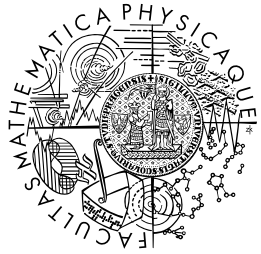

FACULTY
OF MATHEMATICS
AND PHYSICS
Charles University

DOCTORAL THESIS

Petra Vahalová

Ultra-weak photon emission from biological samples

Institute of Photonics and Electronics of the Czech Academy of Sciences
&
Institute of Physics of Charles University

Supervisor of the doctoral thesis:	Ing. Michal Cifra, Ph.D., Institute of Photonics and Electronics of the Czech Academy of Sciences
Study programme:	Biophysics, chemical and macromolecular physics
Study branch:	Physics

Prague 2023

I declare that I carried out this doctoral thesis independently, and only with the cited sources, literature and other professional sources. It has not been used to obtain another or the same degree.

I understand that my work relates to the rights and obligations under the Act No. 121/2000 Sb., the Copyright Act, as amended, in particular the fact that the Charles University has the right to conclude a license agreement on the use of this work as a school work pursuant to Section 60 subsection 1 of the Copyright Act.

In Prague, 3 May, 2023 .....

Author's signature

ACKNOWLEDGEMENTS

Special thanks to:

Dr. Michal Cifra, Dr. Daniel Havelka, Soňa Voslářová, and other colleagues from the Institute of Photonics and Electronics of the Czech Academy of Sciences.

Dr. Viliam Kolivoška from J. Heyrovský Institute of Physical Chemistry of the Czech Academy of Sciences.

Deepest thanks to:

Jakub Kalina, Petr Nehasil and my parents.

Untranslatable thanks:

Děkuji horám, jež mi pomohly sílu odhalit.
Děkuji rostlinám, které mi dopřály zpomalit.
Děkuji vodám, z nichž jsem mohla pít.
Děkuji zvířatům, která mi ukázala jak žít.

Title: Ultra-weak photon emission from biological samples

Author: Petra Vahalová

Department: Institute of Photonics and Electronics of the Czech Academy of Sciences & Institute of Physics of Charles University

Supervisor: Michal Cifra, Ph.D., Institute of Photonics and Electronics of the Czech Academy of Sciences

Abstract: Oxidative processes are an inseparable part of the life of almost all living organisms. They help to maintain homeostasis but they can also stand behind various dysfunctions or diseases. Therefore, an effective method for monitoring oxidative processes in biosamples is an essential tool for medicine, agriculture, and food industry. In this thesis, an overview of available methods for monitoring oxidation in biosamples with a special focus on biological autoluminescence (BAL) is provided. This thesis uses the term BAL to encapsulate various synonyms including the commonly used term ultra-weak photon emission. BAL correlations with various physical, chemical, and biological factors (as original research and an overview from other authors) are also presented. Specifically, the relationships between spontaneous BAL of yeast *Saccharomyces cerevisiae* and the selected physical and chemical parameters (pH, oxygen partial pressure, and cell concentration) during cell growth were established. Additionally, the correlation of BAL intensity from yeast cells or protein bovine serum albumin (BSA) and the number of reactive oxygen species (ROS) that originated as a result of the Fenton reaction were measured. Physical enhancement of BAL from BSA by pulsed electric field was also studied and a basic reaction mechanism of electrogenerated ROS in protein sample leading to BAL was proposed. This work supports BAL employment as a non-invasive monitoring and diagnostic method in various important fields.

Keywords: biological autoluminescence, ultra-weak photon emission, chemiluminescence, oxidative processes, monitoring methods, albumin, yeast, pulsed electric field

Contents

1 Introduction

All metabolically active organisms in presence of oxygen evince really low photon emission. The light is endogenously generated and does not require any external input. It is widely accepted that this light is a luminescence that originates from electron-excited states, which are produced during oxidation reactions of biomolecules, mainly caused by reactive oxygen species (ROS). This phenomenon of weak endogenous chemiluminescence spontaneously occurring in living organisms is mentioned under various synonyms in scientific literature, such as ultra-weak photon emission or biological autoluminescence (BAL). Although the term used in the title of this work is ultra-weak photon emission, I decided to use the term biological autoluminescence (BAL) in the rest of this thesis. The deeper explanation for this decision can be found below in the text. The following introduction to the BAL is a modified version of the Introduction in the paper in Chapter 4.

1.1 Reactive oxygen species

Reactive oxygen species (ROS) stand at the beginning of the path ending by light emission (BAL). They are formed in all metabolically active organisms under the presence of oxygen. They are released during respiration in mitochondria [1, 2] or during a respiratory burst in activated phagocytes [3, 4] (top left part of Fig. 1.1). ROS are also produced by peroxisomes, plasma membrane, cytosol [1, 5], endoplasmic reticulum [6], and extracellular space [7]. Some cellular enzymatic reactions (e.g., those driven by NADPH oxidase, xanthine oxidase, nitric oxidase synthase [8, 9], 5-lipoxygenase [10], or cytochrome P450 [11]) can also lead to the creation of ROS. Besides an immune response to pathogens, they participate in cell signaling and affect various cell processes [3, 4, 12] (lower left part of Fig. 1.1). For example, they take part in the regulation of the cell cycle, differentiation, proliferation, growth, and apoptosis [13]. Moreover, they play a role in regulation of cytoskeleton and cytoskeleton-supported functions of cells, e.g., migration and adhesion [4, 8, 14].

Also, external factors can lead to the ROS formation in an organism, for example, environmental conditions, such as heat, drought, ionizing radiation (including UV), air pollution (SO_2, CO, NO_x), presence of heavy metals cations (e.g., Hg^{2+}, Cd^{2+}, Pb^{2+}) or influence of electric field (EF) [15–17] (top right part of Fig. 1.1).

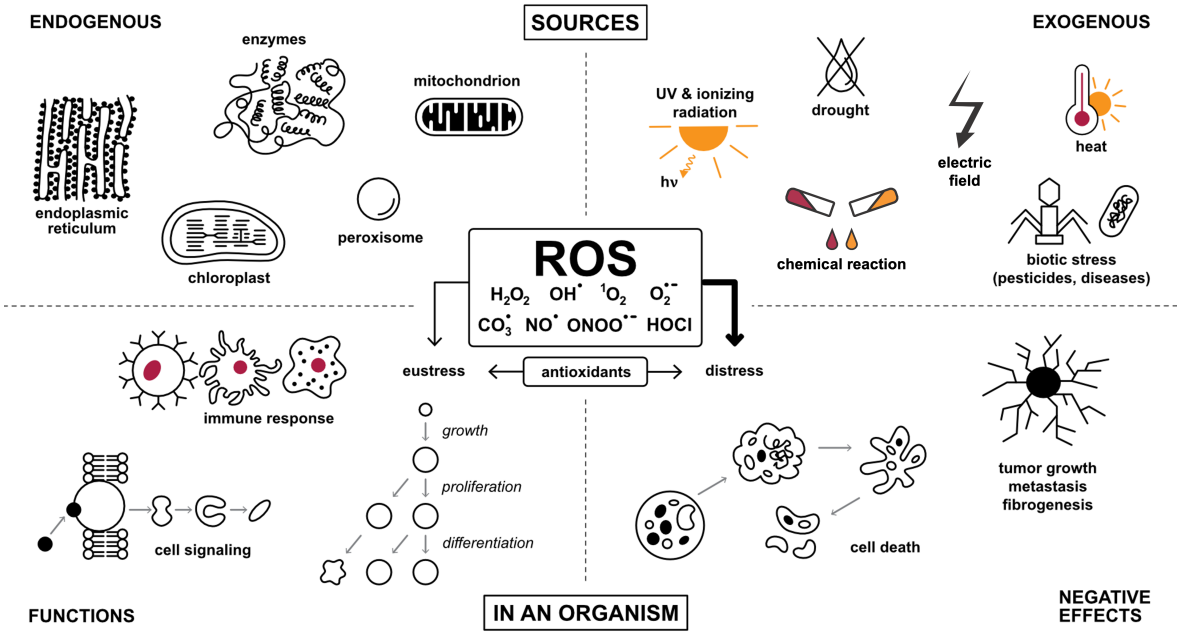

Figure 1.1: The scheme of ROS endogenous and exogenous sources, their functions in an organism, and undesirable consequences of ROS excess. (Modified figure from Chapter 4.)

The non-natural surplus of ROS can have negative effects on an organism such as can lead to tumor growth, metastasis, fibrogenesis, or even cell death [12] (lower right part of Fig. 1.1).

1.2 Antioxidants

Redox homeostasis is essential for proper cellular physiology. An oxidant level can be increased intentionally (e.g., during a respiratory burst or an enzymatic reaction) or inadvertently (e.g., during exposure to pollutants, radiation or inappropriate de/activation of immune cells) [16, 18, 19]. A low increase in the ROS number leads to an adaptive response. However, the excessive production of ROS usually leads to a significant redox balance disruption and can cause cell damage or even cell death that can express as various dysfunctions or diseases on the level of a whole organism [4, 12]. The state when the ability of an organism to eliminate an excess of reactive intermediates is not sufficient is called oxidative stress. On the other hand, deflection of ROS level on the other side (too low level) can also lead to incorrect cell functions, e.g., to inaccuracy of cell signaling [20]. The main role in maintaining the redox balance is played by the antioxidant system. Antioxidants come in many forms, they can be enzymatic or non-enzymatic, endogenous or nutrient-derived, proteins or in form of different molecules. These compounds can intervene in different phases of ROS action, they can prevent the initiation or propagation of ROS damage or they can terminate the radical reaction chain [21].

1.3 Oxidative products

Various products can be formed during reactions of ROS with biomolecules. The prime target of an oxidant attack on a cell is lipids as a major constituent of membranes. Full-length oxidation products, chain-shortened phospholipids, and the corresponding fragments of oxidized fatty acyl chains can be formed during lipid oxidation [22, 23]. We can distinguish products according to the manner and degree of lipid modification – from simpler ones (hydroxides, hydroperoxides, epoxides, ketones) to more complex (isoprostane-like structures, cyclopentenone rings), or with further rearrangement (ring opening to yield isolevuglandins). Changes in lipid structure in membranes, such as peroxidation of polyunsaturated fatty acids, can also change membrane properties (e.g., decrease membrane fluidity and disruption of membrane-bound proteins) subsequently causing an increase in the radical formation and additional modification of polyunsaturated fatty acids to a wide range of products [24]. Some of them, such as aldehydes (e.g., malondialdehyde and 4-hydroxynonenal) can be also employed as "second toxic messengers" because of their relatively high reactivity and rather long life that enables them to diffuse quite far from the point of their origin [25].

However, another major target of a ROS attack is proteins. They constitute approximately 70 % of the dry mass of most cells and have a high rate constant for reaction with many oxidants [16,26]. Three main pathways are appearing during protein reactions with radicals – hydrogen atom abstraction from C–H, O–H, N–H, or S–H bonds, electron abstraction from electron-rich sites (oxidation), and radical addition to electron-rich centers (aromatic rings and sulfur species) [27]. The formation of a particular product depends on many factors such as substrate concentration, environmental conditions (e.g., oxygen concentration, pH), reaction rates, or location of radical action on a protein itself (e.g., peptide backbone or aliphatic side chains). In [16, Table 2] are examples of selected major products produced during oxidation of protein side chains. Protein oxidation often causes also further post-translational protein modifications that can include amino acid alteration or changes in protein structure related to changes in protein properties (e.g., charge, hydrophobicity/hydrophilicity) and functions (e.g., to the loss or (occasional) gain of activity) [16].

Nevertheless, any organic matter can be a target of oxidant action, not only lipids and proteins, but also carbohydrates, DNA, RNA, low-molecular-mass species, or antioxidants [26]. DNA, as a storage of genetic information, also demands special attention. ROS can react with the bases and also with sugar moieties of DNA, producing single- and double-strand breaks in the DNA backbone, adducts of base and sugar groups, and cross-links with other molecules, lesions that block replication [28–30].

Selected products formed during oxidation of biomolecules [16, 31, 32] (reused from Chapter 4):

- **proteins** - hydroperoxides (ROOH), carbonyls e.g., aldehydes and ketones (RCO, RCOR), alcohols (hydroxides) (ROH), peroxides (ROOR), dithiols (RSSR), nitrated/chlorinated Tyr, Trp, Phe, oxidized Tyr, Trp, His, Met, Lys, Leu, Ileu, Val

- **lipids**: chlorinated/nitrated lipids (isoprostanes, isoleukotrienes), hydroperoxides, peroxides (malondialdehyde, 4-hydroxy-2-nonenal, acrolein), alcohols, epoxides, hydrocarbons, aldehydes (oxysterols)
- **DNA/RNA**: aldehyde/other base adducts, nitrated/deaminated bases, oxidized bases

1.4 Further consequences of oxidative stress

The presence of ROS in an unsuitable amount in inappropriate places in an organism results in activation of the antioxidant defense system and in the formation of other reactive species and various oxidative products (from antioxidants or other biomolecules). Modifications of biomolecules often lead to changes in molecule properties and functions that can reflect also in higher cell structures of which the modified molecule is a part of. For example, peroxidation of lipids in a membrane decreases membrane's fluidity, membrane-bound proteins (such as proton pumps or ion channels) can be released or damaged, the membrane and its parts can lose their functions (e.g., the cell loses membrane potential or ion concentration gradient across the membrane), which can end with serious cell damage or even cell death [24]. Changes in proton concentration, in other words, changes in pH, can affect also various cell processes. However, not only pH but also many other physical or chemical parameters can be finally influenced. Worth to mention also oxygen partial pressure, often observed parameter during the research focusing on monitoring oxidative stress [21, 33]. Disruption of cellular metabolism or cell death on a larger scale can affect a wide variety of physiological processes in an organism or can manifest as various diseases (such as neurodegenerative diseases, diabetes, or atherosclerosis). Therefore, seen from the other end, analysis of consequences such as changes in cell viability, metabolism, or other cell functions can provide us useful information about the oxidative state of a sample [21, 24].

1.5 Biological autoluminescence

As mentioned above, during a reaction of ROS with a biomolecule, various products or intermediates can be formed. Two of them are dioxetanes and tetroxides, unstable highly energetic intermediates that decompose to electron excited species [34]. The surplus energy can be used for further chemical reactions, released in form of heat during vibrational decay or can be transferred to a nearby suitable energy acceptor. There is also the possibility to release the excess energy in form of photons during the radiative transition to the ground state. However, this reaction pathway has much lower probability compared to others. Therefore, just a few photons are released from the sample during oxidative processes. For this ultra-weak photon emission, the term biological autoluminescence (BAL) is used in this thesis. The general scheme of reactions leading to BAL is in Fig. 1.2, the more detailed one can be found in [34, Fig. 1].

The intensity of endogenous BAL can vary from tens to several hundreds of photons$\cdot s^{-1}\cdot cm^{-2}$ [35]. BAL induced by external stimuli can be even 2–3 orders of magnitude higher than the endogenous emission of the same sample [36]. However, the distance of a sample from a detector and other optical effects such as

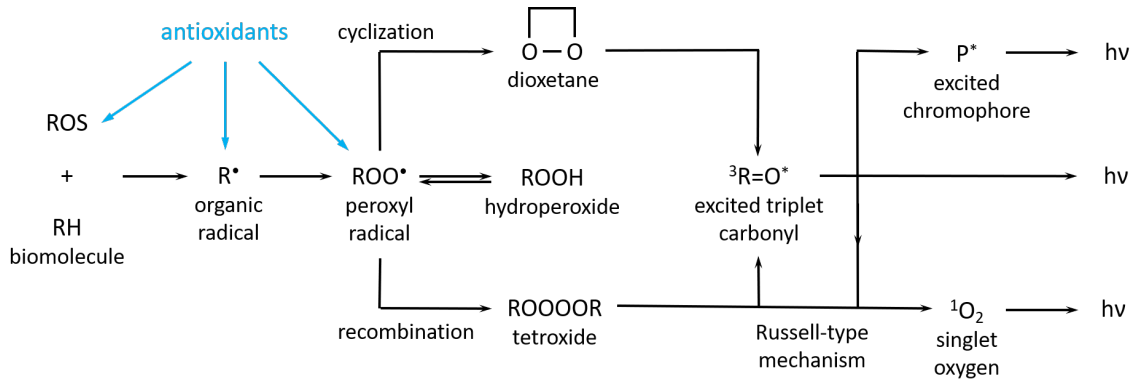

Figure 1.2: General scheme of reactions leading to BAL. (Take over from Chapter 4.) At first, ROS react with a biomolecule RH to generate an organic radical R$^\bullet$. In the presence of molecular oxygen, one-electron oxidation of R$^\bullet$ can lead to the formation of a peroxyl radical ROO$^\bullet$ which can abstract hydrogen from another RH and form ROOH and R$^\bullet$. Another possibility for the ROOH creation is a reaction of RH with singlet oxygen $^1O_2$ via so called 'ene' reaction [34]. The cyclization of ROO$^\bullet$ or the cycloaddition of $^1O_2$ to RH lead to the formation of high-energetic cyclic intermediate 1,2-dioxetane ROOR. Another high-energetic intermediate tetroxide ROOOOR can be a product of the recombination of ROO$^\bullet$. The decomposition of ROOR and ROOOOR results in the formation of triplet excited carbonyl ^{3}R=O*; alternatively, in case of ROOOOR can also result in $^1O_2$ (Russell-type mechanism) [34]. An excited carbonyl ^{3}R=O* can release the excess energy in form of photons or transfer the energy to a near suitable acceptor such as chromophore P or molecular oxygen O_2. Subsequently formed molecules of excited chromophore P* or $^1O_2$ can also emit photons. The light emission can be suppressed by antioxidants that decrease the probability of the ROS formation or transform them into less reactive or non-reactive forms.

absorption, scattering, diffraction, reflection, and refraction may significantly decrease the detected number of photons captured by a detector.

The spectral range of the light emission is from 350 to 1300 nm depending on the type of an emitter. Triplet excited carbonyls ^{3}R=O* emit in the region 350–550 nm, excited chromophores in 550–750 nm (^{1}P*) and 750–1000 nm (^{3}P*), depending on their type [36]. Deexcitation of singlet oxygen $^1O_2$ can be accompanied by monomol (i.e. monomolecular) photon emission at 1270 nm (in case of the molecular transition to the ground (triplet) state) or with dimol (i.e. bimolecular) emission at 634 and at 703 nm (in case of a collision of two $^1O_2$). Nevertheless, various emitters are formed with different probabilities. For example, the yield of $^1O_2$ during the recombination of two peroxyl radicals is 3–14 %, while the yield of ^{3}R=O* during the same reaction is 3–4 orders of magnitude lower [34]. Not only BAL emission but also radiation caused by thermal excitation ranges over the near IR region. It is really hard to distinguish them; therefore, BAL measurements are more focused on the visible and near UV parts of the spectrum.

1.6 Biological autoluminescence - terminology

In scientific literature, various terms are employed for the endogenous photon emission from biological samples. The term used in the title of the thesis *ultra-weak photon emission* stresses really low intensity of the

phenomenon and its particle(photon)-like character. However, it does not contain any reference to the origin of the light. Therefore, another term *biological autoluminescence (BAL)* is used in this work, that seems more appropriate and informative from the current point of view of our research group. The "luminescence" refers to the fact that the light emission is not of a thermal origin. "Auto" refers to the endogenous origin of substances required for luminescence, thus no external luminescence probes have to be added to the studied system. And "biological" refers to the type of samples from that autoluminescence is detected – from biological systems or samples derived or extracted from them. Other terms also used for this phenomenon are *low-level chemiluminecence* [37, 38], *autoluminescence* [39], *biophotons* or *biophoton emission* [35, 40]. The chosen term usually expresses the research group's perspective of the phenomenon.

2 State of the art

Diseases are inseparable parts of our lives. Therefore, present society tries to find out ways how to prevent, diagnose, and cure these dysfunctions. Because current diagnostic methods are often painful and destructive for the analyzed biosamples, new effective and gentle methods overcoming these limitations are in great demand. The development of new monitoring methods plays an important role not only in medicine, but also in agriculture, food industry, or dermatology.

2.1 Monitoring oxidative processes in biosamples

Plenty of diseases, including those occupying the first places in the leaderboard of worldwide causes of death – cardiovascular diseases [41, 42] and cancer [43], are closely related to an increased number of ROS in affected body parts. An overview of available methods for monitoring oxidative processes from the perspective of molecular markers and processes focused on biochemical systems, cell and tissue cultures is provided in Chap. 4.

2.2 BAL and its correlations with various physical, chemical and biological parameters

To employ a method as a diagnostic tool, it is essential to know all factors influencing an output signal or data and the way how they do that. The conditions for reliable distinguishing between a healthy undisturbed biosample and the same type of sample affected by oxidative processes (potentially leading to various diseases) can be variable for different studied samples. Therefore, it is really important to know how a particular biosystem is influenced by specific conditions.

In this work, the main focus is on a particular chemiluminescent method – BAL that is label-free, non-invasive, real-time and with rather low operational costs. An overview of BAL correlations with various physical, chemical and biological parameters and aspects influencing BAL signal is provided in Chap. 4.

2.3 Biosamples

In the experimental part of the thesis, yeast *Saccharomyces cerevisiae* and protein bovine serum albumin (BSA) were chosen as model systems for studying the BAL phenomenon. Yeast *Saccharomyces cerevisiae* is a single-celled eukaryotic organism with the same complexity of internal cell structure as plants, animals or humans. At the same time, they have a short generation time (as a single cell), can be easily cultured and it is also easier to evaluate the effects of various factors on them. Because of abundant usage in food industry [44, 45] and biotechnology [46] they are intensively studied and so also well characterized. BSA is a small, stable, easily available protein that is commonly used as a reference protein for the determination of other protein concentrations (Bradford protein assay) [47]. Additionally, it is usually used as a blocker in immunochemistry [48] and has also several other usages in biochemical applications [49–52]. It is also a useful model for setting of experiments with human serum albumin because of their 76% structural similarity [53].

There have been several studies of spontaneous BAL from yeast. For example, Quickenden et al. [54–58] focused on spontaneous BAL (its intensity and spectral distribution) in the exponential and stationary phase of yeast growth. Similarly, methods based on chemiluminescence measurement have been used to determine the presence or the concentration of BSA in the sample [59, 60] or to explore its binding behavior (e.g., with cephalosporin analogs) [61].

2.4 Pulsed electric field and its influence on proteins

So far technologies using pulsed electric field (PEF) have been employed in various fields of interest. For example, PEF has found applications in medicine (e.g., in electrochemotherapy [62–64], non-thermal tissue ablation [65], or in drug and gene delivery or therapy [66–69]), in food industry (e.g., for non-thermal pasteurization [70, 71] or to increase yields of active food compounds extraction [72–74]) and in biotechnology (e.g., to modify the function of the biomolecules, such as the self-assembly of protein complexes [75] or change (usually decrease) in the enzyme activity [76–79]).

Similarly, like for ROS, lipids are a primary target of PEF action [80] while proteins are the major ones that are also interesting for food industry. Therefore, many experimental and theoretical works focusing on influence of EF on proteins have arisen. For example, molecular dynamic simulations helped to reveal that EF application on a protein sample can change the shape of the protein [81], its molecular surface area [82–84], the secondary structure [85–88], and even can lead to protein unfolding [83, 85, 89]. EF can also affect dipole moment [81, 84, 90, 91] or the propensity towards protein and peptide complex formation or dis/aggregation [91, 92].

The computational results are often supported by various experimental works, although these two approaches usually employ different types of protein samples. For example, changes in the fluorescence spectra of intrinsic aromatic amino acids or in the UV-circular dichroism spectra of proteins have been observed

after PEF application indicating changes in the molecular structure [75, 79, 93] and in the secondary structure [77, 78, 93–97], respectively. Structural changes and (partial) unfolding have been also confirmed by the analysis of hydrophobic and newly accessible SH groups in the protein sample after PEF treatment [93, 98]. PEF applications on a protein leading to its denaturation [99] or aggregation of proteins [79,100,101] have been also demonstrated by experiments. Naturally, each change requires specific conditions (such as temperature or buffer composition) and PEF parameters (e.g., EF strength, number of pulses, or frequency) depending on a protein sample type.

It was also shown that PEF treatment of the sample can enhance the ROS generation [17], in which case the number of ROS depends on electrode material and PEF protocol (such as a number of pulses or frequency) [102]. PEF applications leading to cell electroporation and oxidative changes have been often studied on complex cellular samples [103–108] or on lipids [109–111] as the main constituent of cell membranes. Nevertheless, just a few works concern with oxidative effects of PEF treatment on well-defined protein samples [97, 112].

2.5 Applications employing chemiluminescence

Potential employment of chemiluminescence as a diagnostic method for serious diseases such as cancer [113–120] or neurodegenerative Alzheimer's disease [121–124] have been intensively studied. Accurate assessment of ROS concentrations or their type in a sample [125, 126] may also help in the diagnosis of other health issues such as infertility [127, 128] or could be important in food analysis [129]. Not only ROS but also various biomolecules (such as proteins, enzymes, substrates or metabolites) [130–138] or artificial compounds [138–140] are important markers in medicine, pharmacy or food industry and could be measured with the help of chemiluminescence. Additionally, chemiluminescence could be employed to detect the changes in calcium concentration in living cells [141, 142], to replace the radioactive labels in immunoassays [118, 143, 144], or to study the influence of UV radiation on human skin with a potential application in dermatology [145, 146]. Chemiluminescence has found applications not only in detection, determination or diagnosis but also in therapy of diseases, such as in the photodynamic therapy of cancer [147, 148].

Combinations of chemiluminescence with other techniques or principles help to make the tool even more powerful. For example, in analytical applications chemiluminescence detection is often coupled with various separation techniques such as liquid chromatography [134,136,149] or capillary electrophoresis [150]. It could be also connected with immunoassays [132, 135].

The advantages of employment of chemiluminescent reactions are quite simple measurement instrumentation, low operation cost, very low detection limits and wide dynamic range. Chemiluminescent labels could find employment in non-isotopic immunoassays with potential applications in human, veterinary or forensic medicine, agriculture, or food industry. On the other hand, lack of specificity and low sensitivity to some

physical-chemical factors are major disadvantages of the chemiluminescent method. [138, 144].

3 Goals of the thesis

This thesis has the following goals:

- Provide an overview of available methods for monitoring oxidation in biosamples and their basic characteristics and capabilities.
- Discuss a potential usage of BAL as a monitoring method of oxidative processes in biosamples and provide an overview of BAL correlations with various physical, chemical and biological factors.
- Discuss possibilities of BAL enhancement.
- Confirm that ROS participate in the reaction mechanism leading to BAL
- Propose a basic reaction mechanism of electrogenerated ROS in a protein sample leading to BAL.
- Contribute to an extension of current knowledge of correlations between BAL and physical, chemical or biological parameters related to
  - spontaneous BAL of cell culture.
  - chemically enhanced BAL (by a hydroxyl radical originated from the Fenton reaction) on a level of cells or proteins.
  - physically enhanced BAL (by PEF) from a protein.
- Support the possibility of BAL employment as a non-invasive monitoring and diagnostic method in medicine, agriculture, and food industry.

4 Biological autoluminescence as a perturbance-free method for monitoring oxidation in biosystems

This chapter is a version of:

Petra Vahalová and Michal Cifra,
Biological autoluminescence as a perturbance-free method for monitoring oxidation in biosystems,
Progress in Biophysics and Molecular Biology, volume 177, pages 80 - 108, 2023.
DOI: doi.org/10.1016/j.pbiomolbio.2022.10.009

Author contributions:

Petra Vahalová:
Conceptualization, Data curation, Formal analysis (lead), Investigation (lead), Methodology, Visualization (lead), Writing – original draft (lead): most of the text, Writing – review and editing (lead)

Michal Cifra:
Conceptualization, Formal analysis (supporting), Funding acquisition, Investigation (supporting), Project administration, Resources, Supervision, Validation, Visualization (supporting), Writing – original draft (supporting) , Writing – review and editing (supporting)

Candidate's contribution: 80 %

The manuscript carries the following acknowledgements:

We acknowledge major financial support from the Czech Science Foundation, project no. GX20-06873X. Neuron collective is acknowledged for graphical design and The Science Editorium for the manuscript structure and language check. Viliam Kolivoška is acknowledged for proofreading the manuscript and providing many useful suggestions.

Progress in Biophysics and Molecular Biology 177 (2023) 80–108

Contents lists available at ScienceDirect

Progress in Biophysics and Molecular Biology

journal homepage: www.elsevier.com/locate/pbiomolbio

Biological autoluminescence as a perturbance-free method for monitoring oxidation in biosystems

Petra Vahalová, Michal Cifra *

Institute of Photonics and Electronics of the Czech Academy of Sciences, Prague, 18200, Czech Republic

ARTICLE INFO

Keywords:
Biological luminescence
Oxidative stress
Monitoring methods

ABSTRACT

Biological oxidation processes are in the core of life energetics, play an important role in cellular biophysics, physiological cell signaling or cellular pathophysiology. Understanding of biooxidation processes is also crucial for biotechnological applications.

Therefore, a plethora of methods has been developed for monitoring oxidation so far, each with distinct advantages and disadvantages. We review here the available methods for monitoring oxidation and their basic characteristics and capabilities. Then we focus on a unique method — the only one that does not require input of additional external energy or chemicals — which employs detection of biological autoluminescence (BAL). We highlight the pros and cons of this method and provide an overview of how BAL can be used to report on various aspects of cellular oxidation processes starting from oxygen consumption to the generation of oxidation products such as carbonyls. This review highlights the application potential of this completely non-invasive and label-free biophotonic diagnostic method.

1. Introduction

Biological reduction-oxidation (redox) processes play an important role in life biophysical processes (Zhu and Thompson, 2019) as well as in biotechnology at both the fundamental and industrial level (Hollmann et al., 2011). Here, our major focus is a particular non-invasive method for oxidation monitoring based on biological autoluminescence (BAL) (Cifra and Pospišil, 2014) and its distinct features and advantages. To put BAL into the context of the current redox molecular biology, biochemistry, and biophysics paradigm, we start with a brief overview of existing methods used for monitoring of oxidation and then provide an overview of BAL.

From a biological and biomedical perspective, biological oxidation (reduction-oxidation, in general) is a key process in cellular bioenergetics in eukaryotes, namely ATP production via oxidative phosphorylation in mitochondria (Zhu and Thompson, 2019; Stoldt et al., 2018). Oxidative species, such as reactive oxygen species (ROS), are involved in physiological signal transduction at a cellular level (Zhang et al., 2016; Finkel, 2011; Stadtman and Levine, 2002); however, excessive oxidation leads to oxidative stress, causing or accompanying various health conditions including neurodegenerative and cardiovascular diseases (Puntarulo, 2005; Datz et al., 2013; Schneijder et al., 1992; Crichton et al., 2002; Sian-Hülsmann et al., 2011).

Enzymatic and non-enzymatic redox processes involving biomolecules have also found extensive use in bioelectronics, biotechnology and environmental technology. For instance, at the fundamental research level, redox proteins have been rationally designed (Gilardi and Fantuzzi, 2001) for applications in electrochemical/amperometric sensors (Gorton and Domınguez, 2002) for medical and environmental monitoring. At the industrial level, applications of redox processes have been mainly driven by demand in the food and pharmaceutical industries. As of 2006, the bioredox catalysis approach has accounted for one third of commercialized processes employing enzymes, mostly employed in green chemistry and synthesis (Gibson and Parales, 2000) for the food and pharmaceutical industry. Of these processes, approximately half have comprised oxidation processes [(Hollmann et al., 2011), Fig. 8 therein], [(Liese et al., 2006; Ch. 7 in Stadtman and Levine, 2002)]. There is also a major push for sustainable "green" chemistry (Gibson and Parales, 2000), which is often inspired by biological processes and redox enzymes. Redox enzymes, isolated or in cells, which introduce an oxygen atom to the substrate, such as dioxygenases, peroxidases, oxidases (glucose oxidase, laccase) and dehydrogenases (Hollmann et al., 2011; Urlacher et al., 2004), can serve various biotechnological purposes. Indeed, enzymes can perform regio- or

* Corresponding author.
E-mail address: cifra@ufe.cz (M. Cifra).

https://doi.org/10.1016/j.pbiomolbio.2022.10.009
Received 29 June 2022; Received in revised form 20 October 2022; Accepted 24 October 2022
Available online 3 November 2022

stereoselective oxidation (Urlacher et al., 2004) needed for various synthesis processes. The synthesis of biopolymers and gels is a booming field inspired from biology. For example, in laccase, tyrosinase, and horseradish peroxidase, enzymes catalyze oxidation-based synthesis of several types of biopolymers from phenolic building blocks (Grönqvist et al., 2005; Jeon et al., 2012). As another example of enzymatic oxidation processes, tyrosinases also catalyze oxidation processes (melanin pigment synthesis) involved in color formation in skin and hair of mammals, but also in unwanted browning of plant-derived foods (Mattinen et al., 2008). Some redox enzymes, such as laccase, also have a bifunctional role so that they take part in both catabolic (bond--breaking) and anabolic (bond-forming) oxidation functions (Jeon and Chang, 2013). Another technology that utilizes oxidation processes are bioinspired fuel cells (Chaudhuri and Lovley, 2003). There, redox proteins coupled to external electrodes have been developed to harness energy from the substrates to power external electrical circuits (Nöll and Nöll, 2011; Willner et al., 2009; Barrière et al., 2006). Such "green" chemical electricity sources are in line with Goal 7 of "Affordable and clean energy" of United Nations Sustainable Development Goals program (United Nations, 2019). Advanced oxidation processes, which include enzymatic and non-enzymatic (e.g., Fenton-reaction-based) approaches, are also employed for the degradation (Gibson and Parales, 2000) of waste substances and wastewater treatment and management (decolourisation and detoxification) in general (Ledakowicz et al., 2001; Babuponnusami and Muthukumar, 2014).

As demonstrated above, both enzymatic and non-enzymatic redox processes are widely employed in research and industry. Therefore, there is a need for effective monitoring methods of oxidation processes and oxidative products. There is a large variety of methods to monitor and detect oxidation markers and processes (Hawkins and Davies, 2019; Celi, 2011; Osório and Cardeal, 2013). They vary according to the specificity, sample destructiveness, sample volume, time needed to obtain the result, handling, instrumental complexity, and costs.

In this review, we concisely review methods for monitoring and detection from the perspective of molecular markers and processes of oxidation with a major focus on biochemical systems, and cell and tissue cultures. Then we focus on a particular chemiluminescent method that is completely label-free, non-invasive and perturbance-free, real-time and with rather low operational costs – biological auto(chemi)luminescence (BAL) – which relies solely on probes endogenous to the sample. For studies on BAL in higher organisms and humans, we refer the reader to other publications, e.g. (Zapata et al., 2021; Van Wijk et al., 2013, 2014; Ou-Yang, 2014; Wijk and Van, 2008).

2. Biological oxidation: current paradigm in brief

2.1. Reactive oxygen species

Reactive oxygen species (ROS) are at the beginning of the reaction chain leading to BAL. They are produced in all metabolically active organisms under the presence of oxygen. We can distinguish two types of ROS - radicals with unpaired electron (e.g., superoxide anion radical $O_2^{\bullet -}$, hydroxyl $HO^{\bullet}$, peroxyl $ROO^{\bullet}$, alkoxyl $RO^{\bullet}$, alkyl $R^{\bullet}$ radicals) and less reactive two-electron (i.e. molecules with paired electrons) ROS (e.g., hydrogen peroxide H_2O_2, organic hydroperoxides ROOH, singlet oxygen $^1O_2$, or ozone O_3) (Hawkins and Davies, 2019; Sies and Jones, 1038). Reactive nitrogen (such as nitrogen monoxide (nitric oxide) $NO^{\bullet}$, peroxynitrite $ONOO^{-\bullet}$, or nitrogen dioxide $NO_2^{\bullet}$ radical) and chlorine species (e.g., hypochlorous acid - HOCl) can be also classified into the ROS category because in addition to containing nitrogen or chlorine, respectively, they also contain oxygen (Li et al., 2016).

ROS are mainly created as a natural by-product of aerobic metabolism. Mitochondria are considered as the major ROS source in mammalian cells (Balaban et al., 2005; Starkov, 2008). Other cell compartments in which ROS are produced are peroxisomes, cytosol, plasma membrane (Balaban et al., 2005; O'Donnell and Azzi, 1996), endoplasmic reticulum (Gross et al., 2006), and extracellular space (McNally et al., 2003). ROS are released during metabolic processes, such as cellular respiration processes, and as by-products of several cellular enzymatic reactions (e.g. those driven by 5-lipoxygenase (Catalano et al., 2005), cytochrome P450 (Gonzalez, 2005), NADPH oxidase, xanthine oxidase, or nitric oxidase synthase (San Martín and Griendling, 2010; Alfadda and Sallam, 2012)). ROS are released during a respiratory burst in activated phagocytes (macrophages, neutrophils, and dendritic cells) as a response of an immune system to foreign invasion (Cristiana and Elena, 2018; Wilson and González-Billault, 2015). They play an important role in cell signaling and influence a wide variety of cell processes (Sies and Jones, 1038; Cristiana and Elena, 2018; Wilson and González-Billault, 2015). They help to regulate the cell cycle, differentiation, proliferation, growth, and apoptosis (Brieger et al., 2012). They

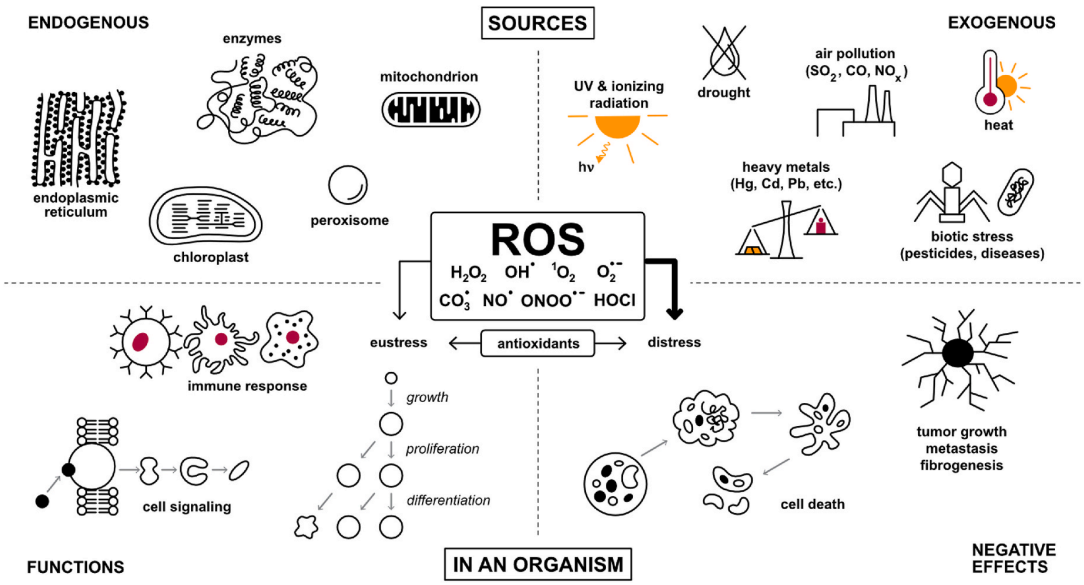

Fig. 1. The scheme of ROS endogenous and exogenous sources, their functions in an organism, and undesirable consequences of ROS excess.

also take part in cytoskeletal regulation and cytoskeleton-supported cell functions, such as migration and adhesion (San Martín and Griendling, 2010; Wilson and González-Billault, 2015; Valdivia et al., 2015) (left part of Fig. 1).

ROS can also be formed in an organism as a result of the influence of environmental condition, such as heat, drought, ionizing radiation (including UV), air pollution (SO_2, CO, NO_x), or presence of heavy metals cations (Hg^{2+}, Cd^{2+}, Pb^{2+}, etc.) (Das and Roychoudhury, 2014). The excess of ROS can lead to pathological states as tumor growth, metastasis, fibrogenesis, or even cell death (Sies and Jones, 1038) (right part of Fig. 1).

2.2. Antioxidants

A balance between reduction and oxidation (redox homeostasis) is indispensable for proper cellular physiology (Wilson and González-Billault, 2015). Disruption of the ROS balance in cells arises from both external agents and endogenous processes that generate reactive species, either intentionally (e.g., during pathogen killing or enzymatic reactions) or accidently (e.g., exposure to radiation, pollutants, or drugs) (Hawkins and Davies, 2019; Merck, 2015). It usually leads to a significant increase in ROS levels, also called oxidative stress (an imbalance between ROS production and the ability of an organism to detoxify reactive intermediates quickly enough). A low increase in the oxidant level leads to an adaptive response; however, substantial excess of ROS leads to cell damage or death, which are associated with several dysfunctions and diseases on a scale of a whole organism (Sies and Jones, 1038; Wilson and González-Billault, 2015). On the other hand, a too low ROS level can lead to improper cell functions, such as errors in signaling pathways (Yun et al., 2009). The antioxidant defense system helps to maintain this redox homeostasis. Enzymes and other compounds that prevent the initiation or propagation of ROS damage or that act as radical chain terminating agents constitute the primary antioxidant defense system (Jamnik and Raspor, 2005). We can distinguish antioxidants as endogenous or nutrient-derived, enzymatic or non-enzymatic, proteins or other molecules.

Antioxidant defense system includes (Jamnik and Raspor, 2005; Percival, 1996; Abuja and Albertini, 2001; Cabiscol Català et al., 2000):

- **endogenous antioxidant protection system**
  - *antioxidant enzymes*: catalases, superoxide dismutases, reductases (e.g. glutathione- or thioredoxin reductase), peroxidases (e.g. glutathione peroxidase), dehydrogenases (e.g. glucose-6-phosphate dehydrogenases), oxidoreductases (e.g. sulfirodoxin, thioredoxin), thioltransferase (e.g. glutaredoxin)
  - *metal binding proteins*: ferritin (iron), lactoferrin (iron), transferrin (iron), myoglobin (iron), albumin (copper), ceruloplasmin (copper), metallothionein (copper)
  - *other compounds*: bilirubin, thiols (e.g., glutathione, lipoic acid, N-acetyl cysteine), NADPH and NADH, ubiquinol (coenzyme Q10), uric acid
- **nutrient-derived antioxidants**
  - *water soluble*: ascorbic acid (vitamin C), polyphenols (such as flavonoids)
  - *lipid soluble*: tocopherols and tocotrienols (vitamin E), carotenoids (such as β-caroten, lycopene, lutein, zeaxanthin)

2.3. Oxidative products

All organic components of a biological system (e.g., proteins, lipids, carbohydrates, DNA, RNA, low-molecular-mass species, antioxidants) can be damaged by reactions with oxidants (Hawkins et al., 2009). Lipids, as a substantial part of membranes, are a prime target of ROS. Lipid peroxidation of polyunsaturated fatty acids in a membrane causes changes in its properties (decrease in membrane fluidity and disruption of membrane-bound proteins), resulting in the formation of more radicals and the degradation of polyunsaturated fatty acids to a variety of products (Cabiscol Català et al., 2000). For example, aldehydes (such as malondialdehyde and 4-hydroxynonenal) are very reactive but rather long lived so they can diffuse quite far from the point of their origin and act as "second toxic messengers" (Esterbauer et al., 1991). There is a wide variety of products that result from lipid oxidation including full-length oxidation products, chain-shortened phospholipids, and the corresponding fragments of oxidized fatty acyl chains (Spickett and Pitt, 2015; Reis and Spickett, 2012). Also, the extent and manner of modifications can vary from a simple one (hydroperoxides, hydroxides, epoxides, ketones) to more complex (isoprostane-like structures, cyclopentenone rings), or with further rearrangement (ring opening to yield isolevuglandins).

Proteins compose approximately 70% of the dry mass of most cells and have a high rate constant for reaction with many oxidants; therefore, they are the major target for the damage caused by ROS (Hawkins and Davies, 2019; Hawkins et al., 2009). This can result in changes to protein structure, functions, properties, catalytic turnover, and to the loss or (occasional) gain of activity (Hawkins and Davies, 2019). The majority of radical reactions with proteins occur via three major pathways: hydrogen atom abstraction from C–H, N–H, O–H, or S–H bonds, electron abstraction from electron-rich sites (oxidation), and radical addition to electron-rich centers (aromatic rings and sulfur species) (Hawkins and Davies, 2001). Depending on the reaction rates, "location of attack" (e.g., peptide backbone or aliphatic side chains), substrate and oxygen concentration, pH, and other factors, various radicals and other products are formed. For example, selected major products generated from oxidation of protein side chains are shown in (Hawkins and Davies, 2019). Radicals, two-electron oxidants, metal-oxo complexes and secondary products of their reactions generate a wide variety of post-translational protein modifications that alter the amino acid and protein composition and structure, charge, hydrophobicity/hydrophilicity, folding and function (Hawkins and Davies, 2019).

DNA, as a carrier of genetic information, is also an important target. Reactive species attack both the bases and sugar moieties, producing single- and double-strand breaks in the backbone, adducts of base and sugar groups, and cross-links with other molecules, lesions that block replication (Sies, 1993; Sies and Menck, 1992; Hartwig, 1996).

Selected products from the oxidation of biomolecules (Hawkins and Davies, 2014, 2019; Dalle-Donne et al., 2003):

- **proteins** - hydroperoxides (ROOH), carbonyls e.g. aldehydes and ketones (RCO, RCOR), alcohols (hydroxides) (ROH), peroxides (ROOR), dithiols (RSSR), nitrated/ chlorinated Tyr, Trp, Phe, oxidized Tyr, Trp, His, Met, Lys, Leu, Ileu, Val
- **lipids**: chlorinated/nitrated lipids (isoprostanes, isoleukotrienes), hydroperoxides, peroxides (malondialdehyde, 4-hydroxy-2-nonenal, acrolein), alcohols, epoxides, hydrocarbons, aldehydes (oxysterols)
- **DNA/RNA**: aldehyde/other base adducts, nitrated/deaminated bases, oxidized bases

2.4. Further consequences of oxidative stress

Reactions of ROS with biomolecules lead to the formation of other ROS and various oxidative products and provoke an antioxidant defense response; however, a wide variety of physiological processes are also influenced. The changes in a cell that are caused by ROS can be reflected in physical or chemical parameters such as oxygen partial pressure or pH (Jamnik and Raspor, 2003, 2005). The modification of biomolecules causes changes in their functions and the properties of cellular structures of which they are a part. For example, lipid peroxidation decreases membrane fluidity, membrane-bound proteins can be damaged or released, and the membrane loses its properties and functions (Cabiscol Català et al., 2000). Cellular metabolism can be disrupted and cell death or manifestations of various diseases of an organism (such as

neurodegenerative diseases, diabetes, and atherosclerosis) can be observed. Therefore, monitoring of cell viability, changes in metabolism and other cell functions can provide useful information about the oxidative state of a sample (Jamnik and Raspor, 2005; Cabiscol Català et al., 2000).

2.5. Biological autoluminescence

Reaction of ROS with biomolecules can lead to the creation of unstable, highly energetic intermediates that decompose to electron excited species. Electron excited species can take several further pathways (e.g., vibrational decay to produce heat, further chemical reactions). One of them, having low probability compared to others, is the radiative transition to the ground state, where the excess energy is released in the form of photon. This ultra-low photon emission is called biological autoluminescence (BAL). The general scheme of reactions leading to BAL is in Fig. 2, more detailed one can be found in [(Pospíšil et al., 2019), Fig. 1 therein].

The intensity of endogenous BAL ranges from tens to several hundreds of photons· s^{-1}· cm^{-2} (Balasigamani et al., 1997); however, BAL induced by external stimuli can be 2-3 orders of magnitude higher than the endogenous emission (Cifra and Pospišil, 2014). The amount of detected photons is further reduced because of the distance of a sample from a detector and other optical effects such as absorption, scattering, diffraction, reflection, and refraction.

The main emitter molecular species, which lead to BAL, are triplet excited carbonyls $^3R=O^*$, singlet $^1P^*$ and triplet excited chromophores $^3P^*$, and singlet oxygen $^1O_2$. Triplet carbonyls $^3R=O^*$ emit in the region 350–550 nm, chromophores in 550–750 nm ($^1P^*$) and 750–1000 nm ($^3P^*$), depending on their type (Cifra and Pospišil, 2014). The transition of singlet oxygen $^1O_2$ to the ground (triplet) state is accompanied by monomol (i.e. monomolecular) photon emission at 1270 nm. A collision of two $^1O_2$ can result in dimol (e.g. bimolecular) emission at 634 and at 703 nm. However, different emitters are created with various probabilities. For example, during recombination of two peroxyl radicals, the yield of $^3R=O^*$ formed is 3–4 orders of magnitude less than the yield of $^1O_2$, which is 3–14% (Pospíšil et al., 2019). Because the BAL intensity in the near IR region is comparable with photon emission caused by thermal excitation and therefore often difficult to distinguish from each other, BAL analysis is more focused on the visible and near UV parts of the spectrum.

One may legitimately ask whether there are other physical luminescent phenomena that contribute to BAL. The question can be reduced to where the energy comes from to generate the electron excited state. In a wide range of physical systems, there are well-known luminescent phenomena where the energy for electron excitation is generated without chemical reactions, such as sonoluminescence (Suslick and Flannigan, 2008) or triboluminescence (Xie and Li, 2018). However, there is little evidence that these mechanisms would routinely contribute to the BAL that is ordinarily observed in experiments, because extreme situations such as high-power input or macroscopic rupture of the material is usually needed to observe non-chemically generated luminescence of biomaterials (Li and Haneman, 1999). Furthermore, Slawinski provided a short analysis of how the following hypothetical mechanisms involving collective molecular interactions could combine to electron excitation in cells (Sławiński, 1988): release of superhelical DNA twist, molecular interactions in the electric field of biomembranes, possibility of population inversion and stimulated emission in electrogenic structures, and collective excitations in perturbed water and cytosol. However, current evidence does not suggest that these mechanisms would be the routine source of BAL (Cifra et al., 2015). The school of thought of Fritz-Albert Popp proposes that the biological endogenously produced electron excited state and the subsequently generated photons are not just a by-products of chemical reactions, but actually have a biological function: the photons collectively form a (bio)photon field within cells and organisms and this field has a biological use as a self-organizing biological agent (Popp et al., 1994; Popp, 2009) due to proposed optical coherence (Popp and Kilmister, 1986). Within this school of thought, DNA was proposed to be a photon storage (Rattemeyer et al., 1981) but the particular source of the electronic excitation energy was not explicitly experimentally considered. Although these are exciting proposals, the evidence so far has not convinced the scientific community because of the ambiguities (Cifra et al., 2015) of the interpretations of the experiments including those on the physical and statistical parameters of BAL (Popp and Li, 1993; Popp et al., 1988).

2.6. Biological autoluminescence: terminology

The phenomenon of endogenous light emission from biological samples is mentioned under various synonyms in the scientific literature. We use the term biological autoluminescence because it seems to

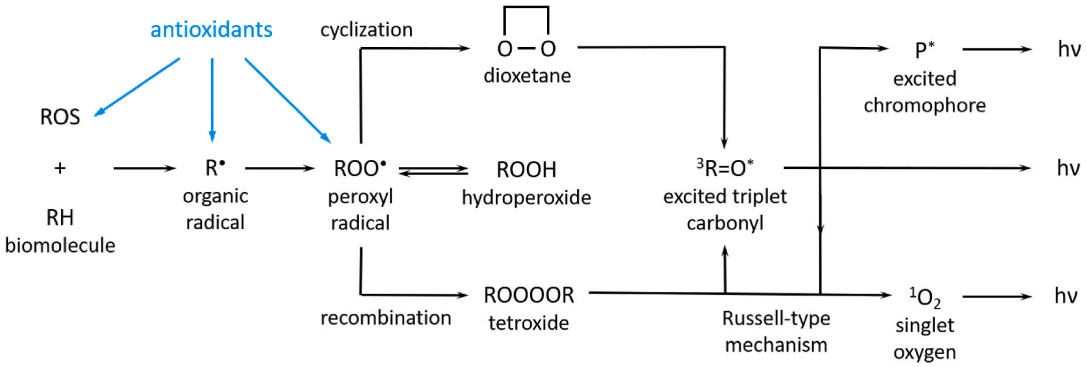

Fig. 2. General scheme of reactions leading to BAL. At first, ROS react with a biomolecule RH to generate an organic radical $R^•$. In the presence of molecular oxygen, one-electron oxidation of $R^•$ can lead to the formation of a peroxyl radical $ROO^•$ which can abstract hydrogen from another RH and form ROOH and $R^•$. Another possibility for ROOH creation is a reaction of RH with singlet oxygen $^1O_2$ via so called 'ene' reaction (Pospíšil et al., 2019). The cyclization of $ROO^•$ or the cycloaddition of $^1O_2$ to RH lead to the formation of high-energetic cyclic intermediate 1,2-dioxetane ROOR. Another high-energetic intermediate tetroxide ROOOOR can be a product of the recombination of $ROO^•$. The decomposition of ROOR and ROOOOR results in the formation of triplet excited carbonyl $^3R=O^*$; alternatively, in case of ROOOOR can also results in $^1O_2$ (Russell-type mechanism) (Pospíšil et al., 2019). An excited carbonyl $^3R=O^*$ can released excess energy in form of photon or transfer energy to a near suitable acceptor such as chromophore P or molecular oxygen O_2. Subsequently formed molecules of excited chromophore P^* or $^1O_2$ can also emit photons. The light emission can be suppressed by antioxidants that decrease the probability of ROS formation or transform them into less reactive or non-reactive forms.

be the most appropriate and informative for several reasons. The "luminescence" refers to the important fact that the phenomenon involves light emission that is not of a thermal origin, in contrast to thermal radiation. "Auto" refers to the aspect that the light process and the molecular substances required for luminescence to occur are endogenous to the system under study. It also refers to the fact that to observe luminescence, no external luminescence probes have to be added to the system: the light emitting species are produced within the system. "Biological" refers to the fact that the focus is on autoluminescence of biological systems or samples derived or extracted from biological systems.

Other terms for BAL are used in the literature: *Ultra-weak photon emission* (Cifra and Pospišil, 2014) merely describes that it is a light phenomenon of very low intensity and it has a particle(photon)-like character and it does not explicitly specify any mechanism of the light generation. *Low level chemiluminescence* (Cadenas et al., 1980; Boveris et al., 1980a) highlights the fact that the mechanism of BAL is due to chemical excitation of electrons to higher energy levels in respective molecules, which then can become emitters of BAL. *Autoluminescence* (Havaux et al., 2006) emphasizes the origin of BAL - without any external stimuli. *Biophotons* or *biophoton emission* (Balasigamani et al., 1997; Cohen and Popp, 1997) highlight the biological origin of the light emission, the particle (photon) nature of the light and/or a potential biological function of BAL. The choice of term usually expresses the authors' perspective on the phenomenon.

3. Methods for monitoring oxidative/free radical processes in cell cultures

Information about the oxidative state of a cell or an organism can be obtained from a direct ROS level measurement. Another way can be to assess the level of oxidation by quantifying the loss of parent materials, the formation of specific products, or detecting generic markers of such reactions (e.g., protein carbonyls, DNA strand breaks, protein thiol levels) (Hawkins and Davies, 2014). The detection of changes in intermediate reversible metabolite levels/ratios or antioxidant concentrations and activities can also tell us more about the oxidative state of a sample (Abuja and Albertini, 2001; Veskoukis et al., 2018). As well as, we can examine changes in selected cell processes (such as growth (Carmona et al., 2019; Munna, 2013)), cell compartment properties and functions (e.g., membrane fluidity (de la Haba et al., 2013; Benderitter et al., 2003) and permeability (Schlenker et al., 2000; Tiwari et al., 2002)), physical/chemical parameters (such as oxygen consumption (Carmona et al., 2019; Tiwari et al., 2002)), or others. Also, the presence of some agents (such as some metals) can increase the probability of oxidation, so monitoring of these pro-oxidants can provide useful information about sample state (Valenzuela et al., 2018; The British Nutrition Foundation, 1995). Therefore, a wide range of methods have been used for monitoring oxidative processes from various perspectives (Table 1).

Table 1
Methods for monitoring oxidative processes and products of oxidation: classification from various perspectives.

methods	optical electrochemical chromatography-based spin-trapping EPR mass spectroscopy
molecular species and processes	ROS detection oxidation products detection antioxidant presents intermediate reversible metabolites detection
level of complexity of studied sample	macromolecules cell cultures whole organism

The chosen method depends on the level of complexity of the studied sample (e.g., yeast culture), which marker of oxidation we want to follow (e.g., protein carbonyls) and which method we want to use for its detection (e.g., chemiluminescence). Of course, each method has its own advantages and disadvantages as evident in [(Celi, 2011), Table 1 therein], in which various methods used for oxidative stress assessment by the monitoring of several selected biomarkers are compared. A list of selected common biomarkers of oxidative stress, enzyme families, small molecules, and genes studied in the oxidative stress field is provided in a document from EMD Milipore Corp. (Merck (2015), Tables 1, 2, 6, 7 therein]. Selected antibodies and dyes used in oxidative stress research and common fluorescent dyes to study mitochondria are also listed there [(Merck, 2015), Tables 4, 5, 9 therein].

In this review, we examine methods according to various oxidation markers (second row of Table 1). We discuss methods of direct ROS measurement and measurement of oxidative damage of proteins, lipids, DNA, and saccharides through their oxidative products. We also cover the assessment of oxidative state based on measurement of selected intermediate reversible metabolites and assessment of antioxidant status by total antioxidant capacity, antioxidant enzyme activity, or the determination of nonenzymatic antioxidant levels. At the end, correlations of various physical, chemical and biological parameters and process with oxidative stress will be discussed.

3.1. Reactive oxygen species

The biggest limitation of direct ROS detection is their short lifetime and high reactivity (Prasad et al., 2019). The most common and powerful method for ROS examination is electron paramagnetic resonance (EPR), also called electron spin resonance, spectroscopy, which can be combined with other techniques to (partially) overcome challenges connected with the short lifetime of radicals (Hawkins and Davies, 2014), including rapid-flow methods, *in situ* photolysis or radiolysis, freeze-quenching, and the most widely used spin trapping (Hawkins and Davies, 2019). A spin trap (typically a nitrone or nitroso compound) reacts with the present reactive radicals and creates longer-lived radical adducts that can be subsequently detected (Davies, 2016).

A combination of various methods is usually used for detection, quantification, and characterization of a selected radical in a studied sample. For example, Kumar et al. monitored protein radicals in *Arabidopsis* using an immuno-spin trapping technique based on the detection of 5,5-dimethyl-1-pyrroline N-oxide (DMPO) nitrone adducts using the anti-DMPO antibody (Kumar et al., 2019). Imaging of protein radicals was performed by confocal laser scanning microscopy using fluorescein conjugated to the anti-DMPO antibody. For further characterization of protein radicals (where the protein radicals are formed and with which processes is their formation associated) standard blotting techniques using PSII protein-specific antibodies and monitoring of the dis/appearance of the protein bands were used.

Other widely used tools for ROS detection are fluorescent probes. They are used to detect localized production of ROS *in vivo* (Sedlářová and Luhová, 2017). For example, staining with 5-(and −6)-carboxy-2′, 7′-dichlorodihydrofluorescein diacetate can be used to assess the amount of H_2O_2, $OH^{\bullet}$, or $ROO^{\bullet}$ in a sample or with dihydroethidium to detect superoxide anion radical ($^1O_2^{\bullet-}$) molecules (Katerji et al., 2019). Trotti et al. evaluated a quite new spectrophotometric assay d-ROMs (diacron reactive oxygen metabolites) test to measure derivatives of reactive oxygen metabolites, specifically hydroperoxides in serum (Trotti et al., 2002). Biological characteristics of the studied material that should be taken into account and handling factors that influence the results of histochemical staining with fluorochromes are discussed in the review by Sedlářová and Luhová (Sedlářová and Luhová, 2017). However, not only permeable fluorescent dyes can be used for localization of

ROS production. Carmona et al. monitored physiological H_2O_2 fluctuations in fission yeast cells using a genetically encoded peroxiredoxin-based probe roGFP2-Tpx1.C169S (Carmona et al., 2019).

These examples show the selection of methods for ROS detection. In the cases, when not the primary ROS are to be analyzed but the consequence of their reactions, it is appropriate to analyze oxidation products of biomolecules.

3.2. Oxidation products

ROS react with all organic components of biological matter; therefore, a wide variety of products can be formed during oxidation reactions. An oxidation extent in the sample can be evaluated according to distribution and quantity of specific products of an oxidative reaction (such as 8-oxo-7,8-dihydroguanine (Nakabeppu et al., 2017)) or typical chemical structures (such as carbonyls (Weber et al., 2015)). However, some methods for determining a selected oxidation marker are more specific than others. Therefore, also accuracy of the oxidation level can be more precise for some products and methods than for others.

As proteins are highly abundant and react rapidly with many oxidants, they are major targets of oxidative damage (Hawkins and Davies, 2019). To assess protein amino acid composition and their associated modifications, a sample goes through several preparation steps. The sample is separated by liquid chromatography (LC; e.g., high-performance liquid chromatography, HPLC, or ultra performance liquid chromatography), subsequent detection and quantification can be performed by UV–visible absorption, fluorescence, mass spectrometry (MS), or electrochemical detection. A schematic diagram of the whole process can be found in [(Hawkins and Davies, 2019), Fig 6. therein].

Other common targets for ROS attacks are lipids, as a substantial part of biological membranes. A number of mass spectrometric techniques have been used to analyze lipid oxidation products. Electron capture atmospheric pressure chemical ionization MS or gas chromatography (GC) MS can also be used to study lipid oxidation products (Yin and Porter, 2005). Ag^+ coordination ion spray MS is a powerful tool to analyze intact lipid peroxides (Yin and Porter, 2005). Long-time sample preparation is a common problem in a wide range of analytical methods. To eliminate this problem, HPLC coupled with electrospray ionization tandem MS (ESI-MS/MS) can be utilized for regioisomer-independent quantification of fatty acid oxidation products (Ahern et al., 1038). The advantages and disadvantages of various forms of MS and its combinations with other techniques are discussed in (Spickett and Pitt, 2015). Reis and Spickett highlighted the combination of MS with HPLC and they also presented nuclear magnetic resonance spectroscopy as a complementary method to MS (Reis and Spickett, 2012). Various methods for the detection of protein lipoxidation and summarization of a combination of strategies that can be employed for the chemical and structural characterization of vimentin lipoxidation and the assessment of the consequences of oxidation are discussed in (Aldini et al., 2015).

In the text below, selected oxidation products formed during reaction of ROS with biological matter (Fig. 3) and possible methods of their detection are discussed.

3.2.1. Carbonyls

Oxidative stress induces carbonylation of biomolecules such as lipids, proteins, and nucleic acids, see Fig. 3. Out of these three, the protein carbonyl detection methods are the most widespread. Not only do proteins have a higher occurrence in cells than other biomolecules, but protein carbonyls can also be formed from lipid or sugar oxidation products (see Fig. 1 in (Weber et al., 2015)). A broad spectrum of chemical probes can be used for the analysis of carbonylated proteins. One of the ordinarily used probes is 2,4-dinitrophenylhydrazine (DNPH), in which case DNPH-modification of protein carbonyls could be detected by spectrophotometric measurements, gel-based or HPLC-based analysis, immunofluorescent imaging, or enzyme-linked immunosorbent assay (ELISA) measurement (Weber et al., 2015; Yan and Forster, 2011). Their advantages, pitfalls, sensitivity, and linearity are compared in (Rogowska-Wrzesinska et al., 2014). Commercial kits are also available. Lysis buffer components can potentially affect the oxidation state of the sample, see (Rogowska-Wrzesinska et al., 2014). Therefore, several methods improving the standard DNPH assay (Mesquita et al., 2014; Georgiou et al., 2018) or using different fluorescent hydrazides (Bodipy, Cy3, and Cy5 hydrazides) (Tamarit et al., 2012) have been published. Other probes that can be used are tritiated sodium borohydride ([3H]NaBH4), biotin probes (biotin-hydrazide, N′-aminooxymethylcarbonylhydrazino-D-biotin), [14C]iodoacetamide or various fluorescence probes (fluorescein-5-thiosemicarbazide, Alexa 488 fluorescence hydroxylamine, N-aminoperylene-3,4,9,10-tetracarboxylic-bisimides, near infrared fluorescence probes) (Yan and Forster, 2011; Yan and Sohal, 2000). A comparison of these protein

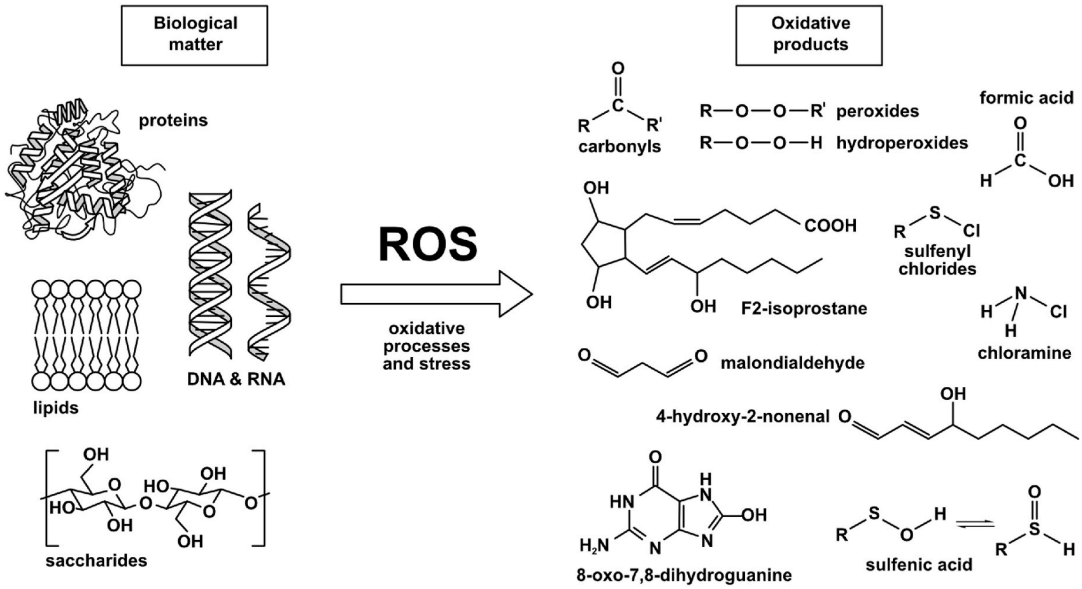

Fig. 3. Oxidation products formed during oxidative processes and oxidative stress in an organisms.

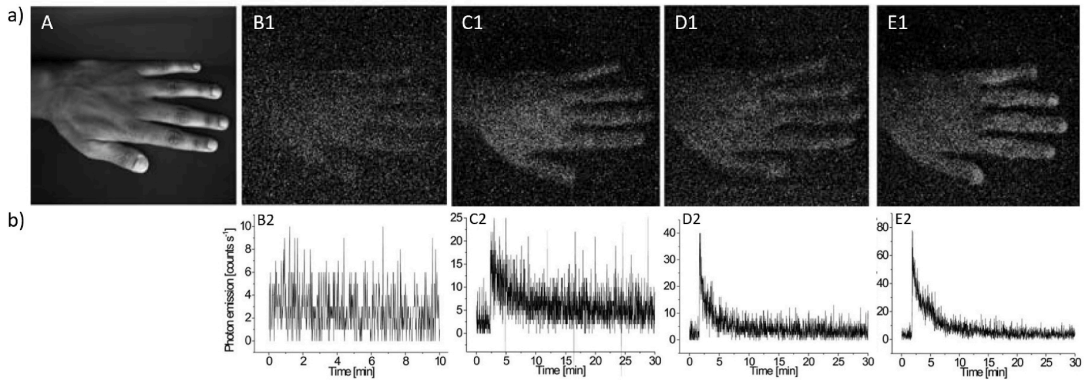

Fig. 4. Amplifying effect of various ROS types on BAL intensity of the hand dorsal side measured by a) CCD camera (30 min integration time) and b) PMT. A) The photograph of the dorsal side of the hand, B) its spontaneous BAL, and BAL induced by C) superoxide anion radical (25 mM xanthine + 0.05 U ml^{-1} xanthine oxidase], D) hydrogen peroxide (50 mM), and E) hydroxyl radical (50 mM H_2O_2 + 10 mM $FeSO_4$). The figure is reproduced from (Prasad and Pospišil, 2011) with the permission.

carbonyl probes is provided in (Yan and Forster, 2011). From an analytical method's point of view, spectrophotometric assays, HPLC, GC, fluorescent methods, radioactive labelling, immunoassays (ELISA, Western blot), (gel-)electrophoresis, or MS can be used for the protein carbonyls assessment (Purdel et al., 2014).

3.2.2. Peroxides, hydroperoxides, isoprostanes

Hydroperoxides (ROOH) are major products of protein and lipid damage in the presence of O_2. Various methods have been developed to assess lipid peroxidation. One of most common methods is the direct measurement of UV absorption at 234 nm, the characteristic wavelength for conjugated dienes in lipid hydroperoxides (Abuja and Albertini, 2001; Yin and Porter, 2005). However, a strong limitation of this method is the UV absorption of other compounds in the sample at similar wavelengths. The addition of an another substance to the oxidized sample can shift the measured absorbance wavelength to assess hydroperoxides. For example, hydroperoxide quantification can be done by iodometric titration (absorbance measurement at 358 nm) (Jessup et al., 1994), the ferrous oxidation of xylenol orange (FOX) assay (absorbance measurement at 560 nm) (Gay and Gebicki, 2003), or by boronic acid probes (a fluorometric assay for real-time analysis) (Michalski et al., 2014). Quantitative and qualitative analysis of lipid hydroperoxides can be also done using an assay based on HPLC and microperoxidase/isoluminol-dependent chemilumescence (Frei et al., 1988; Miyazawa et al., 1994).

Isoprostanes are prostaglandin-like endoperoxides formed *in vivo* during peroxidation of arachidonic acid (Fam and Morrow, 2003). The most common products of this reaction are F_2-isoprostenes containing an F-type prostane ring. Other classes of isoprostanes formed during the isoprostane pathway are D_2/E_2-isoprostanes, A_2/J_2-isoprostanes, isothromboxanes, and isoketals. Isoporostane-like compounds can also be formed from other polyunsaturated fatty acids, for example, neuroprostanes from docosahexaenoic acid. F_2-isoprostanes can be measured by GC/negative ion chemical ionization MS assay, other methods employing GC/MS or LC/MS, or by immunoassays (Fam and Morrow, 2003). Other classes of isoprostanes and neuroprostanes can also be measured by similar GC/MS assays.

3.2.3. Malondialdehyde and 4-hydroxy-2-nonenal

Malondialdehyde (MDA) is a low-molecular-weight end product of radical-induced decomposition of polyunsaturated fatty acids. At low pH and elevated temperature, MDA readily reacts with 2-thiobarbituric acid (TBA) generating a fluorescent adduct (Janero, 1990). The produced thiobarbituric acid reactive substances (TBARS) can be measured by spectrophotometric methods (Celi, 2011). A formed pigment shows an absorption maximum at 532 nm and fluorescence emission at 553 nm (Yin and Porter, 2005). However, this method has several disadvantages such as non-specificity, non-reproducibility, or no quantitative relationship with lipid peroxidation (Celi, 2011). The TBARS assay detect not only MDA but also a wide range of other lipid peroxidation products (Griffiths et al., 2002). Moreover, results of this frequently used method for MDA level measurement differ according to the assay conditions, as demonstrated, for example, by experiments with cattle (Castillo et al., 2005, 2006; Bernabucci et al., 2002; Bouwstra et al., 2008). Colorimetry, luminometry, chemiluminescence, HPLC, or GC/MS are other possible methods for direct assessment of MDA level in a sample (Celi, 2011).

Another frequently studied product of phospholipid peroxidation is 4-hydroxy-2-nonenal (HNE) (Spickett and Pitt, 2015). HNE can form Schiff bases or Michael adducts with residues in proteins (Spickett, 2013). HNE adducts to protein can be immunodetected by ELISA and western blotting using polyclonal and monoclonal antibodies. To identify the protein and exact location and nature of the modifications, MS is usually used.

3.2.4. Chlor/bromamines, sulfenic acids, and related species

Hypohalous acids (HOCl and HOBr) react avidly with nucleophiles containing nitrogen or sulfur atoms (such as amines, amides, thiols, or thioethers) (Davies et al., 2008). Generated N-chloro and N-bromo species can be quantified by their UV absorption bands (~ 250 and 290 nm, respectively), usually accompanied with a probe such as 5-thio-2--nitrobenzoic acid (TNB) to avoid overlap with other species that could be present in a complex sample (Hawkins and Davies, 2019). However, the probe TNB is not specific for any particular species. Oxidation of TNB to the corresponding dimer (DTNB) also occurs with, e.g., peroxides, singlet oxygen, or ONOOH (peroxynitrous acid). Quantification is achieved by measurement of the TNB absorbance decrease (at 412 nm). Another detection method is iodometric titration, but it has low specificity, too. N-Chloro species can also be examined by LC/MS.

Major intermediates formed by oxidants with Cys residues and related species or during reaction of $RS^{\bullet}$ with $NO^{\bullet}$ or $NO_2^{\bullet}$ are sulfenic acids (RSOH), sulfenyl chlorides (RSCl), S-nitrosated (RSNO, S-nitrosylated), and S-nitrated ($RSNO_2$) species. Most of these species (except RSNO) react rapidly with other thiols (and other nucleophiles and oxidants) to give disulfides (RSSR), thiosulfinates (RS(O)SR), sulfinic (RS(O)OH) or sulfonic acid ($RS(O)_2OH$) (Hawkins and Davies, 2019) and Fig. 3. Sulfenic acid group within proteins (RS(OH)) can be detected directly by X-ray crystallography, nuclear magnetic resonance spectroscopy, or MS. Because of several limitations of these direct methods, chemical approaches are also used (Furdui and Poole, 2014). The

detection of RSOH usually relies on chemical derivatization or trapping methods (Hawkins and Davies, 2019). Various nucleophilic and electrophilic probes (such as dimedone, benzylamide, or NBD chloride) can also be used (Furdui and Poole, 2014; Gupta et al., 2016).

3.2.5. DNA/RNA oxidative damage

Because nucleic acids are essential for life of all known organisms, the damage of these molecules can have far-reaching and substantial negative consequences in an organism. Therefore, monitoring of DNA/RNA oxidative damage (e.g., through their oxidative products) is an important part of the research focused on oxidative stress. Optimization of DNA/RNA extraction and the use of HPLC coupled to electrochemical detection or associated with (electrospray-ionization) tandem MS or GC/MS allow the measurement of oxidative damage to DNA/RNA and reveal several modified nucleosides and bases (Cadet, 2003; Ravanat et al., 2002; Halliwell and Dizdaroglu, 1992; McKinlay et al., 2144). Several examples of free-radical-induced products of pyrimidines and purines in DNA are shown in Fig. 11 in (Dizdaroglu, 1991). Because guanine exhibits the lowest ionization potential among nucleic acid components, it is the preferential target of one-electron oxidizing agents (Cadet, 2003). One of the major DNA/RNA base modifications is 8-oxo-7,8-dihydroguanine (Collins et al., 1996; Wurtmann and Wolin, 2009). However, 8-oxo-7,8-dihydroguanine is the major form in neutral solutions (Nakabeppu et al., 2017). Opening of the imidazole ring of 8-oxo-7,8-dihydroguanine, followed by one-electron reduction and protonation, gives another product of guanine 2,6-diamino-4-hydroxy-5-formamidopyrimidine (FapyGua) (Halliwell and Dizdaroglu, 1992). To assess low levels of oxidative DNA damage, an alternative method involving base excision DNA repair enzymes can be used. Bacterial formamidopyrimidine DNA N-glycosylase and endonuclease III cleave oxidized DNA at the sites of modified purine and pyrimidine bases, respectively. The extent of the DNA nicks is subsequently determined using sensitive methods, e.g., the (modified) comet assay (Collins et al., 1996) or the alkaline unwinding technique (Hartwig, 1996). To assess oxidative damage to DNA/RNA, it is also possible to use monoclonal antibodies. For example, antibodies 1F7 and 15A3 have been developed and characterized by competitive ELISA for quantification of DNA-derived 8-hydroxydeoxyguanosine as well as RNA-derived 8-hydroxyguanosine, markers of nucleid acids oxidative damage (Yin et al., 1995; Nunomura et al., 1999). ROS react mostly with the bases; however, a small amount also react with the sugar part leading to the release of intact bases, to alterations of the sugar part or to strand breaks (Dizdaroglu, 1991). Several examples of hydroxyl-radical-induced products of the sugar part in DNA are shown in Fig. 14 in (Dizdaroglu, 1991).

3.2.6. Carbohydrate oxidation

Carbohydrates are a common energy source; therefore, their oxidation is a widely researched topic. In organisms, carbohydrate oxidations usually lead to specific products because of specific enzyme catalyzation (carbohydrate oxidases) (Dickens, 1936; Savino and Fraaije, 2021). On the other side, chemical industry tries to find out proper substrates and catalysts to produce organic acids and furan compounds via catalytic oxidation reactions (Zhang and Huber, 2018). Generally, in the industrial chemistry, catalytic oxidation of carbohydrates or carbohydrate derivatives can form a wide spectrum of compounds including formic acid, acetic acid, glycolic acid, gluconic acid, glucaric acid, malonic acid, oxalic acid, 2,5-diformylfuran, 5-hydroxymethyl-2-furancarboxylic acid, 5-formyl-2-furancarboxylic acid, and 2,5-furandicarboxylic acid (Zhang and Huber, 2018). Other examples of carbohydrate oxidation products can be found in the classic review (Guthrie, 1962). Guthrie discussed products from monosaccharides, oligosaccharides, and also polysaccharides formed after their periodate (IO_4) oxidation. Oxidation also breaks the asymmetry of the sugar molecule, thus oxidation of the same derivative of several different sugars may lead to the same oxidation products (e.g. oxidation of any methyl-α-D-pentopyranoside yields in the same product) (Guthrie, 1962).

A wide variety of oxidation products of carbohydrates brings also a wide variety of the detection methods. For example, one of typical products of saccharide oxidation is formic acid. Its free from can be determined using acido-basic methods and both the free and bound (as a formyl derivative) forms can be determined using iodometric, or potentiometric titration, spectrophotometry (Babor et al., 1973; Meile et al., 2014), or gravimetric methods (Fedoroňko et al., 1973). HPLC and GC/MS were used to quantify advanced glycation products, such as pentosidine (Sell and Monnier, 1989) and carboxymethyllysine (Ahmed et al., 1986). Irreversible advanced glycation of proteins participates in the ageing process and it is amplified in diabetes (Miyata et al., 2000). The levels of pentosidine, carboxymethyllysine, and MDA-lysine in plasma proteins of hemodialysis patients are even higher than in diabetic subjects without uremia (Miyata et al., 1998; Shinzatovan Yperselede Strihou, 1996). Lagercrantz used EPR to observed production of anion radicals of semidone type during oxidation of aqueous alkaline solution of α-hydroxyketones with low oxygen concentration (Lagercrantz, 1964). Šimkovic et al. demonstrated that alkaline oxidative degradation of various saccharides (monosaccharides, microcrystalline cellulose, starch, and (4-O-methylglucurono)xylan) gives the same aromatic semidone radical 2,5-dihydro-p-benzosemiquinone using EPR spectroscopy and quantum chemical calculations (Šimkovic et al., 1983).

3.3. Intermediate reversible metabolites; NADH, NADPH

Nicotinamide adenine dinucleotide (NAD^+/NADH) and its phosphorylated form ($NADP^+$/NADPH) play important roles in fundamental cell processes. They are involved in cellular metabolism, signaling pathways, and regulatory processes, such as reductive biosyntheses, detoxification, immune defense, or gene regulation (Agledal et al., 2010). They also have a strong impact on redox biology. NADPH participates in the function of three antioxidant enzymes (peroxiredoxins, glutathione peroxidase, catalase) (Veskoukis et al., 2018). Thus, cellular levels of NADH or NADPH are strictly controlled in organisms. NADPH and related redox biomarkers (NADH, NAD + kinase, NADPH oxidase, peroxirodoxin, thioredoxin, thioredoxin reductase, nitrogen monoxide synthase) can be assessed spectrophotometrically in blood and tissue (Veskoukis et al., 2018). Reduced forms NADH/NADPH exhibit light absorption at 340 ± 30 nm (peak half-width) and fluorescent emission at 460 ± 50 nm (Blacker et al., 1038) with maximum intensity at 447 nm that corresponding with NADH in mitochondria (Eng et al., 1989). In contrast, their oxidized forms (NAD^+/$NADP^+$) do not absorb or fluoresce significantly at these wavelengths (Eng et al., 1989) – a fact which can be conveniently used for their detection. However, disadvantages of this spectrophotometric method is low sensitivity and high interference. Therefore, various substances are added to the sample to obtain required specificity via selective binding. For example, thiazolyl blue tetrazolium bromide (MTT) can be added to the sample based on the protocol of Wagner and Scott (1994). Then an absorbance change is monitored at 570 nm, at which the product of MTT reduction (formazan) exhibits an absorbance maximum. Assays for other related redox biomarkers can be found in Table 1 in Veskoukis's review (Veskoukis et al., 2018). It is also possible to enhance NADPH fluorescence, e.g., by using metagenome-derived blue fluorescent protein (You et al., 2019). Other methods available for NADH/NADPH measurement are enzymatic oxidation, enzyme-coupled cycling reactions, metabolite analysis by LC, and MS (Vidugiriene, 2013). NADPH and NADH fluorescence in living cells can be distinguished by fluorescence lifetime imaging (Blacker et al., 1038). It is also possible to monitor cellular NADH/NADPH dynamics by genetically encoded fluorescent sensors (Tao et al., 2017; Cameron et al., 2016; Bilan et al., 2014; Zhao et al., 2016).

Besides NAD^+ and $NADP^+$, flavin adenine dinucleotide (FAD), flavin mononucleotide (FMN), or coenzyme Q (CoQ) are other organic cofactors that participate in redox reactions and can provide useful

information about the oxidative state of a sample. They can be detected similarly as $NAD(P)^+$. For example, free FAD in buffer excited at 450 nm emits around 528 nm, with a slight blue shift in protein environment (Chorvat and Chorvatova, 2006), as well as in the presence of 80% (by volume) of glycerol (Heikal, 2010).

3.4. Antioxidants

The antioxidant status of a biological sample is an important indicator of oxidative stress. There are three main methods for the assessment of the total antioxidant activity (the sum of the contributions of all antioxidants present in a biological samples) in biological samples (Abuja and Albertini, 2001). The first one is called the total peroxyl radical-trapping potential (TRAP) method and it is based on introducing free radicals to the sample and determining the time at which all available antioxidants are consumed by these radicals. Radicals are typically produced e.g. from thermal decomposition of 2,2′-diazobis (2-amidinopropane)dihydrochloride (AAPH) (Valkonen and Kuusi, 1997) or 2,2′-azo-bis(2-amidinopropane) (ABAP) (Desmarchelier et al., 1997) and oxidizable molecular probes (such as dichlorofluorescein, DCFH) are used to detect and quantify oxidation (Karadag et al., 2009). In the second method, the trolox equivalent antioxidant capacity (TEAC) test, the radical cations $ABTS^+$ (2,2′-azinobis(3-ethylbenzothiazoline 6-sulfonate)) are used, comparing the efficiency to a reference trolox C (Abuja and Albertini, 2001). In another assay, FRAP (fluorescence recovery after photobleaching), ferric ion in a complex with tripyridiltriazine is reduced to a colored ferrous complex by sample antioxidants (Abuja and Albertini, 2001). The third main method, oxygen radical absorbance capacity (ORAC), employs measurement of the oxidative loss of the intrinsic fluorescence of B- or R-phycoerythrin (Abuja and Albertini, 2001). Antioxidant activity can also be measured indirectly by cyclic voltammetry, which enables the measurement of the overall concentration of reductants because the majority of low molecular weight antioxidants are reducing agents (Abuja and Albertini, 2001).

Glutathione (GSH), a cellular antioxidant present intracellularly and in human plasma, is oxidized to its disulfide (GSSG) (Deponte, 2013). Reverse reaction (from GSSG back to the GSH form) is mediated by GSH reductase using NADPH as a cofactor. Determination of the GSH/GSSG ratio can serve as an oxidation stress indicator. To prevent GSH autooxidation during sample processing, samples are usually treated with N-ethylmaleimide, other options include 2-vinylpyridine or iodoacetic acid (Asensi et al., 1999). Then, GSSG can be determined by HPLC. A modification of the glutathione S-transferase method of Brigelius (Asensi et al., 1999; Brigelius et al., 1983) can be used for GSH measurement. The adduct S-(2,4-dinitrophenyl)glutathione formed during reaction of 1-chloro-2,4-dinitrobenzene with GSH catalyzed by glutathione S-trasferase has an absorbance maximum at 340 nm (Asensi et al., 1999). The GSH concentration can also be determined via the consumption of NADPH during the reverse reaction mediated by GSH reductase (Deponte, 2013). The reverse reaction can also be used to determine levels of GSH and the total of GSH and GSSG spectrophotometrically; then, the GSSG level is the difference between these two values (Hawkins and Davies, 2019). Genetically encoded probes, such as roGFP fused to glutaredoxin, are another way to determine GSSG concentration. It is also possible to determine GSH and GSSG simultaneously by capillary electrophoresis (Muscari et al., 1998). Additionally, the ratio of another antioxidant, ascorbate and its two-electron oxidation product dehydroascorbate could also serve as an oxidative status indicator (Lykkesfeldt et al., 1997; Sinha et al., 2014). Levels of antioxidants retinoids and carotenoids (pro/vitamin A) can be measured by atmospheric pressure chemical ionization (APCI) LC/MS or reverse-phase HPLC (Katerji et al., 2019). To assess the level of α-tocopherol (vitamin E), there are several methods based on the reduction of Fe^{3+} to Fe^{2+} ions by α-tocopherol (Emmerie and Engel, 1938; Hashim and Schuttringer, 1966; Hidiroglou et al., 1989; Desai, 1984; Nirmala and Narendhirakannan, 2011). Vitamin E level can also be analyzed by GC/MS (Picardo et al., 1996; Grammatico et al., 1998) or by reverse-phase HPLC (Miller et al., 1984; Taibi and Nicotra, 2002).

The level of sample oxidation can also be assessed by measuring the antioxidant enzyme activity, such as that of superoxide dismutase (SOD), catalase, peroxidases, glutathione reductase, or glutathione S-transferase (Sinha et al., 2014). A different protocol is used to determine the activity of the different enzymes. For example, SOD activity is indirectly determined by measuring the inhibition of nitroblue tetrazolium reduction (reduction is caused by $^1O_2^{\bullet}$) at 560 nm (Beauchamp and Fridovich, 1971) and catalase activity is determined by monitoring the rate of decomposition of H_2O_2 at 240 nm (Aebi, 1984).

3.5. Physical, chemical, and biological parameters correlated with oxidative stress

In this section, we briefly discuss the parameters that correlate with oxidative stress. For example, Tiwari et al. studied the influence of oxidative stress caused by a mixture of glucose and glucose oxidase (producing H_2O_2) on mitochondrial functions and properties in non-photosynthetic *Arabidopsis* cells (Tiwari et al., 2002). They observed that mitochondrial electron transport was increased by oxidative stress, resulting in H_2O_2 generation amplification, ATP depletion, and cell death. Amplified H_2O_2 production also led to opening of the mitochondrial permeability transition pores and the release of cytochrome *c* from mitochondria (Tiwari et al., 2002). The mitochondrial permeability transition was assessed by measuring the mitochondrial swelling via a decrease in the absorbance at 546 nm. Electron transport and oxygen consumption in oxidatively stressed mitochondria were measured using a Clark type oxygen electrode. Evan's blue was used to quantify cell viability. De la Haba et al. analyzed plasma membrane fluidity after cell oxidation with H_2O_2 by two-photon microscopy (in combination with the environment-sensitive probe Laurdan) (de la Haba et al., 2013). They demonstrated that oxidative stress increases membrane rigidity. Benderitter et al. studied the influence of ionizing (γ) radiation on the human erythrocyte membrane (Benderitter et al., 2003). Besides other things, they found that the fatty acid pattern changed (increased content of saturated fatty acids) using GC. Furthermore, they found by fluorescence anisotropy that the membrane fluidity increased but the lipid-protein interface became more rigid. Schlenker et al. elicited oxidative stress in HTC rat hepatome cells by H_2O_2 or by combination of D-alanine with D-amino acid oxidase (Schlenker et al., 2000). Subsequently, they evaluated changes in a relative cell volume from a video recording of single cells under a microscope or the cell volume was measured electronically by a Coulter Multisizer for cells in suspension. To determine membrane cation permeability, they measured whole-cell currents using patch clamp recording techniques. As the consequence of the oxidative stress, they found rapid decrease of cell volume followed by an 100-fold increase in membrane cation permeability and then partial volume recovery. Munna et al. determined the effects of oxidative stress caused by H_2O_2 on a culture of *Escherichia coli* (Munna, 2013). They observed lowered cell viability, growth, and culturability. Concentrations of cell samples were established by measuring the absorbance at 600 nm. Cell morphology and arrangement of colonies were evaluated after staining under a light microscope. Bi et al. showed significant increase in water channel protein aquaporin 4 expression after H_2O_2 treatment of primary astrocyte cultures through immunoblotting (Bi et al., 2017). Oxidative stress also elicits a genetic response that leads to a significant increase in the cellular resistance to oxidative agents (Cabiscol Català et al., 2000). Therefore, oxidative stress response can also be assessed by examining the changes in transcriptome and proteome (Jamnik and Raspor, 2005). The above examples show that there is plenty of parameters that correlate with oxidative stress; as a consequence, there is also a wide range of methods that can be used to analyze them.

4. Biological autoluminescence: method and correlations

BAL is a weak optical radiation (typically < 1000 photons $\cdot$ cm^{-2} $\cdot$ s^{-1} in the 350–1270 nm range) released during biological and biochemical processes that involve oxidation. Therefore, the physical nature of BAL detection is the detection of weak light. The requirement for this type of detection is a sufficiently sensitive light detector for collecting the light from the biosample and that the probed biosample is located at a place with no light background.

Here we list the operational characteristics of BAL, which together make the method unique.

1. label-free: no input of external chemical probes to the sample is needed to observe BAL.
2. non-invasive: no mechanical contact of the biosample with the probe, no external light or other physical stimuli are required. This is in contrast with all other methods, where the biosample is either destroyed during the analysis (e.g. mass spectroscopy), or where a probe of a physical detector has to be in contact with the sample (e.g., some electrochemical methods), or has to send some form of energy to perturb the sample in order to analyze it (e.g. electrochemical, fluorescence and light absorbance methods). That also means that the sample analyzed for its BAL is reusable for further analysis.
3. real-time: the detection of BAL can be performed in real-time during the sample treatment and handling, therefore allowing for the detection of the dynamic response of the sample in normal, physiological conditions or undergoing oxidative treatment or stress.
4. low operation complexity and operation costs: the simplest setups for the detection of BAL require only a light-tight enclosure and an appropriately sensitive photodetector with a PC interface. The samples must be handled in low light conditions. No further consumables are needed.
5. scalable: larger sample provides higher signal

The drawback of BAL is a lack of specificity. The specificity can be increased when optical spectra and other signal parameters are analyzed. For example particular BAL emitters have their own optical spectra, which could be potentially used to assess particular processes or species (Nerudová et al., 2015). Anyway, to employ BAL as a marker for a particular process or chemical species, a standard analytical method has to be used to establish a correlation of BAL with that process or species for expected operating conditions in a particular sample type. Then, BAL can serve as a convenient method for monitoring any changes of oxidation processes in real-time.

BAL can be detected by photomultiplier tubes (PMT), see [(Fels et al., 2015) 187, Ch. 3] for details. They have very low noise per unit area of sensitive surface (photocathode), high gain (10^5–10^7), and reasonable quantum efficiency (ratio of the number of the detected photocounts to the number of the impinging photons) of photon detection ($\sim$ 15–40% at peak sensitivity) (Cifra and Pospíšil, 2014). Their time resolution is up to a few nanoseconds. Imaging of BAL can be performed by charge-coupled device (CCD) cameras (Kobayashi, 2014). However, the time resolution of a CCD camera is quite low (in the order of minutes) for BAL measurement. To decrease the noise, detectors are often cooled, but cooling might also decrease the detection sensitivity in the red region of the spectrum.

For quantitative assessment of the actually generated and emitted number of photons, one needs to consider the technical and physical optical aspects, which we briefly discuss here. The detected number of BAL photons is always lower than the actually generated number of molecular electronically excited states and emitted photons. On the molecular level, the main reason is that the emission of photons from the excited state is only one of the processes that competes for the excited state energy (Turro, 2004). The excited state of a molecule can also chemically react (not producing photon) or the excited state energy can be released non-radiatively (i.e. without emission of a photon) through molecular vibrations to heat. Excited state energy can also be transferred to other molecules (acceptors), which can then emit the energy in the form of a photon, use the energy to react chemically, or dissipate energy vibrationally (to heat), as in the case of the original excited state. In any case, once the photon is emitted, it can also be absorbed by molecules contained in the matter through which it has to travel to the photodetector. Therefore, even if the detector detection efficiency in terms of the collection angle and quantum efficiency is taken into account, the number of detected photons will be lower than the number of photons actually emitted by the original molecular emitters. This self-absorption in the biosample is of particular concern in opaque and pigment-rich samples, but not as much in small volumes and transparent samples, which also includes single layer (adherent) cell cultures.

To unleash the full potential of BAL measurement as an effective monitoring and diagnostic tool, it is essential to clarify the mechanisms which underlie BAL in particular samples: exact sources (reaction pathways and final emitters) of BAL, agents and other parameters influencing the BAL intensity, time dependence, and spectral distribution. Below we review the major correlations between various agents and BAL analyzed so far. Summary of these correlations with BAL and the corresponding references, sorted according a complexity of a studied system to '$<$ cell' (biomolecules, organelles, and other biosamples less complex than a cell) and 'cell+' (cell and more complex samples), are summarized in Table 2. We propose that the molecular species and processes, which correlate with BAL parameters (mostly intensity), can be monitored by BAL when all other conditions are the same in the biosystem or biosample under study.

4.1. BAL and ROS

Reactive oxygen species (ROS) are initiators, intermediates, and products of reactions leading to BAL. Therefore, increasing ROS production usually leads to an increase of the BAL intensity. This type of behavior in the case of increasing hydrogen peroxide concentration has been observed by many authors (Kageyama et al., 2006; Vahalová et al., 2021; Bereta et al., 2021; Salin and Bridges, 1981; Saeidfirozeh et al., 2018; Cheun et al., 2007; Rác et al., 2015; Rastogi and Pospíšil, 2010; Iida et al., 2002). Salin et al. observed a significant increase in the BAL intensity after the addition of hydrogen peroxide to wounded root soybean segments not only in aerobic but also in anaerobic conditions (Salin and Bridges, 1981). Wefers et al. distinguished two phases of emitted chemiluminescence associated with oxygen concentration, the first one (decrease of light emission to 4%) was dependent on exogenously added or endogenously generated hydrogen peroxide, whereas the second phase (decrease of BAL to 2.5%) did not require hydrogen peroxide (but an organic peroxy species) (Wefers et al., 1985). The types of emissive species formed during oxidative reactions in the samples exposed to hydrogen peroxide have also been studied (Rác et al., 2015; Rastogi and Pospíšil, 2010). For example, Iida et al. and Pathak et al. studied the contribution of superoxide anion radical to BAL (Pathak et al., 2017; Iida et al., 2002). Not only hydrogen peroxide can be an initiator of the BAL intensity changes. Prasad and Pospíšil compared amplifying effects of tree different types of ROS on BAL intensity of the dorsal side of the hand, see Fig. 4 (Prasad and Pospišil, 2011). However, the most inspected ROS is singlet oxygen. It has a really special role in BAL production. Singlet oxygen can be the initiator of an oxidative reaction, its intermediate product, and also the final product leading to the light emission. For example, a ROS molecule (singlet oxygen or another ROS) can react with a biomolecule leading to the creation of a hydroperoxide that subsequently decomposes to a singlet oxygen (Fig. 2. This new singlet oxygen can react with another nearby chemical substance or can release excess energy in the form of heat or light emission (BAL). Singlet oxygen formation during oxidative reactions in the samples exposed to hydrogen peroxide leading to BAL emission has been studied in (Rác et al., 2015; Rastogi and Pospíšil, 2010).

Table 2
References to BAL correlations with ROS generation by various ways or with specific ROS type (e.g. singlet oxygen), with antioxidants and other ROS/BAL modulators, with triplet excited carbonyls, and with chromophore-like compounds. The column '< cell' refers to works where the biochemical model systems or extracted organelles were used as the samples and the column 'cell +' refers to works at the level of isolated cells, cell cultures, or tissues.

Correlation	References (cell<)	References (cell+)
ROS & ROS formation agents		
redox enzymes		
horseradish peroxidase	(Sławińska and Sławiński, 1988; Wefers et al., 1985; Mano et al., 2014; Medeiros et al., 1987; Medeiros and Sies, 1989; Bastos et al., 2017; Dunford et al., 1984; Schulte-Herbruggen and Sies, 1989; Velosa et al., 2007; Cilento and Adam, 1988; Bechara et al., 1979; Cilento, 1984; Oliveira et al., 1978; Bohne et al., 1986; Bohne et al., 1986; Durán and Cilento, 1980; Soares and Bechara, 1982; de Medeiros and Bechara, 1986)	
lipoxygenase	Abeles (1986)	(Birtic et al., 2011; Prasad et al., 2016, 2017; Maccarrone et al., 1997, 1999; Prasad and Pospíšil, 2011; Boveris et al., 1980b)
cytochrome P450 monooxygenase		(Inagaki et al., 2007, 2009; Kato et al., 2014)
myeloperoxidase	(Andersen et al., 1977; Kiryu et al., 1999)	(Andersen et al., 1977; Klebanoff, 1980; Hampton et al., 1998)
other enzymes	(Abeles, 1986; Sławiński et al., 1981; Kanofsky, 1983, 2000; Prochaska et al., 1987; Wefers et al., 1984; Adam and Cilento, 1982)	(Allen, 1979; Kageyama et al., 2006; Tang and Dai, 2014)
Fenton reaction	(Shen et al., 1991; Khabiri et al., 2008)	(Birtic et al., 2011; Khabiri et al., 2008; Vahalová et al., 2021; Bereta et al., 2021)
other sources	(Cadenas et al., 1980; Lissi et al., 1994)	(Salin and Bridges, 1981; Saeidfirozeh et al., 2018; Cheun et al., 2007; Lloyd et al., 1979)
singlet oxygen (generating agents listed)		
hydroperoxides	(Miyamoto et al., 2003a; Pathak et al., 2017; Prado et al., 1111; Uemi et al., 2011; Di Mascio et al., 2016; Prado et al., 2009; Miyamoto et al., 2003b)	Prasad et al. (2016)
endoperoxides	(Di Mascio et al., 2016, 2019; Miyamoto et al., 2003b; Di Mascio and Sies, 1989; Uemi et al., 2009; Ronsein et al., 2011; Kazakov et al., 2007)	
dioxetanes	(Mano et al., 2014; Briviba et al., 1996)	
endogenous photosensitizers	(Pathak et al., 2017; Baier et al., 2006)	
exogenous photosensitizers	(Kochevar and Redmond, 2000; Hall and Chignell, 1987)	Kochevar and Redmond (2000)
excitation energy transfer from $^3R = O^*$	(Mano et al., 2014; Pathak et al., 2017)	Prasad et al. (2016)
horseradish peroxidase	(Wefers et al., 1985; Mano et al., 2014; Medeiros et al., 1987; Medeiros and Sies, 1989)	
lipoxygenase		(Prasad et al., 2016, 2017)
myeloperoxidase	Kiryu et al. (1999)	(Klebanoff, 1980; Hampton et al., 1998)
other enzymes	(Abeles, 1986; Kanofsky, 1983, 2000; Prochaska et al., 1987; Wefers et al., 1984; Adam and Cilento, 1982)	Allen (1979)
other sources	(Miyamoto et al., 2003b, 2009, 2012; Held et al., 1978; Di Mascio et al., 1994; Gupta et al., 2009; Cadet et al., 2009)	(Rác et al., 2015; Rastogi and Pospíšil, 2010)
superoxide anion radical	(Medeiros et al., 1987; Wefers et al., 1984; Pathak et al., 2017; Wefers and Sies, 1983; Iida et al., 2002)	(Hampton et al., 1998; Allen, 1979; Kageyama et al., 2006)
Antioxidants and other BAL modulators		
non-enzymatic antioxidants		
α-tocopherol	Kuzmenko et al. (1999)	(Maccarrone et al., 1997, 1998)
ascorbic acid	(Wefers et al., 1985; Lissi et al., 1994)	(Maccarrone et al., 1997, 1998; Vahalová et al., 2021; Salin and Bridges, 1981; Rastogi and Pospíšil, 2010; Č ervinková et al., 2015; Radotić et al., 1990)
mannitol	(Medeiros and Sies, 1989; Wefers et al., 1984; Hideg and Inaba, 1991; Torinuki and Miura, 1981)	(Maccarrone et al., 1997, 1998; Salin and Bridges, 1981; Č ervinková et al., 2015; Radotić et al., 1990)
glutathione	Wefers et al. (1985)	Červinková et al. (2015)
others	Kuzmenko et al. (1999)	Prasad et al. (2020a)
enzymatic antioxidants		
catalase	(Wefers et al., 1984, 1985; Iida et al., 2002; Hideg, 1993; Nakano et al., 1975)	(Birtic et al., 2011; Maccarrone et al., 1999; Allen, 1979; Salin and Bridges, 1981; Radotić et al., 1990)
superoxide dismutase	(Wefers et al., 1984, 1985; Medeiros et al., 1987; Medeiros and Sies, 1989; Iida et al., 2002; Hideg and Inaba, 1991; Torinuki and Miura, 1981; Hideg, 1993; Nakano et al., 1975)	(Allen, 1979; Salin and Bridges, 1981; Radotić et al., 1990; Prasad et al., 2020a; Hideg, 1993)
non-natural antioxidants & BAL quenchers		
sodium azide	(Prado et al., 2009; Hall and Chignell, 1987; Hideg, 1993; Hideg et al., 1991; Deneke and Krinsky, 1977; Albertini and Abuja, 1998)	Salin and Bridges (1981)
TEMPO		(Maccarrone et al., 1997, 1998)
trolox	Lissi et al. (1994)	(Maccarrone et al., 1997, 1998)
potassium cyanide	(Hideg and Inaba, 1991; Hideg, 1993; Hideg et al., 1991)	
antimycin A	(Hideg, 1993; Hideg et al., 1991)	
salicylhydroxamic acid	(Hideg and Inaba, 1991; Hideg, 1993; Hideg et al., 1991)	Kageyama et al. (2006)

(*continued on next page*)

Table 2 (*continued*)

Correlation	References (cell<)	References (cell+)
EDTA	Albertini and Abuja (1998)	Maccarrone et al. (1997)
Tiron		(Kageyama et al., 2006; Salin and Bridges, 1981; Kobayashi et al., 2006)
sorbate ions (for $^3R = O^*$)	(Bechara et al., 1979; Catalani et al., 1987; Timmins et al., 1997)	
others	(Hideg and Inaba, 1991; Albertini and Abuja, 1998)	(Kageyama et al., 2006; Salin and Bridges, 1981; Kataoka et al., 2001)
BAL enhancers		
D_2O	(Wefers et al., 1985; Medeiros and Sies, 1989; Prado et al., 2009; Hall and Chignell, 1987; Torinuki and Miura, 1981)	Salin and Bridges (1981)
DABCO	(Medeiros and Sies, 1989; Kazakov et al., 2007; Torinuki and Miura, 1981; Hideg, 1993; Hideg et al., 1991; Deneke and Krinsky, 1977)	
NAD(P)H	(Hideg and Inaba, 1991; Hideg, 1993; Hideg et al., 1991)	
chlorophyll *a*	(Medeiros and Sies, 1989; de Medeiros and Bechara, 1986)	
others	(Medeiros and Sies, 1989; Hideg et al., 1991; Deneke and Krinsky, 1977)	(Abeles, 1986; Maccarrone et al., 1997; Salin and Bridges, 1981)
Oxidation products		
carbonyls		
malondialdehyde	Noll et al. (1987)	(Havaux et al., 2006; Prasad et al., 2016)
variety of carbonyl species originally in excited state, see section BAL emitters lower		
hydroperoxides - see singlet oxygen subsection under ROS & ROS formation agents		
endoperoxides - see singlet oxygen subsection under ROS & ROS formation agents		
dioxetanes - see singlet oxygen subsection under ROS & ROS formation agents		
Electron excited species		
triplet excited carbonyls (generating agents listed)		
thermal decomposition of dioxetanes	(Mano et al., 2014; Bastos et al., 2017; Velosa et al., 2007; Cilento and Adam, 1988; Pathak et al., 2017; Catalani et al., 1987; Adam and Baader, 1985; White et al., 1974; Bechara and Wilson, 1980)	Cilento and Adam (1988)
HRP/O_2/IBAL	(Bastos et al., 2017; Dunford et al., 1984; Schulte-Herbruggen and Sies, 1989; Velosa et al., 2007; Cilento and Adam, 1988; Bechara et al., 1979; Cilento, 1984; Oliveira et al., 1978; Bohne et al., 1986; Durán and Cilento, 1980)	
HRP/O_2/other substrates	(Mano et al., 2014; Medeiros and Sies, 1989; Cilento and Adam, 1988; Bohne et al., 1986; Soares and Bechara, 1982; de Medeiros and Bechara, 1986)	
decomposition of tetroxide	(Pospíšil et al., 2019; Pathak et al., 2017)	
others	(Mendenhall et al., 1991; Niu and Mendenhall, 1992; Russell, 1957; Farneth and Johnson, 1984; Sharov et al., 1998; Schuh et al., 1984)	(Prasad et al., 2016; Rác et al., 2015; Escobar et al., 1990)
excited chromophores, dyes or other suitable energy acceptors		
energy transfer from $^3R = O^*$	(Bastos et al., 2017; Bechara et al., 1979; Cilento, 1984; Bohne et al., 1986; Durán and Cilento, 1980; Bechara and Wilson, 1980)	Prasad et al. (2016)
singlet oxygen - see above in ROS section		

Abbreviations used in the table.
$^3R = O^*$ = excited triplet carbonyls.
DABCO = 1,4-diazabicyclo[2.2.2]octane.
EDTA = 2,2′,2″,2‴-(Ethane-1,2-diyldinitrilo)tetraacetic acid.
HRP = horseradish peroxidase.
IBAL = isobutyraldehyde.
TEMPO = (2,2,6,6-tetramethylpiperidin-1-yl)oxyl.
Tiron = disodium 4,5-dihydroxy-1,3-benzenedisulfonate.
Trolox = water-soluble analog of α-tocopherol.

4.1.1. Formation of singlet oxygen

Singlet molecular oxygen can be formed in the sample in various ways. It can be chemically produced by the decomposition of lipids, proteins, or DNA hydroperoxides (Prasad et al., 2016; Miyamoto et al., 2003a; Pathak et al., 2017; Prado et al., 1111; Uemi et al., 2011; Di Mascio et al., 2016; Prado et al., 2009), endoperoxides (Di Mascio et al., 2016, 2019; Di Mascio and Sies, 1989; Uemi et al., 2009; Ronsein et al., 2011), or dioxetanes (Briviba et al., 1996). To study the nascent singlet oxygen, combination of various techniques have been used: from spectroscopic measurement of bimolecular and monomolecular decay or direct characterization of the near-infrared light emission (Prado et al., 1111; Uemi et al., 2011; Prado et al., 2009) to employing HPLC/MS (Uemi et al., 2011; Di Mascio et al., 2016; Prado et al., 2009) or EPR spin-trapping spectroscopy (Prasad et al., 2016).

Physical processes leading to singlet oxygen generation include photosensitization – photoexcitation of photosensitizers, compounds that absorb the energy of a visible or UV light photon to become an excited singlet state (Ronsein et al., 2011; Pantopoulos, 2011). This excited singlet photosensitizer is rapidly converted to an excited triplet state, which can transfer energy nonradiatively to molecular oxygen generating singlet oxygen. Porphyrins, flavins, or quinones belong to such endogenous photosensitizers (Pathak et al., 2017; Baier et al., 2006). Methylene blue and Rose Bengal are examples of exogenous photosensitizers (Kochevar and Redmond, 2000). However, photosensitization can occasionally take place in other way. It can lead to the formation of charged radicals derived from the photosensitizer or superoxide anion radical $O_2^{\bullet -}$ (Ronsein et al., 2011; Cadet et al., 2009). The excitation energy transfer to molecular oxygen (and subsequent formation of $^1O_2$) can also occur from excited triplet carbonyls, which can be also studied by BAL measurement (Mano et al., 2014; Prasad et al., 2016; Pathak et al., 2017).

Various enzymes (e.g., peroxidases (Kanofsky, 2000), myeloperoxidase (Kiryu et al., 1999; Klebanoff, 1980; Hampton et al., 1998), lactoperoxidase (Kanofsky, 1983)) also play an important role in singlet oxygen formation. Other chemical sources are reactions of hydrogen

peroxide with hypochlorite ClO^- (Kiryu et al., 1999; Hampton et al., 1998; Held et al., 1978), halides (Klebanoff, 1980; Kanofsky, 1983), or peroxynitrite $N(O)OO^-$ (Di Mascio et al., 1994). The measurement of monomol light emission at 1270 nm is typically used for detection of singlet oxygen generation during decomposition of peroxynitrate $N(O)_2OO^-$ and peroxynitrite $N(O)OO^-$ (Miyamoto et al., 2009; Gupta et al., 2009).

4.1.2. Redox enzymes and their role in ROS formation

As mentioned above, endogenous sources of singlet oxygen, or other ROS, are often enzymes. Several authors have analyzed the correlation between BAL intensity and oxidative processes catalyzed by various enzymes without a deep analysis of BAL origin. BAL can be generated by hydrogen peroxide and horseradish peroxidase (Sławińska and Sławiński, 1988) or the enzymatic oxidation of polyunsaturated fatty acids (such as linolenic acid) by lipoxygenase (Abeles, 1986; Birtic et al., 2011; Prasad et al., 2016; Maccarrone et al., 1997, 1999; Prasad and Pospíšil, 2011). Photon emission can probably be enhanced by cytochrome P450 monooxygenase, which plays an important role in the metabolic detoxification of sulfonylurea herbicides (Inagaki et al., 2007, 2009; Kato et al., 2014). The emission spectra of various enzymatic systems (such as lipoxygenase, myeloperoxidase, or cytochrome *c* with hydrogen peroxide) have also been studied (Abeles, 1986; Boveris et al., 1980b; Andersen et al., 1977; Sławiński et al., 1981).

The presence of various ROS, especially singlet oxygen, during BAL emission has also been widely researched. Singlet oxygen can be the product of reactions catalyzed by myeloperoxidase, xanthine oxidase, microsomal lipid oxidase, prostaglandin oxygenase, lipoxidase, aldehyde oxidase, galactose oxidase, dihydroorotate oxidase, NADPH-cytochrome reductase, or ferredoxin- and NADPH-reductase (Abeles, 1986; Adam and Cilento, 1982). Formation of singlet oxygen via enzymatic lipid peroxidation initiated by lipoxygenase was discussed in depth by (Prasad et al., 2016, 2017). The light emission attributed to singlet oxygen de-excitation as a result of oxidation of reduced glutathione (Wefers et al., 1985; Medeiros et al., 1987) or ribose in the presence of hydrogen peroxide (Medeiros and Sies, 1989) catalyzed by horseradish peroxidese was also observed. The role of NAD(P)H:quinone oxidoreductase in generation of BAL, probably involving singlet oxygen light emission, has also been studied (Prochaska et al., 1987; Wefers et al., 1984). Dicoumarol, as an inhibitor of the NAD(P)H:quinone reductase, led to an increase of BAL, whereas elevation of the enzyme activity by 2(3)-tertbutyl-4-hydroxyanisole reduced the menadione-dependent chemiluminescence. Formation of singlet oxygen and BAL were also observed during activation of NADPH oxidase (NADPH:O_2 oxidoreductase) during the acute inflammatory response of phagocytes (Abeles, 1986; Allen, 1979). However, other ROS, such as superoxide anion $O_2^{\bullet-}$, hydroxyl radical $HO^{\bullet}$, hydrogen peroxide, or hypochlorite OCl^-, can also be produced during the reactions catalyzed by this enzyme.

Medeiros et al. reported the involvement of superoxide anion radicals in the production of photoemissive species during the oxidation of reduced glutathion by horseradish peroxidase (Medeiros et al., 1987). Wefers et al. used superoxide dismutase to demonstrate the involvement of superoxide anion radicals in reactions that are responsible for the second phase of BAL in microsomal suspensions supplemented with 1-naphthol in the presence of NADPH (Wefers et al., 1984). Reaction of xanthine, hypoxanthine, or acetaldehyde with xanthine oxidase also leads to formation of superoxide radical and, therefore, to enhancement of BAL (Abeles, 1986; Kageyama et al., 2006; Wefers and Sies, 1983; Iida et al., 2002). Bohne et al. (1986) observed that oxidation of several catechols (benzene-1,2-diol) (e.g., 4-tert-butylcatechol) by catechol oxidase leads to the generation of o-quinone in an electronically excited state.

In the above-mentioned studies, various enzymes inhibitors were often used to reveal details about the ROS/BAL generation mechanisms specific for the studied sample. For example, catechol and caffeic acid (Prasad et al., 2016, 2017; Prasad and Pospíšil, 2011), or salicylhydroxamic acid (Abeles, 1986) were used to inhibit lipoxygenase, piperonyl butoxide and malathion for cytochrome P450 monooxygenase (Inagaki et al., 2007, 2009; Kato et al., 2014), diphenylene iodonium for NADPH oxidase (Kageyama et al., 2006), or dicoumarol to inhibit NAD(P)H: quinone reductase (Prochaska et al., 1987; Wefers et al., 1984).

Because mitochondria are considered as the major source of ROS in mamalian cells (Balaban et al., 2005; Starkov, 2008), the influence of different parts of the mitochondrial electron transport chain (usually affected by addition of various enzyme inhibitors or other compounds) on BAL signal was also studied (Cadenas et al., 1980; Lloyd et al., 1979). For example, cytochrome *c* oxidase inhibitor sodium azide partly prevented the BAL activity (Tang and Dai, 2014). Cadenas et al. observed that externally added cytochrom *c* considerably increased the light emission and oxygen consumption of antimycin-inhibited bovine heart submitochondrial particles (Cadenas et al., 1980). Miyamoto et al. reported that the interaction of cytochrome *c* with cardiolipin leads to singlet oxygen generation, which was monitored by luminescence measurements at 1270 nm (Miyamoto et al., 2012). Similar to the hemeprotein cytochrome *c*, BAL has been also observed during the oxidation of other hemeproteins such as hemoglobin and methemoglobin by hydrogen peroxide (Lissi et al., 1994).

4.1.3. Cations of transition metals and their role in ROS formation

As mentioned above, ROS can be produced in reactions catalyzed by various enzymes. Cations of transition metals usually play an essential role in the catalytic sites of enzymes, such as iron in horseradish peroxidase (HRP; in heme form) or lipoxygenase. Free metal ions are also crucial in redox reactions as they are redox active. An often used chemical source of ROS is so-called Fenton reaction, which is initiated by the reaction of hydrogen peroxide with ferrous (Fe^{2+}) iron leading to the generation of very reactive hydroxyl radical. During secondary reactions, $HO_2^{\bullet}$, H_2O_2, $^1O_2$, $O_2^{\bullet-}$, or $CO_3^{\bullet-}$ are also created with various reaction constants and yields (Ivanova et al., 2012). For example, the Fenton reaction was employed to induce lipid oxidation in *Arabidopsis* plants (Birtic et al., 2011) or to initiate peroxidation of linoleic acid (Shen et al., 1991), leading to BAL that was primarily attributed to the dimolar emission of singlet oxygen. Khabiri et al. analyzed the BAL intensity of protein/amino acid solutions oxidized as well as porcine skin by H_2O_2 in the presence of Fe^{2+} by sensitive PMT (Khabiri et al., 2008). As complementary methods, they measured an increase in the amount of carbonyls in protein and used MS analysis of oxidation products of amino acids. Authors interpreted their data as that BAL produced by oxidation-stressed skin was mainly due to photon emission of tryptophan or its oxidation products, whereby tryptophan (or its oxidation product) acts as an energy acceptor from other excited species of oxidation-modified amino acids. *In vivo*, Lissi et al. observed BAL during irreversible deactivation of hemoglobin, methemoglobin, or hemin with excess of hydrogen peroxide (Lissi et al., 1994).

4.2. Antioxidants and other modulators of BAL

Many works have been performed to demonstrate the relation between BAL and the addition or presence of antioxidants. Typically, the BAL intensity is decreased in the presence of antioxidants. The reason is that antioxidants deactivate ROS, preventing the attack of biomolecules that initiates the reaction chain leading to BAL (see the scheme in Fig. 2). Substances with antioxidative effects can be categorized to natural and non-natural (prepared by chemical synthesis) ones. Natural antioxidants are typically divided into two classes: enzymatic and non-enzymatic.

Most widely studied non-enzymatic antioxidants are α-tocopherol (vitamin E) (Maccarrone et al., 1997, 1998; Kuzmenko et al., 1999), ascorbic acid (ascorbates, vitamin C) (Wefers et al., 1985; Maccarrone et al., 1997, 1998; Vahalová et al., 2021; Lissi et al., 1994; Salin and Bridges, 1981; Rastogi and Pospíšil, 2010; Červinková et al., 2015; Radotić et al., 1990), carnosic acid (Kuzmenko et al., 1999), glutathione (Wefers et al., 1985), histidine (Prasad et al., 2020a), and mannitol (Medeiros and Sies, 1989; Maccarrone et al., 1997, 1998; Salin and

Bridges, 1981; Radotić et al., 1990).

Other works analyzed the effects of enzymatic antioxidants, which are much more specific than non-enzymatic ones. The inhibition of BAL has been explored mainly using two classes of enzymatic antioxidants: catalase (acting on H_2O_2) (Wefers et al., 1985; Birtic et al., 2011; Maccarrone et al., 1999; Allen, 1979; Salin and Bridges, 1981; Iida et al., 2002; Radotić et al., 1990; Hideg, 1993) and superoxide dismutase (SOD) (acting on superoxid anion radical) (Wefers et al., 1984, 1985; Medeiros et al., 1987; Medeiros and Sies, 1989; Allen, 1979; Iida et al., 2002; Hideg and Inaba, 1991; Prasad et al., 2020a; Hideg, 1993). Both non-enzymatic and enzymatic antioxidants typically have a suppressing effect on BAL intensity, see Fig. 5.

Several non-natural antioxidant substances also have a suppressing effect on the BAL intensity; for example, 2,6-di-tert-butyl-4-methylphenol (Albertini and Abuja, 1998), DNPH ((2,4-dinitrophenyl)hydrazine) (Kataoka et al., 2001), sodium azide (Salin and Bridges, 1981; Prado et al., 2009; Hideg, 1993; Hideg et al., 1991; Deneke and Krinsky, 1977), salicylhydroxamic acid (Hideg and Inaba, 1991; Hideg, 1993; Hideg et al., 1991), metal cation chelator EDTA (2,2′,2″,2‴-(Ethane-1,2-diyldinitrilo)tetraacetic acid) (Maccarrone et al., 1997; Albertini and Abuja, 1998), (2,2,6,6-tetramethylpiperidin-1-yl)oxyl (TEMPO) (Maccarrone et al., 1997, 1998), disodium 4,5-dihydroxy-1,3-benzenedisulfonate (tiron) (Kageyama et al., 2006; Salin and Bridges, 1981; Kobayashi et al., 2006), or trolox (water-soluble analog of α-tocopherol) (Lissi et al., 1994; Maccarrone et al., 1998). The BAL intesity can also be decreased by hydroquinone (Salin and Bridges, 1981) or p-benzoquinone (Hideg and Inaba, 1991). Respiratory inhibitors such as antimycin A and potassium cyanide have also decreasing effect on BAL (Hideg and Inaba, 1991; Hideg, 1993; Hideg et al., 1991). Excess of Cu^+ during plant growing or the 0.2 mM solution of $Co(NO_3)$ can lead to BAL inhibition (Abeles, 1986). For example, sodium azide and certain sorbate salts (such as 2,4-hexadienoate) may have an inhibitory effect on the BAL intensity by direct quenching of particular electron excited states species such as singlet oxygen (by sodium azide (Deneke and Krinsky, 1977)) or triplet excited carbonyl (by sorbate ions (Bechara et al., 1979; Catalani et al., 1987; Timmins et al., 1997)). Intercalating dye ethidium bromide (Cilento and Adam, 1988) or conjugated dienes, indoles, quinones, and tyrosine derivatives (Velosa et al., 2007) have also been used to quench the triplet carbonyls.

Conversely, BAL (as well as singlet oxygen generation) can be enhanced by various compounds, such as D_2O (Wefers et al., 1985; Medeiros and Sies, 1989; Salin and Bridges, 1981; Prado et al., 2009; Torinuki and Miura, 1981), NAD(P)H (Hideg and Inaba, 1991; Hideg, 1993; Hideg et al., 1991), chlorophyll *a* (Medeiros and Sies, 1989; de Medeiros and Bechara, 1986), xanthene dyes (Medeiros and Sies, 1989), and 1,4-diazabicyclo[2.2.2]octane (DABCO) (Medeiros and Sies, 1989; Hideg, 1993; Hideg et al., 1991; Deneke and Krinsky, 1977). Increase of the light emission can also be caused by N,N′-dimethylpiperazine (Deneke and Krinsky, 1977), 13-hydroperoxyoctadecadienoic acid (Maccarrone et al., 1997), triethylamine, tryptophan, diphenylisobenzofuran (Salin and Bridges, 1981), or Hg^{2+} (Abeles, 1986).

The body of evidence presented so far in this section suggests that BAL can be employed to monitor the addition or the presence of antioxidants, quenchers, or enhancers, with several works even reporting the effects of distinct concentrations (Wefers et al., 1985; Kageyama et al., 2006; Vahalová et al., 2021; Lissi et al., 1994; Kazakov et al., 2007; Hall and Chignell, 1987; Červinková et al., 2015). Effects of three non-enzymatic antioxidants at three different concentrations on BAL intensity of differentiated HL-60 cells are shown in Fig. 5b. However, to achieve specificity to particular chemical pathways, the system has to be well characterized.

When the system is not yet well characterized, using the same additives and observing that they have a different or no effect in a different system can be leveraged to analyze the underlying mechanisms that lead to BAL. For example, the addition of enzymatic antioxidants superoxide dismutase or catalase to washed rat liver microsomes in the presence of Fe^{3+}-ADP and NADPH did not cause any significant decrease of chemiluminescence, in which case spectroscopic measurements indicated that the singlet oxygen was probably the main emitter (Nakano et al., 1975). Similarly, incubation of wounded soybean root tissue with superoxide dismutase had no significant effect on BAL signal (Salin and Bridges, 1981), indicating that superoxide anion radical is not involved in the BAL generation. Additionally, non-enzymatic antioxidant mannitol, presented as a hydroxyl $HO^{\bullet}$ radical scavenger (Salin and Bridges, 1981), has different effects on BAL intensity of different systems. Slightly suppressing effect on BAL intensity after addition of mannitol was observed in ribose/horseradish peroxidase/H_2O_2 system (50 mM mannitol) (Medeiros and Sies, 1989), on wounded root soybean segments (500 mM mannitol) (Salin and Bridges, 1981), or on human erythroleukemia K562 cells where BAL was induced by addition of 13-hydroperoxyoctadecadienoic acid (300, 600, and 900 μM mannitol) (Maccarrone et al., 1997) or by electroporation (100 mM mannitol) (Maccarrone et al., 1998). In contrast, mannitol (1, 5, and 10 mM) injection into differentiated HL-60 cells caused small increase of the BAL intensity (Červinková et al., 2015), see Fig. 5b, part C. Moreover, treatment of maize roots with 500 mM mannitol led to significant increase of BAL intensity (Radotić et al., 1990). The authors suppose that this unexpected behavior is a consequence of reaction series initiated by

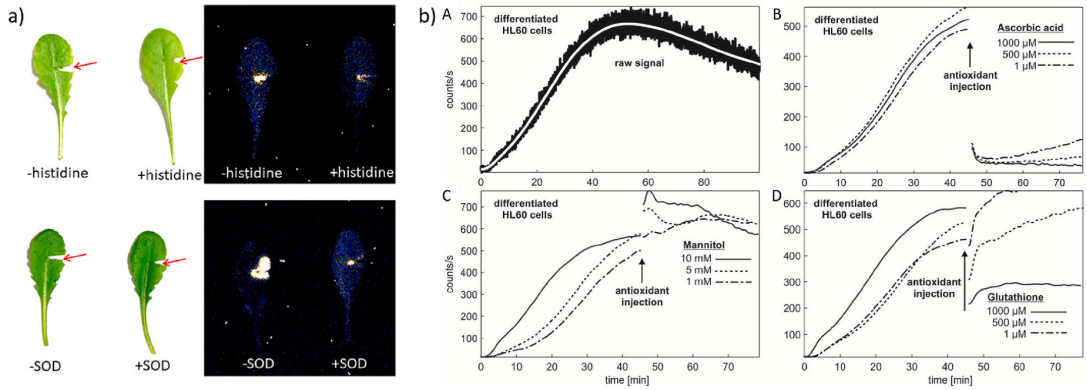

Fig. 5. Effect of various antioxidants on BAL intensity. a) The photographs (on the left) and corresponding 2D images of BAL (on the right) of wounded leaves of *Arabidopsis thaliana* in the absence (−) and presence (+) of 10 mM histidine (up) and 400 U ml^{-1} superoxide dismutase (SOD) (down). Integration time of BAL images was 30 min. b) BAL signal from differentiated HL-60 cells - raw signal without any modulator (A) and modulated by ascorbic acid (B), mannitol (C), and glutathione (D). All experiments with antioxidants were performed at three different antioxidant concentrations. The figure is reproduced from (Prasad et al., 2020a) (a) and (Červinková et al., 2015) (b) with the permission.

degradation of root tissue by mannitol (softening of roots after 30 min incubation in mannitol was observed) and subsequent reactions initiated by H_2O_2 and peroxidase (the authors monitored the change in the BAL intensity of treated and untreated samples induced by H_2O_2, 6% v/v) (Radotić et al., 1990).

4.3. BAL and oxidative reactions products

The reactions of ROS with biomolecules can lead to the formation of various products, e.g., organic radicals, hydroperoxides, endoperoxides, dioxetanes, tetroxides, ground state or triplet excited carbonyls, excited chromophores, or singlet oxygen (Pospíšil et al., 2019). Several of them are already mentioned above, mainly in connection with the generation of singlet oxygen. In this subsection, excited triplet carbonyl, another essential emitter, malondialdehyde, a secondary product of lipid peroxidation, several other lipid oxidative products (such as isoprostanes or prostaglandins), and selected nitrogen-containing compounds (such as amino acids) are discussed.

4.3.1. Carbonyls

As indicated above, the generation of singlet oxygen can accompany or precede the formation of carbonyls. In one of the pathways, the carbonyls are formed in a triplet electronically excited state (Bechara et al., 1979; Cilento et al., 1994). Under appropriate conditions, this state can emit photon, hence manifesting as BAL. Therefore the generation rate of carbonyls directly and positively correlates with BAL intensity. When BAL spectra are measured, the correlation is so significant that it is used as a direct evidence of the presence of triplet excited carbonyls: the peak of the emission is typically between 400 and 500 nm (Bechara et al., 1979; Cilento, 1984; Escobar et al., 1990), often supported by phosphorescence measurement of aldehydes (excited states obtained by external light excitation) (Oliveira et al., 1978; Schuh et al., 1984).

BAL measurements using highly sensitive CCD cameras and low-noise PMTs have helped to detect the formation of triplet excited carbonyls in several various oxidized systems, such as human multiple myeloma cells U266 exposed to H_2O_2 (Rác et al., 2015), unicellular green alga *Chlamydomonas reinhardtii*, in which lipid peroxidation was induced by heat stress (Prasad et al., 2016), during protein oxidation in PSII membranes deprived of Mn_4O_5Ca complex (Pathak et al., 2017), or during the transformation of peroxynitrite (ONOO-) to nitrate (Sharov et al., 1998).

The most common process that leads to the formation of electronically excited triplet carbonyls is thermal decomposition of dioxetanes (Mano et al., 2014; Bastos et al., 2017; Velosa et al., 2007; Cilento and Adam, 1988; Pathak et al., 2017; Adam and Baader, 1985; White et al., 1974). Excited carbonyls can also be formed in singlet form, especially if dioxetanes contain groups that are good electron donors (Cilento and Adam, 1988). However, thermolysis of simple dioxetanes (alkyl, alkoxy, etc.) preferentially generates excited triplet carbonyl compounds. Not only the type of dioxetane, but also its modification can change its thermal stability or triplet and singlet excitation yields. For example, the thermal stability and triplet and singlet excitation yields increase with the degree of methylation, whereas the pattern of methylation does not have a significant effect on the thermal stability of studied 1,2-dioxetanes (Adam and Baader, 1985). According to Bastos et al., the quantum yield of triplet state carbonyl species Φ_T during decomposition of 1, 2-dioxetanes is up to 50% compared with that of singlet state species $\Phi_S < 0.1\%$ (Bastos et al., 2017). Velosa et al. determined that the maximum quantum yield from the generation of triplet carbonyls during 1,2-dioxetanes thermolysis was 60 % (Velosa et al., 2007).

Excited triplet carbonyls can also be formed enzymatically. The most often used systems for excited triplet carbonyl generation are oxygenated ones with a peroxidase, such as isobutyraldehyde (IBAL) oxidation catalyzed by HRP in the presence of molecular oxygen (Dunford et al., 1984; Schulte-Herbruggen and Sies, 1989; Velosa et al., 2007; Cilento, 1984; Oliveira et al., 1978). Dunford et al. observed that the chemiluminescence, reflecting excited triplet carbonyl content in a sample, and oxygen uptake rate in IBAL/O_2/HRP system increased together with increasing concentration of HRP, at first linearly and at approximately 0.5 μM the curves started reaching their limit values (Dunford et al., 1984). In the studied IBAL concentration range, they also observed an increase of BAL and oxygen uptake rate with increasing IBAL concentration. Oliveira et al. used higher concentrations of HRP in a system with the same compounds and they revealed that, in contrast, a HRP concentration higher than 2 μM caused a decrease in the oxygen uptake rate (Oliveira et al., 1978). The generation of excited triplet carbonyls and BAL emission were also observed during horseradish peroxidase-catalyzed aerobic oxidation of 2-methylpropanal (Mano et al., 2014), 3-methylacetoacetone (Soares and Bechara, 1982), ribose in the presence of hydrogen peroxide (Medeiros and Sies, 1989), lysozyme, bovine serum albumin, and protamine adducts with glycolaldehyde (de Medeiros and Bechara, 1986). Cilento and Adam mentioned also using phenylacetaldehyde, indole-3-acetic acid, or Schiff bases as substrates for these type of reactions (peroxidase/O_2 system) (Cilento and Adam, 1988). Other enzymes such as NADPH oxidase, lipoxygenase, or cytochrome P450 can be also used for oxidation of chemical substances in order to generate excited triplet carbonyls (Nukui et al., 2013).

Other processes that lead to the formation of excited triplet carbonyl species are decomposition of tetroxides (Pospíšil et al., 2019; Pathak et al., 2017), dismutation of alkoxyl radicals bearing geminal hydrogen atom(s) ($\Phi_T = 0.1$–8%) (Mendenhall et al., 1991), the Russell reaction in which recombination of alkylperoxyl radicals with geminal hydrogen atom(s) forms singlet oxygen (Φ_S = 3–14%) (Niu and Mendenhall, 1992), triplet carbonyl ($\Phi_T \leq 0.1\%$), and alcohol as final products (Russell, 1957), or the retro Paterno–Büchi reaction, i.e., the reverse [2 + 2] cycloaddition of an alkene to a carbonyl compound ($\Phi_T \leq 0.01\%$) (Farneth and Johnson, 1984).

Because the radiative de-excitation (i.e. photon emission) of excited triplet carbonyls is a spin-forbidden process, energy transfer to nearby suitable energy acceptors (such as various chromophores or molecular oxygen) occurs frequently (Bastos et al., 2017; Cilento, 1984; Bohne et al., 1986; Durán and Cilento, 1980; Prasad et al., 2016; Bechara and Wilson, 1980). There are also several other pathways how excited triplet carbonyls can release the surplus energy (except for BAL and energy transfer): vibrational relaxation (thermal deactivation), cis–trans isomerization of conjugated dienes, [2 + 2] cycloaddition to olefins (Paterno–Büchi reaction), abstraction of hydrogen from appropriate donors (e.g., polyunsaturated fatty acids), and Norrish cleavage (e.g., R-scission leading to several products) (Velosa et al., 2007). These other pathways decrease the probability of photon emission from excited triplet carbonyls, or other energy acceptors, which received the energy from excited triplet carbonyls and, therefore, also decrease the BAL intensity of a studied sample.

Several authors have studied the correlation between BAL and the level of malondialdehyde (MDA), a secondary product of lipid peroxidation which also contains a carbonyl group. Generally, the higher the BAL intensity the higher the MDA level (Havaux et al., 2006; Prasad et al., 2016; Noll et al., 1987). Prasad et al. employed a highly sensitive CCD camera to evaluate the effects of the time under heat stress on the BAL intensity of *Chlamydomonas reinhardtii*. They observed that a longer oxidation time increases the BAL intensity and also MDA concentration in a sample (Prasad et al., 2016). Havaux et al. studied *Arabidopsis* plats - wild type, single mutant deficient in ascorbate, and double mutant deficient in ascorbate and zeaxanthin exposed to four-days-lasting high light stress (Havaux et al., 2006). The double mutant evinced the highest integrated BAL signal intensity (the BAL signal integration time was 60 min) and simultaneously the highest MDA level in leaves. Noll et al. observed that the BAL dynamics were significantly delayed after the MDA dynamics in case of lipid peroxidation in rat liver microsomes promoted by NADPH/ADP-iron, whereas the BAL and MDA dynamics

had very similar causes in the case of sample oxidation promoted by NADPH/CCl_4 (Noll et al., 1987). The maximal rate of MDA formation and BAL intensities were different for various initiators and also for various tested oxygen partial pressures (Table I in (Noll et al., 1987)).

4.3.2. Other metabolites

Burgos et al. monitored respiratory burst (induced by phorbol 12-myristate 13-acetate) of differentiated neutrophil-like HL-60 cells using BAL (Burgos et al., 2017). The produced lipid metabolites related to caused oxidative stress (isoprostanes, prostaglandins, lysosphingolipids, and nitro-fatty acids) were analyzed in cell extracts and in culture medium using LC-MS. The authors observed that the amount of 8-iso-prostaglandin E2, 8-isoprostaglandin E1, prostaglandin E1, and sphinganine C18:0 significantly increased in cell lysates during respiratory burst, whereas sphingosine C18:1 decreased. From extracellular metabolites (in culture medium), only prostaglandin E2, prostaglandin D2, and ±5-isoprostane F2α-IV significantly increased during respiratory burst. The authors concluded that BAL is probably correlated only with intracellular signalling metabolic intermediates (Burgos et al., 2017). Similar group of authors lead by Burgos evaluated also the correlation of BAL with selected amino acids and other nitrogen-containing compounds (Burgos et al., 2016). They used the same model sample (differentiated neutrophil-like HL-60 cells) and capillary electrophoresis-mass spectrometry for targeted metabolomics. Authors revealed the inverse relation of the changes in BAL intensity and in putrescine, glutathione, sarcosine, creatine, β-alanine, methionine, and hydroxyproline levels. They proposed that methionine pathway may contribute to the observed changes in BAL intensity of HL-60 cells.

4.4. Physical, chemical, and biological parameters correlated with oxidative processes, oxidative metabolism and oxidative stress and their effects on BAL

BAL reflects the sample oxidation. Rate, level, and time course of sample oxidation, and so also BAL intensity, time course, and spectral distribution, depending on the set of various parameters, e.g., sample composition and geometry, oxygen concentration, temperature, or pH (Bohne et al., 1986; Rychly et al., 2004) (Fig. 6). The change in oxidative state of the sample also induces changes in various biological processes, which can be also studied by monitoring of BAL (Vahalová et al., 2021).

4.4.1. Oxygen presence and consumption

The oxygen concentration is the most important factor that influences the BAL. The presence of oxygen is essential for the BAL

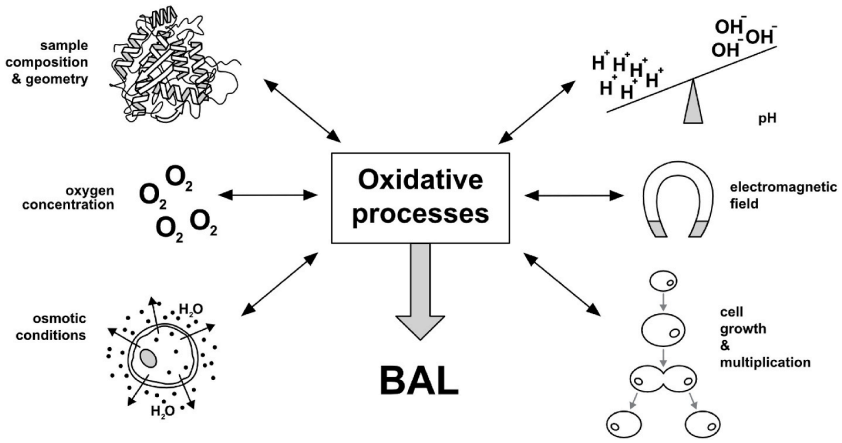

Fig. 6. Examples of parameters influenced by oxidative processes in an organism and simultaneously influencing oxidative processes and so also BAL.

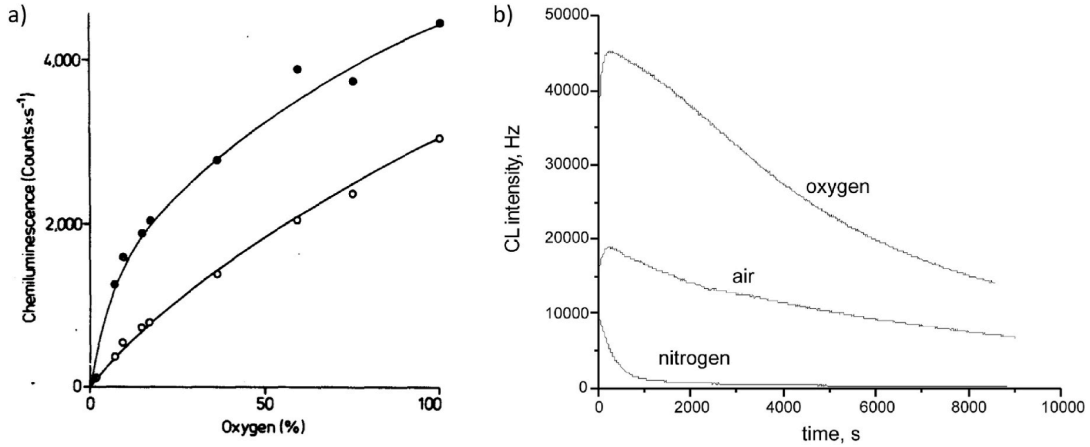

Fig. 7. Effect of oxygen concentration on BAL intensity. a) Oxygen dependence of BAL (≥610 nm) of reduced glutathione/horseradish peroxidase system displayed two phases (peaks in the time series) on both chemiluminescence phases: phase I (○) and phase II (●). b) Time dependence of BAL (CL) intensity of Whatman cellulose (circular cuts 6 mm) at 220 °C in the atmospheres with three different concentrations of oxygen. The figures are reproduced from (Wefers et al., 1985) (a) and (Rychlý et al., 2002) (b) with the permission.

measurements and has been confirmed by many authors. For example, a significant BAL decrease of oxidized samples in anaerobic compared to aerobic conditions (Prasad and Pospíšil, 2011; Rajfur, 1994) or even complete drop of BAL signal on the level of BAL signal of a sterile or non-oxidized medium have been observed in oxidized samples gassed by nitrogen (Abeles, 1986; Wefers et al., 1984; Torinuki and Miura, 1981; Laager et al., 2009; Strlič et al., 2000; Oros and Alves, 2018) or made anaerobic by addition of glucose/glucose oxidase/catalase (Bohne et al., 1986). The increase in BAL intensity with increasing oxygen concentration in the sample is illustrated by Fig. 7 and has been shown also in (Allen, 1979; Quickenden and Tilbury, 1983; Kobayashi et al., 1999). In several studied systems (consisting of the sample, oxidizing system, and in some cases other substances such as an enzyme inhibitor), authors have observed two components of BAL: oxygen-dependent and oxygen-independent (Lloyd et al., 1979; Ohya et al., 2000).

Multiple authors have also analyzed the oxygen consumption and rate of oxygen uptake. Usually, the BAL intensity and oxygen uptake rate increase with the incubation time (Noll et al., 1987) or increasing concentration of the reactants (biomolecular substrate and oxidation reagents) (Dunford et al., 1984; Wefers and Sies, 1983; Sharov et al., 1998; Napetschnig and Sies, 1987; Knudsen et al., 2000). The time required for the parameters to reach a maximum value seems to be dependent on the type of a system that promoted the oxidation of the sample or steady-state oxygen partial pressure (Noll et al., 1987). For example, BAL started to increase with a significant delay after oxygen uptake in a system in which lipid peroxidation in rat liver microsomes was promoted by NADPH/ADP-iron (Noll et al., 1987). Furthermore, as the pO_2 was reduced (from 30.0 mm Hg to 3.0 mm Hg), the lag phase became even longer. At the lowest tested pO_2 (0.5 mm Hg), no BAL was detected at all, whereas oxygen uptake was still observed. On the other hand, BAL and oxygen uptake have really similar time courses at all tested pO_2 in case of lipid peroxidation promoted by NADPH/CCl_4. Also the time course of oxygen uptake can vary a lot depending on the studied system and conditions. Knudsen et al. studied chemiluminescence and oxygen uptake during reactions of selected aldehydes and β-diketones promoted by peroxynitrite (Knudsen et al., 2000). In case of β-diketones 3-methyl-2,4-pentanedione and 2,4-pentanedione, oxygen was depleted within seconds. Total oxygen uptake of aldehyde isobutanal decreased by approximately 80% and then remained constant. Oxygen uptake of 2-pentanone and 3-methyl-2-butanone decreased very slowly during 70 s of measurement. Another examples of time courses of BAL accompanied by measurement of oxygen uptake are shown in (Bechara et al., 1979; Soares and Bechara, 1982; Baader et al., 1985).

To sum up, the BAL intensity is substantially influenced by the oxygen concentration. However, the rate and time course of oxygen uptake (and BAL) can vary a lot depending on a type of studied system,

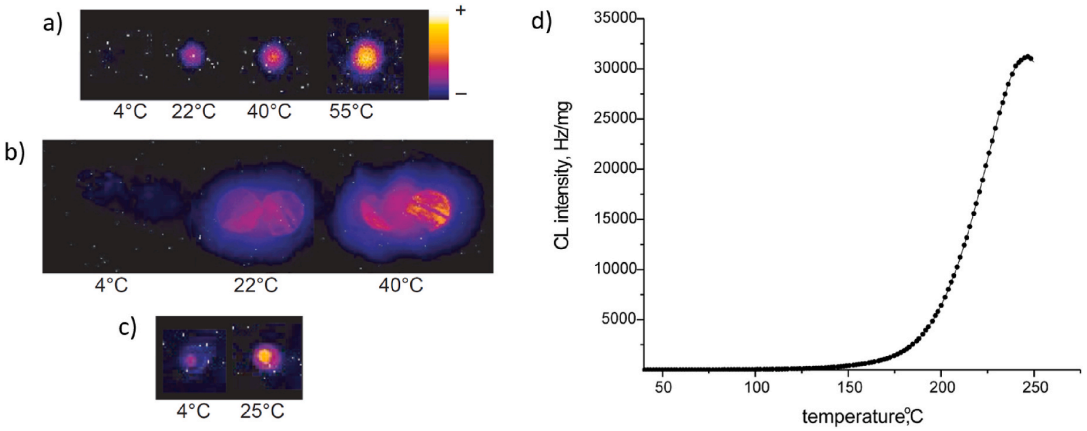

Fig. 8. Temperature dependence of BAL. 2D images of BAL from a) oxidized linolenic acid, b) light-stressed leaf disks from Arabidopsis plants, and c) oxidized lysozyme. Linolenic acid and lysozyme were oxidized by singlet oxygen generated by illumination in the presence of methylene blue. Data are representative images from three independent measurements. d) Temperature dependence of BAL (CL) intensity of oxidized Whatman cellulose (circular cut 9 mm) in oxygen. Measured points (heating rate 2.5 °C/min) are represented by dots and the theoretical fit by full line. The figures are reproduced from (Birtic et al., 2011) (a–c) and (Rychlý et al., 2002) (d) with the permission.

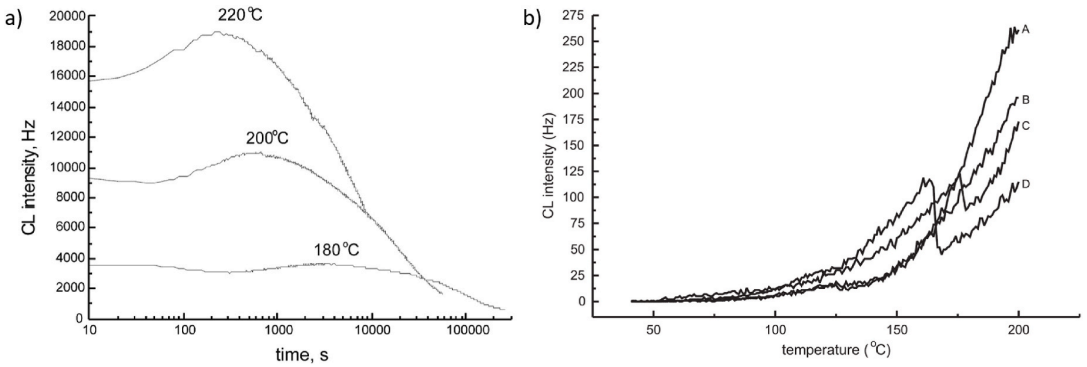

Fig. 9. a) Time dependence of BAL (CL) intensity accompanying the thermal oxidation of Whatman cellulose (circular cuts 6 mm) in the air at three different temperatures. b) Temperature dependence of BAL (CL) in nitrogen atmosphere for four different saccharides: A) cellobiose, B) lactose, C) laevoglucosan, and D) maltose. Rate of heating was 5 °C/min. The figures are reproduced from (Rychlý et al., 2002) (a) and (Strlič et al., 2000) (b) with the permission.

oxidating of the sample, concentrations of the reactants, an incubation time, and experimental conditions (such as steady-state oxygen partial pressure, temperature, or pH).

4.4.2. Temperature

Temperature also has significant effects on BAL. Maintaining a stable temperature during experiments is critical for reproducibility of experiments (Vahalová et al., 2021; Bereta et al., 2021). Rychlý, Strlič et al. studied the thermal oxidation of cellulose using chemiluminescence measurements. In the studied range of temperatures, the BAL intensity increased with increasing temperature (Birtic et al., 2011; Rychlý et al., 2002; Rychly et al., 2004; Strlič et al., 2000), see Fig. 8. Temperature extremes can lead to substantial damage or even death of cells and, therefore, increased BAL intensity (Abeles, 1986). The change of temperature also changed the course of BAL intensity time-dependence (Rychlý et al., 2002), see Fig. 9a. Furthermore, a type of oxidized substrate (Fig. 9b) or pre-treatment conditions can significantly modify the temperature dependence of BAL (Strlič et al., 2000). Temperature also has a significant effect on the rate constants of chemiluminescence decay (Abeles, 1986; Rychlý et al., 2002; Rychly et al., 2004).

4.4.3. pH dependence

BAL is also strongly dependent on pH. For example, Birtic et al. used highly sensitive CCD camera to observe amplifying effect of increasing pH on BAL intensity of oxidized linolenic acid, see Fig. 10a (Birtic et al., 2011). The usual shape of a BAL intensity-pH dependence curve is a sigmoidal (Miyamoto et al., 2009; Sharov et al., 1998). Soares and Bechara measured the chemiluminescence and oxygen depletion to find out that the horseradish peroxidase-catalyzed aerobic oxidation of 3-methyl-2,4-pentanedione yields biacetyl, partly in the electronically excited triplet state (Soares and Bechara, 1982). Besides other things, they observed a strong pH effect on the rate of oxygen uptake. The reaction became 200 times faster when the pH was raised from 7 to 8. Knudsen et al. obtained pH profiles of the peroxynitrite-promoted oxidation of isobutanal and 3-methyl-2,4-pentanedione by measuring the total oxygen consumption, see Fig. 10b (Knudsen et al., 2000). The pH profile of 3-methyl-2,4-pentanedione corresponded with the peroxynitrous acid titration curve, indicating that peroxynitrite anions act as the oxidant. In case of isobutanal, just a subtle increase of oxygen uptake was observed in the pH region close to the peroxynitrous acid pK_a value. However, its pH profile also suggested that the peroxynitrite anion and the peroxynitrous acid were the oxidizing agents. The time courses of BAL intensity can also vary depending on the pH (Bohne et al., 1986).

4.4.4. Magnetic field

Several authors have studied the influence of a magnetic field on BAL. It was reported that a low magnetic field (62 Oe) promoted respiration and growth of bean seedlings by 10% and also increased the chemiluminescence by 40% (Abeles, 1986). On the other hand, higher magnetic fields decreased respiration, growth, and BAL. Cheun et al. observed that the overall BAL intensities and decay characteristics were similar for both samples: Madin-Darby canine kidney cells exposed to a 60 Hz AC magnetic field (14 Gauss) and control non-exposed cells (Cheun et al., 2007). However, chemiluminescence decay patterns in

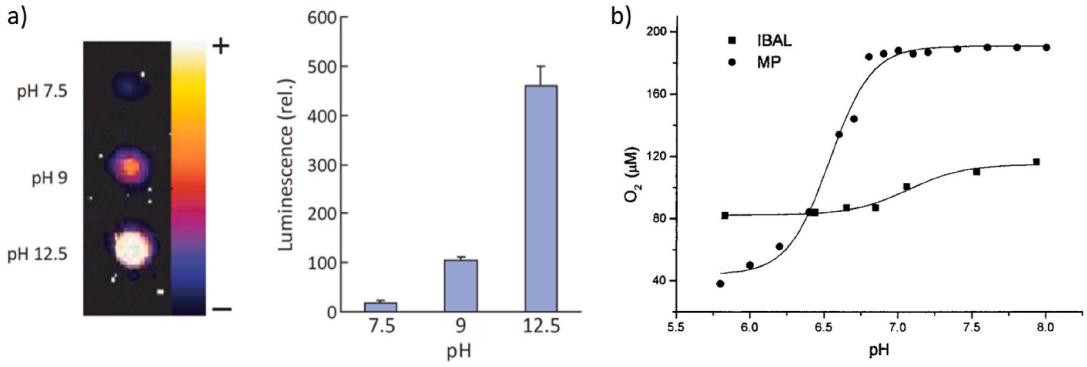

Fig. 10. Amplifying effect of increasing pH on a) BAL intensity and on b) total oxygen consumption. a) BAL signal imaged by CCD camera and corresponding sums of the signals from oxidized linolenic acid at three different pHs (adjusted by addition of 5 N NaOH). The samples were oxidized by singlet oxygen produced by light and methylene blue. Bar graph shows mean values and standard deviations of five independent measurements. b) pH profiles of isobutanal (IBAL) and 3-methyl-2,4-pentanedione (MP). 10 mM IBAL and 1 mM MP in 500 mM phosphate buffer (pH 7.2) were treated with 500 μM peroxynitrite. Reprinted with permission from (Birtic et al., 2011) (a) and (Knudsen et al., 2000), copyright 2022 American Chemical Society (b).

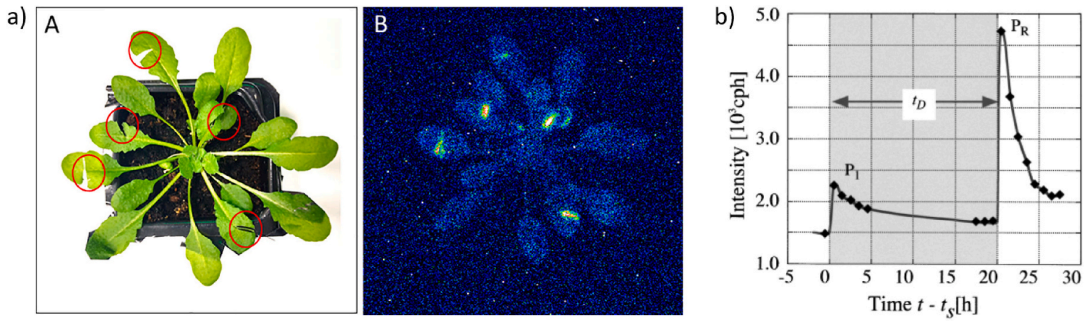

Fig. 11. Influence of a) wounding and b) drought on BAL intensity of plant samples. a) A photograph (A) with wounding locations highlighted by red circles and the corresponding 2D image of BAL intensity (B) of the plant *Arabidopsis thaliana*. b) Changes of BAL intensity of red bean seeds during drought stress (shaded area) and after rewatering. t_D - drought period, t_S - time between placing germinating seeds into a growth chamber (RH = 82% and T = 24 °C) and the beginning of drought stress application. The figure is reproduced from (Prasad et al., 2020a) (a) and (Ohya et al., 2002) (b) with the permission.

detail were slightly different: BAL decay of an exposed sample had a peak at the initial part, more apparent with higher H_2O_2 concentration (H_2O_2 was used to amplify the BAL signal). The decay behavior is important in order to understand the effect of a magnetic field on the mechanism of ROS generation. Also, Bereta et al. did not observe any significant difference in BAL intensities and their dynamics between a control yeast cell culture and a sample exposed to a low-frequency magnetic field (800 Hz, 1.5 mT) (Bereta et al., 2021). However, their measurements showed a significant time shift between the maxima of BAL dynamics of the control and the exposed sample: the BAL intensity maximum and subsequent rapid decrease occurred earlier in the samples exposed to a magnetic field. Because a BAL dynamic of a yeast culture is closely related to its metabolism (Vahalová et al., 2021), exposure of the yeast sample to the magnetic field probably influenced metabolic processes and caused earlier change of metabolism type (and so earlier rapid decrease of BAL intensity).

4.4.5. Sample structural properties

The structural properties of samples can also affect the BAL emission during sample oxidation. For example, Kočar et al. studied the influence of sample crystallinity, morphology, and size on chemiluminescence during atmospheric oxidation of cellulose (Kočar et al., 2004). Samples from microcrystalline cellulose with various crystallinity (30.7, 26.4, 14.6, and 0.0%) had similar content of carbonyl groups and similar courses of BAL intensity. However, the morphology had a significant effect on the BAL signal. More refined fibers had a larger specific surface area exposed to atmospheric oxygen, larger content of peroxides inside the material, and, therefore, higher observed chemiluminescence emission. Samples of 0.11, 0.21, 0.47, and 0.70 mm diameter were compared with the usual sample size of 9 mm. The two smallest samples gave too low signals to allow background subtraction without introducing a substantial error. The BAL from the samples of diameter 0.47 and 0.70 mm was comparable with the samples of 9 mm diameter. Iida et al. observed that BAL intensity of browned products (a heated mixture of 1 M arabinose and 1 M of an amino acid (Ala, Cys, Glu, Lys, Phe, Try, or His) in distilled water, soy sauce, and coffee) was influenced by the amino acid structure (Iida et al., 2002).

4.4.6. Biological processes, cell growth and multiplication

BAL has also been found to correlate with the occurrence of several biological processes. The most intensively studied process is cell growth and cell division, either in cell cultures (Vahalová et al., 2021; Bereta et al., 2021; Červinková et al., 2015; Quickenden and Tilbury, 1983; Konev et al., 1966; Quickenden and Hee, 1974; Tilbury and Quickenden, 1988; Vogel et al., 1998; Vogel and Süssmuth, 1998; Kobayashi and Inaba, 2000; Kim et al., 2007a) or whole tissue (Chen et al., 2002; Takeda et al., 2004): the most extensively studied biological tissues were germinating seeds (Saeidfirozeh et al., 2018; Colli, 1955; Gallep and Dos Santos, 2007; Moraes et al., 2012; de Mello, 2014; Gallep et al., 2014, 2018; Rafieiolhosseini et al., 2016; Gallep and Robert, 2020).

From microbial cell cultures, the best explored cell type for BAL during the cell culture growth is the yeast *Saccharomyces* and its various species (Vahalová et al., 2021; Bereta et al., 2021; Červinková et al., 2015; Quickenden and Tilbury, 1983; Quickenden and Hee, 1974; Tilbury and Quickenden, 1988). Quickenden and Que Hee found that the most intense BAL signals appear in the *Saccharomyces cerevisiae* at the latter part of the logarithmic stage and early stationary stage (Quickenden and Hee, 1974). They also estimated that there is approximately 0.07–0.7 photons per cell division emitted in the logarithmic stage. In their follow-up work, Quickenden and Tilbury observed that both standard and respiratory deficient ("petite") mutants of *S. cerevisiae* displayed BAL signals but with different BAL kinetics and intensities at different stages (Quickenden and Tilbury, 1983). When the molecular oxygen was removed from the medium by nitrogen saturation, both cell types could grow, but there were no BAL signals. The authors concluded that BAL does not arise "from any of the reactions in the fermentative and respiratory pathways" and, considering findings in (Lloyd et al., 1979), suggested that $O_2^{\bullet -}$ is involved in BAL generating reactions in the growing yeast cell cultures. These findings are interesting because they link a process (cell growth) to the involvement of particular molecular species, particularly $O_2^{\bullet -}$. This link is now supported by multiple works, see superoxide dismutase (enzyme that removes $O_2^{\bullet -}$) line in Table 2. In newer studies on BAL from growing *Saccharomyces cerevisiae* cultures, it was found that within the first approximately 16 h, the BAL signal increases, then starts to decrease and then drops to almost background within 30 min (Bereta et al., 2021; Červinková et al., 2015). Later, we demonstrated that the BAL signal, after it dropped to low values, can be recovered by adding glucose to the cell culture (Vahalová et al., 2021). These results indicated that the strong BAL signal from yeast cell cultures is dependent on the pathways involving glucose consumption. Cultures of amoeba *Dictyostelium discoideum* also display a change of BAL signals during its development stages (Kobayashi and Inaba, 2000). The authors showed that this amoeba cell culture displays a short (< 1 h) transient increase of BAL after starvation and then a slow transient increase of BAL intensity during the development stage corresponding to the developmental stage of the aggregation stream and formation of mounds. BAL of plant tissues, particularly germinating seeds, in which dramatic cell growth is taking place, have been explored by several research groups. Mung beans (*Vigna radiata*) have been shown to steadily increase the BAL intensity when observed on a time scale up to several days (Rafieiolhosseini et al., 2016) and similarly for *Arabidopsis thaliana* (Saeidfirozeh et al., 2018). Results from multiple studies led by Gallep suggest that the gravimetric tides, which display semi-circadian periodicity, modulate the BAL signal intensity from germinating seeds (mostly wheat and coffee) (Gallep and Dos Santos, 2007; Moraes et al., 2012; de Mello, 2014; Gallep et al., 2014; Gallep and Robert, 2020). Although the mechanisms of how the seeds sense the minute changes of the gravity is not clear, it seems that these changes are affecting the redox metabolism and ROS activity leading to modulation of BAL (Gallep et al., 2018). When HeLa cells were analyzed for their BAL intensity during cell culture growth (Kim et al., 2007a, 2007b), the authors found an increase of the signal (on day two or three), and then a decrease. The authors claimed that the BAL signal intensity seems to be correlated with cell proliferation rate, as observed from the cell growth curve.

The correlation of BAL with the cell growth can be summarized as follows: In the initial phases of the growth of the cell cultures and tissue, there is typically a positive correlation of cell number (concentration) multiplied by the growth rate (per single cell) with the BAL intensity. This can be interpreted based on the fact that the total amount of actively metabolizing mass (hence total ROS production rate) is increasing during the logarithmic phase of growth and then decreases as the growth ceases (Vahalová et al., 2021). This development is therefore manifested as an increase of BAL intensity, reaching the maximum, and then a decrease (Vahalová et al., 2021; Vogel and Süssmuth, 1998; Kobayashi and Inaba, 2000; Kim et al., 2007a, 2007b). In particular cases, there are also oscillations of BAL intensity induced by external rhythms as explained above (Moraes et al., 2012; Gallep et al., 2014). Interestingly, certain growth media without the cells can manifest quite strong autoluminescent signals, particularly after autoclaving. In such media, the presence of cells can have a quenching effect on the total luminescence signal, which has been suggested to take place due to cell-mediated enhancement of termination reactions (such as for bacterial cells *Escherichia coli*) (Vogel et al., 1998; Vogel and Süssmuth, 1998, 1999; Vogel, 1998).

The correlation of BAL with other important biological processes has also been studied. Slawinski reported a general overview of BAL and its relation to physiological processes (Sławiński, 2005). He concluded, based on his works and studies from other authors (Sławiński, 1990; Kochel, 1990, 1995), that rapid irreversible homeostasis perturbation,

which causes the death of the tested organism, also results in rapid and irreversible (meaning that the repeated stimulus would not provide repeated response) BAL enhancement. Particularly, in (Sławiński, 2003) he showed that the chemical stressors, which do not directly cause oxidative reactions leading to BAL (such as formaldehyde or acetone), can induce a burst of BAL after treating organisms with lethal concentrations. This was demonstrated on multiple species ranging from yeast and protozoa to insects and snails (Sławiński, 2003). Maccarrone et al. went even deeper into the relationship of BAL and cell death (Maccarrone et al., 1999). Based on their results, they suggested that BAL is an early marker of apoptotic (but not necrotic) programs involving hydrogen peroxide generation and 5-lipoxygenase activation.

4.4.7. Other factors influencing BAL emission

BAL emission from plants is also affected by wounding (mechanical injury) that leads to enhancement of the photon emission observed by several authors. For example, Prasad et al. studied the formation of ROS in wounded leaves of *Arabidopsis thaliana* (Prasad et al., 2020a). Using fluorescence imaging and BAL measurements, the authors showed that ROS (superoxide anion radical and singlet oxygen) are produced after wounding. Subsequent oxidation of biomolecules (mainly of polyunsaturated fatty acids) leads to the generation of reactive intermediate products and electronically excited species (Prasad et al., 2020a). The enhanced BAL signal of mechanically injured parts is shown in Fig. 11a. In another article from the same first author, the BAL signal from injured parts of the leaves of *Arabidopsis thaliana* was visible even after 270 min (Prasad et al., 2020b). To evaluate the spectral changes of BAL, the kinetics of BAL from mechanically injured leaves (20 s after wounding) was measured using PMT with cut-on absorption filters with transmission ranges of ≥400 nm and ≥610 nm. The values of BAL were comparable for measurements without a filter and with the ≥400 nm filter, whereas the use of the ≥610 nm filter resulted in a decrease of the BAL signal by approximately a half (Prasad et al., 2020b). Birtic et al. also imaged wounded *Arabidopsis* plants with a cooled CCD camera; moreover, they compared BAL emission of a wild-type plant with three other mutants (Birtic et al., 2011). A mutant (dd2), incapable of hydroxy-fatty acid metabolism, display significantly higher BAL intensity than wild-type. On the other hand, no BAL signal was measured for the other two mutants, lipoxygenase 2 RNA interference plants (LOX2i-2, LOX2i-9). The luminescence observed after mechanical stress has been attributed to chlorophyll (Flor-Henry et al., 2004), lipid peroxidation (Birtic et al., 2011), physiological and bioelectrical changes (Winkler et al., 2009), or increased peroxidase activity due to cell damage together with the release of phenoloxidases (Salin and Bridges, 1981; Radotic et al., 1998).

The BAL increase depends on localization of the wounding on the plant and wounding extent. For example, Salin and Bridges studied chemiluminescence of root and stem segments from etiolated soybean plants after mechanical injury (Salin and Bridges, 1981). They observed that root tissue evinced higher spontaneous BAL intensity than stem tissue and the increase in BAL signal between the control and wounded sample was much higher for roots than for stems. *Cucurbita pepo variaca styriacae* was used as the experimental system by Winkler et al. (2009). The authors observed that BAL intensity of wounded seed leaves of the seedlings was more than two times higher after wounding than before wounding; the BAL signal after wounding slowly increased until a rather constant level. In contrast, the BAL intensity of the stem doubled (for two cuts of stem) after wounding and than decreased hyperbolically, after approximately 200 s BAL signal was comparable to the one before wounding. More cuts of the sample resulted in an increase in the BAL signal. The highest increase in BAL intensity was observed after the total destruction of the plant (subsequent decrease is a better fit by an exponential function). Almost 15-fold higher BAL was observed after plant destruction than from an intact plant, whereas already injured plants displayed a lower BAL increase after total destruction (ca. 8 times) (Winkler et al., 2009). These observations showed the influence of pretreatment on BAL intensity.

BAL modulation has also been observed after an exposure of a sample to various other physical or chemical stress factors, such as various types of radiation. For example, Torinuki and Miura observed 2.5 times higher BAL signal from rat epidermal homogenate after UV irradiation against a control sample (Torinuki and Miura, 1981). Similarly, Evelson et al. observed a significant increase in *in vivo* BAL intensity after exposure of mouse skin to UVA radiation (Evelson et al., 1997). A maximum chemiluminescence intensity (13-fold increase) was recorded after 45–60 min of UVA exposure. Kim et al. evaluated radiation degradation of low density polyethylene using BAL (Kim et al., 2007c). Cobalt-60 was used as a source of gamma-ray radiation. The authors observed increasing BAL signal with increasing radiation dose (from 10 to 500 kGy). Bögl and Heide used the same source of gamma rays (^{60}Co) with radiation doses of up to 10 kGy to irradiate 19 different spices, whole onion, milk powder and frozen chicken (Bögl and Heide, 1977). Photosensitizer luminol was used to increase the chemiluminescence intensity. Except for the sage sample (which had the same chemiluminescence intensity without and after treatment), the other samples displayed from 2 to 933 times higher chemiluminescence immediately after irradiation and from 1.6 to 370 times higher chemiluminescence 1 month after irradiation (not all samples were measured 1 month later) (Bögl and Heide, 1977). Zhu et al. showed that an increase in gamma-ray radiation dose up to 3 Gy (^{60}Co) increased the BAL intensity and cell mortality of lymphocytes (Zhu et al., 2004). Furthermore, the irradiation of a sample with X-rays can cause an increase in chemiluminescence, as observed by Zaqaryan and Badalyan on rats' whole blood sample (Zaqaryan and Badalyan, 2016).

Other examples of stress factors that change the BAL intensity of a sample are osmotic conditions and salt concentration. Ohya et al. studied the effects of drought on BAL from red beans (*Vigna angularis*) during germination and seedling stages. (Ohya et al., 2002). They observed an initial increase of BAL intensity of the root apex and a subsequent slow decrease during 20-h exposure of the sample to drought. Ensuing re-watering again caused a steep BAL increase, this time leading to approximately two times higher intensity than after drought application (Ohya et al., 2002), see. Fig. 11b. Water resupply after drought to soybean seedling also led to strong light emission from the tip of the root (Xing et al., 1999). On the other hand, the authors were not able to detect BAL from the root of the etiolated seedling of germinating soybean without water. Ohya et al. also studied the effects of NaCl treatment on red bean seedlings (Ohya et al., 2000). They observed that BAL intensity after NaCl treatment decreased with increasing NaCl concentration (0.01–1 M), except for treatment with saturated NaCl solution (4.5 M), which led to substantial BAL increase accompanied by destruction of cell membranes. Also, a 1 M NaCl concentration was lethal for a sample (protoplasm effusion), whereas samples survived at lower NaCl concentrations. Physiological differences between the sample treated with 0.01 M NaCl and the reference were hardly visible. A NaCl concentration of 0.1 M caused a change to the root cap color. Salt stress also caused suppression of root elongation, which was much more significant at an early growth stage than at a later one (Ohya et al., 2000). Finally, toxic compounds can also substantially modulate BAL intensity of samples (Radotic et al., 1998). For example, Tian et al. studied the influence of a commercial insecticide (beta-cypermethrin) and an insecticidal plant (*Cicuta virosa* L. var. *latisecta*) on spontaneous BAL emission from larvae of two different types of insect (*Spodoptera litura* and *Zophobas morio*) (Tian et al., 2014). BAL intensities from *S. litura* decreased with increasing concentration of beta-cypermethrin (0, 0.1, and 1 μg/ml), whereas BAL from *Z. morio* was higher for the treated samples with beta-cypermethrin (at 0.156, 0.313, and 0.625 μg/ml) than for the control sample. BAL from *S. litura* larvae treated with petroleum ether or fraction of *C. virosa* L. var. *latisecta* (insecticidal plants), which showed little activity in the bioassay with the two mentioned insects, increased with increasing dose (10, 100, and 1000 μg/ml), whereas changes of the BAL from *Z. morio* after the same

treatment were irregular (Tian et al., 2014).

5. Conclusion and outlook

In this review, we have highlighted the importance of reduction-oxidation processes in molecular and cellular biophysics, biotechnology and outlined the current paradigm of biological oxidation. First, we made a brief review of the current methods to detect and analyze the molecular species and processes related to biological oxidation. The main part of our review focuses on biological autoluminescence, which enables real-time, nondestructive, reagent-free and energy perturbance-free monitoring of oxidative processes. To that end, we reviewed how various classes of reactive oxygen species, redox enzymes, metal ions, antioxidants, and oxidative products are correlated to BAL signals. We also covered correlations of BAL signals with major physical, chemical and biological parameters. It is the first review which covers this topic from the perspective of BAL as a monitoring method at the biotechnological level.

We believe that the biotechnological and analytical power of BAL has not been harnessed in its full potential. In the applications, we see the following ones as the lowest-hanging fruits. Once calibrated to other standard methods, BAL could be used for a variety of biotechnological applications where optical access is available and non-contact sensing is desirable, e.g., monitoring of drug synthesis or other chemical synthesis processes that involve action of redox enzymes, monitoring the instantaneous growth rate in cell cultures, or monitoring of integral cellular stress. BAL could be also used, once properly calibrated by other standard techniques, for sensing the presence of a variety of reactive oxygen species, redox active metal cations, antioxidants and prooxidants, and oxidation products of biomolecules, such as carbonyl groups.

We conclude that biological autoluminescence is a label-free and perturbance-free method to monitor oxidation processes in biological samples with many potential diagnostic applications in biophysics and molecular biology as well as in biotechnology and environmental research and industry.

Author contributions statement

Contributions according to CRediT https://credit.niso.org/:

P.V.: Conceptualization, Data curation, Formal analysis (lead), Investigation (lead), Methodology, Visualization (lead), Writing – original draft (lead): most of the text, Writing – review and editing (lead).

M.C.: Conceptualization, Formal analysis (supporting), Funding acquisition, Investigation (supporting), Project administration, Resources, Supervision, Validation, Visualization (supporting), Writing – original draft (supporting), Writing – review and editing (supporting).

Declaration of competing interest

The authors declare that they have no competing interests.

Acknowledgements

We acknowledge major financial support from the Czech Science Foundation, project no. GX20-06873X. Neuron collective is acknowledged for graphical design and The Science Editorium for the manuscript structure and language check. Viliam Kolivoška is acknowledged for proofreading the manuscript and providing many useful suggestions.

Abbreviations

BAL = biological autoluminescence, CCD = charge-coupled device, DABCO = 1,4-diazabicyclo[2.2.2]octane, DMPO = 5,5-dimethyl-1-pyrroline N-oxide, DNPH = 2,4-dinitrophe-nylhydrazine, EDTA = 2,2′,2″,2‴-(Ethane-1,2-diyldinitrilo)tetraacetic acid, ELISA = enzyme-linked immunosorbent assay, EPR = electron paramagnetic resonance, FAD = flavin adenine dinucleotide, GC = gas chromatography, GSH = glutathione, GSSG = glutathione disulfide, HNE = 4-hydroxy-2-nonenal HPLC - high-performance liquid chromatography, HRP = horseradish peroxidase IBAL = isobutyraldehyde, LC = liquid chromatography, MDA = malondialdehyde, MS = mass spectrometry, MTT = thiazolyl blue tetrazolium bromide, NAD^+/NADH = nicotinamide adenine dinucleotide, $NADP^+$/NADPH = nicotinamide adenine dinucleotide phosphate, PMT = photomultiplier tube ROS = reactive oxygen species, SOD = superoxide dismutase, TBARS = thiobarbituric acid reactive substances, TEMPO = (2,2,6,6-tetramethylpiperidin-1-yl)oxyl, Tiron = disodium 4,5-dihydroxy-1,3-benzenedisulfonate, trolox = water-soluble analog of α-tocopherol, TNB = 5-thio-2-nitrobenoic acid.

References

Abeles, F., 1986. Plant chemiluminescence. Annu. Rev. Plant Physiol. 37 (1), 49–72.
Abuja, P.M., Albertini, R., 2001. Methods for monitoring oxidative stress, lipid peroxidation and oxidation resistance of lipoproteins. Clin. Chim. Acta 306 (1–2), 1–17. https://doi.org/10.1016/S0009-8981(01)00393-X. URL. https://linkinghub.elsevier.com/retrieve/pii/S000989810100393X.
Adam, W., Baader, W.J., 1985. Effects of methylation on the thermal stability and chemiluminescence properties of 1, 2-dioxetanes. J. Am. Chem. Soc. 107 (2), 410–416. URL. http://pubs.acs.org/doi/abs/10.1021/ja00288a022.
Adam, W., Cilento, G., 1982. Chemical and Biological Generation of Excited States. Elsevier.
Aebi, H., 1984. [13] Catalase in vitro. In: Methods in Enzymology, vol. 105. Elsevier, pp. 121–126.
Agledal, L., Niere, M., Ziegler, M., 2010. The phosphate makes a difference: cellular functions of NADP. Redox Rep. : Communications in Free Radical Research 15 (1), 2–10. https://doi.org/10.1179/174329210X12650506623122. URL. https://www.ncbi.nlm.nih.gov/pmc/articles/PMC7067316/.
K. W. Ahern, V. Serbulea, C. L. Wingrove, Z. T. Palas, N. Leitinger, T. E. Harris, Regioisomer-independent quantification of fatty acid oxidation products by HPLC-ESI-MS/MS analysis of sodium adducts, Sci. Rep. 9 (1). doi:10.1038/s41598-019-47693-5. URL http://www.nature.com/articles/s41598-019-47693-5.
Ahmed, M.U., Thorpe, S.R., Baynes, J.W., 1986. Identification of N epsilon-carboxymethyllysine as a degradation product of fructoselysine in glycated protein. J. Biol. Chem. 261 (11), 4889–4894. https://doi.org/10.1016/S0021-9258(19)89188-3. URL. https://linkinghub.elsevier.com/retrieve/pii/S0021925819891883.
Albertini, R., Abuja, P.M., 1998. Monitoring of low density lipoprotein oxidation by low-level chemiluminescence. Free Radic. Res. 29 (1), 75–83. https://doi.org/10.1080/10715769800300091. URL. http://www.tandfonline.com/doi/full/10.1080/10715769800300091.
Aldini, G., Domingues, M.R., Spickett, C.M., Domingues, P., Altomare, A., Sánchez-Gómez, F.J., Oeste, C.L., Pérez-Sala, D., 2015. Protein lipoxidation: detection strategies and challenges. Redox Biol. 5, 253–266. https://doi.org/10.1016/j.redox.2015.05.003. URL. https://linkinghub.elsevier.com/retrieve/pii/S2213231715000464.
Alfadda, A.A., Sallam, R.M., 2012. Reactive oxygen species in health and disease. J. Biomed. Biotechnol. https://doi.org/10.1155/2012/936486. URL. https://www.ncbi.nlm.nih.gov/pmc/articles/PMC3424049/.
Allen, R.C., 1979. Chemiluminescence from eukaryotic and prokaryotic cells: reducing potential and oxygen requirements. Photochem. Photobiol. 30 (1), 157–163, 10.1111/j.1751-1097.1979.tb07129.x. https://onlinelibrary.wiley.com/doi/pdf/10.1111/j.1751-1097.1979.tb07129.x. https://onlinelibrary.wiley.com/doi/abs/10.1111/j.1751-1097.1979.tb07129.x.
Andersen, B.R., Brendzel, A.M., Lint, T.F., 1977. Chemiluminescence spectra of human myeloperoxidase and polymorphonuclear leukocytes. Infect. Immun. 17 (1), 62–66.
Asensi, M., Sastre, J., Pallardo, F.V., Lloret, A., Lehner, M., Garcia-de-la Asuncion, J., Viña, J., 1999. [23] Ratio of reduced to oxidized glutathione as indicator of oxidative stress status and DNA damage. In: Methods in Enzymology, vol. 299. Elsevier, pp. 267–276. https://doi.org/10.1016/S0076-6879(99)99026-2. https://linkinghub.elsevier.com/retrieve/pii/S0076687999990262.
Baader, W., Bohne, C., Cilento, G., Dunford, H., 1985. Peroxidase-catalyzed formation of triplet acetone and chemiluminescence from isobutyraldehyde and molecular oxygen. J. Biol. Chem. 260 (18), 10217–10225 publisher: ASBMB.
Babor, K., Kaláč, V., Tihlárik, K., 1973. Periodate oxidation of saccharides. III.* Comparison of the methods for determining the consumption of sodium periodate and the amount of formic acid formed. Chem. Zvesti 27 (5), 676–680.
Babuponnusami, A., Muthukumar, K., 2014. A review on Fenton and improvements to the Fenton process for wastewater treatment. J. Environ. Chem. Eng. 2 (1), 557–572. https://doi.org/10.1016/j.jece.2013.10.011. URL. http://linkinghub.elsevier.com/retrieve/pii/S2213343713002030.
Baier, J., Maisch, T., Maier, M., Engel, E., Landthaler, M., Bäumler, W., 2006. Singlet oxygen generation by UVA light exposure of endogenous photosensitizers. Biophys. J. 91 (4), 1452–1459. https://doi.org/10.1529/biophysj.106.082388. URL. https://www.ncbi.nlm.nih.gov/pmc/articles/PMC1518628/.
Balaban, R.S., Nemoto, S., Finkel, T., 2005. Mitochondria, Oxidants, and Aging, Cell 120 (4), 483–495. https://doi.org/10.1016/j.cell.2005.02.001. URL. https://linkinghub.elsevier.com/retrieve/pii/S0092867405001091.

Balasigamani, D., Usa, M., Inaba, H., 1997. Biophotons: ultraweak light emission from living systems. Curr. Opin. Solid State Mater. Sci. 2 (2), 188–193. https://doi.org/10.1016/S1359-0286(97)80064-2. URL. http://www.sciencedirect.com/science/article/pii/S1359028697800642.

Barrière, F., Kavanagh, P., Leech, D., 2006. A laccase–glucose oxidase biofuel cell prototype operating in a physiological buffer. Electrochim. Acta 51 (24), 5187–5192. https://doi.org/10.1016/j.electacta.2006.03.050. URL. https://linkinghub.elsevier.com/retrieve/pii/S001346860600288X.

Bastos, E.L., Farahani, P., Bechara, E.J., Baader, W.J., 2017. Four-membered cyclic peroxides: carriers of chemical energy. J. Phys. Org. Chem. 30 (9), e3725 https://doi.org/10.1002/poc.3725. URL.

Beauchamp, C., Fridovich, I., 1971. Superoxide dismutase: improved assays and an assay applicable to acrylamide gels. Anal. Biochem. 44 (1), 276–287. https://doi.org/10.1016/0003-2697(71)90370-8. URL. https://linkinghub.elsevier.com/retrieve/pii/0003269771903708.

Bechara, E.J., Wilson, T., 1980. Alkyl substituent effects on dioxetane properties. Tetraethyl-, dicyclohexylidene-, and 3, 4-dimethyl-3, 4-di-n-butyldioxetanes. A discussion of decomposition mechanisms. J. Org. Chem. 45 (26), 5261–5268.

Bechara, E.J., Oliveira, O.M., Duran, N., Baptista, R.C.d., Cilento, G., 1979. Peroxidase catalyzed generation of triplet acetone. Photochem. Photobiol. 30 (1), 101–110. URL. http://onlinelibrary.wiley.com/doi/10.1111/j.1751-1097.1979.tb07121.x/full.

Benderitter, M., Vincent-Genod, L., Pouget, J.P., Voisin, P., 2003. The cell membrane as a biosensor of oxidative stress induced by radiation exposure: a multiparameter investigation. Radiat. Res. 159 (4), 471–483. URL. http://www.jstor.org/stable/3580714.

Bereta, M., Teplan, M., Chafai, D.E., Radil, R., Cifra, M., 2021. Biological autoluminescence as a noninvasive monitoring tool for chemical and physical modulation of oxidation in yeast cell culture. Sci. Rep. 11, 328. https://doi.org/10.1038/s41598-020-79668-2. URL.

Bernabucci, U., Ronchi, B., Lacetera, N., Nardone, A., 2002. Markers of oxidative status in plasma and erythrocytes of transition dairy cows during hot season. J. Dairy Sci. 85 (9), 2173–2179. https://doi.org/10.3168/jds.S0022-0302(02)74296-3. URL. https://linkinghub.elsevier.com/retrieve/pii/S0022030202742963.

Bi, C., Tham, D.K.L., Perronnet, C., Joshi, B., Nabi, I.R., Moukhles, H., 2017. The oxidative stress-induced increase in the membrane expression of the water-permeable channel aquaporin-4 in astrocytes is regulated by caveolin-1 phosphorylation. Front. Cell. Neurosci. 11 https://doi.org/10.3389/fncel.2017.00412. URL. https://www.ncbi.nlm.nih.gov/pmc/articles/PMC5742350/.

Bilan, D.S., Matlashov, M.E., Gorokhovatsky, A.Y., Schultz, C., Enikolopov, G., Belousov, V.V., 2014. Genetically encoded fluorescent indicator for imaging NAD+/NADH ratio changes in different cellular compartments. Biochim. Biophys. Acta 1840 (3), 951–957. https://doi.org/10.1016/j.bbagen.2013.11.018. URL. https://www.ncbi.nlm.nih.gov/pmc/articles/PMC4398388/.

Birtic, S., Ksas, B., Genty, B., Mueller, M.J., Triantaphylidès, C., Havaux, M., 2011. Using spontaneous photon emission to image lipid oxidation patterns in plant tissues. Plant J. 67 (6), 1103–1115.

T. S. Blacker, Z. F. Mann, J. E. Gale, M. Ziegler, A. J. Bain, G. Szabadkai, M. R. Duchen, Separating NADH and NADPH fluorescence in live cells and tissues using FLIM, Nat. Commun. 5. doi:10.1038/ncomms4936. URL https://www.ncbi.nlm.nih.gov/pmc/articles/PMC4046109/.

Bögl, W., Heide, L., 1977. Chemiluminescence measurements as an identification method for gamma-irradiated foodstuffs. Radiat. Phys. Chem. 25 (1–3), 173–185. https://doi.org/10.1016/0146-5724(85)90262-6, 1985. https://linkinghub.elsevier.com/retrieve/pii/0146572485902626.

Bohne, C., Campa, A., Cilento, G., Nassi, L., Villablanca, M., 1986. Chlorophyll: an efficient detector of electronically excited species in biochemical systems. Anal. Biochem. 155 (1), 1–9.

Bouwstra, R., Goselink, R., Dobbelaar, P., Nielen, M., Newbold, J., van Werven, T., 2008. The relationship between oxidative damage and vitamin E concentration in blood, milk, and liver tissue from vitamin E supplemented and nonsupplemented periparturient heifers. J. Dairy Sci. 91 (3), 977–987. https://doi.org/10.3168/jds.2007-0596. URL. https://linkinghub.elsevier.com/retrieve/pii/S0022030208713535.

Boveris, A., Cadenas, E., Reiter, R., Filipowski, M., Nasake, Chance, B., 1980a. Organ chemiluminescence—noninvasive assay for oxidative radical reaction. Proc. Natl. Acad. Sci. U.S.A. 77, 347–351. URL. http://www.jstor.org/stable/pdf/8201.pdf.

Boveris, A., Sanchez, R.A., Varsavsky, A.I., Cadenas, E., 1980b. Spontaneous chemiluminescence of soybean seeds. FEBS (Fed. Eur. Biochem. Soc.) Lett. 113 (1), 29–32. https://doi.org/10.1016/0014-5793(80)80487-X. https://febs.onlinelibrary.wiley.com/doi/pdf/10.1016/0014-5793%2880%2980487-X. https://febs.onlinelibrary.wiley.com/doi/abs/10.1016/0014-5793%2880%2980487-X.

K. Brieger, S. Schiavone, J. Miller, K. Krause, Reactive oxygen species: from health to disease, Swiss Med. Wkly.doi:10.4414/smw.2012.13659. URL http://doi.emh.ch/smw.2012.13659.

Brigelius, R., Muckel, C., Akerboom, T.P., Sies, H., 1983. Identification and quantitation of glutathione in hepatic protein mixed disulfides and its relationship to glutathione disulfide. Biochem. Pharmacol. 32 (17), 2529–2534. https://doi.org/10.1016/0006-2952(83)90014-X. URL. https://linkinghub.elsevier.com/retrieve/pii/000629528390014X.

Briviba, K., Saha-Möller, C., Adam, W., Sies, H, 1996. Formation of singlet oxygen in the thermal decomposition of 3-hydroxymethyl-3,4,4-trimethyl-1,2-dioxetane, a chemical source of triplet-excited ketones. Biochem. Mol. Biol. Int. 38 (4), 647–651. URL. https://europepmc.org/article/med/8728092.

Burgos, R.C.R., Červinková, K., van der Laan, T., Ramautar, R., van Wijk, E.P., Cifra, M., Koval, S., Berger, R., Hankemeier, T., van der Greef, J., 2016. Tracking biochemical changes correlated with ultra-weak photon emission using metabolomics. J. Photochem. Photobiol. B Biol. 163, 237–245. https://doi.org/10.1016/j.jphotobiol.2016.08.030. URL. http://linkinghub.elsevier.com/retrieve/pii/S1011134416302871.

Burgos, R.C.R., Schoeman, J.C., Winden, L.J.v., Červinková, K., Ramautar, R., Van Wijk, E.P.A., Cifra, M., Berger, R., Hankemeier, T., Greef, J.v. d., 2017. Ultra-weak photon emission as a dynamic tool for monitoring oxidative stress metabolism. Sci. Rep. 7 (1), 1229. https://doi.org/10.1038/s41598-017-01229-x. URL. http://www.nature.com/articles/s41598-017-01229-x.

Cabiscol Català, E., Tamarit Sumalla, J., Ros Salvador, J., 2000. Oxidative stress in bacteria and protein damage by reactive oxygen species. Int. Microbiol. 3 (1), 3–8. Publisher: Springer-Verlag Ibérica.

Cadenas, E., Boveris, A., Chance, B., 1980. Low-level chemiluminescence of bovine heart submitochondrial particles. Biochem. J. 186 (3), 659–667. URL. http://www.biochemj.org/content/186/3/659.abstract.

Cadet, J., 2003. Oxidative damage to DNA: formation, measurement and biochemical features. Mutat. Res. Fund Mol. Mech. Mutagen 531 (1–2), 5–23. https://doi.org/10.1016/j.mrfmmm.2003.09.001. URL. https://linkinghub.elsevier.com/retrieve/pii/S0027510703001593.

Cadet, J., Douki, T., Ravanat, J.-L., Di Mascio, P., 2009. Sensitized formation of oxidatively generated damage to cellular DNA by UVA radiation. Photochem. Photobiol. Sci. 8 (7), 903. https://doi.org/10.1039/b905343n. URL. http://xlink.rsc.org/?DOI=b905343n.

Cameron, W.D., Bui, C.V., Hutchinson, A., Loppnau, P., Gräslund, S., Rocheleau, J.V., 2016. Apollo-NADP+: a spectrally tunable family of genetically encoded sensors for NADP+. Nat. Methods 13 (4), 352–358. https://doi.org/10.1038/nmeth.3764. URL. http://www.nature.com/articles/nmeth.3764.

Carmona, M., de Cubas, L., Bautista, E., Moral-Blanch, M., Medraño-Fernández, I., Sitia, R., Boronat, S., Ayté, J., Hidalgo, E., 2019. Monitoring cytosolic H2O2 fluctuations arising from altered plasma membrane gradients or from mitochondrial activity. Nat. Commun. 10 (1), 4526. https://doi.org/10.1038/s41467-019-12475-0. URL. http://www.nature.com/articles/s41467-019-12475-0.

Castillo, C., Hernandez, J., Bravo, A., Lopez-Alonso, M., Pereira, V., Benedito, J., 2005. Oxidative status during late pregnancy and early lactation in dairy cows. Vet. J. 169 (2), 286–292. https://doi.org/10.1016/j.tvjl.2004.02.001. URL. https://linkinghub.elsevier.com/retrieve/pii/S1090023304000449.

Castillo, C., Hernández, J., Valverde, I., Pereira, V., Sotillo, J., Alonso, M.L., Benedito, J., 2006. Plasma malonaldehyde (MDA) and total antioxidant status (TAS) during lactation in dairy cows. Res. Vet. Sci. 80 (2), 133–139. https://doi.org/10.1016/j.rvsc.2005.06.003. URL. https://linkinghub.elsevier.com/retrieve/pii/S0034528805001128.

Catalani, L.H., Wilson, T., Bechara, E.J.H., 1987. Two water-soluble fluorescence probes for chemiexcitation studies: sodium 9,10-dibromo- and 9, 10-diphenylanthracene-2-sulfonate. Synthesis, properties and application to triplet acetone and tetramethyldioxetane. Photochem. Photobiol. 45 (2), 273–281. https://onlinelibrary.wiley.com/doi/pdf/10.1111/j.1751-1097.1987.tb05375.x. https://onlinelibrary.wiley.com/doi/abs/10.1111/j.1751-1097.1987.tb05375.x.

Catalano, A., Rodilossi, S., Caprari, P., Coppola, V., Procopio, A., 2005. 5-Lipoxygenase regulates senescence-like growth arrest by promoting ROS-dependent p53 activation. EMBO J. 24 (1), 170–179. https://doi.org/10.1038/sj.emboj.7600502. URL. https://www.ncbi.nlm.nih.gov/pmc/articles/PMC544914/.

Celi, P., 2011. Biomarkers of oxidative stress in ruminant medicine. Immunopharmacol. Immunotoxicol. 33 (2), 233–240. https://doi.org/10.3109/08923973.2010.514917. URL. http://www.tandfonline.com/doi/full/10.3109/08923973.2010.514917.

Červinková, K., Nerudová, M., Hašek, J., Cifra, M., 2015. Chemical modulation of the ultra-weak photon emission from Saccharomyces cerevisiae and differentiated HL-60 cells. In: Tománek, P., Senderáková, D., Páta, P. (Eds.), Photonics, Devices, and Systems VI, vol. 9450. SPIE, pp. 169–175. https://doi.org/10.1117/12.2070424 backup Publisher: International Society for Optics and Photonics. doi:10.1117/12.2070424. URL.

Chaudhuri, S.K., Lovley, D.R., 2003. Electricity generation by direct oxidation of glucose in mediatorless microbial fuel cells. Nat. Biotechnol. 21 (10), 1229–1232. https://doi.org/10.1038/nbt867. URL. http://www.nature.com/articles/nbt867.

Chen, W.-L., Xing, D., He, Y.-H., 2002. Determination the vigor of rice seed with different degrees of aging with ultraweak chemiluminescence during early imbibition. Acta Bot. Sin. 44 (11), 1376–1379.

Cheun, B.S., Yi, S.H., Baik, K.Y., Lim, J.K., Yoo, J.S., Shin, H.W., Soh, K.S., 2007. Biophoton emission of MDCK cell with hydrogen peroxide and 60 Hz AC magnetic field. J. Environ. Biol. 28 (4), 735–740. URL. http://jeb.co.in/journal_issues/200710_oct07/paper_07.pdf.

Chorvat, D., Chorvatova, A., 2006. Spectrally resolved time-correlated single photon counting: a novel approach for characterization of endogenous fluorescence in isolated cardiac myocytes. Eur. Biophys. J. 36 (1), 73–83. https://doi.org/10.1007/s00249-006-0104-4. URL. http://link.springer.com/10.1007/s00249-006-0104-4.

Cifra, M., Pospíšil, P., 2014. Ultra-weak photon emission from biological samples: definition, mechanisms, properties, detection and applications. J. Photochem. Photobiol. B Biol. 139, 2–10. https://doi.org/10.1016/j.jphotobiol.2014.02.009. URL. https://www.sciencedirect.com/science/article/pii/S1011134414000463.

Cifra, M., Brouder, C., Nerudová, M., Kučera, O., 2015. Biophotons, coherence and photocount statistics: a critical review. J. Lumin. 164, 38–51. https://doi.org/10.1016/j.jlumin.2015.03.020. URL. http://linkinghub.elsevier.com/retrieve/pii/S0022231315001568.

Cilento, G., 1984. Generation of electronically excited triplet species in biochemical systems. Pure Appl. Chem. 56 (9), 1179–1190.

Cilento, G., Adam, W., 1988. Photochemistry and photobiology without light. Photochem. Photobiol. 48 (3), 361–368.
Cilento, G., de Baptista, R.C., Brunetti, I.L., 1994. Triplet carbonyls: from photophysics to biochemistry. J. Mol. Struct. 324 (1–2), 45–48.
Cohen, S., Popp, F., 1997. Biophoton emission of the human body. J. Photochem. Photobiol. B Biol. 40 (2), 187–189.
Colli, L., 1955. Further measurement of the bioluminescence of the seedings. Experientia 11, 479–481.
Collins, A.R., Dusinska, M., Gedik, C.M., Stetina, R., 1996. Oxidative damage to DNA: do we have a reliable biomarker? Environ. Health Perspect. 104, 5.
Crichton, R.R., Wilmet, S., Legssyer, R., Ward, R.J., 2002. Molecular and cellular mechanisms of iron homeostasis and toxicity in mammalian cells. J. Inorg. Biochem. 91 (1), 9–18. https://doi.org/10.1016/S0162-0134(02)00461-0. URL. http://www.sciencedirect.com/science/article/pii/S0162013402004610.
Cristiana, F., Elena, A., 2018. Reactive Oxygen Species (ROS) in Living Cells. BoD – Books on Demand google-Books-ID: hnCQDwAAQBAJ.
Dalle-Donne, I., Rossi, R., Giustarini, D., Milzani, A., Colombo, R., 2003. Protein carbonyl groups as biomarkers of oxidative stress. Clin. Chim. Acta 329 (1–2), 23–38. https://doi.org/10.1016/S0009-8981(03)00003-2. URL. http://linkinghub.elsevier.com/retrieve/pii/S0009898103000032.
Das, K., Roychoudhury, A., 2014. Reactive oxygen species (ROS) and response of antioxidants as ROS-scavengers during environmental stress in plants. Front. Environ. Sci. 2, 53–65. https://doi.org/10.3389/fenvs.2014.00053. URL. http://journal.frontiersin.org/article/10.3389/fenvs.2014.00053/abstract.
Datz, C., Felder, T.K., Niederseer, D., Aigner, E., 2013. Iron homeostasis in the metabolic syndrome. Eur. J. Clin. Invest. 43 (2), 215–224. https://doi.org/10.1111/eci.12032. URL. https://onlinelibrary.wiley.com/doi/abs/10.1111/eci.12032.
Davies, M.J., 2016. Detection and characterisation of radicals using electron paramagnetic resonance (EPR) spin trapping and related methods. Methods 109, 21–30. https://doi.org/10.1016/j.ymeth.2016.05.013. URL. https://linkinghub.elsevier.com/retrieve/pii/S1046202316301438.
Davies, M.J., Hawkins, C.L., Pattison, D.I., Rees, M.D., 2008. Mammalian heme peroxidases: from molecular mechanisms to health implications. Antioxidants Redox Signal. 10 (7), 1199–1234. https://doi.org/10.1089/ars.2007.1927. URL. http://www.liebertpub.com/doi/10.1089/ars.2007.1927.
de la Haba, C., Palacio, J.R., Martínez, P., Morros, A., 2013. Effect of oxidative stress on plasma membrane fluidity of THP-1 induced macrophages. Biochim. Biophys. Acta Biomembr. 1828 (2), 357–364. https://doi.org/10.1016/j.bbamem.2012.08.013. URL. https://linkinghub.elsevier.com/retrieve/pii/S0005273612002945.
de Medeiros, M.H., Bechara, E.J., 1986. Chemiluminescent aerobic oxidation of protein adducts with glycolaldehyde catalyzed by horseradish peroxidase. Arch. Biochem. Biophys. 248 (1), 435–439. https://doi.org/10.1016/0003-9861(86)90441-8. URL. https://linkinghub.elsevier.com/retrieve/pii/0003986186904418.
de Mello, C., 2014. Gallep, Ultraweak, spontaneous photon emission in seedlings: toxicological and chronobiological applications: UPE in seedlings - applications. Luminescence 29 (8), 963–968. https://doi.org/10.1002/bio.2658. URL.
Deneke, C.F., Krinsky, N.I., 1977. Inhibition and enhancement of singlet oxygen ('Ag) dimol chemiluminescence. Photochem. Photobiol. 25 (3), 299–304.
Deponte, M., 2013. Glutathione catalysis and the reaction mechanisms of glutathione-dependent enzymes. Biochim. Biophys. Acta Gen. Subj. 1830 (5), 3217–3266. https://doi.org/10.1016/j.bbagen.2012.09.018. URL. https://linkinghub.elsevier.com/retrieve/pii/S0304416512002735.
Desai, I.D., 1984. [16] Vitamin E analysis methods for animal tissues. In: Methods in Enzymology, vol. 105. Academic Press, pp. 138–147. https://doi.org/10.1016/S0076-6879(84)05019-9 of Oxygen Radicals in Biological Systems. https://www.sciencedirect.com/science/article/pii/S0076687984050199.
Desmarchelier, C., Repetto, M., Coussio, J., Llesuy, S., Ciccia, G., 1997. Total reactive antioxidant potential (TRAP) and total antioxidant reactivity (TAR) of medicinal plants used in southwest amazonia (Bolivia and Peru). Int. J. Pharmacogn. 35 (4), 288–296. https://doi.org/10.1076/phbi.35.4.288.13303. URL. https://www.tandfonline.com/doi/full/10.1076/phbi.35.4.288.13303.
Di Mascio, P., Sies, H., 1989. Detection and quantification of singlet oxygen generated by thermolysis of a water-soluble endoperoxide. J. Am. Chem. Soc. 111, 2909–2914.
Di Mascio, P., Bechara, E.J.H., Medeiros, M.H.G., Briviba, K., Sies, H., 1994. Singlet molecular oxygen production in the reaction of peroxynitrite with hydrogen peroxide. FEBS (Fed. Eur. Biochem. Soc.) Lett. 355 (3), 287–289. https://febs.onlinelibrary.wiley.com/doi/pdf/10.1016/0014-5793%2894%2901224-5. https://febs.onlinelibrary.wiley.com/doi/abs/10.1016/0014-5793%2894%2901224-5.
Di Mascio, P., Martinez, G.R., Miyamoto, S., Ronsein, G.E., Medeiros, M.H.G., Cadet, J., 2016. Singlet molecular oxygen: Düsseldorf – São Paulo, the Brazilian connection. Arch. Biochem. Biophys. 595, 161–175. https://doi.org/10.1016/j.abb.2015.11.016. URL. http://www.sciencedirect.com/science/article/pii/S0003986115003707.
Di Mascio, P., Martinez, G.R., Miyamoto, S., Ronsein, G.E., Medeiros, M.H.G., Cadet, J., 2019. Singlet molecular oxygen reactions with nucleic acids, lipids, and proteins. Chem. Rev. 119 (3), 2043–2086. https://doi.org/10.1021/acs.chemrev.8b00554. URL. https://pubs.acs.org/doi/10.1021/acs.chemrev.8b00554.
Dickens, F., 1936. Mechanism of carbohydrate oxidation. Nature 138 (3503), 1057–1057, publisher: Nature Publishing Group.
Dizdaroglu, M., 1991. Chemical determination of free radical-induced damage to DNA. Free Radic. Biol. Med. 10 (3–4), 225–242. https://doi.org/10.1016/0891-5849(91)90080-M. URL. https://linkinghub.elsevier.com/retrieve/pii/089158499190080M.
Dunford, H., Baader, W.J., Bohne, C., Cilento, G., 1984. On the mechanism of peroxidase-catalyzed chemiluminescence from isobutyraldehyde. Biochem. Biophys. Res. Commun. 122 (1), 28–32 doi:10.1016/0006-291X(84)90434-0. URL. https://linkinghub.elsevier.com/retrieve/pii/0006291X84904340.
Durán, N., Cilento, G., 1980. Long-range triplet-singlet energy transfer from enzyme generated triplet acetone to xanthene dyes. Photochem. Photobiol. 32 (1), 113–116, 10.1111/j.1751-1097.1980.tb03997.x. URL. https://onlinelibrary.wiley.com/doi/pdf/10.1111/j.1751-1097.1980.tb03997.x. https://onlinelibrary.wiley.com/doi/abs/10.1111/j.1751-1097.1980.tb03997.x.
Emmerie, A., Engel, C., 1938. Colorimetric determination of α-tocopherol (vitamin E). Recl. Trav. Chim. Pays-Bas 57 (12), 1351–1355 (publisher: Wiley Online Library).
Eng, J., Lynch, R., Balaban, R., 1989. Nicotinamide adenine dinucleotide fluorescence spectroscopy and imaging of isolated cardiac myocytes. Biophys. J. 55 (4), 621–630. https://doi.org/10.1016/S0006-3495(89)82859-0. URL. https://linkinghub.elsevier.com/retrieve/pii/S0006349589828590.
Escobar, J.A., Cilento, G., Nascimento, A.L.T.O., 1990. Effects induced in neutrophils by a precursor of triplet acetone. Photochem. Photobiol. 51 (6), 713–717. https://doi.org/10.1111/php.1990.51.6.713. URL.
Esterbauer, H., Schaur, R.J., Zollner, H., 1991. Chemistry and biochemistry of 4-hydroxynonenal, malonaldehyde and related aldehydes. Free Radic. Biol. Med. 11 (1), 81–128. https://doi.org/10.1016/0891-5849(91)90192-6. URL. https://linkinghub.elsevier.com/retrieve/pii/0891584991901926.
Evelson, P., Ordóñez, C.P., Llesuy, S., Boveris, A., 1997. Oxidative stress and in vivo chemiluminescence in mouse skin exposed to UVA radiation. J. Photochem. Photobiol. B Biol. 38 (2–3), 215–219. https://doi.org/10.1016/S1011-1344(96)07437-4. URL. https://linkinghub.elsevier.com/retrieve/pii/S1011134496074374.
Fam, S., Morrow, J., 2003. The isoprostanes: unique products of arachidonic acid oxidation-A review. Curr. Med. Chem. 10 (17), 1723–1740. https://doi.org/10.2174/0929867033457115. URL. http://www.eurekaselect.com/openurl/content.php?genre=article&issn=0929-8673&volume=10&issue=17&spage=1723.
Farneth, W.E., Johnson, D.G., 1984. Chemiluminescence in the infrared photochemistry of oxetanes: the formal reverse of ketone photocycloaddition. J. Am. Chem. Soc. 106 (6), 1875–1876. https://doi.org/10.1021/ja00318a074. URL. https://pubs.acs.org/doi/abs/10.1021/ja00318a074.
Fedoroňko, M., Füleová, E., Danieliszyn, W., 1973. Estimation of DL-glyceraldehyde, dihydroxyacetone, methylglyoxal, and their mixtures by oxidation with sodium periodate. Chem. Zvesti 7.
Fels, D., Cifra, M., Scholkmann, F. (Eds.), 2015. Fields of the Cell. Research Signpost, Trivandrum, India. URL. https://www.researchgate.net/publication/281409607_Fields_of_the_cell.
Finkel, T., 2011. Signal transduction by reactive oxygen species. J. Cell Biol. 194 (1), 7–15. https://doi.org/10.1083/jcb.201102095. URL. http://www.jcb.org/lookup/doi/10.1083/jcb.201102095.
Flor-Henry, M., McCabe, T.C., De Bruxelles, G.L., Roberts, M.R., 2004. Use of a highly sensitive two-dimensional luminescence imaging system to monitor endogenous bioluminescence in plant leaves. BMC Plant Biol. 4 (1), 19. https://bmcplantbiol.biomedcentral.com/articles/10.1186/1471-2229-4-19.
Frei, B., Yamamoto, Y., Niclas, D., Ames, B.N., 1988. Evaluation of an isoluminol chemiluminescence assay for the detection of hydroperoxides in human blood plasma. Anal. Biochem. 175 (1), 120–130 publisher: Elsevier.
Furdui, C.M., Poole, L.B., 2014. Chemical approaches to detect and analyze protein sulfenic acids. Mass Spectrom. Rev. 33 (2), 126–146. https://doi.org/10.1002/mas.21384. URL. https://www.ncbi.nlm.nih.gov/pmc/articles/PMC3946320/.
Gallep, C.M., Dos Santos, S.R., 2007. Photon-counts during germination of wheat (Triticum aestivum) in wastewater sediment solutions correlated with seedling growth. Seed Sci. Technol. 35 (3), 607–614. URL. http://www.ingentaconnect.com/content/ista/sst/2007/00000035/00000003/art00008.
Gallep, C.d.M., Robert, D., 2020. Time-resolved ultra-weak photon emission as germination performance indicator in single seedlings. J. Photochem. Photobiol., A 1, 100001. https://doi.org/10.1016/j.jpap.2020.100001. URL. https://linkinghub.elsevier.com/retrieve/pii/S2666469020300014.
Gallep, C.M., Moraes, T.A., Červinková, K., Cifra, M., Katsumata, M., Barlow, P.W., 2014. Lunisolar tidal synchronism with biophoton emission during intercontinental wheat-seedling germination tests. Plant Signal. Behav. 9 (5), e28671 https://doi.org/10.4161/psb.28671. URL. http://www.tandfonline.com/doi/abs/10.4161/psb.28671.
Gallep, C.M., Viana, J.F., Cifra, M., Clarke, D., Robert, D., 2018. Peter Barlow's insights and contributions to the study of tidal gravity variations and ultra-weak light emissions in plants. Ann. Bot. 122 (5), 757–766. https://doi.org/10.1093/aob/mcx176. URL. http://academic.oup.com/aob/advance-article/doi/10.1093/aob/mcx176/4782486.
Gay, C.A., Gebicki, J.M., 2003. Measurement of protein and lipid hydroperoxides in biological systems by the ferric–xylenol orange method. Anal. Biochem. 315 (1), 29–35. https://doi.org/10.1016/S0003-2697(02)00606-1. URL. https://linkinghub.elsevier.com/retrieve/pii/S0003269702006061.
Georgiou, C.D., Zisimopoulos, D., Argyropoulou, V., Kalaitzopoulou, E., Salachas, G., Grune, T., 2018. Protein and cell wall polysaccharide carbonyl determination by a neutral pH 2,4-dinitrophenylhydrazine-based photometric assay. Redox Biol. 17, 128–142. https://doi.org/10.1016/j.redox.2018.04.010. URL. https://linkinghub.elsevier.com/retrieve/pii/S2213231718302088.
Gibson, D.T., Parales, R.E., 2000. Aromatic hydrocarbon dioxygenases in environmental biotechnology. Curr. Opin. Biotechnol. 11 (3), 236–243. https://doi.org/10.1016/S0958-1669(00)00090-2. URL. https://linkinghub.elsevier.com/retrieve/pii/S0958166900000902.
Gilardi, G., Fantuzzi, A., 2001. Manipulating redox systems: application to nanotechnology. Trends Biotechnol. 19 (11), 468–476. https://doi.org/10.1016/S0167-7799(01)01769-3. URL. https://linkinghub.elsevier.com/retrieve/pii/S0167779901017693.
Gonzalez, F.J., 2005. Role of cytochromes P450 in chemical toxicity and oxidative stress: studies with CYP2E1. Mutat. Res. Fund Mol. Mech. Mutagen 569 (1–2), 101–110.

https://doi.org/10.1016/j.mrfmmm.2004.04.021. URL. https://linkinghub.elsevier.com/retrieve/pii/S0027510704003756.
Gorton, L., Domınguez, E., 2002. Electrocatalytic oxidation of NAD(P)H at mediator-modified electrodes. Rev. Mol. Biotechnol. 82, 22.
Grammatico, P., Maresca, V., Roccella, F., Roccella, M., Biondo, L., Catricalà, C., Picardo, M., 1998. Increased sensitivity to peroxidizing agents is correlated with an imbalance of antioxidants in normal melanocytes from melanoma patients. Exp. Dermatol. 7 (4), 205–212. https://doi.org/10.1111/j.1600-0625.1998.tb00325.x. URL.
Griffiths, H.R., Møller, L., Bartosz, G., Bast, A., Bertoni-Freddari, C., Collins, A., Cooke, M., Coolen, S., Haenen, G., Hoberg, A.-M., 2002. Others, Biomarkers, Molecular Aspects of Medicine, vol. 23. publisher: Pergamon, pp. 101–208, 1-3.
Grönqvist, S., Viikari, L., Niku-Paavola, M.-L., Orlandi, M., Canevali, C., Buchert, J., 2005. Oxidation of milled wood lignin with laccase, tyrosinase and horseradish peroxidase. Appl. Microbiol. Biotechnol. 67 (4), 489–494. https://doi.org/10.1007/s00253-004-1800-6. URL. http://link.springer.com/10.1007/s00253-004-1800-6.
Gross, E., Sevier, C.S., Heldman, N., Vitu, E., Bentzur, M., Kaiser, C.A., Thorpe, C., Fass, D., 2006. Generating disulfides enzymatically: reaction products and electron acceptors of the endoplasmic reticulum thiol oxidase Ero1p. Proc. Natl. Acad. Sci. USA 103 (2), 299–304. https://doi.org/10.1073/pnas.0506448103. URL. http://www.pnas.org/cgi/doi/10.1073/pnas.0506448103.
Gupta, D., Harish, B., Kissner, R., Koppenol, W.H., 2009. Peroxynitrate is formed rapidly during decomposition of peroxynitrite at neutral pH. Dalton Trans. 29, 5730. https://doi.org/10.1039/b905535e. URL. http://xlink.rsc.org/?DOI=b905535e.
Gupta, V., Paritala, H., Carroll, K.S., 2016. Reactivity, selectivity, and stability in sulfenic acid detection: a comparative study of nucleophilic and electrophilic probes. Bioconjugate Chem. 27 (5), 1411–1418. https://doi.org/10.1021/acs.bioconjchem.6b00181. URL. https://pubs.acs.org/doi/10.1021/acs.bioconjchem.6b00181.
Guthrie, R., 1962. The “dialdehydes” from the periodate oxidation of carbohydrates. In: Advances in Carbohydrate Chemistry, vol. 16, pp. 105–158. Elsevier.
Hall, R.D., Chignell, C.F., 1987. Steady-state near-infrared detection of singlet molecular oxygen: a Stern-Volmer quenching experiment with sodium azide. Photochem. Photobiol. 45 (4), 459–464.
Halliwell, B., Dizdaroglu, M., 1992. Commentary the measurement of oxidative damage to DNA by HPLC and GC/MS techniques. Free Radic. Res. Commun. 16 (2), 75–87. https://doi.org/10.3109/10715769209049161. URL. http://www.tandfonline.com/doi/full/10.3109/10715769209049161.
Hampton, M.B., Kettle, A.J., Winterbourn, C.C., 1998. Inside the neutrophil phagosome: oxidants, myeloperoxidase, and bacterial killing. J. Am. Soci. Hematol. 92 (9), 3007–3017.
Hartwig, A., 1996. Sensitive analysis of oxidative DNA damage in mammalian cells: use of the bacterial Fpg protein in combination with alkaline unwinding. Toxicol. Lett. 88 (1–3), 85–90. https://doi.org/10.1016/0378-4274(96)03722-8. URL. https://linkinghub.elsevier.com/retrieve/pii/0378427496037228.
Hashim, S.A., Schuttringer, G.R., 1966. others, Rapid determination of tocopherol in macro-and microquantities of plasma. Results obtained in various nutrition and metabolic studies. Am. J. Clin. Nutr. 19, 137–145.
Havaux, M., Triantaphylides, C., Genty, B., 2006. Autoluminescence imaging: a non-invasive tool for mapping oxidative stress. Trends Plant Sci. 11 (10), 480–484.
Hawkins, C.L., Davies, M.J., 2001. Generation and propagation of radical reactions on proteins. Biochim. Biophys. Acta Bioenerg. 1504 (2–3), 196–219. https://doi.org/10.1016/S0005-2728(00)00252-8. URL. http://linkinghub.elsevier.com/retrieve/pii/S0005272800002528.
Hawkins, C.L., Davies, M.J., 2014. Detection and characterisation of radicals in biological materials using EPR methodology. Biochim. Biophys. Acta Gen. Subj. 1840 (2), 708–721. https://doi.org/10.1016/j.bbagen.2013.03.034. URL. https://linkinghub.elsevier.com/retrieve/pii/S0304416513001281.
Hawkins, C.L., Davies, M.J., 2019. Detection, identification, and quantification of oxidative protein modifications. J. Biol. Chem. 294 (51), 19683–19708. https://doi.org/10.1074/jbc.REV119.006217. URL. https://www.ncbi.nlm.nih.gov/pmc/articles/PMC6926449/.
Hawkins, C.L., Morgan, P.E., Davies, M.J., 2009. Quantification of protein modification by oxidants. Free Radic. Biol. Med. 46 (8), 965–988. https://doi.org/10.1016/j.freeradbiomed.2009.01.007. URL. https://linkinghub.elsevier.com/retrieve/pii/S089158490900029X.
Heikal, A.A., 2010. Intracellular coenzymes as natural biomarkers for metabolic activities and mitochondrial anomalies. Biomarkers Med. 4 (2), 241–263. https://doi.org/10.2217/bmm.10.1. URL. https://www.futuremedicine.com/doi/10.2217/bmm.10.1.
Held, A.M., Halko, D.J., Hurst, J.K., 1978. Mechanisms of chlorine oxidation of hydrogen peroxide. J. Am. Chem. Soc. 100 (18), 5732–5740. https://doi.org/10.1021/ja00486a025. URL. https://pubs.acs.org/doi/abs/10.1021/ja00486a025.
Hideg, È., 1993. On the spontaneous ultraweak light emission of plants. J. Photochem. Photobiol. B Biol. 18 (2), 239–244.
Hideg, E., Inaba, H., 1991. Biophoton emission (ultraweak photoemission) from dark adapted spinach chloroplasts. Photochem. Photobiol. 53 (1), 137–142.
Hideg, È., Kobayashi, M., Inaba, H., 1991. Spontaneous ultraweak light emission from respiring spinach leaf mitochondria. Biochim. Biophys. Acta Bioenerg. 1098 (1), 27–31.
Hidiroglou, N., McDowell, L.R., Balbuena, O., 1989. Plasma tocopherol in sheep and cattle after ingesting free or acetylated Tocopherol1,2. J. Dairy Sci. 72 (7), 7.
Hollmann, F., Arends, I.W.C.E., Buehler, K., Schallmey, A., Bühler, B., 2011. Enzyme-mediated oxidations for the chemist. Green Chem. 13 (2), 226–265. https://doi.org/10.1039/C0GC00595A. URL. http://xlink.rsc.org/?DOI=C0GC00595A.
Iida, T., Yoshiki, Y., Someya, S., Okubo, K., 2002. Generation of reactive oxygen species and photon emission from a browned product. Biosci., Biotechnol., Biochem. 66 (8), 1641–1645. https://doi.org/10.1271/bbb.66.1641. URL. http://www.tandfonline.com/doi/full/10.1271/bbb.66.1641.
Inagaki, H., Imaizumi, T., Wang, G.-X., Tominaga, T., Kato, K., Iyozumi, H., Nukui, H., 2007. Spontaneous ultraweak photon emission from rice (Oryza sativa L.) and paddy weeds treated with a sulfonylurea herbicide. Pestic. Biochem. Physiol. 89 (2), 158–162. https://doi.org/10.1016/j.pestbp.2007.05.005. URL. http://linkinghub.elsevier.com/retrieve/pii/S004835750700082X.
Inagaki, H., Imaizumi, T., Wang, G.-X., Tominaga, T., Kato, K., Iyozumi, H., Nukui, H., 2009. Sulfonylurea-resistant biotypes of Monochoria vaginalis generate higher ultraweak photon emissions than the susceptible ones. Pestic. Biochem. Physiol. 95 (3), 117–120.
Ivanova, I.P., Trofimova, S.V., Piskarev, I.M., Aristova, N.A., Burhina, O.E., Soshnikova, O.O., 2012. Mechanism of chemiluminescence in Fenton reaction, 01 J. Biophys. Chem. 3, 88–100. https://doi.org/10.4236/jbpc.2012.31011.
Jamnik, P., Raspor, P., 2003. Stress response of yeastcandida intermedia to Cr(VI). J. Biochem. Mol. Toxicol. 17 (6), 316–323. https://doi.org/10.1002/jbt.10093. URL.
Jamnik, P., Raspor, P., 2005. Methods for monitoring oxidative stress response in yeasts. J. Biochem. Mol. Toxicol. 19 (4), 195–203. https://doi.org/10.1002/jbt.20091 doi: 10.1002/jbt.20091.
Janero, D.R., 1990. Malondialdehyde and thiobarbituric acid-reactivity as diagnostic indices of lipid peroxidation and peroxidative tissue injury. Free Radic. Biol. Med. 9 (6), 515–540. https://doi.org/10.1016/0891-5849(90)90131-2. URL. https://linkinghub.elsevier.com/retrieve/pii/0891584990901312.
Jeon, J.-R., Chang, Y.-S., 2013. Laccase-mediated oxidation of small organics: bifunctional roles for versatile applications. Trends Biotechnol. 31 (6), 335–341. https://doi.org/10.1016/j.tibtech.2013.04.002. URL. https://linkinghub.elsevier.com/retrieve/pii/S0167799913000747.
Jeon, J.-R., Baldrian, P., Murugesan, K., Chang, Y.-S., 2012. Laccase-catalysed oxidations of naturally occurring phenols: from in vivo biosynthetic pathways to green synthetic applications. Microb. Biotechnol. 5 (3), 318–332. https://sfamjournals.onlinelibrary.wiley.com/doi/pdf/10.1111/j.1751-7915.2011.00273.x.doi:10.1111/j.1751-7915.2011.00273.x. https://sfamjournals.onlinelibrary.wiley.com/doi/abs/10.1111/j.1751-7915.2011.00273.x.
Jessup, W., Dean, R.T., Gebicki, J.M., 1994. [29] Iodometric determination of hydroperoxides in lipids and proteins. In: Methods in Enzymology, vol. 233. Elsevier, pp. 289–303. https://doi.org/10.1016/S0076-6879(94)33032-8. URL. https://linkinghub.elsevier.com/retrieve/pii/S0076687994330328.
Kageyama, C., Kato, K., Iyozumi, H., Inagaki, H., Yamaguchi, A., Furuse, K., Baba, K., 2006. Photon emissions from rice cells elicited by N-acetylchitooligosaccharide are generated through phospholipid signaling in close association with the production of reactive oxygen species. Plant Physiol. Biochem. 44 (11–12), 901–909. https://doi.org/10.1016/j.plaphy.2006.09.010. URL. http://linkinghub.elsevier.com/retrieve/pii/S098194280600132X.
Kanofsky, J.R., 1983. Singlet oxygen production by lactoperoxidase. J. Biol. Chem. 258 (10), 5991–5993. https://doi.org/10.1016/S0021-9258(18)32358-5. URL. https://linkinghub.elsevier.com/retrieve/pii/S0021925818323585.
Kanofsky, J.R., 2000. [6] Assay for singlet-oxygen generation by peroxidases using 1270-nm chemiluminescence. In: Methods in Enzymology, vol. 319, pp. 59–67. https://doi.org/10.1016/S0076-6879(00)19008-1. Elsevier. https://linkinghub.elsevier.com/retrieve/pii/S0076687900190081.
Karadag, A., Ozcelik, B., Saner, S., 2009. Review of methods to determine antioxidant capacities. Food Anal. Methods 2 (1), 41–60. https://doi.org/10.1007/s12161-008-9067-7. URL. http://link.springer.com/10.1007/s12161-008-9067-7.
Kataoka, Y., Cui, Y., Yamagata, A., Niigaki, M., Hirohata, T., Oishi, N., Watanabe, Y., 2001. Activity-dependent neural tissue oxidation emits intrinsic ultraweak photons. Biochem. Biophys. Res. Commun. 285 (4), 1007–1011. https://doi.org/10.1006/bbrc.2001.5285. URL. http://linkinghub.elsevier.com/retrieve/pii/S0006291X01952854.
Katerji, M., Filippova, M., Duerksen-Hughes, P., 2019. Approaches and Methods to Measure Oxidative Stress in Clinical Samples: Research Applications in the Cancer Field, Oxidative Medicine and Cellular Longevity 2019, pp. 1–29. https://doi.org/10.1155/2019/1279250. URL. https://www.hindawi.com/journals/omcl/2019/1279250/.
Kato, K., Iyozumi, H., Kageyama, C., Inagaki, H., Yamaguchi, A., Nukui, H., 2014. Application of ultra-weak photon emission measurements in agriculture. J. Photochem. Photobiol. B Biol. 139, 54–62. https://doi.org/10.1016/j.jphotobiol.2014.06.010. URL. http://linkinghub.elsevier.com/retrieve/pii/S1011134414002024.
Kazakov, D.V., Kazakov, V.P., Maistrenko, G.Y., Mal’zev, D.V., Schmidt, R., 2007. On the effect of 1,4-diazabicyclo[2.2.2]octane on the singlet-oxygen dimol emission: chemical generation of (^{1} O $_2$) $_2$ in peroxide reactions. J. Phys. Chem. 111 (20), 4267–4273. https://doi.org/10.1021/jp070629p. URL. http://pubs.acs.org/doi/abs/10.1021/jp070629p.
Khabiri, F., Hagens, R., Smuda, C., Soltau, A., Schreiner, V., Wenck, H., Wittern, K.-P., Duchstein, H.-J., Mei, W., 2008. Non-invasive monitoring of oxidative skin stress by ultraweak photon emission (UPE)-measurement. I: mechanisms of UPE of biological materials. Skin Res. Technol. 14 (1), 103–111.
Kim, J., Kim, Y.-u., Lee, Y.J., Kobayashi, M., Tsutsumi, Y., Kondo, R., Lee, S.K., Soh, K.-S., 2007a. Spontaneous ultraweak photon emission during the growth of the cell population of cultured HeLa cell line. J. Health Sci. 53 (4), 481–485.
Kim, J., Kim, Y.-u., Lee, Y.J., Han, J., You, H., Kondo, R., Lee, S.K., Soh, K.-S., 2007b. Analysis of changes in the intensities of spontaneous ultraweak photon emission during the growth of the cell population of cultured HeLa cell line. In: World Congress on Medical Physics and Biomedical Engineering 2006. Springer,

pp. 3619–3622. URL. http://link.springer.com/chapter/10.1007/978-3-540-36841-0_916.
Kim, K.Y., Lee, C., Ryu, B.H., 2007c. Chemiluminescence properties of gamma-ray irradiated LDPE. In: 2007 IEEE International Conference on Solid Dielectrics, IEEE, Winchester, pp. 231–234. https://doi.org/10.1109/ICSD.2007.4290794. URL. http://ieeexplore.ieee.org/document/4290794/.
Kiryu, C., Makiuchi, M., Miyazaki, J., Fujinaga, T., Kakinuma, K., 1999. Physiological production of singlet molecular oxygen in the myeloperoxidase-H2O2-chloride system. FEBS (Fed. Eur. Biochem. Soc.) Lett. 443 (2), 154–158. https://doi.org/10.1016/S0014-5793(98)01700-1. https://febs.onlinelibrary.wiley.com/doi/pdf/10.1016/S0014-5793%2898%2901700-1. https://febs.onlinelibrary.wiley.com/doi/abs/10.1016/S0014-5793%2898%2901700-1.
Klebanoff, S.J., 1980. Oxygen metabolism and the toxic properties of phagocytes. Ann. Intern. Med. 93 (3), 480. https://doi.org/10.7326/0003-4819-93-3-480. URL. http://annals.org/article.aspx?doi=10.7326/0003-4819-93-3-480.
Knudsen, F.S., Penatti, C.A.A., Royer, L.O., Bidart, K.A., Christoff, M., Ouchi, D., Bechara, E.J.H., 2000. Chemiluminescent aldehyde and β-diketone reactions promoted by peroxynitrite. Chem. Res. Toxicol. 13 (5), 317–326. https://doi.org/10.1021/tx990176i. URL. https://pubs.acs.org/doi/10.1021/tx990176i.
Kobayashi, M., 2014. Highly sensitive imaging for ultra-weak photon emission from living organisms. J. Photochem. Photobiol. B Biol. 139, 34–38. https://doi.org/10.1016/j.jphotobiol.2013.11.011. URL. http://linkinghub.elsevier.com/retrieve/pii/S1011134413002558.
Kobayashi, M., Inaba, H., 2000. Photon statistics and correlation analysis of ultraweak light originating from living organisms for extraction of biological information. Appl. Opt. 39 (1), 183–192. URL. https://www.osapublishing.org/abstract.cfm?uri=ao-39-1-183.
Kobayashi, M., Takeda, M., Sato, T., Yamazaki, Y., Kaneko, K., Ito, K.-I., Kato, H., Inaba, H., 1999. In vivo imaging of spontaneous ultraweak photon emission from a rat's brain correlated with cerebral energy metabolism and oxidative stress. Neurosci. Res. 34 (2), 103–113. http://www.sciencedirect.com/science/article/pii/S0168010299000401.
Kobayashi, M., Sasaki, K., Enomoto, M., Ehara, Y., 2006. Highly sensitive determination of transient generation of biophotons during hypersensitive response to cucumber mosaic virus in cowpea. J. Exp. Bot. 58 (3), 465–472. https://doi.org/10.1093/jxb/erl215. URL. http://jxb.oxfordjournals.org/lookup/doi/10.1093/jxb/erl215.
Kočar, D., Luiz Pedersoli, J., Strlič, M., Kolar, J., Rychlý, J., Matisová-Rychlá, L., 2004. Chemiluminescence from paper. Polym. Degrad. Stabil. 86 (2), 269–274. https://doi.org/10.1016/j.polymdegradstab.2004.05.005. URL. http://linkinghub.elsevier.com/retrieve/pii/S0141391004001296.
Kochel, B., 1990. Perturbed living organisms: a cybernetic approach founded on photon emission stochastic processes. Kybernetes 19 (6), 16–25. https://doi.org/10.1108/eb005865 publisher: MCB UP Ltd. doi:10.1108/eb005865. URL.
Kochel, B., 1995. Perturbed living organisms: a cybernetic approach to oscillatory luminescence. Kybernetes 24 (4), 53–76. https://doi.org/10.1108/03684929510089358 publisher: MCB UP Ltd. doi:10.1108/03684929510089358.
Kochevar, I.E., Redmond, R.W., 2000. [2] Photosensitized production of singlet oxygen. In: Methods in Enzymology, vol. 319. Elsevier, pp. 20–28. https://doi.org/10.1016/S0076-6879(00)19004-4. https://linkinghub.elsevier.com/retrieve/pii/S0076687900190044.
Konev, S., Lyskova, T., Gd, N., 1966. Very weak bioluminescence of cells in ultraviolet region of spectrum and its biological role. BIOPHYSICS-USSR 11 (2), 410.
Kumar, A., Prasad, A., Sedlářová, M., Pospíšil, P., 2019. Characterization of protein radicals in Arabidopsis. Front. Physiol. 10 https://doi.org/10.3389/fphys.2019.00958. URL. https://www.frontiersin.org/articles/10.3389/fphys.2019.00958/full.
Kuzmenko, A.I., Morozova, R.P., Nikolenko, I.A., Donchenko, G.V., Richheimer, S.L., Bailey, D.T., 1999. Chemiluminescence determination of the in vivo and in vitro antioxidant activity of RoseOx® and carnosic acid. J. Photochem. Photobiol. B Biol. 48 (1), 63–67 (publisher: Elsevier).
Laager, F., Becker, N., Park, S.-H., Soh, K.-S., 2009. Effects of lac operon activation, deletion of the yhha gene, and the removal of oxygen on the ultra-weak photon emission of Escherichia coli. Electromagn. Biol. Med. 28 (3), 240–249. https://doi.org/10.1080/15368370903065820. URL http://www.informaworld.com/openurl?genre=article&doi=10.1080/15368370903065820&magic=crossref——D404A21C5BB053405B1A640AFFD44AE3.
Lagercrantz, C., 1964. Formation of stable free radicals in alkaline solutions of some monosaccharides. Acta Chem. Scand. 18, 1321–1324.
Ledakowicz, S., Solecka, M., Zylla, R., 2001. Biodegradation, decolourisation and detoxification of textile wastewater enhanced by advanced oxidation processes. J. Biotechnol. 89 (2–3), 175–184. https://doi.org/10.1016/S0168-1656(01)00296-6. URL. https://linkinghub.elsevier.com/retrieve/pii/S0168165601002966.
Li, W., Haneman, D., 1999. Rupture luminescence from natural fibers. J. Chem. Phys. 111 (22), 10314–10320. https://doi.org/10.1063/1.480379. URL. http://aip.scitation.org/doi/10.1063/1.480379.
Li, R., Jia, Z., Trush, M.A., 2016. Defining ROS in biology and medicine, reactive oxygen species (apex. N.C.) 1 (1), 9–21. https://doi.org/10.20455/ros.2016.803. URL. https://www.ncbi.nlm.nih.gov/pmc/articles/PMC5921829/.
Liese, A., Seelbach, K., Wandrey, C., 2006. Industrial Biotransformations. John Wiley & Sons.
Lissi, E.A., Escobar, J., Pascual, C., Castillo, M.d., Schmitt, T.H., Mascio, P.D., 1994. Visible chemiluminescence associated with the reaction between methemoglobin or oxyhemoglobin with hydrogen peroxide. Photochem. Photobiol. 60 (5), 405–411. URL. http://onlinelibrary.wiley.com/doi/10.1111/j.1751-1097.1994.tb05124.x/full.
Lloyd, D., Boveris, A., Reiter, R., Filipkowski, M., Chance, B., 1979. Chemiluminescence of acanthamoeba castellanii. Biochem. J. 184 (1), 149–156. URL. http://www.biochemj.org/content/184/1/149.abstract.
Lykkesfeldt, J., Loft, S., Nielsen, J.B., Poulsen, H.E., 1997. Ascorbic acid and dehydroascorbic acid as biomarkers of oxidative stress caused by smoking. Am. J. Clin. Nutr. 65 (4), 959–963. https://doi.org/10.1093/ajcn/65.4.959. URL. https://academic.oup.com/ajcn/article/65/4/959/4655543.
Maccarrone, M., Rosato, N., Agró, A.F., 1997. Lipoxygenase products induce ultraweak light emission from human erythroleukemia cells. J. Biolumin. Chemilumin. 12 (6), 285–293.
Maccarrone, M., Fantini, C., Agrò, A.F., Rosato, N., 1998. Kinetics of ultraweak light emission from human erythroleukemia K562 cells upon electroporation. Biochim. Biophys. Acta Biomembr. 1414 (1), 43–50.
Maccarrone, M., Salucci, M.L., Melino, G., Rosato, N., Finazzi-Agro, A., 1999. The early phase of apoptosis in human neuroblastoma CHP100 cells is characterized by lipoxygenase-dependent ultraweak light emission. Biochem. Biophys. Res. Commun. 265 (3), 758–762.
Mattinen, M.-L., Lantto, R., Selinheimo, E., Kruus, K., Buchert, J., 2008. Oxidation of peptides and proteins by Trichoderma reesei and Agaricus bisporus tyrosinases. J. Biotechnol. 133 (3), 395–402, 10.1016/j.jbiotec.2007.10.009. URL. https://linkinghub.elsevier.com/retrieve/pii/S0168165607016690.
C.M. Mano, F.M. Prado, J. Massari, G.E. Ronsein, G.R. Martinez, S. Miyamoto, J. Cadet, H. Sies, M.H.G. Medeiros, E.J.H. Bechara, P. Di Mascio, 2014. Excited singlet molecular O2 (1Δg) is generated enzymatically from excited carbonyls in the dark, Sci. Rep. 4. doi:10.1038/srep05938. URL http://www.nature.com/articles/srep05938.
A. McKinlay, W. Gerard, S. Fields, Global analysis of RNA oxidation in Saccharomyces cerevisiae, Biotechniques 52 (2). doi:10.2144/000113801. URL https://www.future-science.com/doi/10.2144/000113801.
McNally, J.S., Davis, M.E., Giddens, D.P., Saha, A., Hwang, J., Dikalov, S., Jo, H., Harrison, D.G., 2003. Role of xanthine oxidoreductase and NAD(P)H oxidase in endothelial superoxide production in response to oscillatory shear stress. Am. J. Physiol. Heart Circ. Physiol. 285 (6), H2290–H2297. https://doi.org/10.1152/ajpheart.00515.2003. URL. https://www.physiology.org/doi/10.1152/ajpheart.00515.2003.
Medeiros, M.H., Sies, H., 1989. Chemiluminescent oxidation of ribose catalyzed by horseradish peroxidase in presence of hydrogen peroxide. Free Radic. Biol. Med. 6 (6), 565–571. https://doi.org/10.1016/0891-5849(89)90062-2. URL. https://linkinghub.elsevier.com/retrieve/pii/0891584989900622.
Medeiros, M.H., Wefers, H., Sies, H., 1987. Generation of excited species catalyzed by horseradish peroxidase or hemin in the presence of reduced glutathione and H2O2. Free Radic. Biol. Med. 3 (2), 107–110 publisher: Elsevier.
Meile, K., Zhurinsh, A., Spince, B., 2014. Aspects of periodate oxidation of carbohydrates for the analysis of pyrolysis liquids. J. Carbohydr. Chem. 33 (3), 105–116 publisher: Taylor & Francis).
Mendenhall, G.D., Sheng, X.C., Wilson, T., 1991. Yields of excited carbonyl species from alkoxyl and from alkylperoxyl radical dismutations. J. Am. Chem. Soc. 113 (23), 8976–8977.
Merck, 2015. Modern methods in oxidative stress research. URL. https://www.merckmillipore.com/CZ/cs/life-science-research/antibodies-assays/antibodies-overview/Research-Areas/neuroscience/oxidative-stress/NLib.qB.eW0AAAFPwH11gPuJ,nav.
Mesquita, C.S., Oliveira, R., Bento, F., Geraldo, D., Rodrigues, J.V., Marcos, J.C., 2014. Simplified 2,4-dinitrophenylhydrazine spectrophotometric assay for quantification of carbonyls in oxidized proteins. Anal. Biochem. 458, 69–71. https://doi.org/10.1016/j.ab.2014.04.034. URL. https://linkinghub.elsevier.com/retrieve/pii/S0003269714001936.
Michalski, R., Zielonka, J., Gapys, E., Marcinek, A., Joseph, J., Kalyanaraman, B., 2014. Real-time measurements of amino acid and protein hydroperoxides using coumarin boronic acid. J. Biol. Chem. 289 (32), 22536–22553. https://doi.org/10.1074/jbc.M114.553727. URL. https://www.ncbi.nlm.nih.gov/pmc/articles/PMC4139259/.
Miller, K.W., Lorr, N.A., Yang, C.S., 1984. Simultaneous determination of plasma retinol, α-tocopherol, lycopene, α-carotene, and β-carotene by high-performance liquid chromatography. Anal. Biochem. 138 (2), 340–345 publisher: Elsevier.
Miyamoto, S., Martinez, G.R., Medeiros, M.H.G., Di Mascio, P., 2003a. Singlet molecular oxygen generated from lipid hydroperoxides by the Russell mechanism: studies using ^{18}O-labeled linoleic acid hydroperoxide and monomol light emission measurements. J. Am. Chem. Soc. 125 (20), 6172–6179. https://doi.org/10.1021/ja029115o. URL. https://pubs.acs.org/doi/10.1021/ja029115o.
Miyamoto, S., Martinez, G.R., Martins, A.P.B., Medeiros, M.H.G., Di Mascio, P., 2003b. Direct evidence of singlet molecular oxygen [O2(1dg)] production in the reaction of linoleic acid hydroperoxide with peroxynitrite. J. Am. Chem. Soc. 125 (15), 4510–4517. https://doi.org/10.1021/ja029262m. URL. http://pubs.acs.org/doi/abs/10.1021/ja029262m.
Miyamoto, S., Ronsein, G.E., Corrêa, T.C., Martinez, G.R., Medeiros, M.H.G., Di Mascio, P., 2009. Direct evidence of singlet molecular oxygen generation from peroxynitrate, a decomposition product of peroxynitrite. Dalton Trans. 29, 5720. https://doi.org/10.1039/b905560f. URL. http://xlink.rsc.org/?DOI=b905560f.
Miyamoto, S., Nantes, I.L., Faria, P.A., Cunha, D., Ronsein, G.E., Medeiros, M.H.G., Di Mascio, P., 2012. Cytochrome c-promoted cardiolipin oxidation generates singlet molecular oxygen. Photochem. Photobiol. Sci. 11 (10), 1536. https://doi.org/10.1039/c2pp25119a. URL. http://xlink.rsc.org/?DOI=c2pp25119a.
Miyata, T., Fu, M.-X., Kurokawa, K., van Ypersele De Strihou, C., Thorpe, S.R., Baynes, J. W., 1998. Autoxidation products of both carbohydrates and lipids are increased in uremic plasma: is there oxidative stress in uremia? Kidney Int. 54 (4), 1290–1295.

https://doi.org/10.1046/j.1523-1755.1998.00093.x. URL. https://linkinghub.elsevier.com/retrieve/pii/S0085253815307523.
Miyata, T., Kurokawa, K., Strihou, C.V.Y.D., 2000. Advanced glycation and lipoxidation end products: role of reactive carbonyl compounds generated during carbohydrate and lipid metabolism. J. Am. Soc. Nephrol. 11 (9), 1744–1752. https://doi.org/10.1681/ASN.V1191744 publisher: American Society of Nephrology Section: REVIEW. https://jasn.asnjournals.org/content/11/9/1744.
Miyazawa, T., Fujimoto, K., Suzuki, T., Yasuda, K., 1994. [34] Determination of phospholipid hydroperoxides using luminol chemiluminescence—high-performance liquid chromatography. In: Methods in Enzymology, vol. 233. Elsevier, pp. 324–332.
Moraes, T.A., Barlow, P.W., Klingelé, E., Gallep, C.M., 2012. Spontaneous ultra-weak light emissions from wheat seedlings are rhythmic and synchronized with the time profile of the local gravimetric tide. Naturwissenschaften 99 (6), 465–472. https://doi.org/10.1007/s00114-012-0921-5. URL. http://link.springer.com/10.1007/s00114-012-0921-5.
Munna, M.S., 2013. Influence of exogenous oxidative stress on Escherichia coli cell growth, viability and morphology. Am. J. Biosci. 1 (4), 59. https://doi.org/10.11648/j.ajbio.20130104.12. URL. http://www.sciencepublishinggroup.com/journal/paperinfo.aspx?journalid=219&doi=10.11648/j.ajbio.20130104.12.
Muscari, C., Pappagallo, M., Ferrari, D., Giordano, E., Capanni, C., Caldarera, C., Guarnieri, C., 1998. Simultaneous detection of reduced and oxidized glutathione in tissues and mitochondria by capillary electrophoresis. J. Chromatogr. B Biomed. Sci. Appl. 707 (1–2), 301–307. https://doi.org/10.1016/S0378-4347(97)00595-1. URL. https://linkinghub.elsevier.com/retrieve/pii/S0378434797005951.
Nakabeppu, Y., Ohta, E., Abolhassani, N., 2017. MTH1 as a nucleotide pool sanitizing enzyme: friend or foe? Free Radic. Biol. Med. 107, 151–158. https://doi.org/10.1016/j.freeradbiomed.2016.11.002. URL. https://linkinghub.elsevier.com/retrieve/pii/S0891584916310310.
Nakano, M., Noguchi, T., Sugioka, K., Fukuyama, H., Sato, M., 1975. Spectroscopic evidence for the generation of singlet oxygen in the reduced nicotinamide adenine dinucleotide phosphate-dependent microsomal lipid peroxidation system. J. Biol. Chem. 250 (6), 2404–2406.
Napetschnig, S., Sies, H., 1987. Generation of photoemissive species by mitomycin C redox cycling in rat liver microsomes. Biochem. Pharmacol. 36 (10), 1617–1621. https://doi.org/10.1016/0006-2952(87)90045-1. URL. https://linkinghub.elsevier.com/retrieve/pii/0006295287900451.
Nerudová, M., Červinková, K., Hašek, J., Cifra, M., 2015. In: Tománek, P., Senderáková, D., Páta, P. (Eds.), Optical Spectral Analysis of Ultra-weak Photon Emission from Tissue Culture and Yeast Cells. SPIE Proceedings, p. 94500O. https://doi.org/10.1117/12.2069897. URL. http://proceedings.spiedigitallibrary.org/proceeding.aspx?doi=10.1117/12.2069897.
Nirmala, J.G., Narendhirakannan, R., 2011. Detection and genotyping of high-risk HPV and evaluation of anti-oxidant status in cervical carcinoma patients in Tamil nadu state, India - a case control study. Asian Pac. J. Cancer Prev. APJCP (12), 2689–2695.
Niu, Q.J., Mendenhall, G.D., 1992. Yields of singlet molecular oxygen from peroxyl radical termination. J. Am. Chem. Soc. 114 (1), 165–172. https://doi.org/10.1021/ja00027a024. URL. https://pubs.acs.org/doi/abs/10.1021/ja00027a024.
Nöll, T., Nöll, G., 2011. Strategies for "wiring" redox-active proteins to electrodes and applications in biosensors, biofuel cells, and nanotechnology. Chem. Soc. Rev. 40 (7), 3564. https://doi.org/10.1039/c1cs15030h. URL. http://xlink.rsc.org/?DOI=c1cs15030h.
Noll, T., De Groot, H., Sies, H., 1987. Distinct temporal relation among oxygen uptake, malondialdehyde formation, and low-level chemiluminescence during microsomal lipid peroxidation. Arch. Biochem. Biophys. 252 (1), 284–291. https://doi.org/10.1016/0003-9861(87)90033-6. URL. https://linkinghub.elsevier.com/retrieve/pii/0003986187900336.
Nukui, H., Inagaki, H., Iyozumi, H., Kato, K., 2013. Biophoton emissions in sulfonylurea-herbicide-resistant weeds. In: Price, A. (Ed.), Herbicides - Advances in Research. InTech. URL. http://www.intechopen.com/books/herbicides-advances-in-research/biophoton-emissions-in-sulfonylurea-herbicide-resistant-weeds.
Nunomura, A., Perry, G., Pappolla, M.A., Wade, R., Hirai, K., Chiba, S., Smith, M.A., 1999. RNA oxidation is a prominent feature of vulnerable neurons in alzheimer's disease. J. Neurosci. 19 (6), 1959–1964. https://doi.org/10.1523/JNEUROSCI.19-06-01959.1999. URL. http://www.jneurosci.org/lookup/doi/10.1523/JNEUROSCI.19-06-01959.1999.
Ohya, T., Kurashige, H., Okabe, H., Kai, S., 2000. Early detection of salt stress damage by biophotons in red bean seedling, Japanese. J. Appl. Phys. 39 (1, No. 6A), 3696–3700. https://doi.org/10.1143/JJAP.39.3696. URL. http://stacks.iop.org/1347-4065/39/3696.
Ohya, T., Yoshida, S., Kawabata, R., Okabe, H., Kai, S., 2002. Biophoton emission due to drought injury in red beans: possibility of early detection of drought injury. Jpn. J. Appl. Phys. 41 (Part 1, No. 7A), 4766–4771. https://doi.org/10.1143/JJAP.41.4766. URL. https://iopscience.iop.org/article/10.1143/JJAP.41.4766.
Oliveira, O., Haun, M., Durán, N., O'Brien, P., O'Brien, C., Bechara, E., Cilento, G., 1978. Enzyme-generated electronically excited carbonyl compounds, Acetone phosphorescence during the peroxidase-catalyzed aerobic oxidation of isobutanal. J. Biol. Chem. 253 (13), 4707–4712 publisher: American Society for Biochemistry and Molecular Biology.
Oros, C.L., Alves, F., 2018. Leaf wound induced ultraweak photon emission is suppressed under anoxic stress: observations of Spathiphyllum under aerobic and anaerobic conditions using novel in vivo methodology. PLoS One 13 (6), e0198962. https://doi.org/10.1371/journal.pone.0198962. URL. http://dx.plos.org/10.1371/journal.pone.0198962.
Osório, V.M., Cardeal, Z.L., 2013. Analytical methods to assess carbonyl compounds in foods and beverages. J. Braz. Chem. Soc. https://doi.org/10.5935/0103-5053.20130236. URL. http://www.gnresearch.org/doi/10.5935/0103-5053.20130236.
Ou-Yang, H., 2014. The application of ultra-weak photon emission in dermatology. J. Photochem. Photobiol. B Biol. 139, 63–70. https://doi.org/10.1016/j.jphotobiol.2013.10.003. URL. http://linkinghub.elsevier.com/retrieve/pii/S1011134413002224.
O'Donnell, V.B., Azzi, A., 1996. High rates of extracellular superoxide generation by cultured human fibroblasts: involvement of a lipid-metabolizing enzyme. Biochem. J. 318 (Pt 3), 805–812. URL. https://www.ncbi.nlm.nih.gov/pmc/articles/PMC1217690/.
Pantopoulos, K., 2011. Oxygen radicals and related species. In: Principles of Free Radical Biomedicine. Nova Science Publishers, Inc., New York oCLC: 952771919.
Pathak, V., Prasad, A., Pospíšil, P., 2017. Formation of singlet oxygen by decomposition of protein hydroperoxide in photosystem II. PLoS One 12 (7), e0181732. https://doi.org/10.1371/journal.pone.0181732. URL. https://dx.plos.org/10.1371/journal.pone.0181732.
Percival, M., 1996. Antioxidants. Clin. Nutr. Insight 1, 1–6.
Picardo, M., Grammatico, P., Roccella, F., Roccella, M., Grandinetti, M., del Porto, G., Passi, S., 1996. Imbalance in the antioxidant pool in melanoma cells and normal melanocytes from patients with melanoma. J. Invest. Dermatol. 107 (3), 322–326. https://doi.org/10.1111/1523-1747.ep12363163. URL. https://linkinghub.elsevier.com/retrieve/pii/S0022202X15426727.
Popp, F.-A., 2009. Cancer growth and its inhibition in terms of coherence. Electromagn. Biol. Med. 28 (1), 53–60. https://doi.org/10.1080/15368370802711805. URL. http://www.tandfonline.com/doi/full/10.1080/15368370802711805.
Popp, F.-A., 1986. On the coherence of ultraweak photonemission from living tissues. In: Kilmister, C.W. (Ed.), Disequilibrium and Self-Organisation, Mathematics and its Applications. Springer Netherlands, Dordrecht, pp. 207–230. https://doi.org/10.1007/978-94-009-4718-4_16, 10.1007/978-94-009-4718-4_16. URL.
Popp, F.-A., Li, K.-h., 1993. Hyperbolic relaxation as a sufficient condition of a fully coherent ergodic field. Int. J. Theor. Phys. 32 (9), 1573–1583.
Popp, F.-A., Li, K., Mei, W., Galle, M., Neurohr, R., 1988. Physical aspects of biophotons. Cell. Mol. Life Sci. 44 (7), 576–585.
Popp, F.-A., Gu, Q., Li, K.-H., 1994. Biophoton emission: experimental background and theoretical approaches. Mod. Phys. Lett. B 8 (21n22), 1269–1296.
Pospíšil, P., Prasad, A., Rác, M., 2019. Mechanism of the formation of electronically excited species by oxidative metabolic processes: role of reactive oxygen species. Biomolecules 9 (7), 258. https://doi.org/10.3390/biom9070258. URL. https://www.mdpi.com/2218-273X/9/7/258.
Prado, F.M., Scalfo, A.C., Miyamoto, S., Medeiros, M.H.G., Mascio, P.D.. Generation of singlet molecular oxygen by lipid hydroperoxides and nitronium ion, photochemistry and photobiology n/a (n/a). https://onlinelibrary.wiley.com/doi/pdf/10.1111/php.13236. https://onlinelibrary.wiley.com/doi/abs/10.1111/php.13236.
Prado, F.M., Oliveira, M.C., Miyamoto, S., Martinez, G.R., Medeiros, M.H., Ronsein, G.E., Di Mascio, P., 2009. Thymine hydroperoxide as a potential source of singlet molecular oxygen in DNA. Free Radic. Biol. Med. 47 (4), 401–409. https://doi.org/10.1016/j.freeradbiomed.2009.05.001. URL. https://linkinghub.elsevier.com/retrieve/pii/S0891584909002664.
Prasad, A., Pospíšil, P., 2011. Linoleic acid-induced ultra-weak photon emission from Chlamydomonas reinhardtii as a tool for monitoring of lipid peroxidation in the cell membranes. PLoS One 6 (7), e22345. https://doi.org/10.1371/journal.pone.0022345. URL. http://dx.plos.org/10.1371/journal.pone.0022345.
Prasad, A., Pospišil, P., 2011. Two-dimensional imaging of spontaneous ultra-weak photon emission from the human skin: role of reactive oxygen species. J. Biophot. 4 (11–12), 840–849. https://doi.org/10.1002/jbio.201100073. URL.
Prasad, A., Ferretti, U., Sedlářová, M., Pospíšil, P., 2016. Singlet oxygen production in Chlamydomonas reinhardtii under heat stress. Sci. Rep. 6, 20094 https://doi.org/10.1038/srep20094. URL. http://www.nature.com/articles/srep20094.
Prasad, A., Sedlářová, M., Kale, R.S., Pospíšil, P., 2017. Lipoxygenase in singlet oxygen generation as a response to wounding: in vivo imaging in Arabidopsis thaliana. Sci. Rep. 7 (1), 9831. https://doi.org/10.1038/s41598-017-09758-1. URL. http://www.nature.com/articles/s41598-017-09758-1.
Prasad, A., Pospíšil, P., Tada, M., 2019. Editorial: reactive oxygen species (ROS) detection methods in biological system. Front. Physiol. 10, 1316. https://doi.org/10.3389/fphys.2019.01316. URL. https://www.frontiersin.org/article/10.3389/fphys.2019.01316/full.
Prasad, A., Sedlářová, M., Balukova, A., Rác, M., Pospíšil, P., 2020a. Reactive oxygen species as a response to wounding: in vivo imaging in Arabidopsis thaliana. Front. Plant Sci. 10, 1660. https://doi.org/10.3389/fpls.2019.01660. URL. https://www.frontiersin.org/article/10.3389/fpls.2019.01660/full.
Prasad, A., Gouripeddi, P., Devireddy, H.R.N., Ovsii, A., Rachakonda, D.P., Wijk, R.V., Pospíšil, P., 2020b. Spectral distribution of ultra-weak photon emission as A response to wounding in plants: an in vivo study. Biology 9 (6), 139. https://doi.org/10.3390/biology9060139 number: 6 Publisher: Multidisciplinary Digital Publishing Institute. https://www.mdpi.com/2079-7737/9/6/139.
Prochaska, H.J., Talalay, P., Sies, H., 1987. Direct protective effect of NAD(P)H:quinone reductase against menadione-induced chemiluminescence of postmitochondrial fractions of mouse liver. J. Biol. Chem. 262 (5), 1931–1934 publisher: American Society for Biochemistry and Molecular Biology. URL. http://www.jbc.org/content/262/5/1931.
Puntarulo, S., 2005. Iron, oxidative stress and human health. Mol. Aspect. Med. 26 (4), 299–312. https://doi.org/10.1016/j.mam.2005.07.001. URL. http://www.sciencedirect.com/science/article/pii/S009829970500035X.
Purdel, N.C., Margina, D., Ilie, M., 2014. Current methods used in the protein carbonyl assay. Annual Research & Review in Biology 4 (12), 2015.

Quickenden, T.I., Hee, S.S.Q., 1974. Weak luminescence from the yeast Saccharomyces cerevisiae and the existence of mitogenetic radiation. Biochem. Biophys. Res. Commun. 60 (2), 764–770.
Quickenden, T., Tilbury, R., 1983. Growth dependent luminescence from cultures of normal and respiratory deficient Saccharomyces cerevisiae. Photochem. Photobiol. 37 (3), 337–344.
Rác, M., Sedlářová, M., Pospíšil, P., 2015. The formation of electronically excited species in the human multiple myeloma cell suspension. Sci. Rep. 5, 8882. https://doi.org/10.1038/srep08882. URL. http://www.nature.com/articles/srep08882.
Radotić, K., Redenović, Č., Jeremić, M., Vučinić, Ž., 1990. Effect of propagators and inhibitors on the ultraweak luminescence from maize roots. J. Biolumin. Chemilumin. 5 (4), 221–225. URL. http://onlinelibrary.wiley.com/doi/10.1002/bio.1170050403/full.
Radotic, K., Radenovic, C., Jeremic, M., 1998. Spontaneous ultraweak bioluminescence in plants: origin, mechanisms and properties. Gen. Physiol. Biophys. 17, 289–308. URL. http://www.gpb.sav.sk/1998/1998_04_289.pdf.
Rafieiolhosseini, N., Poplová, M., Sasanpour, P., Rafii-Tabar, H., Alhossaini, M.R., Cifra, M., 2016. Photocount statistics of ultra-weak photon emission from germinating mung bean. J. Photochem. Photobiol. B Biol. 162, 50–55. https://doi.org/10.1016/j.jphotobiol.2016.06.001. URL. http://linkinghub.elsevier.com/retrieve/pii/S1011134416304328.
Rajfur, Z., 1994. Photon emission from chemically perturbed yeast cells. J. Biolumin. Chemilumin. 9 (2), 59–63 publisher: Wiley Online Library.
Rastogi, A., Pospíšil, P., 2010. Effect of exogenous hydrogen peroxide on biophoton emission from radish root cells. Plant Physiol. Biochem. 48 (2–3), 117–123. https://doi.org/10.1016/j.plaphy.2009.12.011. URL. http://linkinghub.elsevier.com/retrieve/pii/S0981942810000069.
Rattemeyer, M., Popp, F.-A., Nagl, W., 1981. Evidence of photon emission from DNA in living systems. Naturwissenschaften 68 (11), 572–573.
Ravanat, J.-L., Douki, T., Duez, P., Gremaud, E., Herbert, K., Hofer, T., Lasserre, L., Saint-Pierre, C., Favier, A., Cadet, J., 2002. Cellular background level of 8-oxo-7, 8-dihydro-2'-deoxyguanosine: an isotope based method to evaluate artefactual oxidation of DNA during its extraction and subsequent work-up. Carcinogenesis 23 (11), 1911–1918 (publisher: Oxford University Press).
Reis, A., Spickett, C.M., 2012. Chemistry of phospholipid oxidation. Biochim. Biophys. Acta Biomembr. 1818 (10), 2374–2387. https://doi.org/10.1016/j.bbamem.2012.02.002. URL. https://linkinghub.elsevier.com/retrieve/pii/S0005273612000387.
Rogowska-Wrzesinska, A., Wojdyla, K., Nedić, O., Baron, C.P., Griffiths, H.R., 2014. Analysis of protein carbonylation — pitfalls and promise in commonly used methods. Free Radic. Res. 48 (10), 1145–1162. https://doi.org/10.3109/10715762.2014.944868. URL. http://www.tandfonline.com/doi/full/10.3109/10715762.2014.944868.
Ronsein, G.E., Martinez, G.R., de Almeida, E.A., Miyamoto, S., Gennari de Medeiros, M. H., Di Mascio, P., 2011. Role of singlet molecular oxygen in the oxidative damage to biomolecules. In: Abele, D., Vázquez-Medina, J.P., Zenteno-Savín, T. (Eds.), Oxidative Stress in Aquatic Ecosystems. John Wiley & Sons, Ltd, Chichester, UK, pp. 344–358. https://doi.org/10.1002/9781444345988.ch25. URL.
Russell, G.A., 1957. Deuterium-isotope effects in the autoxidation of aralkyl hydrocarbons. Mechanism of the interaction of peroxy radicals. J. Am. Chem. Soc. 79 (14), 3871–3877. URL. http://pubs.acs.org/doi/pdf/10.1021/ja01571a068.
Rychlý, J., Strlič, M., Matisová-Rychlá, L., Kolar, J., 2002. Chemiluminescence from paper I. Kinetic analysis of thermal oxidation of cellulose. Polym. Degrad. Stabil. 78 (2), 357–367. URL. http://www.sciencedirect.com/science/article/pii/S0141391002001878.
Rychly, J., Matisovarychla, L., Lazar, M., Slovak, K., Strlic, M., Kocar, D., Kolar, J., 2004. Thermal oxidation of cellulose investigated by chemiluminescence. The effect of water at temperatures above 100?C. Carbohydr. Polym. 58 (3), 301–309. https://doi.org/10.1016/j.carbpol.2004.07.006. URL. http://linkinghub.elsevier.com/retrieve/pii/S0144861704002577.
Saeidfirozeh, H., Shafiekhani, A., Cifra, M., Masoudi, A.A., 2018. Endogenous chemiluminescence from germinating Arabidopsis thaliana seeds. Sci. Rep. 8 (1), 16231 https://doi.org/10.1038/s41598-018-34485-6. URL. http://www.nature.com/articles/s41598-018-34485-6.
Salin, M.L., Bridges, S.M., 1981. Chemiluminescence in wounded root tissue: evidence for peroxidase involvement. Plant Physiol. 67 (1), 43–46. https://doi.org/10.1104/pp.67.1.43. URL. http://www.plantphysiol.org/cgi/doi/10.1104/pp.67.1.43.
San Martín, A., Griendling, K.K., 2010. Redox control of vascular smooth muscle migration. Antioxidants Redox Signal. 12 (5), 625–640. https://doi.org/10.1089/ars.2009.2852. URL. https://www.ncbi.nlm.nih.gov/pmc/articles/PMC2829046/.
Savino, S., Fraaije, M.W., 2021. The vast repertoire of carbohydrate oxidases: an overview. Biotechnol. Adv. 51, 107634 https://doi.org/10.1016/j.biotechadv.2020.107634. URL. https://www.sciencedirect.com/science/article/pii/S0734975020301361.
Schlenker, T., Feranchak, A.P., Schwake, L., Stremmel, W., Roman, R.M., Fitz, J., 2000. Functional interactions between oxidative stress, membrane Na+ permeability, and cell volume in rat hepatoma cells. Gastroenterology 118 (2), 395–403. https://doi.org/10.1016/S0016-5085(00)70222-8. URL. https://linkinghub.elsevier.com/retrieve/pii/S0016508500702228.
Schneijder, P., Kok, F., Hermus, R., 1992. Iron, oxidative stress, and disease risk. Cancer Causes Control 3, 457–473.
Schuh, M.D., Speiser, S., Atkinson, G.H., 1984. Time-resolved phosphorescence spectra of acetaldehyde and perdeuterioacetaldehyde vapor. J. Phys. Chem. 88 (11), 2224–2228.
Schulte-Herbruggen, T., Sies, H., 1989. The peroxidase/oxidase activity of soybean lipoxygenase-I. Triplet excited carbonyls from the reaction with isobutanal and the effect of glutathione. Photochem. Photobiol. 49 (5), 697–704. URL. http://onlinelibrary.wiley.com/doi/10.1111/j.1751-1097.1989.tb08443.x/full.
Sedlářová, M., Luhová, L., 2017. Re-evaluation of imaging methods of reactive oxygen and nitrogen species in plants and fungi: influence of cell wall composition. Front. Physiol. 8, 826. https://doi.org/10.3389/fphys.2017.00826. URL. http://journal.frontiersin.org/article/10.3389/fphys.2017.00826/full.
Sell, D.R., Monnier, V.M., 1989. Structure elucidation of a senescence cross-link from human extracellular matrix. J. Biol. Chem. 264 (36), 21597–21602. https://doi.org/10.1016/S0021-9258(20)88225-8. URL. https://linkinghub.elsevier.com/retrieve/pii/S0021925820882258.
Sharov, V.S., Driomina, E.S., Briviba, K., Sies, H., 1998. Sensitization of peroxynitrite chemiluminescence by the triplet carbonyl sensitizer coumarin-525. Effect of CO2. Photochem. Photobiol. 68 (6), 797–801 doi:10.1111/j.1751-1097.1998.tb05286.x. https://onlinelibrary.wiley.com/doi/pdf/10.1111/j.1751-1097.1998.tb05286.x. https://onlinelibrary.wiley.com/doi/abs/10.1111/j.1751-1097.1998.tb05286.x.
Shen, X., Tian, J., Zhu, Z., Li, X., 1991. Chemiluminescence study on the peroxidation of linoleic acid initiated by the reaction of ferrous iron with hydrogen peroxide. Biophys. Chem. 40 (2), 161–167.
Shinzato, T., van Ypersele, de Strihou, 1996. Accumulation of albumin-linked and free-form pentosidine in the circulation of uremic patients with end-stage renal failure: renal implications in the pathophysiology of. Pentosidine 7 (8), 9.
Sian-Hülsmann, J., Mandel, S., Youdim, M.B.H., Riederer, P., 2011. The relevance of iron in the pathogenesis of Parkinson's disease. J. Neurochem. 118 (6), 939–957. https://doi.org/10.1111/j.1471-4159.2010.07132.x. URL. https://onlinelibrary.wiley.com/doi/abs/10.1111/j.1471-4159.2010.07132.x.
Sies, H., 1993. Damage to plasmid DNA by singlet oxygen and its protection. Mutat. Res. Genet. Toxicol. 299 (3–4), 183–191. https://doi.org/10.1016/0165-1218(93)90095-U. URL. https://linkinghub.elsevier.com/retrieve/pii/016512189390095U.
H. Sies, D. P. Jones, Reactive oxygen species (ROS) as pleiotropic physiological signalling agents, Nat. Rev. Mol. Cell Biol.:10.1038/s41580-020-0230-3. URL http://www.nature.com/articles/s41580-020-0230-3.
Sies, H., Menck, C.F., 1992. Singlet oxygen induced DNA damage. Mutat. Res. 275 (3–6), 367–375. https://doi.org/10.1016/0921-8734(92)90039-r.
Šimkovic, I., Tiňo, J., Plaček, J., Mañásek, Z., 1983. ESR study of alkaline, oxidative degradation of saccharides. Identification of 2, 5-dihydroxy-p-benzosemiquinone. Carbohydr. Res. 116 (2), 263–269 publisher: Elsevier).
Sinha, A.K., AbdElgawad, H., Giblen, T., Zinta, G., De Rop, M., Asard, H., Blust, R., De Boeck, G., 2014. Anti-oxidative defences are modulated differentially in three freshwater teleosts in response to ammonia-induced oxidative stress. PLoS One 9 (4), e95319. https://doi.org/10.1371/journal.pone.0095319. URL. http://dx.plos.org/10.1371/journal.pone.0095319.
Sławińska, D., Sławiński, J., 1988. Sensitized chemiluminescence of coumarins as a possible component of plants ultraweak luminescence. J. Lumin. 40–41, 262–263. https://doi.org/10.1016/0022-2313(88)90185-8. URL. http://www.sciencedirect.com/science/article/pii/0022231388901858.
Sławiński, J., 1988. Luminescence research and its relation to ultraweak cell radiation. Experientia 44 (7), 559–571.
Sławiński, J., 1990. Necrotic photon emission in stress and lethal interactions. Curr Topics Biophys 8, 27–38.
Sławiński, J., 2003. Biophotons from Stressed and Dying Organisms: Toxicological aspects. In: Ind. J. Exp. Biol., 41 Publisher: NISCAIR-CSIR, India, pp. 483–493.
Sławiński, J., 2005. Photon emission from perturbed and dying organisms: biomedical perspectives. Forschende Komplementärmed./Res. Complementary Med. 12 (2), 90–95. https://doi.org/10.1159/000083971. URL. http://www.karger.com/?doi=10.1159/000083971.
Sławiński, J., Galezowski, W., Elbanowski, M., 1981. Chemiluminescence in the reaction of cytochrome c with hydrogen peroxide. Biochim. Biophys. Acta Bioenerg. 637 (1), 130–137. https://doi.org/10.1016/0005-2728(81)90218-8. URL. https://linkinghub.elsevier.com/retrieve/pii/0005272881902188.
Soares, C.L., Bechara, E.H., 1982. Enzymatic generation of triplet biacetyl. Photochem. Photobiol. 36 (1), 117–119 doi:10.1111/j.1751-1097.1982.tb04351.x. URL. https://onlinelibrary.wiley.com/doi/pdf/10.1111/j.1751-1097.1982.tb04351.x. https://onlinelibrary.wiley.com/doi/abs/10.1111/j.1751-1097.1982.tb04351.x.
Spickett, C.M., 2013. The lipid peroxidation product 4-hydroxy-2-nonenal: advances in chemistry and analysis. Redox Biol. 1 (1), 145–152. https://doi.org/10.1016/j.redox.2013.01.007. URL. http://linkinghub.elsevier.com/retrieve/pii/S2213231713000281.
Spickett, C.M., Pitt, A.R., 2015. Oxidative lipidomics coming of age: advances in analysis of oxidized phospholipids in physiology and pathology. Antioxidants Redox Signal. 22 (18), 1646–1666. https://doi.org/10.1089/ars.2014.6098. URL. https://www.ncbi.nlm.nih.gov/pmc/articles/PMC4486145/.
Stadtman, E., Levine, R., 2002. Why have cells selected reactive oxygen species to regulate cell signaling events? Hum. Exp. Toxicol. 21 (2) https://doi.org/10.1191/0960327102ht215oa, 83–83. http://het.sagepub.com/cgi/doi/10.1191/0960327102ht215oa.
Starkov, A.A., 2008. The role of mitochondria in reactive oxygen species metabolism and signaling. Ann. N. Y. Acad. Sci. 1147, 37–52. https://doi.org/10.1196/annals.1427.015. URL. https://www.ncbi.nlm.nih.gov/pmc/articles/PMC2869479/.
Stoldt, S., Wenzel, D., Kehrein, K., Riedel, D., Ott, M., Jakobs, S., 2018. Spatial orchestration of mitochondrial translation and OXPHOS complex assembly. Nat. Cell Biol. 20 (5), 528–534. https://doi.org/10.1038/s41556-018-0090-7. URL. http://www.nature.com/articles/s41556-018-0090-7.
Strlič, M., Kolar, J., Pihlar, B., Rychlỳ, J., Matisová-Rychlá, L., 2000. Chemiluminescence during thermal and thermo-oxidative degradation of cellulose. Eur. Polym. J. 36 (11), 2351–2358. URL. http://www.sciencedirect.com/science/article/pii/S0014305700000112.

Suslick, K.S., Flannigan, D.J., 2008. Inside a collapsing bubble: sonoluminescence and the conditions during cavitation. Annu. Rev. Phys. Chem. 59 (1), 659–683. https://doi.org/10.1146/annurev.physchem.59.032607.093739. URL. http://www.annualreviews.org/doi/10.1146/annurev.physchem.59.032607.093739.

Taibi, G., Nicotra, C., 2002. Development and validation of a fast and sensitive chromatographic assay for all-trans-retinol and tocopherols in human serum and plasma using liquid–liquid extraction. J. Chromatogr. B 780 (2), 261–267. https://doi.org/10.1016/S1570-0232(02)00529-9. URL. https://linkinghub.elsevier.com/retrieve/pii/S1570023202005299.

Takeda, M., Kobayashi, M., Takayama, M., Suzuki, S., Ishida, T., Ohnuki, K., Moriya, T., Ohuchi, N., 2004. Biophoton detection as a novel technique for cancer imaging. Cancer Sci. 95 (8), 656–661. https://doi.org/10.1111/j.1349-7006.2004.tb03325.x. URL.

Tamarit, J., de Hoogh, A., Obis, E., Alsina, D., Cabiscol, E., Ros, J., 2012. Analysis of oxidative stress-induced protein carbonylation using fluorescent hydrazides. J. Proteonomics 75 (12), 3778–3788. https://doi.org/10.1016/j.jprot.2012.04.046. URL. http://www.sciencedirect.com/science/article/pii/S1874391912002679.

Tang, R., Dai, J., 2014. Spatiotemporal imaging of glutamate-induced biophotonic activities and transmission in neural circuits. PLoS One 9 (1), e85643.

Tao, R., Zhao, Y., Chu, H., Wang, A., Zhu, J., Chen, X., Zou, Y., Shi, M., Liu, R., Su, N., Du, J., Zhou, H.-M., Zhu, L., Qian, X., Liu, H., Loscalzo, J., Yang, Y., 2017. Genetically encoded fluorescent sensors reveal dynamic regulation of NADPH metabolism. Nat. Methods 14 (7), 720–728. https://doi.org/10.1038/nmeth.4306. URL. http://www.nature.com/articles/nmeth.4306.

The British Nutrition Foundation, 1995. Springer Netherlands, Dordrecht, Iron. https://doi.org/10.1007/978-94-011-0585-9. http://link.springer.com/10.1007/978-94-011-0585-9.

Tian, Y., Yang, C., Xu, H., 2014. Insect spontaneous ultraweak photon emission as an indicator of insecticidal compounds. J. Photochem. Photobiol. B Biol. 140, 79–84. https://doi.org/10.1016/j.jphotobiol.2014.07.012. https://linkinghub.elsevier.com/retrieve/pii/S1011134414002383.

Tilbury, R.N., Quickenden, T.I., 1988. Spectral and time dependence studies of the ultra weak bioluminescence emitted by the bacterium Escherichia coli. Photochem. Photobiol. 47 (1), 145–150. URL. http://onlinelibrary.wiley.com/doi/10.1111/j.1751-1097.1988.tb02704.x/abstract.

Timmins, G.S., dos Santos, R.E., Whitwood, A.C., Catalani, L.H., Di Mascio, P., Gilbert, B. C., Bechara, E.J.H., 1997. Lipid peroxidation-dependent chemiluminescence from the cyclization of alkylperoxyl radicals to dioxetane radical intermediates. Chem. Res. Toxicol. 10 (10), 1090–1096. https://doi.org/10.1021/tx970075p. URL. https://pubs.acs.org/doi/10.1021/tx970075p.

Tiwari, B.S., Belenghi, B., Levine, A., 2002. Oxidative stress increased respiration and generation of reactive oxygen species, resulting in ATP depletion, opening of mitochondrial permeability transition, and programmed cell death. Plant Physiol. 128 (4), 1271–1281. https://doi.org/10.1104/pp.010999. URL. https://www.ncbi.nlm.nih.gov/pmc/articles/PMC154255/.

Torinuki, W., Miura, T., 1981. Singlet oxygen and ultraweak chemiluminescence in rat skin. Tohoku J. Exp. Med. 135 (4), 387–393. https://doi.org/10.1620/tjem.135.387. URL. http://joi.jlc.jst.go.jp/JST.Journalarchive/tjem1920/135.387?from=CrossRef.

Trotti, R., Carratelli, M., Barbieri, M., 2002. Performance and clinical application of a new, fast method for the detection of hydroperoxides in serum. Panminerva Med. 44 (1), 37–40. URL. https://europepmc.org/article/med/11887090.

Turro, N.J., 2004. Chapter 03 - transitions between electronic states - chemical dynamics and kinetics. In: Modern Molecular Photochemistry. URL:http://turroserver.chem.columbia.edu/courses/MMP_Chapter_Updates/MMP+_Ch3_Text*.pdf.

Uemi, M., Ronsein, G.E., Miyamoto, S., Medeiros, M.H.G., Di Mascio, P., 2009. Generation of cholesterol carboxyaldehyde by the reaction of singlet molecular oxygen [O_2 ($^1\delta_g$)] as well as ozone with cholesterol. Chem. Res. Toxicol. 22 (5), 875–884. https://doi.org/10.1021/tx800447b. URL. https://pubs.acs.org/doi/10.1021/tx800447b.

Uemi, M., Ronsein, G.E., Prado, F.M., Motta, F.D., Miyamoto, S., Medeiros, M.H.G., Di Mascio, P., 2011. Cholesterol hydroperoxides generate singlet molecular oxygen [O_2 ($^1\delta_g$)]: near-IR emission, ^{18}O-labeled hydroperoxides, and mass spectrometry. Chem. Res. Toxicol. 24 (6), 887–895. https://doi.org/10.1021/tx200079d. URL. https://pubs.acs.org/doi/10.1021/tx200079d.

United Nations, 2019. The Sustainable Development Goals Report 2019. United Nations. URL. https://www.un-ilibrary.org/content/publication/55eb9109-en.

Urlacher, V.B., Lutz-Wahl, S., Schmid, R.D., 2004. Microbial P450 enzymes in biotechnology. Appl. Microbiol. Biotechnol. 64 (3), 317–325. https://doi.org/10.1007/s00253-003-1514-1. URL. http://link.springer.com/10.1007/s00253-003-1514-1.

Vahalová, P., Červinková, K., Cifra, M., 2021. Biological autoluminescence for assessing oxidative processes in yeast cell cultures. Sci. Rep. 11 (1), 10852 https://doi.org/10.1038/s41598-021-89753-9. URL. http://www.nature.com/articles/s41598-021-89753-9.

Valdivia, A., Duran, C., Martin, A., 2015. The role of Nox-mediated oxidation in the regulation of cytoskeletal dynamics. Curr. Pharmaceut. Des. 21 (41), 6009–6022. https://doi.org/10.2174/1381612821666151029112624. URL. http://www.eurekaselect.com/openurl/content.php?genre=article&issn=1381-6128&volume=21&issue=41&spage=6009.

Valenzuela, R., Rincón-Cervera, M.Á., Echeverría, F., Barrera, C., Espinosa, A., Hernández-Rodas, M.C., Ortiz, M., Valenzuela, A., Videla, L.A., 2018. Iron-induced pro-oxidant and pro-lipogenic responses in relation to impaired synthesis and accretion of long-chain polyunsaturated fatty acids in rat hepatic and extrahepatic tissues. Nutrition 45, 49–58. https://doi.org/10.1016/j.nut.2017.07.007.

Valkonen, M., Kuusi, T., 1997. Spectrophotometric assay for total peroxyl radical-trapping antioxidant potential in human serum. JLR (J. Lipid Res.) 38 (4), 823–833 publisher: ASBMB.

Van Wijk, R., Van Wijk, E.P., Schroen, Y., Van der Greef, J., 2013. Imaging human spontaneous photon emission: historic development, recent data and perspectives. Trends Photochem. Photobiol. 15, 27–40.

Van Wijk, R., Van Wijk, E.P., van Wietmarschen, H.A., Greef, J.v. d., 2014. Towards whole-body ultra-weak photon counting and imaging with a focus on human beings: a review. J. Photochem. Photobiol. B Biol. 139, 39–46. https://doi.org/10.1016/j.jphotobiol.2013.11.014. URL. http://linkinghub.elsevier.com/retrieve/pii/S1011134413002583.

Velosa, A.C., Baader, W.J., Stevani, C.V., Mano, C.M., Bechara, E.J.H., 2007. 1,3-Diene probes for detection of triplet carbonyls in biological systems. Chem. Res. Toxicol. 20 (8), 1162–1169. https://doi.org/10.1021/tx700074n. URL. http://pubs.acs.org/doi/abs/10.1021/tx700074n.

Veskoukis, A.S., Margaritelis, N.V., Kyparos, A., Paschalis, V., Nikolaidis, M.G., 2018. Spectrophotometric assays for measuring redox biomarkers in blood and tissues: the NADPH network. Redox Rep. 23 (1), 47–56. https://doi.org/10.1080/13510002.2017.1392695. URL. https://www.tandfonline.com/doi/full/10.1080/13510002.2017.1392695.

Vidugiriene, J., 2013. Tools for Cell Metabolism: Bioluminescent NAD(P)/NAD(P)H-Glo™ Assays.

Vogel, R., 1998. About the Quenching of the Chemiluminescence from Liquid Culture Media by Microorganisms and Weak Light Emission Patterns from Bacterial Cultures. Ph.D. thesis.

Vogel, R., Süssmuth, R., 1998. Interaction of bacterial cells with weak light emission from culture media. Bioelectrochem. Bioenerg. 45 (1), 93–101. https://doi.org/10.1016/S0302-4598(98)00067-1. URL. http://linkinghub.elsevier.com/retrieve/pii/S0302459898000671.

Vogel, R., Süssmuth, R., 1999. Weak light emission patterns from lactic acid bacteria. Luminescence 14 (2), 99–105. https://doi.org/10.1002/(SICI)1522-7243(199903/04)14:2<99::AID-BIO519>3.0.CO;2-7. URL.

Vogel, R., Guo, X., Süssmuth, R., 1998. Chemiluminescence patterns from bacterial cultures undergoing bacteriophage induced mass lysis. Bioelectrochem. Bioenerg. 46 (1), 59–64. https://doi.org/10.1016/S0302-4598(98)00123-8. URL. http://linkinghub.elsevier.com/retrieve/pii/S0302459898001238.

Wagner, T.C., Scott, M.D., 1994. Single extraction method for the spectrophotometric quantification of oxidized and reduced pyridine nucleotides in erythrocytes. Anal. Biochem. 222 (2), 417–426 publisher: Elsevier.

Weber, D., Davies, M.J., Grune, T., 2015. Determination of protein carbonyls in plasma, cell extracts, tissue homogenates, isolated proteins: focus on sample preparation and derivatization conditions. Redox Biol. 5, 367–380. https://doi.org/10.1016/j.redox.2015.06.005. URL. http://linkinghub.elsevier.com/retrieve/pii/S2213231715000567.

Wefers, H., Sies, H., 1983. Oxidation of glutathione by the superoxide radical to the disulfide and the sulfonate yielding singlet oxygen. Eur. J. Biochem. 137 (1–2), 29–36. URL. http://onlinelibrary.wiley.com/doi/10.1111/j.1432-1033.1983.tb07791.x/full.

Wefers, H., Toru, K., Sies, H., 1984. Generation of low-level chemiluminescence during the metabolism of 1-naphthol by rat liver microsomes. Biochem. Pharmacol. 33 (24), 4081–4085 publisher: Elsevier.

Wefers, H., Reichmann, E., Sies, H., 1985. Excited species generation in horseradish peroxidase-mediated oxidation of glutathione. J. Free Radic. Biol. Med. 1 (4), 311–318 (publisher: Elsevier).

White, E.H., Miano, J.D., Watkins, C.J., Breaux, E.J., 1974. Chemically produced excited states. Angew Chem. Int. Ed. Engl. 13 (4), 229–243. https://doi.org/10.1002/anie.197402291, 10.1002/anie.197402291. URL.

Wijk, R.V., Van, E.P.A., 2008. Free radicals and low-level photon emission in human pathogenesis: state of the art. Indian J. Exp. Biol. 37.

Willner, I., Yan, Y.-M., Willner, B., Tel-Vered, R., 2009. Integrated enzyme-based biofuel cells-A review. Fuel Cell. 9 (1), 7–24. https://doi.org/10.1002/fuce.200800115, 10.1002/fuce.200800115.

Wilson, C., González-Billault, C., 2015. Regulation of cytoskeletal dynamics by redox signaling and oxidative stress: implications for neuronal development and trafficking. Front. Cell. Neurosci. 9 https://doi.org/10.3389/fncel.2015.00381. URL. https://www.ncbi.nlm.nih.gov/pmc/articles/PMC4588006/.

Winkler, R., Guttenberger, H., Klima, H., 2009. Ultraweak and induced photon emission after wounding of plants. Photochem. Photobiol. 85 (4), 962–965. URL. http://onlinelibrary.wiley.com/doi/10.1111/j.1751-1097.2009.00537.x/full.

Wurtmann, E.J., Wolin, S.L., 2009. RNA under attack: cellular handling of RNA damage. Crit. Rev. Biochem. Mol. Biol. 44 (1), 34–49. https://doi.org/10.1080/10409230802594043. URL. http://www.tandfonline.com/doi/full/10.1080/10409230802594043.

Xie, Y., Li, Z., 2018. Triboluminescence: recalling interest and new aspects. Chem 4 (5), 943–971. https://doi.org/10.1016/j.chempr.2018.01.001. URL. https://www.sciencedirect.com/science/article/pii/S2451929418300238.

Xing, D., Tan, S., Tang, Y., He, Y., Li, D., 1999. Observation of biophoton emission from plants in the process of defense response. Chin. Sci. Bull. 44 (23), 2159–2162 (publisher: Springer).

Yan, L.-J., Forster, M.J., 2011. Chemical probes for analysis of carbonylated proteins: a review. J. Chromatogr. B 879 (17–18), 1308–1315. https://doi.org/10.1016/j.jchromb.2010.08.004. URL. http://linkinghub.elsevier.com/retrieve/pii/S157002321000485X.

Yan, L.-J., Sohal, R.S., 2000. Analysis of oxidative modification of proteins. Curr. prot. protein sci. 20 (1), 14–4.

Yin, H., Porter, N.A., 2005. New insights regarding the autoxidation of polyunsaturated fatty acids. Antioxidants Redox Signal. 7 (1–2), 170–184. https://doi.org/10.1089/ars.2005.7.170. URL. http://www.liebertpub.com/doi/10.1089/ars.2005.7.170.

Yin, B., Whyatt, R.M., Perera, F.P., Randall, M.C., Cooper, T.B., Santella, R.M., 1995. Determination of 8-hydroxydeoxyguanosine by an immunoaffinity chromatography-monoclonal antibody-based ELISA. Free Radic. Biol. Med. 18 (6), 1023–1032.

You, S.-H., Lim, H.-D., Cheong, D.-E., Kim, E.-S., Kim, G.-J., 2019. Rapid and sensitive detection of NADPH via mBFP-mediated enhancement of its fluorescence. PLoS One 14 (2), e0212061. https://doi.org/10.1371/journal.pone.0212061. URL. http://dx.plos.org/10.1371/journal.pone.0212061.

Yun, J., Rocic, P., Pung, Y.F., Belmadani, S., Carrao, A.C.R., Ohanyan, V., Chilian, W.M., 2009. Redox-dependent mechanisms in coronary collateral growth: the "redox window" hypothesis. Antioxidants Redox Signal. 11 (8), 1961–1974. https://doi.org/10.1089/ars.2009.2476. URL. https://www.ncbi.nlm.nih.gov/pmc/articles/PMC2848513/.

Zapata, F., Pastor-Ruiz, V., Ortega-Ojeda, F., Montalvo, G., Ruiz-Zolle, A.V., García-Ruiz, C., 2021. Human ultra-weak photon emission as non-invasive spectroscopic tool for diagnosis of internal states – a review. J. Photochem. Photobiol. B Biol. 216, 112141 https://doi.org/10.1016/j.jphotobiol.2021.112141. URL. https://www.sciencedirect.com/science/article/pii/S1011134421000191.

Zaqaryan, A.E., Badalyan, H.G., 2016. Chemiluminescence of rats' whole blood after X-ray and. γ-irradiation 9 (1), 4.

Zhang, Z., Huber, G.W., 2018. Catalytic oxidation of carbohydrates into organic acids and furan chemicals. Chem. Soc. Rev. 47 (4), 1351–1390. https://doi.org/10.1039/C7CS00213K. URL. http://xlink.rsc.org/?DOI=C7CS00213K.

Zhang, J., Wang, X., Vikash, V., Ye, Q., Wu, D., Liu, Y., Dong, W., 2016. ROS and ROS-mediated cellular signaling. Oxidative Medicine and Cellular Longevity 2016 1–18. https://doi.org/10.1155/2016/4350965. URL. http://www.hindawi.com/journals/omcl/2016/4350965/.

Zhao, Y., Wang, A., Zou, Y., Su, N., Loscalzo, J., Yang, Y., 2016. In vivo monitoring of cellular energy metabolism using SoNar, a highly responsive sensor for NAD+/NADH redox state. Nat. Protoc. 11 (8), 1345–1359. https://doi.org/10.1038/nprot.2016.074. URL. http://www.nature.com/articles/nprot.2016.074.

Zhu, J., Thompson, C.B., 2019. Metabolic regulation of cell growth and proliferation. Nat. Rev. Mol. Cell Biol. 1.

Zhu, D., Xing, D., Wei, Y., Li, X., Gao, B., 2004. Evaluation of the degree of medical radiation damage with a highly sensitive chemiluminescence method. Luminescence 19 (5), 278–282. https://doi.org/10.1002/bio.782. URL. https://onlinelibrary.wiley.com/doi/10.1002/bio.782.

5 Biological autoluminescence for assessing oxidative processes in yeast cell cultures

This chapter is a version of:

Petra Vahalová, Kateřina Červinková and Michal Cifra,
Biological autoluminescence for assessing oxidative processes in yeast cell cultures,
Scientific Reports, volume 11, issue 1, number 10852, 2021.
DOI: doi.org/10.1038/s41598-021-89753-9.

Author contributions:

Petra Vahalová:
Data curation (lead), Formal analysis (lead), Investigation (lead), Methodology (lead), Software, Visualization (lead), Writing – original draft (lead)

Kateřina Červinková:
Data curation (supporting), Formal analysis (supporting), Investigation (supporting), Methodology (supporting)

Michal Cifra:
Conceptualization, Formal analysis (supporting), Funding acquisition, Investigation (supporting), Project administration, Resources, Supervision, Validation, Visualization (supporting), Writing – original draft (supporting), Writing – review & editing

Candidate's contribution: 80 %

The manuscript carries the following acknowledgements:

We acknowledge Czech Science Foundation, project no. 20-06873X for funding. Authors also participate in the COST CA15211 and exchange project between Czech and Slovak Academy of Sciences, no. SAV-18-11. Neuron collective is acknowledged for the support in graphical design and The Science Editorium for the manuscript language check.

The supplementary information is in Appendix (Section B).

scientific reports

OPEN

Biological autoluminescence for assessing oxidative processes in yeast cell cultures

Petra Vahalová, Kateřina Červinková & Michal Cifra✉

Nowadays, modern medicine is looking for new, more gentle, and more efficient diagnostic methods. A pathological state of an organism is often closely connected with increased amount of reactive oxygen species. They can react with biomolecules and subsequent reactions can lead to very low endogenous light emission (biological autoluminescence—BAL). This phenomenon can be potentially used as a non-invasive and low-operational-cost tool for monitoring oxidative stress during diseases. To contribute to the understanding of the parameters affecting BAL, we analyzed the BAL from yeast *Saccharomyces cerevisiae* as a representative eukaryotic organism. The relationship between the BAL intensity and the amount of reactive oxygen species that originates as a result of the Fenton reaction as well as correlation between spontaneous BAL and selected physical and chemical parameters (pH, oxygen partial pressure, and cell concentration) during cell growth were established. Our results contribute to real-time non-invasive methodologies for monitoring oxidative processes in biomedicine and biotechnology.

One of the main missions of modern society is to prevent, manage, and cure diseases. A key requirement to achieve this is the development of effective and ideally non-invasive diagnostic methods. New gentle diagnostic methods will help to overcome limitations of current methods, which can be painful for the patient and destructive for the analyzed biosamples. In addition to human diseases, the development of new diagnostic methods is also important for monitoring diseases of animals or plants, which have a strong impact on agriculture and the food industry. In this work, we contribute to the development of a non-invasive biophotonic method for real-time monitoring of oxidative processes in cell cultures as model organisms.

Multiple diseases, including those that are the leading causes of deaths worldwide, such as cancer[1], neurodegenerative[2], and cardiovascular[3,4] diseases, are closely related to an increased amount of reactive oxygen species (ROS) in affected body parts. In living organisms, incomplete reduction of O_2 during respiration is considered to be a typical source of ROS. However, ROS are also naturally produced during fatty acid metabolism in peroxysomes and by NADPH oxidases in the membrane of macrophages[5]. Non-mitochondrial ROS sources, originating from proteins encoded by NADPH oxidase orthologs, have also been recently discovered in single cell organisms, such as yeast[6]. The level of ROS in an organism can also be increased by ionizing radiation or chemicals[7]. To maintain redox homeostasis, which is necessary for proper functioning of an organism, organisms have developed various defense mechanisms to eliminate undesirable ROS or prevent the damage caused by them. Endogenous antioxidants include antioxidant enzymes (e.g., catalase, superoxide dismutase, or glutathione reductase), metal binding proteins (such as ferritin binding iron or ceruloplasmin binding copper), and several other compounds (e.g., lipoic acid, NAD(P)H, or thioredoxin)[8]. Water-soluble ascorbic acid or lipid-soluble tocopherol are examples of antioxidants usually supplied by nutrients.

Interactions of ROS with biomolecules lead to a cascade of reactions. ROS are initiators of these reactions but also their products. We can distinguish radicals with unpaired electron (e.g., superoxide anion $O_2^{\cdot-}$, peroxynitrite $ONOO^{-\cdot}$, hydroperoxyl $HO_2^{\cdot}$, hydroxyl $HO^{\cdot}$, peroxyl $ROO^{\cdot}$, alkoxyl $RO^{\cdot}$, or alkyl $R^{\cdot}$ radicals) and less reactive two-electron ROS (e.g., hydrogen peroxide H_2O_2, organic hydroperoxides ROOH, or singlet oxygen $^1O_2$) or if they are organic or not[7]. However, these oxidants can convert among themselves under particular circumstances and reaction conditions. The probable mechanism from the reaction of ROS with biological matter to final photon emission (BAL) is briefly described below.

Highly reactive non-organic radicals (mainly $HO^{\cdot}$ or $HO_2^{\cdot}$) adopt an electron from organic matter RH resulting in the formation of an organic radical $R^{\cdot}$[9]. In the presence of molecular oxygen, peroxyl $ROO^{\cdot}$ can be created and subsequently remove the hydrogen from another RH, leading to the formation of ROOH and the restoration of an alkyl $R^{\cdot}$ radical. Cyclization or recombination of $ROO^{\cdot}$ results in the creation of unstable high-energy

Institute of Photonics and Electronics of the Czech Academy of Sciences, Prague, Czechia. ✉email: cifra@ufe.cz

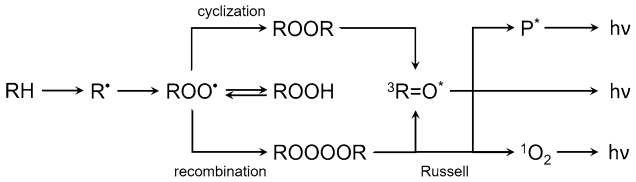

Figure 1. A simplified scheme of reactions of ROS with biological matter and subsequent possible reactions leading to photon emission based on earlier work[9]. Initially, the reaction of ROS with a biomolecule RH leads to the formation of various radicals, which in turn lead to the formation of unstable high-energetic intermediates (ROOR, ROOOOR). Decomposition of these energetic intermediates leads to the formation of electron excited species and subsequent photon emission hν. See details in the text.

intermediates, dioxetanes ROOR[10] and tetroxides ROOOOR[11], respectively. 1,2-dioxetane decomposes to triplet excited ^{3}R=O* and ground R=O carbonyls, and tetroxide, either to triplet excited carbonyl ^{3}R=O*, molecular oxygen, and organic hydroxide ROH or to ground-state carbonyl R=O, singlet oxygen $^1O_2$, and ROH[9]. If a chromophore or molecular oxygen are in proximity of triplet excited carbonyls $^3R = O^*$, energy transfer can occur and lead to the formation of a triplet ^{3}P* or singlet ^{1}P* excited chromophore and singlet oxygen $^1O_2$, respectively. Singlet oxygen can also be the primary product of decomposition of unstable high-energy intermediates. Redundant energy of excited species can be released in the form of heat or as light emission[12]. Triplet excited carbonyls $^3R = O^*$ emit between 350 and 550 nm, chromophores in the region 550–750 nm (^{1}P*) and 750–1000 nm (^{3}P*), depending on their type. Typical emission wavelengths for singlet oxygen $^1O_2$ are 1270 nm for monomol or 634 and 703 nm for dimol photon emission. A simplified scheme of the reactions is shown in Fig. 1.

However, the probabilities of the reactions leading to the formation of excited species and subsequent radiative de-excitation are very low; therefore, the intensity of photon emission is also very low[13]. From tens to several hundreds of photons s^{-1} cm^2 is the range of intensities typical for spontaneous photon emission of a sample[12]. The intensity can increase by 2–3 orders of magnitude in the case of artificially induced photon emission. On the other hand, detector efficiency, distance between the sample and detector, and additional optical effects (such as absorption or scattering in the sample) decrease the amount of photons that can be detected. Several terms are used to describe this phenomenon. Here we use biological autoluminescence (BAL) to emphasize the biological and endogenous origin of this luminescence phenomenon. Other terms used in the literature are ultra-weak photon emission, biophotons, or bio-chemiluminescence[12].

Although the probable general biochemical and biophysical mechanisms of BAL are rather well established[13], the origin and physiology of the processes leading to BAL are different for different organisms in different conditions[14–17].

The amount of ROS in organisms can be affected by endogenous processes but also by the presence of external oxidants and pro-oxidants. Natural and artificial processes can lead to the generation of various types of ROS. One of the common reactions that yields highly reactive hydroxyl radicals besides other products[18] is the Fenton reaction, which involves divalent iron (Fe^{2+}) and hydrogen peroxide (H_2O_2). In organisms, these two chemicals are strictly controlled and separated. However, artificial usage of the Fenton reaction is popular in many industrial fields in which production of the highly reactive radical is desirable.

As a biological system for the analysis of ROS-BAL correlations, we chose yeast *Saccharomyces cerevisiae*, which is a widely used and well characterized model organism in molecular biology research. Furthermore, yeasts and their various strains are also essential in the food industry[19,20] and biotechnology[21]. They are eukaryotic, which is the same as humans, animals, or plants, but single-celled organisms; thus, it is easier to evaluate the effects of various stress factors on the organism.

There have been several studies of spontaneous BAL from yeast. For example, Quickenden et al.[14,22–25] studied the intensity and spectral distribution of spontaneous BAL in the exponential and stationary phase of yeast growth. Other researchers have used various methods to study oxidation caused by the Fenton reaction[26,27]. Ivanova et al.[28] focused on mechanisms of chemiluminescence as a result of the Fenton reaction. To connect these topics and broaden the knowledge about them, we decided to evaluate the correlation between BAL of a living organism, yeast *Saccharomyces cerevisiae*, and artificially increased amount of ROS by the Fenton reaction. We also investigated the correlation between spontaneous BAL and selected physical and chemical parameters (pH, oxygen partial pressure, cell concentration, and concentration of the antioxidant ascorbic acid) to verify the hypothesis of ROS-BAL correlation. See Fig. 2 for the scheme of the paper.

Results and discussion

Biological autoluminescence enhanced by Fenton reagents. First, we evaluated the BAL signal from yeast samples containing three different cell concentrations to determine which concentration resulted in the highest BAL intensity. The BAL intensity was observed during real-time oxidation of yeast cells with 0.5 mM $FeSO_4$ and 2.5 mM H_2O_2 (final concentrations are always provided, unless noted otherwise). The kinetics during the first 60 s are shown in Fig. 3a. Hydrogen peroxide was injected into the sample after 10 seconds of background measurement. The sums of the BAL signal during the first 60 s after injection of H_2O_2 with a subtracted background (first 10 s before the injection of H_2O_2) are shown in Fig. 3b. The average from 3 independent measurements and standard deviation are displayed. We can see that the BAL signal increases together

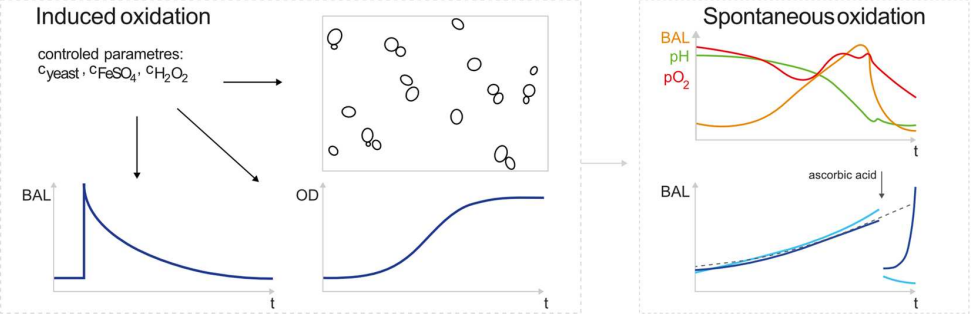

Figure 2. A schematic summary of the parameters and processes related to biological autoluminescence (BAL) explored in this paper. We analyzed the BAL and related parameters both under the conditions of induced and spontaneous (endogenous) oxidation in the yeast cell cultures. For induced oxidation, the amount of free radicals in a sample was regulated (increased) by the Fenton reaction. Then, the effects of various concentration of yeast and Fenton reagents ($FeSO_4$ and H_2O_2) on BAL, growth curves, and cell clustering was analyzed. The BAL due to spontaneous oxidation processes and its correlation with several selected parameters (pH, pO_2, concentration of antioxidant ascorbic acid) were established.

with the yeast concentration up to the limit 10^8 cells mL^{-1}. With increasing yeast concentration, the amount of biomass that ROS can react with is higher and the amount of potential sources of BAL grows. However, above 10^8 cells mL^{-1}, the samples start to become increasingly turbid and also sediment faster, making the lower layers inaccessible for oxygen and the Fenton reagents, hence decreasing the actual amount of biomass that could be directly oxidised. All these factors, we believe, lead to the lower BAL intensity for cell concentrations above 10^8 cells mL^{-1}. Therefore, for subsequent experiments we used a yeast concentration of 10^8 cells mL^{-1}, which exhibited the highest BAL intensity.

We measured the BAL response of yeast cell cultures at a concentration of 10^8 cells mL^{-1} induced by the addition of various concentrations of the Fenton reagents $FeSO_4$ and H_2O_2. The final concentration ranges of the reagents were 50 nM–0.5 mM $FeSO_4$ and 25 μM–25 mM H_2O_2. The sums of the BAL intensities during the first 60 s after injection of H_2O_2 with a subtracted background (calculated from the previous 10 s before the injection of H_2O_2) are shown in Fig. 3c. The given numbers (represented by colours) are the average from 3 measurements with a standard deviation. At the lowest used concentrations (50 nM $FeSO_4$ and 25 μM H_2O_2), a signal comparable to the intensity of a control sample (only Milli-Q water without yeast) was obtained, see Fig. S1. For the measurements at higher concentrations, the BAL signals were substantially higher than those obtained with the control samples. Generally, higher Fenton reagent concentrations resulted in a higher BAL signal.

The influence of oxidation induced by the Fenton reaction (caused by the 0.5 mM $FeSO_4$ and 2.5 mM or 25 mM H_2O_2) on a yeast cells was evaluated under a microscope. In Fig. 3e,f yeast (e) before and (f) after 10 min oxidation with 0.5 mM $FeSO_4$, 2.5 mM H_2O_2 are shown. The yeast concentration (evaluated for cells with a diameter between 3 and 9 μm) was 10^8 cells mL^{-1} for control sample and before oxidation (Fig. 3e) and $3 \cdot 10^7$ cells mL^{-1} after oxidation of the cells (Fig. 3f). For both H_2O_2 concentrations, we did not observe any damaged cells. However, the yeast cells tended to cluster after oxidation. Cell aggregation could be one of the possible reasons for the lower yeast concentration that was measured in the 3–9 μm cell diameter range.

Toledano et al. claimed that the toxic concentration of hydrogen peroxide for yeast is approximately 5 mM (depending on the yeast species)[5], [chap. 6, p.246], which is within the range of the concentrations we evaluated. However, inducing the apoptosis by external oxidants depends on the incubation time. There are also several factors that can modulate the resistance to oxidative stress. For example, yeasts have a higher resistance to oxidative stress in the stationary phase and during respiration, when their metabolic processes (oxidative phosphorylation) employ oxygen and inevitably generate ROS endogenously. Also, previous mild stress condition (including different types of stress) can lead to increased tolerance to oxidative stress. For example, the sudden transfer of yeast cells from room temperature to 30 °C and change of the medium can be experienced as stress[5], [chap. 6]. To assess the viability of cells after the oxidation by Fenton reagents (10 min incubation; 0.5 mM $FeSO_4$, 2.5–250 mM H_2O_2), we performed a Trypan blue assay using identical experimental conditions (yeast strain, buffers, all reagent and cells concentration, duration of oxidation treatments) in our recent work[29]. Under our experimental conditions, the cell viability remained >98 % after treatment with 2.5 mM and 25 mM H_2O_2 and reduced to 87 % after treatment with 250 mM H_2O_2.

The effect of the Fenton reaction ($\approx$ 10 min incubation; 0.5 mM $FeSO_4$, 2.5 - 250 mM H_2O_2) on yeast growth was also evaluated here. As shown in Fig. 3d, the samples treated with a higher concentration of hydrogen peroxide had a longer lag phase. However, the final amount of cells (in the stationary phase) was similar for all samples. The duration of the lag phase depends on several factors such as the temperature, aeration, the conditions in a previous environment, amount of transferred biomass, or yeast health[30], [chap. 9]. More stressed cells probably need more time to overcome unfavourable consequences and to prepare for cell division.

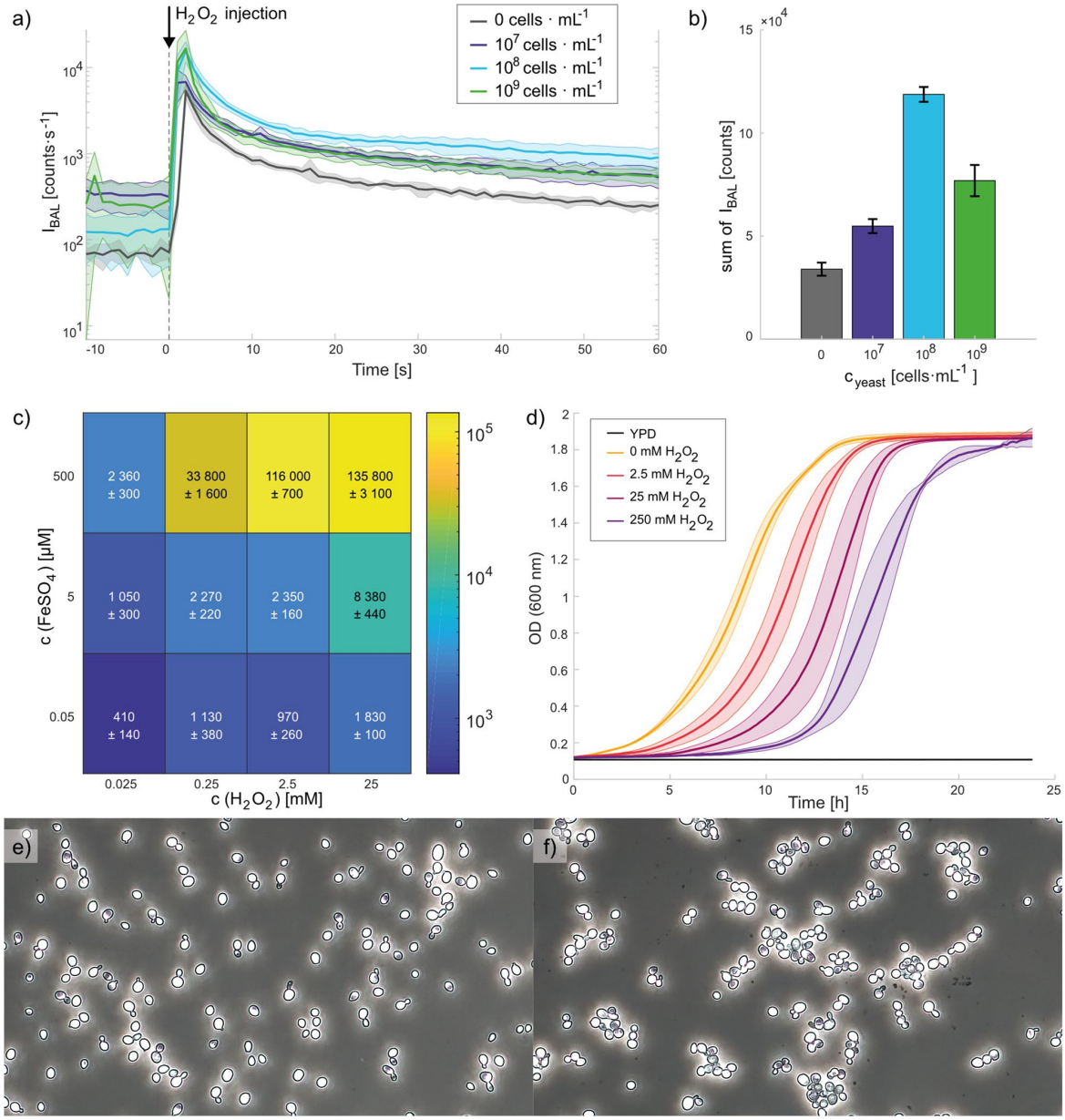

Figure 3. Effects of the Fenton reaction on BAL of yeast, their growth curve, and evaluation of the oxidised yeast under a microscope. First two graphs (**a,b**) show induced BAL of yeast by the Fenton reaction (0.5 mM $FeSO_4$, 2.5 mM H_2O_2) for different concentrations of yeast (10^7–10^9 cells mL^{-1}). Part **c)** displays induced yeast BAL by the Fenton reaction for various concentrations of Fenton reagents (50 nM–0.5 mM $FeSO_4$, 25 µM–25 mM H_2O_2) and a fixed yeast concentration (10^8 cells mL^{-1}). (**a**) BAL kinetics after the injection of hydrogen peroxide into the sample after 10 seconds of background measurement (t = 0). (**b**) Bar graph and (**c**) heat map of the sum of the BAL intensities during the first 60 s after injection of H_2O_2 with a subtracted background (the previous 10 s before the injection of H_2O_2). (**d**) Yeast growth curves after oxidation of cells (10^8 cells mL^{-1}) by the Fenton reaction (~10 min; 0.5 mM $FeSO_4$, 0/2.5/25/250 mM H_2O_2) depicted by OD at 600 nm. In all cases (**a**–**d**), the average from 3 measurements and the standard deviation are shown. Microscopic pictures of a yeast sample in water (**e**) before and (**f**) after the Fenton reaction (~10 min; 0.5 mM $FeSO_4$, 2.5 mM H_2O_2). Yeast concentrations (3–9 µm in a diameter) were 10^8 cells mL^{-1} before and $3 \cdot 10^7$ cells mL^{-1} after oxidation.

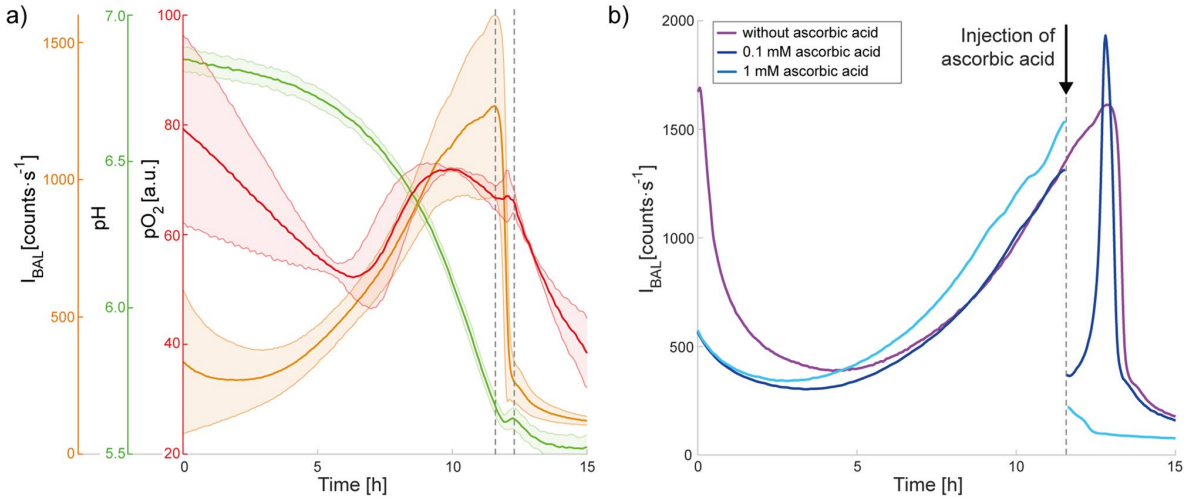

Figure 4. (**a**) Spontaneous BAL of yeast measured in a bioreactor together with the change in pH and pO_2 (average from 3 measurements with a standard deviation). Dashed vertical lines around the twelfth hour delimit the sharp decrease of the BAL intensity and corresponding changes in pH and pO_2. (**b**) Influence of various concentrations of the antioxidant ascorbic acid (0–1 mM) on spontaneous BAL of yeast. The initial concentration of the sample was $5 \cdot 10^5$ cells mL^{-1}.

Spontaneous biological autoluminescence. We also analyzed the spontaneous BAL of yeast culture in a bioreactor during their growth (Fig. 4a). Because the sample was prepared under normal laboratory light conditions, we observed an initial slight decrease of the BAL signal while the sample was adapting to the dark condition in a black box (the decreasing signal was observed also in YPD medium only, see Fig. S2, so we do not attribute it to cellular processes). Then, the signal increased during several hours. At the same time, the pH decreased and pO_2 displayed nonlinear behavior. After approximately 12 h of measurement, the BAL signal sharply decreased, whereas the pH and pO_2 slightly increased. Quickenden et al. observed that the BAL of yeast *Saccharomyces cerevisiae* was similar to nutrient luminescence (i.e. close to background) in anaerobic conditions (nitrogen instead of air)[24]. However, there was still enough oxygen in our samples after approximately 12 h (Fig 4a). As shown in Fig. 3d, a transition from exponential to stationary phase of the cell growth curve occurs after approximately 12 h (in a control sample = without Fenton reagents treatment). This change of phases is called the diauxic shift and it is connected with a change in yeast metabolism from fermentation to aerobic respiration. Therefore, a sharp decrease of the BAL intensity could be caused by internal changes related with the initiation of respiration. This statement might look contradictory at first sight, because within classical understanding of physiological processes underlying BAL, a higher respiration rate (mitochondria-enabled) should lead to a higher rate of ROS generation[31–34], hence to a higher BAL intensity. To explain our observations, we propose the following hypothesis:

1. the ROS generation rate $k_{ROS} = \frac{dROS}{dt}$ per unit of effective amount of metabolically active yeast biomass M_{active} during anaerobic phosphorylation is smaller than the one during the oxidative phosphorylation, i.e., $k_{ROS,anaerobic} < k_{ROS,aerobic}$
2. the metabolic activity of yeast is much higher during anaerobic metabolism than during aerobic metabolism, as demonstrated by the cell growth-rate in the exponential phase versus stationary phase, i.e., $M_{active,anaerobic} \gg M_{active,aerobic}$
3. the BAL intensity I_{BAL} is proportional to $M_{active} k_{ROS}$
4. $M_{active,anaerobic}\ k_{ROS,anaerobic} > M_{active,aerobic}\ k_{ROS,aerobic}$, i.e., $I_{BAL,anaerobic} > I_{BAL,aerobic}$

What could be the potential sources of ROS during anaerobic metabolism and is there any supporting data for our hypothesis? According to[35], non-mitochondrial ROS generation can be related to cellular biosynthesis. Tilbury et al. also suggested that possible source of BAL during the exponential phase of yeast growth (during fermentation) are oxidative side-reactions accompanying protein synthesis[14]. Rinnerthaler et al. found that an important non-mitochondrial source of ROS in yeast is a NADPH-oxidase ortholog Yno1p/Aim14p[6]. Maslanka et al. also evaluated the content of pyridine nucleotide cofactors and the ratios of their reduced and oxidised form. They observed a higher ratio of NADPH/$NADP^+$ for yeast cultivated in the media supporting aerobic respiration[35]. Besides other functions, NADPH is considered to directly operate as an antioxidant to scavenge free radicals and reduce oxidised biomolecules[36]. Jamieson et al.[37] observed significantly higher (oxidative) stress resistance during respiratory growth and stationary phase than during fermentation. Because incomplete reduction of O_2 during respiration is usually considered as the major source of ROS[5], organisms have developed active, antioxidant-based defense mechanisms, which lead to a decreased amount of ROS in cells or repairing

of the damage caused by them. Maslanka et al. observed a dependence of ROS amount and also the ROS source on the type of carbon source/concentration of glucose and on the type of metabolism of yeast *Saccharomyces cerevisiae* wild-type and two mutant strains: Δsod1 and Δsod2[35]. Their results showed that non-mitochondrial ROS sources are an important pool of ROS in yeast, especially during fermentation. They also observed that more ROS are generated by yeast in the medium with higher concentration of glucose when they estimated the level of ROS with dihydroethidium (DHET). Because glucose is an important source of energy for yeast and its concentration in a sample has influence on yeast metabolism, we also performed experiments with glucose. We observed changes in the glucose concentration in the yeast samples during their growth (Fig. S4) and an increase in the yeast BAL intensity when glucose was re-supplied into the sample (Fig. S3). Our data are in agreement with the results of Maslanka et al.[35]. The glucose concentration decreased with increasing yeast concentration. In our second mentioned type of the experiment with glucose, after the BAL signal reaches the peak and drops to a low level, the addition of glucose causes a temporary increase of the BAL intensity (Fig. S3).

To briefly comment on the kinetics of the pH and partial pressure of oxygen (pO_2) in the sample during 15-h yeast growth in the bioreactor (Fig. 4a): The decrease of pH during fermentation is a well-known effect in yeast biotechnology caused by excretion of organic acids and absorption of basic amino acids[38]. The kinetics of pO_2 is much more enigmatic: Initially, there is a decrease of pO_2, then an increase starting after approximately 6–7 h and then a decrease again after 10 h. In general, there are two competing processes that determine the pO_2: O_2 (air) supply to the bioreactor via an injecting tube through a bubbling output and consumption of the O_2 in the sample, which explain the three observed phases of the pO_2 kinetics. The initial decrease of pO_2 might be due to slowly fading auto-oxidation taking place in the YPD medium, which binds O_2. The following increase might be due to O_2 supply starting to dominate over the O_2 consumption. The decrease that starts after 10 h is likely owing to the onset of cellular respiration.

We carried out further experiments to test whether oxidative reactions are indeed involved in spontaneous BAL generation. The amount of ROS in a sample can be increased by the Fenton reaction, as demonstrated in previous studies[26–28]. On the other hand, the sample ROS content can also be artificially decreased by using, for example, an antioxidant. For experiments in which we wanted to suppress ROS (with an expected consequence of suppressing the BAL intensity), a sample with a higher BAL intensity is more suitable for observing a significant signal decrease. Therefore, the influence of the antioxidant ascorbic acid on the BAL of yeast culture was observed at the time points with high BAL intensity (Fig. 4b). The effect of the antioxidant depended on its final concentration in the sample. After injection of ascorbic acid at a lower concentration (0.1 mM), we observed a rapid decrease followed by a steep increase back to the values expected for a sample without antioxidant treatment. The injection of ascorbic acid at a higher final concentration (1 mM) resulted in a steep decrease and no renewal of the signal. The observed effects probably depended on the ratio of the amounts of ROS and antioxidant. At a lower final concentrations of antioxidant, the molecules of ascorbic acid react with ROS and are quickly depleted. Then, the amount of ROS, and thus the BAL signal, increases again without any hindrance. A higher concentration of ascorbic acid either terminates the chain production of ROS or considerably reduces the amount of ROS for such a long time that the yeast can pass through the fermentation to the aerobic respiration phase. Červinková et al.[39] also studied the effects of ascorbic acid (vitamin C), among other antioxidants, on yeast BAL intensity. They tested concentrations of 1, 5, and 10 mM and also did not observe any renewal of the BAL signal. They also tested the influence of ascorbic acid (1, 500, and 1000 μM) on the BAL intensity of HL-60 cells. Even at the lowest used concentration (1 μM), the signal did not recover. As expected, each sample has a different threshold antioxidant concentration and also a different response to various antioxidants[39].

Conclusion

We investigated the correlations between selected physical, chemical, and biological factors and the BAL intensity of yeast samples. The oxidation of a yeast cells using the Fenton reaction caused a higher BAL signal with increasing concentrations of the Fenton reagents. A higher BAL signal was also observed with increasing yeast concentration up to a certain limit, after which the BAL signal decreased again. On the other hand, the addition of the antioxidant ascorbic acid to the sample decreased the BAL intensity for some time depending on the antioxidant dose. We did not observe any damaged yeast cells under a microscope after short-time oxidation, just the tendency of the cells to cluster. However, a higher H_2O_2 concentration caused prolongation of the lag phase of the yeast growth.

During yeast culture growth in a bioreactor, the BAL intensity increased together with the number of cells, the pH and glucose concentration decreased, whereas the change in pO_2 was nonlinear. After approximately 12 h, when the glucose concentration was low and the yeast samples were undergoing the growth phase change (diauxic shift), the BAL signal sharply decreased.

We demonstrated that the BAL intensity of the yeast sample is proportional to the amount of ROS in the sample. Our data indicated that non-mitochondrial sources of ROS also play an important role in the production of ROS and BAL. We were able to monitor various processes closely connected with the change of ROS content in the studied object by observing changes of the BAL intensity over time. However, the ROS content can be affected by many various factors. Beyond chemical factors, it could be also physical factors such as magnetic[29] and electric field, particularly pulsed electric field, which is a part of our ongoing work. In general, knowing which other factors can influence the BAL intensity and the mechanisms involved will allow the development of a new reliable diagnostic method.

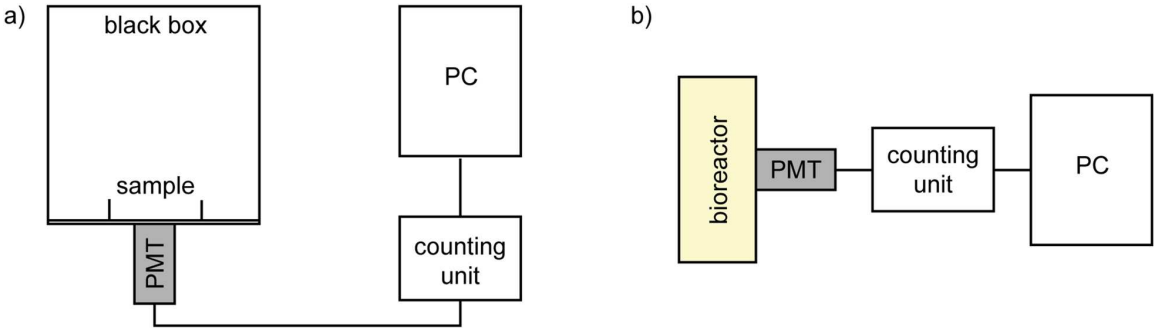

Figure 5. A scheme of the experimental setup for the measurements of BAL during (**a**) induced oxidation in a Petri dish in a black box and (**b**) spontaneous oxidation in a bioreactor. The bioreactor with the photodetector chamber was light-isolated by a black cloth construction.

Methods

Yeast *Saccharomyces cerevisiae* wild type (BY 4741) was used as a model organism. They were cultivated for approximately 24 h in an orbital shaking incubator (Yihder Co., Ltd; LM-420D) at 30 °C, 180 rpm, in standard YPD medium (1 % yeast extract, 2 % peptone, 2 % D-glucose). Then, they were centrifuged (Heraeus Biofuge Stratos) 2 times and the YPD medium was changed to Milli-Q H_2O. Measurement of yeast concentration was performed with a cell counter (Beckman Coulter, Z2 series) in the range 3 - 9 μm. Yeast *Saccharomyces cerevisiae* has a diameter between 1 and 10 μm. Their mean cell size depends on various factors such as growth temperature[40], strain, and age[41].

Biological autoluminescence measurement setup. *Induced BAL.* Induced emission was measured from a 3 mL of yeast sample in Milli-Q water in a Petri dish (Thermo Scientific, diameter 35 mm). The concentration of yeast was between 10^7 and 10^9 cells mL^{-1}. The amount of ROS in the sample was regulated by the Fenton reaction

$$Fe^{2+} + H_2O_2 \rightarrow Fe^{3+} + HO^{\cdot} + OH^{-} \quad (1)$$

After preparation of a yeast sample at a required cell concentration, 50 μL of iron(II) sulfate was added to the sample so that the final $FeSO_4$ concentrations in the sample was 50 nM, 5 μM, or 0.5 mM. Then the sample was placed into a special black box with a photomultiplier module H7360-01 (Hamamatsu Photonics K.K., spectral range 300–650 nm) where the measurements of BAL were performed. After approximately 1 min of BAL measurement, 50 μL of H_2O_2 (final concentrations: 25 μM, 250 μM, 2.5 mM, and 25 mM) was injected into the yeast sample with $FeSO_4$. The whole BAL measurement took approximately 10 minutes. A scheme of the experimental setup is shown in Fig. 5a.

Spontaneous BAL. Spontaneous emission was measured in a bioreactor Biostat Aplus (Sartorius Stedim Biotech) in a dark room. The bioreactor with the photodetector chamber was light-isolated by a black cloth construction to further minimize any background light. Yeasts at an initial concentration of $5 \cdot 10^5$ cells mL^{-1} were stirred (180 rpm), bubbled with air ($\sim$1 L min^{-1}) and maintained at a temperature of 30 °C during their cultivation in YPD medium. 75 μL of antifoaming agent (polypropylene glycol) was added to the 750 mL sample. The measurement time was between 15 and 20 h. The photomultiplier module (H7360-01, Hamamatsu Photonics K.K., spectral range 300–650 nm) was used for BAL measurements. A scheme of the experimental setup is shown in Fig. 5b. Measurement of the pH, pO_2, and temperature was performed by original probes included in the bioreactor.

The initial yeast concentration is lower compared with measurements of BAL intensity after short-time oxidation of yeast cells in water induced by the Fenton reaction. If we want to measure spontaneous BAL of yeast and their growth curve simultaneously, it is better to start at a lower yeast concentration to have a nicer shape of the curve. (The higher initial amount of yeast quickly depletes the glucose , the exponential phase is really short, and the difference between the initial and the final cell concentration is not so distinct.) Also, the measurement of yeast concentration is easier and more precise (without dilution of a sample) in the used concentration range. (Upper limit of a sample concentration is approximately $3 \cdot 10^8$ cells mL^{-1} for the cell counter.)

The experiment for observing the influence of glucose re-supply into the sample on BAL intensity was performed in an Erlenmeyer flask in a black box similar to the measurements of induced BAL. The measurement setup is described in[42]. Cells were cultivated in an orbital shaking incubator (YPD, 30 °C, 180 rpm) for 16 h. The cell concentration in the sample was established with a Bürker chamber. The required amount of yeast cells was transported to 200 mL of cold YPD medium so that the initial yeast concentration was $5 \cdot 10^5$ cells mL^{-1}. The sample was bubbled with filtered room air. After 16 h of spontaneous BAL measurement, 11 mL 40% glucose was added into the sample.

Glucose concentration measurement. The glucose concentration was established with a commercial glucose kit (Glu 1000, Erba Lachema). Optical density was measured at 500 nm and subsequently recalculated to a real glucose concentration in mM (using calibration solutions at known glucose concentration).

Growth curve. Growth curves were measured in a Spark microplate reader (Tecan). After approximately 24-h cultivation of yeast in an orbital shaking incubator (30 °C, 180 rpm) in standard YPD medium, the samples ware centrifuged (2×) and the YPD medium was changed to Milli-Q H_2O. Then, oxidation of the yeast sample (concentration of 10^8 cells mL^{-1}) was performed with the Fenton reaction (0.5 mM $FeSO_4$, 2.5 mM/25 mM/250 mM H_2O_2) for 10 min. The samples were in the shaker (30 °C, 180 rpm) during the oxidation. Then, the samples were centrifuged and the water was changed to fresh YPD medium. After dilution of each sample 100 times, 200 µL of each sample was put in a well of a 96-well plate (Thermo Scientific Nunc, transparent, non-treated, flat bottom, type no. 269620) and covered with a lid. 5–7 replicates of each sample were prepared on the same plate. The optical density at 600 nm was measured every 10 min for 24 h. The samples were shaken for the rest of the time. The temperature during measurement of the growth curves was maintained at 30 °C.

Microscopic imaging. Microscopic imaging before and after the oxidation by the Fenton reaction was performed with the microscope BX50 (Olympus) with the camera Moticam 1080. Phase contrast and an objective magnification of 20× was used.

Data availability

Raw data are available under https://doi.org/10.5281/zenodo.4382342 and described in the supplementary information S1.

Received: 18 December 2020; Accepted: 30 April 2021
Published online: 25 May 2021

References

1. Sabharwal, S. S. & Schumacker, P. T. Mitochondrial ROS in cancer: Initiators, amplifiers or an Achilles' heel?. *Nat. Rev. Cancer* **14**, 709–721. https://doi.org/10.1038/nrc3803 (2014).
2. Lin, M. T. & Beal, M. F. Mitochondrial dysfunction and oxidative stress in neurodegenerative diseases. *Nature* **443**, 787–795. https://doi.org/10.1038/nature05292 (2006).
3. Siegrist, J. & Sies, H. Disturbed redox homeostasis in oxidative distress: A molecular link from chronic psychosocial work stress to coronary heart disease?. *Circ. Res.* **121**, 103–105. https://doi.org/10.1161/CIRCRESAHA.117.311182 (2017).
4. Shah, A. M. Free radicals and redox signalling in cardiovascular disease. *Heart* **90**, 486–487. https://doi.org/10.1136/hrt.2003.029389 (2004).
5. Toledano, M. B., Delaunay, A., Biteau, B., Spector, D. & Azevedo, D. Oxidative stress responses in yeast. In *Yeast Stress Responses* Vol. 1 (eds Hohmann, S. *et al.*) 241–303 (Springer, Berlin Heidelberg, Berlin, Heidelberg, 2003). https://doi.org/10.1007/3-540-45611-2_6.
6. Rinnerthaler, M. *et al.* Yno1p/Aim14p, a NADPH-oxidase ortholog, controls extramitochondrial reactive oxygen species generation, apoptosis, and actin cable formation in yeast. *Proc. Natl. Acad. Sci.* **109**, 8658–8663. https://doi.org/10.1073/pnas.1201629109 (2012).
7. Hawkins, C. L. & Davies, M. J. Detection, identification, and quantification of oxidative protein modifications. *J. Biol. Chem.* **294**, 19683–19708 (2019).
8. Percival, M. Antioxidants. *Clin. Nutr. Ins.* **1**, 1–6 (1996).
9. Pospíšil, P., Prasad, A. & Rác, M. Mechanism of the formation of electronically excited species by oxidative metabolic processes: Role of reactive oxygen species. *Biomolecules* **9**, 258 (2019). https://www.mdpi.com/2218-273X/9/7/258.
10. Vacher, M. *et al.* Chemi- and bioluminescence of cyclic peroxides. *Chem. Rev.* **118**, 6927–6974. https://doi.org/10.1021/acs.chemrev.7b00649 (2018).
11. Miyamoto, S., Martinez, G. R., Medeiros, M. H. & Di Mascio, P. Singlet molecular oxygen generated by biological hydroperoxides. *J. Photochem. Photobiol. B: Biol.* **139**, 24–33 (2014).
12. Cifra, M. & Pospišil, P. Ultra-weak photon emission from biological samples: Definition, mechanisms, properties, detection and applications. *J. Photochem. Photobiol. B: Biol.* **139**, 2–10 (2014).
13. Pospíšil, P., Prasad, A. & Rác, M. Role of reactive oxygen species in ultra-weak photon emission in biological systems. *J. Photochem. Photobiol. B: Biol.* **139**, 11–23 (2014).
14. Tilbury, R. & Quickenden, T. Luminescence from the yeast Candida utilis and comparisons across three genera. *Luminescence* **7**, 245–253 (1992).
15. Hagens, R. *et al.* Non-invasive monitoring of oxidative skin stress by ultraweak photon emission measurement. II: biological validation on ultraviolet A-stressed skin. *Skin Res. Technol.* **0**, 071018045710002. https://doi.org/10.1111/j.1600-0846.2007.00207.x (2007).
16. Kato, K. *et al.* Application of ultra-weak photon emission measurements in agriculture. *J. Photochem. Photobiol. B: Biol.* **139**, 54–62 (2014).
17. Ou-Yang, H. The application of ultra-weak photon emission in dermatology. *J. Photochem. Photobiol. B: Biol.* **139**, 63–70 (2014).
18. Louwerse, M. *Computational modeling of oxidation catalysis: studies concerning Fenton's reaction*. Ph.D. thesis, s.n.], S.l. (2008). OCLC: 229344243.
19. Lambrechts, M. G. & Pretorius, I. S. Yeast and its Importance to Wine Aroma: A review. *S. Afr. J. Enol. Viticult.* **21**, 97–129 (2000). https://www.journals.ac.za/index.php/sajev/article/view/3560. Number: 1.
20. Pires, E. J., Teixeira, J. A., Brányik, T. & Vicente, A. A. Yeast: the soul of beer's aroma—a review of flavour-active esters and higher alcohols produced by the brewing yeast. *Appl. Microbiol. Biotechnol.* **98**, 1937–1949. https://doi.org/10.1038/nrc38036 (2014).
21. Borodina, I. & Nielsen, J. Advances in metabolic engineering of yeast Saccharomyces cerevisiae for production of chemicals. *Biotechnol. J.* **9**, 609–620. https://doi.org/10.1038/nrc38037 (2014).
22. Quickenden, T. I. & Hee, S. S. Q. Weak luminescence from the yeast Saccharomyces cerevisiae and the existence of mitogenetic radiation. *Biochem. Biophys. Res. Commun.* **60**, 764–770 (1974).
23. Quickenden, T. I. & Hee, S. S. Q. The spectral distribution of the luminescence emitted during growth of the yeast Saccharomyces cerevisiae and its relationship to mitogenetic radiation. *Photochem. Photobiol.* **23**, 201–204 (1976).

24. Quickenden, T. & Tilbury, R. Growth dependent luminescence from cultures of normal and respiratory deficient Saccharomyces cerevisiae. *Photochem. Photobiol.* **37**, 337–344 (1983).
25. Quickenden, T. I. & Tilbury, R. N. Luminescence spectra of exponential and stationary phase cultures of respiratory deficient Saccharomyces cerevisiae. *J. Photochem. Photobiol. B: Biol.***8**, 169–174 (1991).
26. Stadtman, E. & Berlett, B. Fenton chemistry. Amino acid oxidation. *J. Biol. Chem.* **266**, 17201–17211 (1991).
27. Baron, C. P., Refsgaard, H. H. F., Skibsted, L. H. & Andersen, M. L. Oxidation of bovine serum albumin initiated by the Fenton reaction—effect of EDTA, tert -butylhydroperoxide and tetrahydrofuran. *Free Radical Res.* **40**, 409–417. https://doi.org/10.1038/nrc38039 (2006).
28. Ivanova, I. P. *et al.* Mechanism of chemiluminescence in Fenton reaction. *J. Biophys. Checm.* **03**, 88–100. https://doi.org/10.1038/nature052920 (2012).
29. Bereta, M., Teplan, M., Chafai, D. E., Radil, R. & Cifra, M. Biological autoluminescence as a noninvasive monitoring tool for chemical and physical modulation of oxidation in yeast cell culture. *Sci. Rep.* **11**, 328. https://doi.org/10.1038/s41598-020-79668-2 (2021).
30. Jacques, K. A., Lyons, T. P. & Kelsall, D. R. *The alcohol textbook: a reference for the beverage, fuel and industrial alcohol industries* 4th edn. (Nottingham University Press, Nottingham, 2003) (**OCLC: 255247331**).
31. Cadenas, E., Boveris, A. & Chance, B. Low-level chemiluminescence of bovine heart submitochondrial particles. *Biochem. J.***186**, 659–667 (1980). http://www.biochemj.org/content/186/3/659.abstract.
32. Narayanaswami, V. & Sies, H. Oxidative damage to mitochondria and protection by ebselen and other antioxidants. *Biochem. Pharmacol.* **40**, 1623–1629 (1990).
33. Kamal, A. H. M. & Komatsu, S. Involvement of reactive oxygen species and mitochondrial proteins in biophoton emission in roots of soybean plants under flooding stress. *J. Proteome Res.* **14**, 2219–2236. https://doi.org/10.1021/acs.jproteome.5b00007 (2015).
34. Sardarabadi, H. *et al.* Enhancement of the biological autoluminescence by mito-liposomal gold nanoparticle nanocarriers. *J. Photochem. Photobiol. B: Biol.* **204**, 111812 (2020).
35. Maslanka, R., Zadrag-Tecza, R. & Kwolek-Mirek, M. Linkage between carbon metabolism, redox status and cellular physiology in the yeast Saccharomyces cerevisiae Devoid of SOD1 or SOD2 Gene. *Genes* **11**, 780 (2020).
36. Kirsch, M. & Groot, H. NAD(P)H, a directly operating antioxidant?. *FASEB J.* **15**, 1569–1574. https://doi.org/10.1038/nature052927 (2001).
37. Jamieson, D. J. Oxidative stress responses of the yeastSaccharomyces cerevisiae. *Yeast***14**, 1511–1527 (1998). https://onlinelibrary.wiley.com/doi/10.1002/(SICI)1097-0061(199812)14:16<1511::AID-YEA356>3.0.CO;2-S.
38. Coote, N. & Kirsop, B. H. Factors responsible for the decrease in pH during beer fermentations. *J. Inst. Brew.* **82**, 149–153. https://doi.org/10.1002/j.2050-0416.1976.tb03739.x (1976).
39. Nerudová, M., Červinková, K., Hašek, J. & Cifra, M. Optical spectral analysis of ultra-weak photon emission from tissue culture and yeast cells. In *SPIE Proceedings* (eds Tománek, P. *et al.*) 94500O (2015). https://doi.org/10.1117/12.2069897.
40. Zakhartsev, M. & Reuss, M. Cell size and morphological properties of yeast Saccharomyces cerevisiae in relation to growth temperature. *FEMS Yeast Res.* **18**. https://doi.org/10.1093/femsyr/foy052/4987208 (2018).
41. Feldmann, H. (ed.) *Yeast: molecular and cell biology* 2nd edn. (Wiley-Blackwell, New York, 2012).
42. Červinková, K., Nerudová, M., Hašek, J. & Cifra, M. Chemical modulation of the ultra-weak photon emission from Saccharomyces cerevisiae and differentiated HL-60 cells. In *Photonics, Devices, and Systems VI, pp 169–175* Vol. 9450 (SPIE, 2015) (eds Tománek, P. *et al.*) (Backup Publisher: International Society for Optics and Photonics). https://doi.org/10.1117/12.2070424.

Acknowledgements

We acknowledge Czech Science Foundation, project no. 20-06873X for funding. Authors also participate in the COST CA15211 and exchange project between Czech and Slovak Academy of Sciences, no. SAV-18-11. Neuron collective is acknowledged for the support in graphical design and The Science Editorium for the manuscript language check.

Author contributions

Contribution roles according to CRediT: https://casrai.org/credit/: P.V.: data curation (lead), formal analysis (lead), investigation (lead), methodology (lead), software (equal), visualization (lead), writing—original draft (lead). K.C.: data curation (supporting), formal analysis (supporting), investigation (supporting), methodology (supporting). M.C.: conceptualization, formal analysis (supporting), funding acquisition, investigation (supporting), project administration, resources, supervision, validation, visualization (supporting), writing—original draft (supporting), writing—review and editing.

Competing interests

The authors declare no competing interests.

Additional information

Supplementary Information The online version contains supplementary material available at https://doi.org/10.1038/s41598-021-89753-9.

Correspondence and requests for materials should be addressed to M.C.

6 Biochemiluminescence sensing of protein oxidation by reactive oxygen species generated by pulsed electric field

This chapter is a version of:

Petra Vahalová, Daniel Havelka, Eva Vaněčková, Tomáš Zakar, Viliam Kolivoška, Michal Cifra, Biochemiluminescence Sensing of Protein Oxidation by Reactive Oxygen Species Generated by Pulsed Electric Field,

Sensors and Actuators B: Chemical, volume 385, number 133676, 2023.

DOI: doi.org/10.1016/j.snb.2023.133676.

Author contributions:

Petra Vahalová:
Data curation, Formal analysis, Investigation (lead), Methodology, Software, Visualization, Writing – original draft (supporting), Writing – review & editing

Daniel Havelka:
Methodology (supporting - luminescence PEF chamber design and testing, and electric field simulation), Software (supporting), Visualization (supporting), Supervision (supporting)

Viliam Kolivoška: Conceptualization, Data curation (supporting), Formal analysis, Investigation (supporting), Methodology, Visualization (supporting), Writing – original draft (lead), Writing – review & editing

Eva Vaněčková: Methodology (supporting)

Tomáš Zakar: Methodology (supporting)

Michal Cifra: Conceptualization, Formal analysis (supporting), Funding acquisition, Investigation (supporting), Project administration, Resources, Supervision, Validation, Writing – original draft (supporting), Writing – review & editing

Djamel Eddine Chafai non-author contributor: Conceptualization (supporting - conceived the idea of BAL PEF experiments and designed the first version of PEF chamber for luminescence detection), Methodology (supporting)

Kateřina Červinková non-author contributor: Methodology (supporting - heating measurement), Investigation (supporting - heating measurement)

Candidate's contribution: 65 %

The manuscript carries the following acknowledgements:

We acknowledge Czech Science Foundation project no. 20-06873X. We also acknowledge non-author contributors: Djamel Eddine Chafai: Conceptualization (supporting – conceived the idea of BAL PEF experiments and designed the first version of PEF chamber for luminescence detection), Methodology (supporting). Kateřina Červinková: Methodology (supporting – heating measurement), Investigation (supporting – heating measurement).

The supplementary information is in Appendix (Section C).

Sensors & Actuators: B. Chemical 385 (2023) 133676

Contents lists available at ScienceDirect

Sensors and Actuators: B. Chemical

journal homepage: www.elsevier.com/locate/snb

Biochemiluminescence sensing of protein oxidation by reactive oxygen species generated by pulsed electric field

Petra Vahalová [a], Daniel Havelka [a], Eva Vaněčková [b], Tomáš Zakar [a], Viliam Kolivoška [b,*], Michal Cifra [a,*]

[a] Institute of Photonics and Electronics of the Czech Academy of Sciences, Prague, 18200, Czechia
[b] J. Heyrovský Institute of Physical Chemistry of the Czech Academy of Sciences, Prague, 18200, Czechia

ARTICLE INFO

Keywords:
Chemiluminescence
Pulsed electric field
Proteins
Albumin
Sensing
Monitoring

ABSTRACT

Pulsed electric field (PEF) technology is an important emerging modality for both biomedicine and the food industry, yet the mechanisms of action of a PEF on a biomolecular level remain unclear. In order to gain a better understanding of this, a sensing platform was developed to enable sensitive detection of oxidative processes induced by the PEF. It was found that the application of PEF in phosphate buffer leads to the electrogeneration of reactive oxygen species (ROS) which in turn triggers intrinsic chemiluminescence. Furthermore, the presence of the bovine serum albumin (BSA) was found to increase the luminescence signal, which was attributed to biochemiluminescence due to the reactions of BSA with the electrogenerated ROS. A carbonyl determination assay was then used to confirm that the BSA molecules had indeed been oxidatively modified. We proposed a scheme describing the reactions leading from charge transfer at the anode/electrolyte interface to the actual photon emission, helping to elucidate the mechanisms of action of PEF on proteins. The results may to open up new avenues for the application of PEF technology.

1. Introduction

Pulsed electric field (PEF) technology has rapidly growing applications in several research and industrial fields: e.g. in medicine (enabling electrochemotherapy [1–3], non-thermal tissue ablation [4], novel methods for drug and gene delivery and therapy [5–8]), in the food industry (enabling non-thermal pasteurization [9,10], increasing yields of active food compounds extraction [11–13]) and in biotechnology (manipulating the function of the biomolecules, such as the self-assembly of protein complexes [14] and enzyme activity [15]). The core physical mechanism of PEF relies on manipulating, through the action on either mobile or bound electric charges, biomolecular structures such as membranes or proteins with an intense electric field (EF) to exert functional changes in biomolecules. Furthermore, the application of an intense EF for a duration of a short (nanosecond–millisecond) pulse (often delivered in series) reduces unwanted thermal effects. While often the primary desired effects of PEF are physical (induction of the transmembrane voltage or deformation of biomolecules), in samples (which are of the vast majority) with substantial electrical conductivity, the passing electric currents inevitably cause electrochemical reactions at sample/electrode interfaces, which are often not well characterized. In this paper, we provide new evidence and demonstrate a novel photonic method for sensing the oxidative effects of PEF on proteins. We also demonstrate the PEF acts on proteins through the generation of reactive oxygen species (ROS) as products of electrochemical reactions taking place at the anode.

While lipid membranes have been a canonical target for PEF [16], there is a rising interest and need to understand the PEF effects on proteins — by mass the most abundant biomolecules in most biological cells, crucial food constituents, and potential bio-nanotechnological workhorses. So far, the effects of intense short-duration EF on proteins have been explored theoretically using computational molecular dynamics simulations and experimentally, mainly for food technology applications. Molecular dynamics simulations considering the influence of an EF [17,18] can predict mechanisms and pathways of the EF effect on proteins structure and dynamics. For instance, an EF has been shown to change the shape of the protein [19], molecular surface area [20–22] dipole moment [19,22–24], secondary structure [25–28] and eventually lead to unfolding [21,25,29]. EF was also found to affect the propensity towards protein and peptide complex formation or dis/aggregation [24,30].

In general, these computational results of PEF effects are directly and indirectly corroborated by various experimental works, albeit there is only a small overlap between protein types analyzed using computational simulations and those probed experimentally. In several

* Corresponding authors.
E-mail addresses: viliam.kolivoska@jh-inst.cas.cz (V. Kolivoška), cifra@ufe.cz (M. Cifra).

https://doi.org/10.1016/j.snb.2023.133676
Received 15 December 2022; Received in revised form 13 March 2023; Accepted 14 March 2023
Available online 17 March 2023

experimental works, the changes in the UV-circular dichroism spectra of proteins after PEF application indicate a change in the secondary structure [31–37]. Often, a change in the fluorescence of intrinsic aromatic amino acids in proteins has been observed, which indicates structural changes in the molecule [14,33,38]. The analysis of hydrophobic groups and newly accessible SH groups has been used to demonstrate structural changes and (partial) unfolding [33,39]. In some cases, the denaturation [40] aggregation of proteins has been observed [38,41,42]. In the case of enzymes, a change (typically decrease) of catalytic activity has been observed after applying PEF [15, 31,36,38]. For these effects to occur, exceeding a certain threshold of EF strength or a number of pulses and an optimal combination of PEF parameters and experimental conditions (e.g., buffer composition, design of the PEF chamber, temperature) must be applied.

Under common PEF treatment conditions of electrically conductive samples, a substantial proportion of electric current induced by the delivered EF is associated to charge transfer (reduction and oxidation) reactions at the interface of the sample and employed electrodes, i.e., Faradaic currents. These electrochemical reactions generate ROS [43], which can subsequently react with biomolecules present in the sample. These reactions are favored by longer pulses (tens and hundreds of microseconds and longer) due to their low-frequency spectral content and by the electrode materials supporting Faradaic processes [44]. Although some works on lipids [45–47] and complex cellular biosamples [48–53] have reported oxidative changes after PEF treatment, oxidative effects of PEF on well-defined protein samples have not yet been reported, even if tested [54].

The oxidation of proteins can be probed by a wide variety of methods with distinct features, sensitivity and specificity [55]. One of the sensitive, label-free, and in-situ methods for sensing of oxidative processes is intrinsic (bio)chemiluminescence, also termed ultra-weak photon emission or biological auto(chemi)luminescence (BAL) [55–57]. In this paper, we demonstrate that intrinsic chemiluminescence and bio-chemiluminescence can be used to sense the electrochemical generation of ROS by PEF and that those ROS cause oxidation of a model protein — bovine serum albumin (BSA). Furthermore, we also propose the reaction mechanism leading to PEF-induced biochemiluminescence.

2. Materials and methods

Materials and Methods are described in Supplementary Information 1.

3. Results and discussion

3.1. PEF induced biochemiluminescence depends on electrode material

Steel is a commonly used electrode material for PEF applications in medicine and the food industry. However, the use of metals as anodes may lead to the electrochemical oxidation of their surface, causing the liberation of metallic cations to the solution, potentially affecting the structure, properties, and function of the present biomolecules. The release of cations may be circumvented by using conductive materials other than metals. Carbon allotropes involving sp^2 atoms are conductive and chemically more inert than metallic elements constituting steel. Even when oxidized, carbon dioxide is formed, which has negligible biological activity compared to metallic cations.

To investigate the role of the anode material in the electrochemical generation of ROS by PEF leading to chemi- and biochemiluminescence, we devised a chamber with either a steel or glassy carbon anode. In both cases, the chamber contained a steel cathode, with the interface to the inspected sample being beyond the reach of the photomultiplier tube (PMT) employed as the sensing device (see Fig. 1). The cathode was partially optically transparent, which enabled the (bio)chemiluminescence signal from the interior of the chamber to be sensed. Such an experimental arrangement (see Fig. 2) allows the specific inspection of anodically generated ROS and their follow-up reactions. To probe the inherent chemiluminescence of electrogenerated ROS without the interference of biomolecules, the experiments were first performed by employing aqueous phosphate buffer (PB). Subsequently, measurements were repeated with an aqueous solution of bovine serum albumin (BSA) taken as a model biomolecule. The concentrations of PB and BSA in their solutions were adjusted so that the conductivity of both these samples was identical. This conductivity equality guarantees that, for a given chamber geometry and applied voltage, the electric current flowing through the chamber (and hence passed charge) is the same, enabling direct comparison of the obtained chemiluminescence and BAL signals and referencing them to the amount of electrogenerated ROS. In all experiments with BSA, we used a constant concentration of 20 mg/mL (i.e. 0.3 mM) to demonstrate the principle. This concentration was chosen to optimize the solution conductivity so that the resistance of the load presented to the PEF generator was high enough. This enabled maintaining the accuracy of applied voltage for the entire pulsing series without the distortion of desired rectangular PEF waveform (see below for details). We also made additional experiments with higher concentrations of BSA (results not shown). The general observation is that the higher the BSA concentration, the higher the current and the higher the BAL signal. Applied PEF consisted of 30 pulses repeated in 1 s intervals, each of them polarizing electrodes at a constant voltage of a given magnitude (see below) for 100 μs (see Fig. 3a for the voltage profile). To obtain the baseline response, monitoring of luminescence was commenced 120 s before the PEF period. To monitor the residual response after pulsing, the signal was measured for another 450 s.

The current transients recorded during the first pulse within PEF performed with a voltage of 1500 V (the highest value applied in this work), for both inspected anode materials and samples is shown in Fig. 3b. The subtle deviations in current magnitudes observed for the carbon and steel anodes were ascribed to a slight difference in the chamber geometry (gap between the anode and the cathode, see Supplementary Information 1 for details). For both the carbon and steel anodes, the PB and BSA samples showed nearly identical current profiles. The small current overshoots evident at the beginning of the pulse and upon its termination originate from the fact that the probed circuit contains capacitors arising from interfacial double layers formed naturally at the anode/electrolyte and cathode/electrolyte interfaces. Constant current observed for most of the pulsing period suggests that reactance contributions to the impedance due to interfacial charging phenomena may be neglected. In the following, we consider that the entire measured current carried through the electrode/electrolyte interfaces is due to the charge transfer involved in respective electrochemical reactions.

The chemiluminescence transients obtained for both electrode materials and samples are shown in Fig. 3c. In contrast to the current transients, the chemiluminescence profiles showed marked differences. On the carbon anode, signals obtained for both the PB and BSA samples have well-developed maxima corresponding to the pulsing period (120 to 150 s). This clearly indicated that anodic charge transfer processes lead to chemiluminescence. A residual signal was observed upon pulsing (150 to 600 s), gradually returning to the baseline response. A blown-up view of the residual signal for the period between 150 and 210 s is shown in the inset of Fig. 3c. To quantify the chemiluminescence during and after pulsing, we performed signal integration in the respective time intervals, with results shown in Fig. 3d. The BSA sample had a higher signal integral than the PB sample both during and after pulsing, implying that protein molecules were involved in reactions leading to biochemiluminescence. The higher BSA/PB signal ratio obtained for the period after pulsing indicated that the residual luminescence signal occurred mainly due to slow processes involving protein molecules.

With the steel anodes, both samples showed only minute chemiluminescence signals, both during and after pulsing. This suggested that

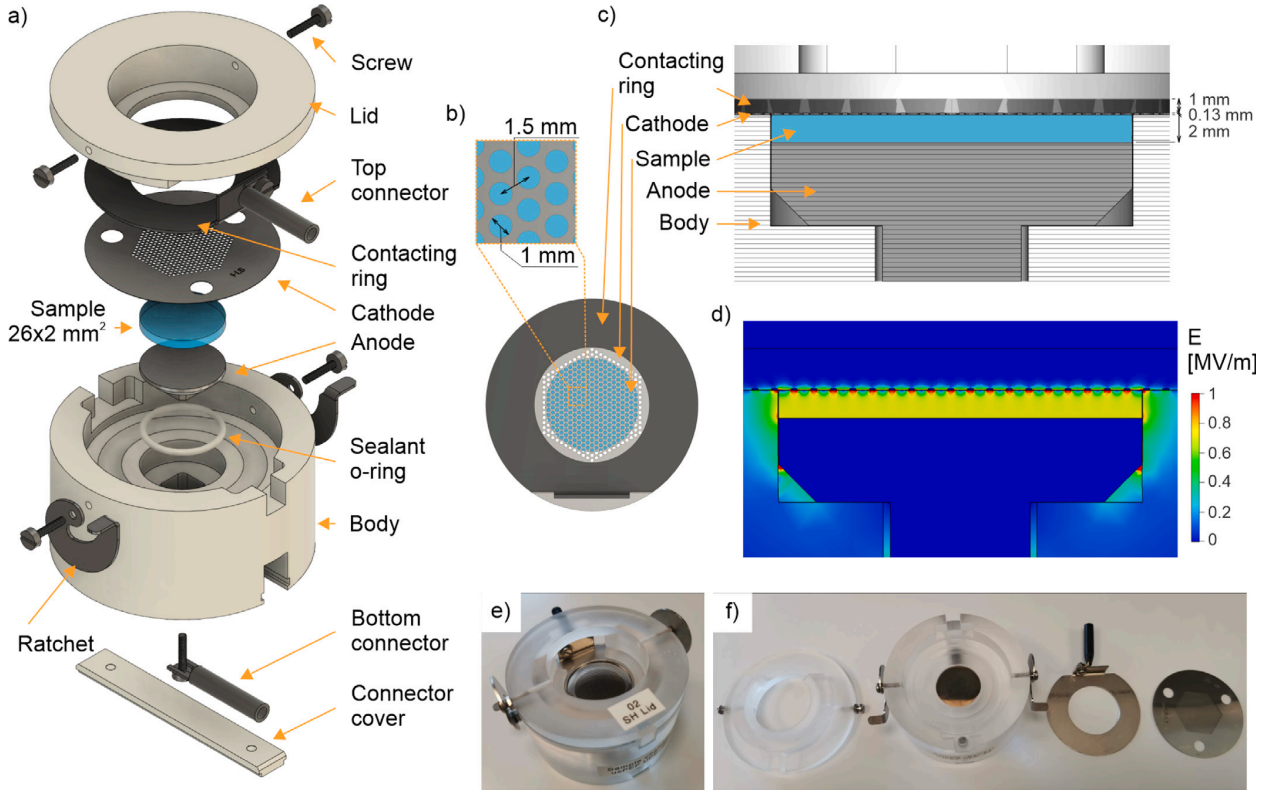

Fig. 1. (a) 3D model of the PEF chamber and its compartments. (b) Top view of contacting ring, cathode and sample with a zoom into the cathode perforation. (c) Cross-sectional view of the chamber (cathode, sample and anode) (d) Numerically simulated electric field strength with used pulse amplitude 1500 V. Photograph of (e) an assembled and (f) a disassembled PEF chamber. See Supplementary Information 1 for more details.

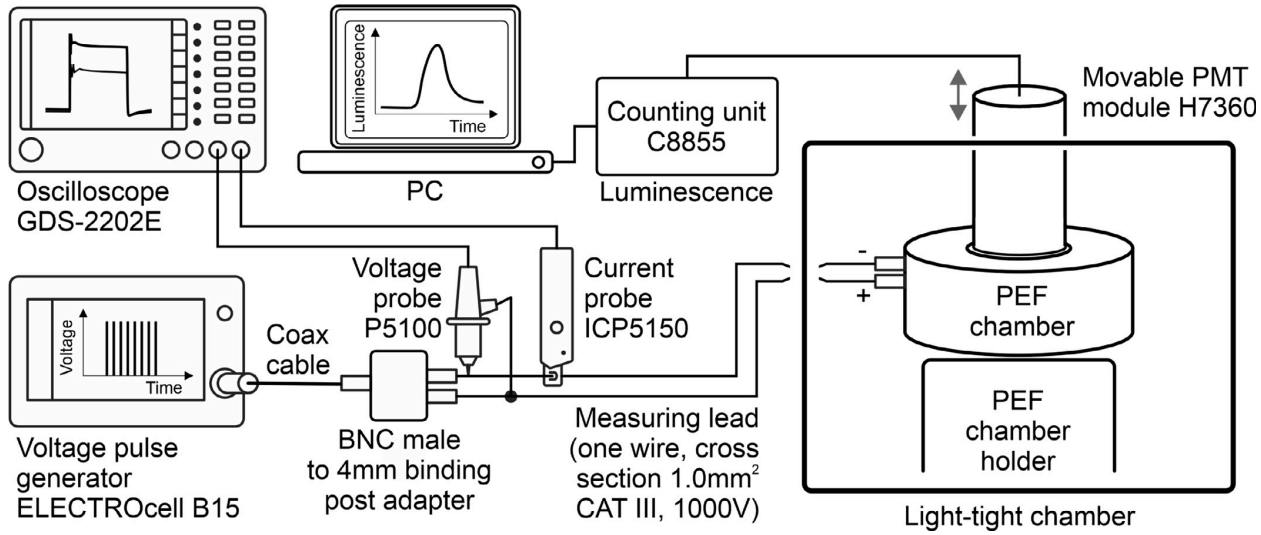

Fig. 2. A schematic diagram of the experimental setup for measuring (bio)chemiluminescence during and after PEF treatment in the dedicated chamber. See Supplementary Information 1 for more details.

on the steel surface, anodic charge transfer processes do not generate ROS at quantities detectable by our PMT setup. Presumably, the high catalytic activity of metal atoms contained in steel in contact with the samples enables fast electrochemical oxidation of water directly to non-emissive triplet molecular oxygen $^3O_2$ as the final product. More detailed analysis of anodic reactions and follow-up interactions among electrogenerated ROS will be presented below. At the steel electrode, it cannot be excluded that the charge transfer is partially realized by the dissolution of metallic atoms. Due to the absence of chemiluminescence signals, steel was not used further as the anode material and all experiments presented in the remainder of this work were performed with the carbon anode.

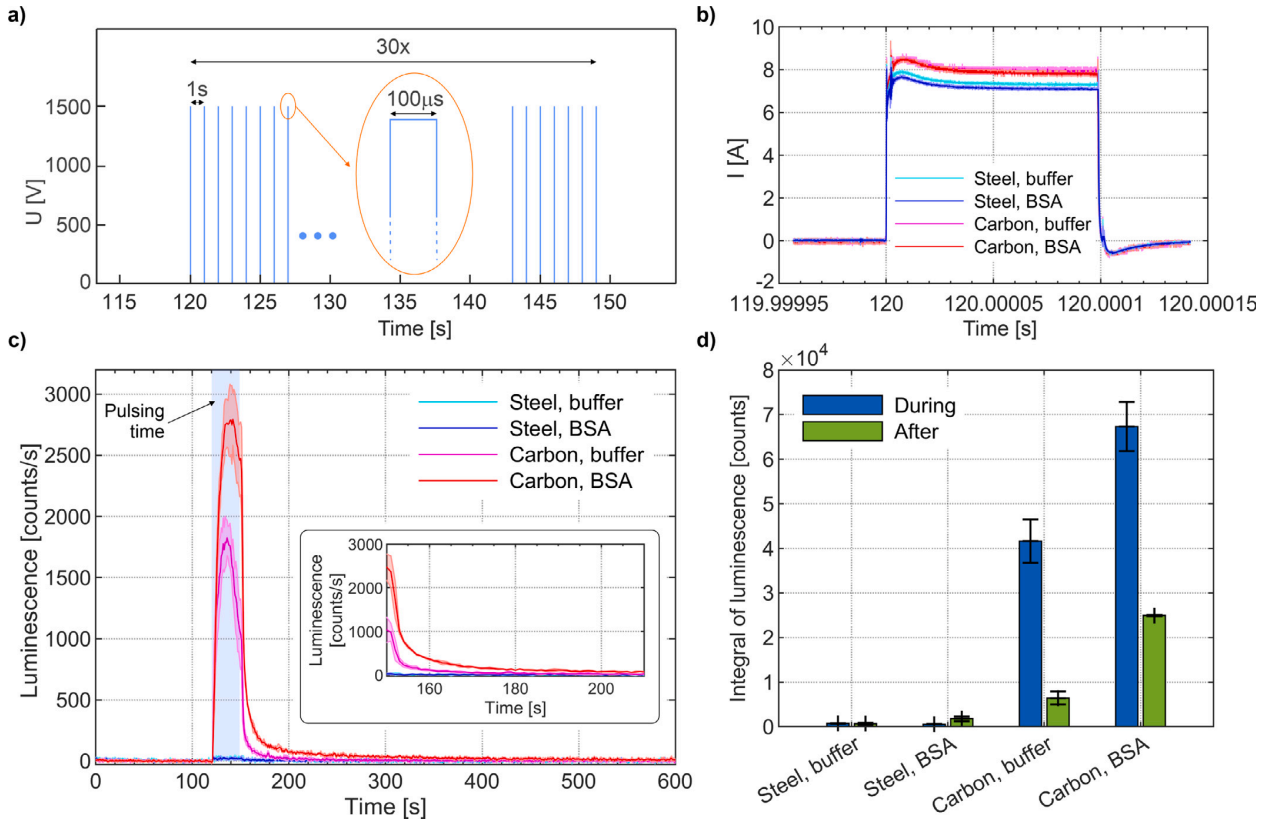

Fig. 3. (a) Voltage profile applied in PEF experiments performed in this work (here shown with amplitude of 1500 V). (b) Current transients obtained in the first voltage pulse for PB and BSA samples employing carbon and steel anode. (c) Luminescence transients recorded before (0 to 120 s), during (120 to 150 s) and after (150 to 600 s) the PEF treatment of above systems; inset is a close-up on the period just after PEF application (150 to 210 s), (d) Luminescence integrals evaluated for *during PEF* and *after PEF* periods.

3.2. Possible mechanisms leading from PEF to biochemiluminescence

To gain deeper mechanistic insights in the anodic process leading to (bio)chemiluminescence in PB and BSA samples, we performed experiments with systematically varied amounts of electrogenerated ROS. This was realized by tuning the applied voltage in PEF to different levels between 300 V and 1500 V. The obtained current–voltage profiles (with current being taken as the average within the first pulse) were nearly identical for the two samples (their conductivity was intentionally adjusted to the same level) and show clear linear dependence (Fig. 4f). The constructed best linear fits had close-to-zero intercept and thus demonstrated the Ohmic behavior of the samples in the PEF chamber.

In the bulk of the electrolyte, the transport of charge is realized by the migration of dissolved ions. For the PB sample, the majority of the charge carriers were Na^+ cation and $H_2PO_4^-$ / HPO_4^{2-} anions. Contributions of H^+ and OH^- ions may be neglected due to the pH neutrality of the sample (~ pH 7.5). BSA dissolved in the neutral environment is negatively charged [58,59]. When dissolved in pure water, BSA anions are balanced by cations originating from the purchased sample. As demonstrated above, under the conditions selected in this work, the entire current is at the electrode/electrolyte interfaces transferred by electrochemical reactions. For the applied voltage amplitude values (300 V to 1500 V), the resulting currents ranged from 1.5 A to 8.0 A (Fig. 4f). These figures were several orders of magnitude higher than diffusion-limited currents expected for substances dissolved at the millimolar range (concentrations of PB constituents and BSA were 0.36 mM/0.83 mM and 0.30 mM in this work). This implied that at such high current, the interfacial charge transfer is realized chiefly by the electrochemical decomposition of water coupled to migration of charge carriers in the EF.

At the cathode, water is reduced to molecular hydrogen, forming OH^- as a by-product. The geometrical arrangement of the employed PEF chamber keeps cathodic reactions hidden (i.e not in the line-of-sight) from the PMT. Furthermore, formed molecular hydrogen has very low reactivity in an aqueous solution and hence cannot influence other processes in the chamber. We conclude that the cathodic hydrogen evolution reaction had no measurable impact on studied (bio)chemiluminescence.

At the anode, water is oxidized, with molecular oxygen as the most chemically stable product (see the proposed reaction scheme in Fig. 5 left). The water oxidation process is composed of four elementary steps (reactions 1 to 4) [60], each of them harvesting one electron to the anode and releasing one H^+ ion to the electrolyte, thus making the local reaction environment acidic. Importantly, three kinds of ROS are generated along the reaction pathway ($OH^\bullet$, $O^{\bullet\bullet}$ and $HO_2^\bullet$). From them, $OH^\bullet$ and $HO_2^\bullet$ radicals mutually recombine (reactions 5 to 7), with singlet molecular oxygen $^1O_2$ being one of the products [61]. $^1O_2$ is converted to its ground triplet state either by a monomolecular decay (reaction 8) or a bimolecular collision (reaction 9); these processes are accompanied by photon emission, with maxima at 1278 nm and 634 nm, respectively [57,62–64]. In our work, the range of wavelengths sensed by the PMT was selected to be from 300 nm to 650 nm with the highest quantum efficiency from 320 nm to 400 nm. The reason was selective sensing of the electron-excited triplet carbonyls formed through reactions of proteins and ROS, which is of our focus (see below), emit in the wavelength range of 350 nm to 500 nm [57]. The fact that PMT senses wavelengths from 300 nm to 650 nm implies that for $^1O_2$ only the emission upon the bimolecular collision (634 nm, reaction 9, [57]) is included in the chemiluminescence signal measured and discussed in this work.

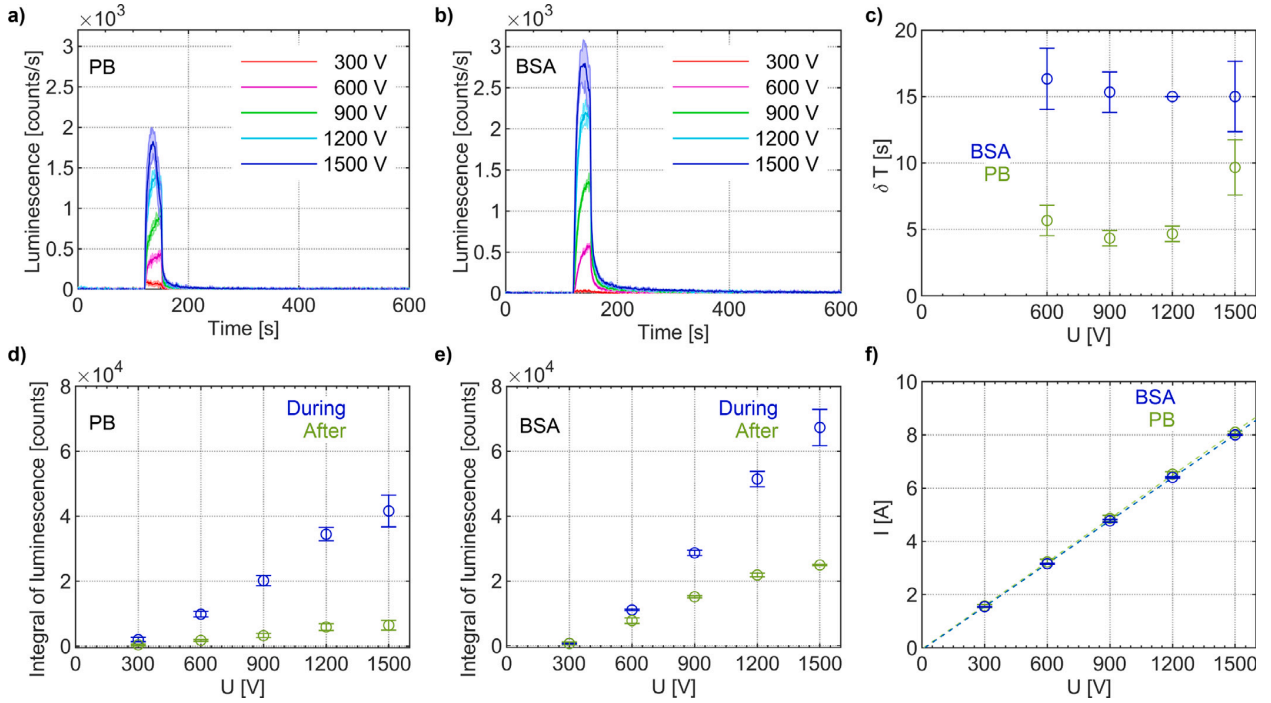

Fig. 4. Luminescence transients recorded for PEF with varied voltage amplitude employing a carbon anode and (a) PB and (b) BSA as the sample. (c) Characteristic decay time in the *after PEF* period. Luminescence integrals obtained for *during PEF* and *after PEF* period for (d) PB and (e) BSA. (f) Current recorded in the first voltage pulse as a function of applied voltage amplitude.

The chemiluminescence transients obtained for the PB sample subjected to PEF of varied voltage amplitude values are shown in Fig. 4a, with integrals evaluated during and after pulsing shown in Fig. 4d. The signal scales with flowing current (Fig. 4f), clearly confirming that the observed chemiluminescence originates from electrogenerated ROS. Pulsing performed at the lowest applied voltage (300 V) leads to close-to-zero chemiluminescence signal, implying that under these circumstances the concentration of electrogenerated ROS is low. Presumably, at low voltages, the catalytic activity of the glassy carbon anode surface is sufficient for facile oxidation of ROS to non-emissive $^3O_2$. (Note that the same effect was observed for the steel anode for voltage amplitude as high as 1500 V.) At voltages higher than 300 V, the rate of ROS generation seems to exceed the capacity of the carbon surface for their further oxidation to $^3O_2$. Formed ROS get desorbed from the anode surface and are transported to the bulk electrolyte by diffusion, where their subsequent mutual collisions (Fig. 5, reactions 5 to 7) are followed by photon emissions (Fig. 5, reactions 8 and 9). Interestingly, at the highest applied voltage (1500 V), the chemiluminescence signal decreased during the pulsing period. We presume that the amount of electrogenerated $^3O_2$ exceeded its solubility limit in water (1.3 mM). As a result, gaseous adsorbates (nanobubbles and nanopancakes) are formed and partially cover the anode surface [65, 66]. Most likely, these gaseous structures create obstacles for the mass transport of ROS, manifesting as a decline in the chemiluminescence signal.

Similar luminescence versus voltage amplitude dependence was also obtained for the BSA sample, with overall more pronounced signals both during and after pulsing (Fig. 4b). The evaluated signal integrals are presented in Fig. 4e. Higher signals confirmed that BSA molecules were involved in processes leading to BAL. At neutral pH, during pulsing, negatively charged BSA molecules move towards the anode, where ROS are formed by the oxidation of water. Hence, it is intuitive to interpret an increase of the signal by collisions between ROS and BSA molecules and follow-up emissive reactions. However, such a seemingly simple picture is complicated by two physicochemical phenomena. (1) Electrochemical oxidation of water generates H^+ as a by-product, forming a local pH gradient at the anode. In the acidic environment, carboxylate moieties in the BSA molecule (imparting a negative charge in the neutral solution) are discharged, while amine groups are protonated. These acido-basic reactions may cause halting or even reversal of the migration motion of BSA molecules, complicating their transport to the anode. (2) Proteins in general, and BSA in particular, tend to adsorb on carbon surfaces, typically creating a monolayer [67,68]. While an accumulation of proteins at reaction interfaces may be beneficial for a signal increase in potential analytical applications, it cannot be excluded that adsorbed molecules affect electrochemical kinetics of ROS formation. Reactions among molecules accompanied by their adsorption on the electrode surface are processes that often complicate interfacial charge transfer. One should always consider the existence of these phenomena when interpreting the results of electrochemical experiments.

During pulsing, the presence of BSA in the sample increases the integral of the chemiluminescence signal by a factor of approximately 1.5 (Fig. 4d, e). The amplification is more pronounced in the after-pulsing period (factor of 3 to 4). This comparison implies that BSA molecules contribute to the luminescence signal chiefly in the post-pulsing period. This observation motivated us to quantify the characteristic times of the luminescence decay in the post-pulsing period. We evaluated the signal at the end of the pulsing period (at 150 s) and determined the time interval required for this signal to fall to 1/10 of its original intensity. The obtained results (Fig. 4c) indicated that the presence of BSA approximately doubles the characteristic decay time. A higher signal maintained for a longer period upon pulsing recorded for the BSA sample suggested that the observed BAL is preceded by sluggish physical (diffusion) and chemical (bimolecular collisions) processes involving protein molecules.

While evaluating the amount and spatial distribution of ROS formed at the anode in the PEF is beyond the scope of this work, we briefly

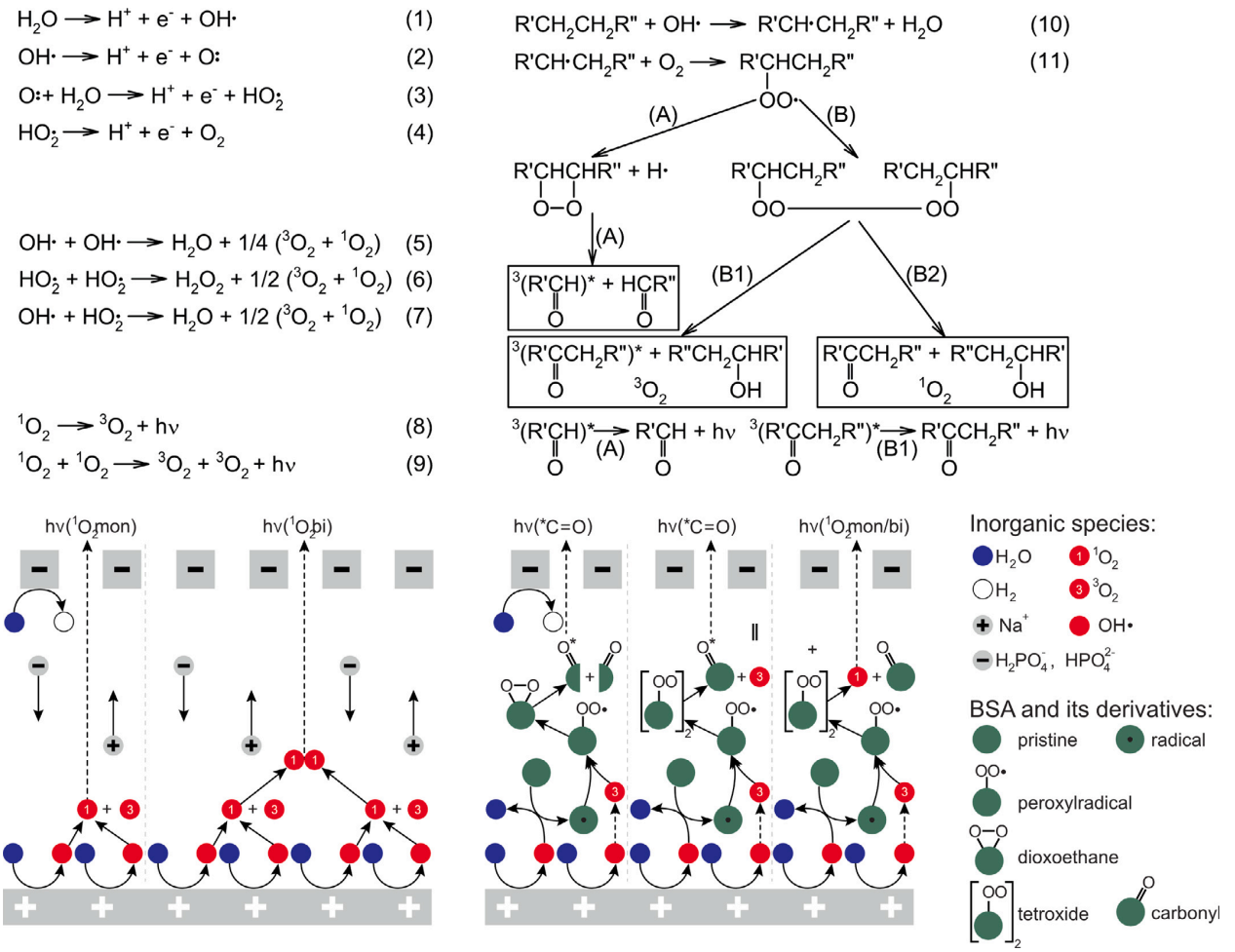

Fig. 5. Upper: Proposed reaction scheme of the anodic ROS generation and BSA oxidation induced by PEF. (1) to (4) Anodic oxidation of water leading to radical ROS and oxygen. (5) to (7) Recombination reactions among radical ROS. Photoemissive monomolecular decay (8) and bimolecular collision and emission (9) of singlet oxygen. (10) and (11) Damage of aliphatic structures in the BSA molecule by ROS and oxygen. Possible reaction routes of further oxidative damage of BSA molecule — dioxethane (A) and tetroxide (B) pathway, with electron-excited triplet carbonyl (B1) and singlet oxygen (B2) as final BAL emitters. Lower: Cartoon cumulatively depicting physical processes (mass transport due to diffusion and migration) and chemical reactions (charge transfer processes at anode (+) and cathode (-), bulk collisions and photoemissive deexcitations) taking place in the PEF chamber filled with PB (left) and BSA (right).

present an approach enabling the estimation of their surface concentrations and the extent to which they penetrate to the bulk of the sample. We applied basic laws governing mass transport/charge transfer phenomena and performed several simplifications to keep the involved mathematics at a widely understandable level (see Supplementary Information 2). We considered that the hydroxyl radical OH• was the only electrogenerated ROS, i.e. only reaction 1, Fig. 5, takes place; the mechanism of the reactions between ROS and BSA will be presented below. This allowed the amount of ROS n to be estimated based on Faraday's law for electrolysis, $n = INΔt/(zF)$, where I is current, N is the number of applied pulses with a width of $Δt$, z is the number of electrons (per molecule) exchanged in the reaction (one for OH•) and F is Faraday's constant (96485 C mol^{-1}). For the applied PEF (30 × 100 μs pulse) and measured currents (1.5 A to 8.0 A), the amount of electrogenerated ROS ranged from 0.5 to 2.5 ·10^{-7} mol. ROS formed at the anode are transported to the bulk of the sample by diffusion. The thickness of the diffusion layer ⟨x⟩ is used to estimate the distance to which ROS penetrate, ⟨x⟩ scales with time t according to the formula $⟨x⟩^2 = 4Dt$, where D is the diffusion coefficient (5.3 ·10^{-9} m^2 s^{-1} for OH•). We applied this relationship to determine the ⟨x⟩ value for the characteristic decay time of luminescence (roughly 15 s, see Fig. 4c). We considered that the entire ROS were generated at once at t = 0 s and corrected this assumption by adding the length of pulsing period (30 s) to the time introduced to the calculation. The obtained result (⟨x⟩ = 0.98 mm) indicated that at the characteristic decay time of luminescence, the "fastest" ROS were transported roughly to the middle of the PEF chamber (see Supplementary Information 1 for the geometry). The concentration profile of ROS electrogenerated at the anode can be approximated by a decreasing linear function, running from c_0 at the anode to 0 mM at ⟨x⟩. This allows c_0 to be estimated based on the relationship $c_0 = 2n/(A⟨x⟩)$, where A is the electrode area (in this work 5.3 ·10^{-4} m^2). For the performed PEF experiments, the resulting c_0 values ranged from 0.18 to 0.96 mM, which is comparable to the concentration of initially introduced BSA (0.30 mM). Importantly, the presented calculations may help design experimental conditions (e.g., chamber geometry, PEF parameters, sample conductivity and duration of experiment) for tuning the concentration and spatial distribution of electrogenerated ROS. In the Supplementary Information

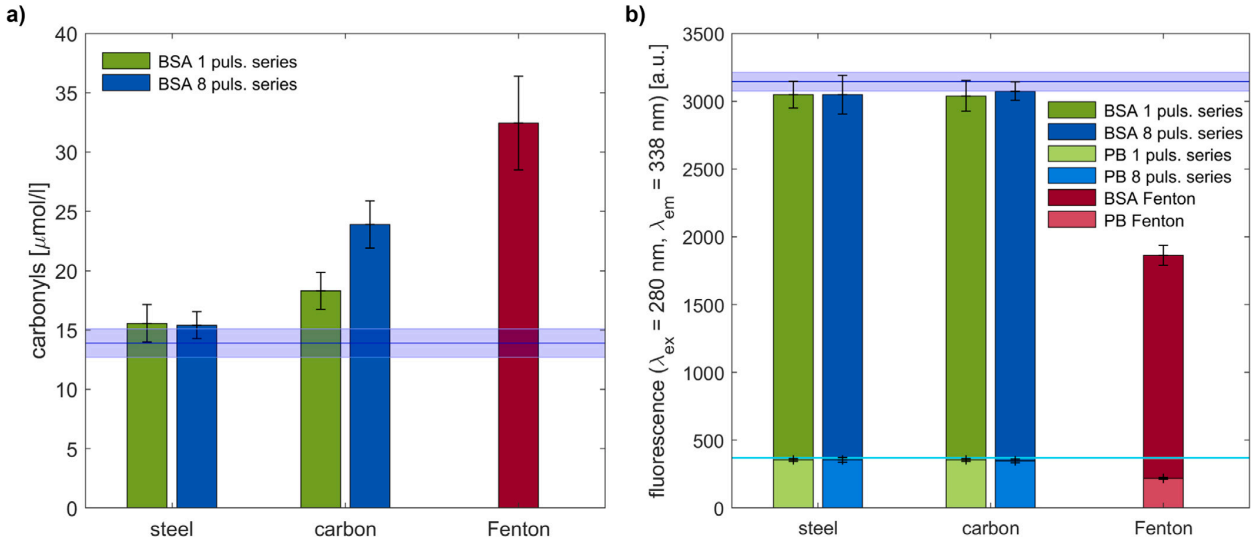

Fig. 6. Carbonyl content (a) and fluorescence (excitation at 280 nm, measurement at 338 nm) response (b) of pristine BSA samples (purple bands), BSA samples subjected to PEF treatment with one (green bars) and eight (blue bars) pulsing series at carbon and steel anode and BSA samples subjected to Fenton reagent (magenta bars). In (b) fluorescence response of pristine (cyan band) and respectively treated (light shades) PB samples is additionally depicted.

2, we provide an excel sheet containing applets enabling the scrutiny of various physicochemical aspects (diffusion, migration, sample conductivity, amount of dissolved gases, amount and concentration profiles of electrogenerated products, temperature increase in the solution due to Joule heating in PEF and diffusive heat transport) relevant to PEF experiments with biomolecules. The temperature increase during the PEF treatment was monitored experimentally employing a thermal camera, see Fig. S1 in the Supplementary Information 1 — the temperature increase was 2.2 °C above the initial temperature after 30 pulses. Such small temperature increase is assumed to have no influence on the chemical structure and BAL of BSA molecules.

In the following, we present a suggested reaction mechanism of the BSA oxidation by ROS generated at the anode in the PEF and subsequent photoemissive reactions, with the scheme presented in Fig. 5,right. A significant portion of the amino acids constituting proteins contain aliphatic sequences, which allows BSA to be generally depicted as a R'CH_2CH_2R" structure, where R' and R" denote the rest of the molecule. Based on the equal current–voltage characteristics obtained for the PB and BSA samples (Fig. 4f), we consider that ROS are electrogenerated irrespective of the protein presence. Following mechanistic models developed for the oxidation of biomolecules [57], we presume that the BSA molecule is first attacked by an OH• radical (Fig. 5, reaction 10), forming a BSA (alkyl) radical. This radical further reacts with an oxygen molecule (either electrogenerated or naturally dissolved in water), forming a BSA peroxyl radical (reaction 11). The latter undergoes one of the following reaction pathways: (A) The terminal oxygen radical atom of the peroxyl group attacks an adjacent carbon atom, causing hydrogen abstraction and formation of 1,2-dioxoethane derivative. It decomposes, forming two separate carbonyl-containing products, one of them being an electron-excited triplet carbonyl that is subsequently converted to the ground singlet state, with the process being accompanied by the emission of a photon. (B) Two BSA peroxyl radicals dimerize forming a tetroxide derivative, which decomposes by a disproportionation reaction to an alcohol, a carbonyl-containing species and molecular oxygen. This reaction either forms electron-excited triplet carbonyl (B1) or $^1O_2$ (B2), with both of them producing photons in follow-up reactions. As mentioned above, $^1O_2$ is converted to its ground triplet state either by a monomolecular (reaction 8) or by a bimolecular emissive process (reaction 9), the latter being sensed by the PMT employed in this work.

3.3. PEF generated ROS cause chemical changes in protein

To corroborate the correctness of the proposed reaction mechanism, we analyzed BSA samples subjected to the PEF treatment for the content of carbonyl moieties. The analysis is based on colorimetric determination of a product of the reaction between carbonyl groups and 2,4-dinitrophenylhydrazine (Brady test, see Supplementary Information 1 for details). As a negative and positive control, the analysis was performed for pristine (untreated) BSA and BSA oxidized by a Fenton reagent (1 μM $FeSO_4$ and 146.5 mM H_2O_2) replacing the PEF treatment. The Fenton reagent generates HO· and OOH· ROS according to the following reaction scheme

$$Fe^{2+} + H_2O_2 \rightarrow Fe^{3+} + HO^{\cdot} + OH^{-} \quad (1)$$

$$Fe^{3+} + H_2O_2 \rightarrow Fe^{2+} + OOH^{\cdot} + H^{+} \quad (2)$$

For comparison, we also include the analysis performed for BSA samples subjected to the PEF treatment employing steel anodes where almost no luminescence signal was observed (see Fig. 3c, d. The content of carbonyls depending on the sample treatment is depicted in Fig. 6a. The result obtained for the pristine BSA is interpreted as a natural content of carbonyl groups in the protein. The treatment of the BSA sample by Fenton reagent leads to a profound increase of the carbonyl content, implying that new carbonyl groups are formed in the sample upon the oxidation of BSA by chemically generated ROS. In contrast, the samples subjected to the PEF treatment show only a subtle increase of the carbonyl amount. The increase is roughly triple for the carbon anode in comparison with the steel anode. It is important to highlight that in PEF-based experiments, ROS are generated only at the anode and are transported to a limited volume of the BSA sample (see the discussion above), whereas in Fenton-reagent-based experiments ROS are present in the entire volume of the sample. To enhance the reach of electrogenerated ROS in the bulk of the sample, we repeated the PEF treatment with number of pulses increased from 30 to 240 (i.e., multiplied 8-times, with 90 s pause between each pulsing series). For the steel anode, the carbonyl content remained almost unaltered, which is in line with the very sluggish ROS formation as deduced from the minute luminescence signal (see Fig. 3c, d. For the carbon anode, an approximately three-fold increase in the amount of carbonyl was observed upon extended pulsing. The deviation between the change

of the carbonyl content and the increase in the number of pulses was ascribed to non-linear nature of the diffusion as a mass transport mechanism preceding the reactions among ROS and BSA.

Samples of BSA treated as described above were further analyzed for the content of aromatic amino acid residues by evaluating the fluorescence signal at 338 nm (Fig. 6b). The fluorescence was excited at 280 nm, which falls within the absorption bands of tyrosine (TYR) and tryptophan (TRP), to selectively probe these residues.

The BSA sample subjected to the Fenton treatment showed a considerable decrease of the fluorescence signal when compared to the pristine sample, indicating that TYR and TRP residues were oxidized. In contrast, all BSA samples treated by PEF showed only a very subtle fluorescence decrease (less than 5 %), implying that the vast majority of TYR and TRP residues remained intact upon pulsing. This result indicated that the oxidation of BSA by electrogenerated ROS takes place in the non-aromatic parts of the molecule. This is in line with the proposed reaction mechanism (Fig. 5), in which the oxidation of the aliphatic parts of the BSA molecule is considered.

Besides luminescence measurements with BSA and electrogenerated ROS in PEF (see Figs. 3 and 4), we additionally employed luminescence measurements to probe chemical oxidation of BSA by Fenton reagent. We found out that observed luminescence signals scale with amounts of H_2O_2 and Fe^{2+} introduced as the ROS precursor and catalyst in the Fenton reagent (see Supplementary Information 1 for details). These finding corroborate that biochemiluminescence observed in PEF is indeed due to reactions among electrogenerated ROS and BSA molecules.

In this paper, we aimed to explore essential mechanistic aspects of PEF-induced oxidative processes in biomolecules leading to BAL. Therefore we focused on a very simple biomolecular system — aqueous solution of BSA. However, the results lie a foundation for the potential use of our method for ROS generation by PEF and their action also in more complex ex vivo or in vivo systems. Some earlier pioneering works [50], which nevertheless provided no mechanistic details of how the ROS are generated, as well as our ongoing work, suggest there is a correlation between cell membrane electroporation and BAL.

4. Conclusions and outlook

In this work, we designed and manufactured a unique experimental platform for sensing the formation of reactive oxygen species and the oxidation of bovine serum albumin as a model biomolecule in pulsed electric fields by (bio)chemiluminescence measurements.

We demonstrate that the anode material has a decisive role in the formation of reactive oxygen species, with glassy carbon producing significant quantities. The introduction of bovine serum albumin led to an increase of the luminescence signal, indicating that its molecules were involved in chemical reactions leading to the photon emission. Based on a general scheme applicable to the oxidation of biomolecules, we proposed a reaction mechanism of bovine serum albumin oxidation by electrogenerated reactive oxygen species, with the observed biochemiluminescence being due to electron-excited triplet carbonyls and singlet oxygen originating from oxidative damage of aliphatic regions in the molecule. The validity of the proposed mechanism was confirmed by the chemical spectroscopic analysis of protein samples. Additionally, we explored the chemical oxidation of bovine serum albumin by Fenton reagent, further corroborating the correctness of the suggested reaction mechanism.

Our work clearly confirms that biochemiluminescence is a valuable tool for in-situ real-time monitoring of oxidative changes in biomolecules induced by reactive oxygen species. At the same time, the obtained results underscore that these species are unavoidably formed in pulsed electric fields, contributing to structural and functional changes (e.g. enzymatic activity) of probed biomolecules. In future work, we intend to perform spectral analysis of electrogenerated biochemiluminescence to provide further evidence for the proposed photon emitters. Apart from pulsed electric field, our investigations will utilize linear sweep voltage profiles enabling closer revelation of reaction mechanisms of reactive oxygen species formation. Furthermore, we aim to explore how various pro-oxidants and anti-oxidants modulate oxidative damage of proteins in pulsed electric fields. Besides that, we will employ other electrolyte anions (nitrate and halogenides) to inspect the formation and oxidation properties of other types of reactive species.

5. Abbreviations & terminology

BAL = biological autoluminescence = (bio)chemiluminescence (*"auto" refers to the fact that species, after being oxidized by ROS, which lead to the luminescence signal are already present (endogenous) in the sample*)
BSA = bovine serum albumin
EF = electric field
PB = phosphate buffer
PEF = pulsed electric field
PMT = photomultiplier tube
ROS = reactive oxygen species

CRediT authorship contribution statement

Petra Vahalová: Data curation, Formal analysis, Investigation, Methodology, Software, Visualization, Writing – original draft, Writing – review & editing. **Daniel Havelka:** Methodology, Software, Visualization, Supervision. **Eva Vaněčková:** Methodology. **Tomáš Zakar:** Methodology. **Viliam Kolivoška:** Conceptualization, Data curation, Formal analysis, Investigation, Methodology, Visualization, Writing – original draft, Writing – review & editing. **Michal Cifra:** Conceptualization, Formal analysis, Funding acquisition, Investigation, Project administration, Resources, Supervision, Validation, Writing – original draft, Writing – review & editing.

Declaration of competing interest

The authors declare the following financial interests/personal relationships which may be considered as potential competing interests: Michal Cifra reports financial support was provided by Czech Science Foundation.

Data availability

The data that supports the findings of this study are available within the article and its supplementary material. The raw data will be provided on demand.

Acknowledgment

We acknowledge Czech Science Foundation project no. 20-06873X. We also acknowledge non-author contributors: **Djamel Eddine Chafai**: Conceptualization (supporting - conceived the idea of BAL PEF experiments and designed the first version of PEF chamber for luminescence detection), Methodology (supporting). **Kateřina Červinková**: Methodology (supporting - heating measurement), Investigation (supporting - heating measurement).

Appendix A. Supplementary data

Supplementary material related to this article can be found online at https://doi.org/10.1016/j.snb.2023.133676.

References

[1] G. Serša, M. Bosnjak, M. Čemažar, R. Heller, Preclinical studies on electrochemotherapy, in: D. Miklavčič (Ed.), Handbook of Electroporation, Springer International Publishing, Cham, 2017, pp. 1511–1525, http://dx.doi.org/10.1007/978-3-319-32886-7_45, URL http://link.springer.com/10.1007/978-3-319-32886-7_45.

[2] V. Todorovic, M. Cemazar, Combined treatment of electrochemotherapy with immunomodulators, in: Handbook of Electroporation, 2016, pp. 1717–1731.

[3] J. Gehl, G. Serša, Electrochemotherapy and its clinical applications, in: D. Miklavčič (Ed.), Handbook of Electroporation, Springer International Publishing, Cham, 2017, pp. 1771–1786, http://dx.doi.org/10.1007/978-3-319-32886-7_91, URL http://link.springer.com/10.1007/978-3-319-32886-7_91.

[4] S. Bhonsle, R.E. Neal, R.V. Davalos, Preclinical studies on irreversible electroporation, in: Handbook of Electroporation, 2016, pp. 1527–1542.

[5] A.A. Bulysheva, R. Heller, Gene electrotransfer for ischemic tissue, in: D. Miklavčič (Ed.), Handbook of Electroporation, Springer International Publishing, Cham, 2017, pp. 1665–1677, http://dx.doi.org/10.1007/978-3-319-32886-7_58, URL http://link.springer.com/10.1007/978-3-319-32886-7_58.

[6] S.A. Shirley, Delivery of cytokines using gene electrotransfer, in: D. Miklavčič (Ed.), Handbook of Electroporation, Springer International Publishing, Cham, 2017, pp. 1755–1768, http://dx.doi.org/10.1007/978-3-319-32886-7_189, URL http://link.springer.com/10.1007/978-3-319-32886-7_189.

[7] L. Liu, M.P. Morrow, M. Bagarazzi, Clinical use of DNA vaccines, in: D. Miklavčič (Ed.), Handbook of Electroporation, Springer International Publishing, Cham, 2017, pp. 1933–1952, http://dx.doi.org/10.1007/978-3-319-32886-7_106, URL http://link.springer.com/10.1007/978-3-319-32886-7_106.

[8] C. Rosazza, S. Haberl Meglic, A. Zumbusch, M.-P. Rols, D. Miklavcic, Gene electrotransfer: A mechanistic perspective, Current Gene Therapy 16 (2) (2016) 98–129, URL http://www.ingentaconnect.com/contentone/ben/cgt/2016/00000016/00000002/art00005.

[9] W. Zhao, R. Yang, Pulsed electric fields for inactivation of endogenous enzymes in foods, in: D. Miklavčič (Ed.), Handbook of Electroporation, Springer International Publishing, Cham, 2017, pp. 2239–2251, http://dx.doi.org/10.1007/978-3-319-32886-7_130, URL http://link.springer.com/10.1007/978-3-319-32886-7_130.

[10] F. Schottroff, A. Krottenthaler, H. Jäger, Stress induction and response, inactivation, and recovery of vegetative microorganisms by pulsed electric fields, in: D. Miklavčič (Ed.), Handbook of Electroporation, Springer International Publishing, Cham, 2017, pp. 2539–2557, http://dx.doi.org/10.1007/978-3-319-32886-7_183, URL http://link.springer.com/10.1007/978-3-319-32886-7_183.

[11] A. Patras, P. Choudhary, A. Rawson, Recovery of primary and secondary plant metabolites by pulsed electric field treatment, in: D. Miklavčič (Ed.), Handbook of Electroporation, Springer International Publishing, Cham, 2017, pp. 2517–2537, http://dx.doi.org/10.1007/978-3-319-32886-7_182, URL http://link.springer.com/10.1007/978-3-319-32886-7_182.

[12] J.R. Sarkis, N. Boussetta, E. Vorobiev, Application of pulsed electric energies for oil and polyphenol extraction from sesame cake and sesame seeds, in: Handbook of Electroporation, 2017, pp. 2699–2712.

[13] E. Vorobiev, N. Lebovka, Application of pulsed electric fields for root and tuber crops biorefinery, in: Handbook of Electroporation, 2017, pp. 2899–2922.

[14] D.E. Chafai, V. Sulimenko, D. Havelka, L. Kubínová, P. Dráber, M. Cifra, Reversible and irreversible modulation of tubulin self-assembly by intense nanosecond pulsed electric fields, Adv. Mater. 31 (39) (2019) 1903636, http://dx.doi.org/10.1002/adma.201903636.

[15] S.Y. Ho, G.S. Mittal, J.D. Cross, Effects of high field electric pulses on the activity of selected enzymes, J. Food Eng. 31 (1) (1997) 69–84, http://dx.doi.org/10.1016/S0260-8774(96)00052-0, URL https://www.sciencedirect.com/science/article/pii/S0260877496000520.

[16] M.L. Yarmush, A. Golberg, G. Serša, T. Kotnik, D. Miklavčič, Electroporation-based technologies for medicine: Principles, applications, and challenges, Annu. Rev. Biomed. Eng. 16 (1) (2014) 295–320, http://dx.doi.org/10.1146/annurev-bioeng-071813-104622, URL http://www.annualreviews.org/doi/10.1146/annurev-bioeng-071813-104622.

[17] N.J. English, C.J. Waldron, Perspectives on external electric fields in molecular simulation: progress, prospects and challenges, Phys. Chem. Chem. Phys. 17 (19) (2015) 12407–12440, http://dx.doi.org/10.1039/C5CP00629E, URL http://xlink.rsc.org/?DOI=C5CP00629E.

[18] B.B. Noble, N. Todorova, I. Yarovsky, Electromagnetic bioeffects: a multiscale molecular simulation perspective, Phys. Chem. Chem. Phys. 24 (11) (2022) 6327–6348, http://dx.doi.org/10.1039/D1CP05510K, URL https://pubs.rsc.org/en/content/articlelanding/2022/cp/d1cp05510k, Publisher: Royal Society of Chemistry.

[19] P. Marracino, D. Havelka, J. Průša, M. Liberti, J. Tuszynski, A.T. Ayoub, F. Apollonio, M. Cifra, Tubulin response to intense nanosecond-scale electric field in molecular dynamics simulation, Sci. Rep. 9 (1) (2019) 10477, http://dx.doi.org/10.1038/s41598-019-46636-4.

[20] J. Wang, S.K. Vanga, V. Raghavan, Structural responses of kiwifruit allergen act d 2 to thermal and electric field stresses based on molecular dynamics simulations and experiments, Food Funct. 11 (2) (2020) 1373–1384, http://dx.doi.org/10.1039/C9FO02427A, URL http://dx.doi.org/10.1039/C9FO02427A, Publisher: The Royal Society of Chemistry.

[21] S.K. Vanga, A. Singh, V. Raghavan, Effect of thermal and electric field treatment on the conformation of ara h 6 peanut protein allergen, Innov. Food Sci. Emerg. Technol. 30 (2015) 79–88, http://dx.doi.org/10.1016/j.ifset.2015.03.003, URL https://www.sciencedirect.com/science/article/pii/S1466856415000508.

[22] J. Průša, M. Cifra, Molecular dynamics simulation of the nanosecond pulsed electric field effect on kinesin nanomotor, Sci. Rep. 9 (1) (2019) 19721, http://dx.doi.org/10.1038/s41598-019-56052-3, URL http://www.nature.com/articles/s41598-019-56052-3.

[23] F. Toschi, F. Lugli, F. Biscarini, F. Zerbetto, Effects of electric field stress on a β-Amyloid peptide, J. Phys. Chem. B 113 (1) (2009) 369–376, http://dx.doi.org/10.1021/jp807896g, URL http://pubs.acs.org/doi/abs/10.1021/jp807896g.

[24] J. Průša, A.T. Ayoub, D.E. Chafai, D. Havelka, M. Cifra, Electro-opening of a microtubule lattice in silico, Comput. Struct. Biotechnol. J. 19 (2021) 1488–1496, http://dx.doi.org/10.1016/j.csbj.2021.02.007, URL https://www.sciencedirect.com/science/article/pii/S2001037021000581.

[25] P. Marracino, F. Apollonio, M. Liberti, G. d'Inzeo, A. Amadei, Effect of high exogenous electric pulses on protein conformation: Myoglobin as a case study, J. Phys. Chem. B 117 (8) (2013) 2273–2279, http://dx.doi.org/10.1021/jp309857b, URL http://pubs.acs.org/doi/abs/10.1021/jp309857b.

[26] P. Ojeda-May, M.E. Garcia, Electric field-driven disruption of a native β-sheet protein conformation and generation of a helix-structure, Biophys. J. 99 (2) (2010) 595–599, http://dx.doi.org/10.1016/j.bpj.2010.04.040, URL http://linkinghub.elsevier.com/retrieve/pii/S0006349510005382.

[27] N.J. English, D.A. Mooney, Denaturation of hen egg white lysozyme in electromagnetic fields: A molecular dynamics study, J. Chem. Phys. 126 (9) (2007) 091105, http://dx.doi.org/10.1063/1.2515315, URL http://scitation.aip.org/content/aip/journal/jcp/126/9/10.1063/1.2515315.

[28] Q. Zhang, D. Shao, P. Xu, Z. Jiang, Effects of an electric field on the conformational transition of the protein: Pulsed and oscillating electric fields with different frequencies, Polymers 14 (1) (2022) 123, http://dx.doi.org/10.3390/polym14010123, URL https://www.mdpi.com/2073-4360/14/1/123, Number: 1 Publisher: Multidisciplinary Digital Publishing Institute.

[29] A. Sinelnikova, T. Mandl, C. Östlin, O. Grånäs, M.N. Brodmerkel, E.G. Marklund, C. Caleman, Reproducibility in the unfolding process of protein induced by an external electric field, Chem. Sci. 12 (6) (2021) 2030–2038, http://dx.doi.org/10.1039/D0SC06008A, URL https://pubs.rsc.org/en/content/articlelanding/2021/sc/d0sc06008a, Publisher: The Royal Society of Chemistry.

[30] N. Todorova, A. Bentvelzen, N.J. English, I. Yarovsky, Electromagnetic-field effects on structure and dynamics of amyloidogenic peptides, J. Chem. Phys. 144 (8) (2016) 085101, http://dx.doi.org/10.1063/1.4941108, URL http://scitation.aip.org/content/aip/journal/jcp/144/8/10.1063/1.4941108.

[31] K. Zhong, X. Hu, G. Zhao, F. Chen, X. Liao, Inactivation and conformational change of horseradish peroxidase induced by pulsed electric field, Food Chem. 92 (3) (2005) 473–479, http://dx.doi.org/10.1016/j.foodchem.2004.08.010, URL https://linkinghub.elsevier.com/retrieve/pii/S0308814604006247.

[32] W. Zhao, R. Yang, Experimental study on conformational changes of lysozyme in solution induced by pulsed electric field and thermal stresses, J. Phys. Chem. B 114 (1) (2010) 503–510, http://dx.doi.org/10.1021/jp9081189, URL https://pubs.acs.org/doi/10.1021/jp9081189.

[33] W. Zhao, R. Yang, R. Lu, Y. Tang, W. Zhang, Investigation of the mechanisms of pulsed electric fields on inactivation of enzyme: Lysozyme, J. Agricult. Food Chem. 55 (24) (2007) 9850–9858, http://dx.doi.org/10.1021/jf072186s, URL https://pubs.acs.org/doi/10.1021/jf072186s.

[34] W. Zhao, R. Yang, Protective effect of sorbitol on enzymes exposed to microsecond pulsed electric field, J. Phys. Chem. B 112 (44) (2008) 14018–14025, http://dx.doi.org/10.1021/jp8062367, URL https://pubs.acs.org/doi/10.1021/jp8062367.

[35] R. Wang, Q.-H. Wen, X.-A. Zeng, J.-W. Lin, J. Li, F.-Y. Xu, Binding affinity of curcumin to bovine serum albumin enhanced by pulsed electric field pretreatment, Food Chem. 377 (2022) 131945, http://dx.doi.org/10.1016/j.foodchem.2021.131945, URL https://linkinghub.elsevier.com/retrieve/pii/S0308814621029514.

[36] A. Guionet, T. Fujiwara, H. Sato, K. Takahashi, K. Takaki, M. Matsui, T. Tanino, T. Ohshima, Pulsed electric fields act on tryptophan to inactivate α-amylase, J. Electrost. 112 (2021) 103597, http://dx.doi.org/10.1016/j.elstat.2021.103597, URL https://www.sciencedirect.com/science/article/pii/S0304388621000462.

[37] H.W. Yeom, Q.H. Zhang, C.P. Dunne, Inactivation of papain by pulsed electric fields in a continuous system, Food Chem. (1999) 7.

[38] W. Jin, Z. Wang, D. Peng, W. Shen, Z. Zhu, S. Cheng, B. Li, Q. Huang, Effect of pulsed electric field on assembly structure of α-amylase and pectin electrostatic complexes, Food Hydrocolloids 101 (2020) 105547, http://dx.doi.org/10.1016/j.foodhyd.2019.105547, URL https://www.sciencedirect.com/science/article/pii/S0268005X19321587.

[39] W. Zhao, R. Yang, Comparative study of inactivation and conformational change of lysozyme induced by pulsed electric fields and heat, Eur. Food Res. Technol. 228 (1) (2008) 47–54, http://dx.doi.org/10.1007/s00217-008-0905-z.
[40] G. Urabe, T. Katagiri, S. Katsuki, Intense pulsed electric fields denature urease protein, Bioelectricity (2019) http://dx.doi.org/10.1089/bioe.2019.0021, bioe.2019.0021, URL https://www.liebertpub.com/doi/10.1089/bioe.2019.0021.
[41] L. Wu, W. Zhao, R. Yang, W. Yan, Pulsed electric field (PEF)-induced aggregation between lysozyme, ovalbumin and ovotransferrin in multi-protein system, Food Chem. 175 (2015) 115–120, http://dx.doi.org/10.1016/j.foodchem.2014.11.136, URL http://linkinghub.elsevier.com/retrieve/pii/S0308814614018743.
[42] Y.-F. Liu, I. Oey, P. Bremer, A. Carne, P. Silcock, Effects of pH, temperature and pulsed electric fields on the turbidity and protein aggregation of ovomucin-depleted egg white, Food Res. Int. 91 (2017) 161–170, http://dx.doi.org/10.1016/j.foodres.2016.12.005, URL https://www.sciencedirect.com/science/article/pii/S0963996916305993.
[43] S. Zhang, R. Yang, W. Zhao, Q. Liang, Z. Zhang, The first ESR observation of radical species generated under pulsed electric fields processing, LWT - Food Sci. Technol. 44 (4) (2011) 1233–1235, http://dx.doi.org/10.1016/j.lwt.2010.11.016, URL https://linkinghub.elsevier.com/retrieve/pii/S0023643810003932.
[44] P. Ruzgys, V. Novickij, J. Novickij, S. Šatkauskas, Influence of the electrode material on ROS generation and electroporation efficiency in low and high frequency nanosecond pulse range, Bioelectrochemistry 127 (2019) 87–93, http://dx.doi.org/10.1016/j.bioelechem.2019.02.002, URL https://linkinghub.elsevier.com/retrieve/pii/S1567539418305176.
[45] W. Zhao, R. Yang, X. Shi, K. Pan, S. Zhang, W. Zhang, X. Hua, Oxidation of oleic acid under pulsed electric field processing, Food Res. Int. 44 (5) (2011) 1463–1467, http://dx.doi.org/10.1016/j.foodres.2011.03.022, URL https://linkinghub.elsevier.com/retrieve/pii/S0963996911001797.
[46] W. Zhao, R. Yang, Pulsed electric field induced aggregation of food proteins: Ovalbumin and bovine serum albumin, Food Bioprocess Technol. 5 (5) (2012) 1706–1714, http://dx.doi.org/10.1007/s11947-010-0464-8.
[47] K. Yogesh, Pulsed electric field processing of egg products: a review, J. Food Sci. Technol. (2016) 12.
[48] B. Gabriel, J. Teissie, Generation of reactive-oxygen species induced by electropermeabilization of Chinese hamster ovary cells and their consequence on cell viability, Eur. J. Biochem. 223 (1) (1994) 25–33, URL http://onlinelibrary.wiley.com/doi/10.1111/j.1432-1033.1994.tb18962.x/full.
[49] M. Maccarrone, N. Rosato, A.F. Agro, Electroporation enhances cell membrane peroxidation and luminescence, Biochem. Biophys. Res. Commun. 206 (1) (1995) 238–245.
[50] M. Maccarrone, C. Fantini, A.F. Agrò, N. Rosato, Kinetics of ultraweak light emission from human erythroleukemia K562 cells upon electroporation, Biochim. Biophys. Acta (BBA)-Biomembranes 1414 (1) (1998) 43–50.
[51] O.N. Pakhomova, V.A. Khorokhorina, A.M. Bowman, R. Rodaitė-Riševičienė, G. Saulis, S. Xiao, A.G. Pakhomov, Oxidative effects of nanosecond pulsed electric field exposure in cells and cell-free media, Arch. Biochem. Biophys. 527 (1) (2012) 55–64, http://dx.doi.org/10.1016/j.abb.2012.08.004, URL http://linkinghub.elsevier.com/retrieve/pii/S0003986112003037.
[52] Y. Zhang, F. Dong, Z. Liu, J. Guo, J. Zhang, J. Fang, Nanosecond pulsed electric fields promoting the proliferation of porcine iliac endothelial cells: An in vitro study, PLoS One 13 (5) (2018) e0196688, http://dx.doi.org/10.1371/journal.pone.0196688, URL https://journals.plos.org/plosone/article?id=10.1371/journal.pone.0196688, Publisher: Public Library of Science.
[53] W. Szlasa, A. Kiełbik, A. Szewczyk, N. Rembiałkowska, V. Novickij, M. Tarek, J. Saczko, J. Kulbacka, Oxidative effects during irreversible electroporation of melanoma cells—in vitro study, Molecules 26 (1) (2021) 154, http://dx.doi.org/10.3390/molecules26010154, URL https://www.mdpi.com/1420-3049/26/1/154, Number: 1 Publisher: Multidisciplinary Digital Publishing Institute.
[54] L. Wu, W. Zhao, R. Yang, X. Chen, Effects of pulsed electric fields processing on stability of egg white proteins, J. Food Eng. 139 (2014) 13–18, http://dx.doi.org/10.1016/j.jfoodeng.2014.04.008, URL https://linkinghub.elsevier.com/retrieve/pii/S026087741400168X.
[55] P. Vahalová, M. Cifra, Biological autoluminescence as a perturbance-free method for monitoring oxidation in biosystems, Prog. Biophys. Mol. Biol. 177 (2023) 80–108, http://dx.doi.org/10.1016/j.pbiomolbio.2022.10.009.
[56] M. Cifra, P. Pospíšil, Ultra-weak photon emission from biological samples: Definition, mechanisms, properties, detection and applications, J. Photochem. Photobiol. B: Biology 139 (2014) 2–10, http://dx.doi.org/10.1016/j.jphotobiol.2014.02.009, URL https://www.sciencedirect.com/science/article/pii/S1011134414000463.
[57] P. Pospíšil, A. Prasad, M. Rác, Mechanism of the formation of electronically excited species by oxidative metabolic processes: Role of reactive oxygen species, Biomolecules 9 (7) (2019) 258, http://dx.doi.org/10.3390/biom9070258, URL https://www.mdpi.com/2218-273X/9/7/258.
[58] A. Salis, M. Boström, L. Medda, F. Cugia, B. Barse, D.F. Parsons, B.W. Ninham, M. Monduzzi, Measurements and theoretical interpretation of points of zero charge/potential of BSA protein, Langmuir 27 (18) (2011) 11597–11604, http://dx.doi.org/10.1021/la2024605, URL http://pubs.acs.org/doi/abs/10.1021/la2024605.
[59] U. Böhme, U. Scheler, Effective charge of bovine serum albumin determined by electrophoresis NMR, Chem. Phys. Lett. 435 (4–6) (2007) 342–345, http://dx.doi.org/10.1016/j.cplett.2006.12.068, URL http://linkinghub.elsevier.com/retrieve/pii/S000926140601894X.
[60] X. Lu, W.-L. Yim, B.H.R. Suryanto, C. Zhao, Electrocatalytic oxygen evolution at surface-oxidized multiwall carbon nanotubes, J. Am. Chem. Soc. 137 (8) (2015) 2901–2907, http://dx.doi.org/10.1021/ja509879r, Publisher: American Chemical Society.
[61] I.P. Ivanova, S.V. Trofimova, I.M. Piskarev, N.A. Aristova, O.E. Burhina, O.O. Soshnikova, Mechanism of chemiluminescence in fenton reaction, J. Biophys. Chem. 03 (01) (2012) 88–100, http://dx.doi.org/10.4236/jbpc.2012.31011, URL http://www.scirp.org/journal/doi.aspx?DOI=10.4236/jbpc.2012.31011.
[62] A.U. Khan, M. Kasha, Chemiluminescence arising from simultaneous transitions in pairs of singlet oxygen molecules, J. Am. Chem. Soc. 92 (11) (1970) 3293–3300.
[63] P. Di Mascio, E.J.H. Bechara, M.H.G. Medeiros, K. Briviba, H. Sies, Singlet molecular oxygen production in the reaction of peroxynitrite with hydrogen peroxide, FEBS Lett. 355 (3) (1994) 287–289, http://dx.doi.org/10.1016/0014-5793(94)01224-5, URL https://febs.onlinelibrary.wiley.com/doi/abs/10.1016/0014-5793%2894%2901224-5, _eprint: https://febs.onlinelibrary.wiley.com/doi/pdf/10.1016/0014-5793%2894%2901224-5.
[64] P. Di Mascio, G.R. Martinez, S. Miyamoto, G.E. Ronsein, M.H.G. Medeiros, J. Cadet, Singlet molecular oxygen reactions with nucleic acids, lipids, and proteins, Chem. Rev. 119 (3) (2019) 2043–2086, http://dx.doi.org/10.1021/acs.chemrev.8b00554, URL https://pubs.acs.org/doi/10.1021/acs.chemrev.8b00554.
[65] L. Zhang, Y. Zhang, X. Zhang, Z. Li, G. Shen, M. Ye, C. Fan, H. Fang, J. Hu, Electrochemically controlled formation and growth of hydrogen nanobubbles, Langmuir 22 (19) (2006) 8109–8113, http://dx.doi.org/10.1021/la060859f, Publisher: American Chemical Society.
[66] S. Yang, P. Tsai, E.S. Kooij, A. Prosperetti, H.J.W. Zandvliet, D. Lohse, Electrolytically generated nanobubbles on highly orientated pyrolytic graphite surfaces, Langmuir 25 (3) (2009) 1466–1474, http://dx.doi.org/10.1021/la8027513, Publisher: American Chemical Society.
[67] V. Kolivoška, M. Gál, Š. Lachmanová, P. Janda, R. Sokolová, M. Hromadová, Nanoshaving of bovine serum albumin films adsorbed on monocrystalline surfaces and interfaces, Collect. Czechoslov. Chem. Commun. 76 (9) (2011) 1075–1087, http://dx.doi.org/10.1135/cccc2011080, URL http://cccc.uochb.cas.cz/76/9/1075/, Publisher: Institute of Organic Chemistry and Biochemistry AS CR, v.v.i..
[68] V. Kolivoška, M. Gál, M. Hromadová, Š. Lachmanová, H. Tarábková, P. Janda, L. Pospíšil, A.M. Turoňová, Bovine serum albumin film as a template for controlled nanopancake and nanobubble formation: In situ atomic force microscopy and nanolithography study, Colloids Surfaces B 94 (2012) 213–219, http://dx.doi.org/10.1016/j.colsurfb.2012.01.028, URL https://www.sciencedirect.com/science/article/pii/S0927776512000537.

Petra Vahalová is a Ph.D. student (Charles University, Ph.D. program Biophysics, chemical and macromolecular physics) in the Bioelectrodynamics research team (Institute of Photonics and Electronics of the Czech Academy of Sciences) working on biological autoluminescence and methods for its modulation and detection.

Dr. Daniel Havelka received the M.Sc. and Ph.D. degrees in Electrical engineering from the Czech Technical University in Prague, in 2010 and 2014, respectively. Since 2008, he has been a member of the Bioelectrodynamics research team at the Institute of Photonics and Electronics, Czech Academy of Sciences, in Prague where he has been involved in the design and development of computational models of microtubule vibration dynamics and electrodynamics. Now he is focused on the development of microwave micro-/nanosensors for dielectric spectroscopy of micro-volume liquid samples.

Dr. Eva Vaněčková is a postdoctoral researcher in the Electrochemistry at the Nanoscale department at J. Heyrovsky Institute of Physical Chemistry of the Czech Academy of Sciences. She received her PhD. at the University of Chemical Technology in Prague, where she was involved in the characterization of composite electrodes. Her current research is focused on the possibilities of using 3D printing and subtractive technologies for the development of gas diffusion electrodes as effective catalytic systems for the electrochemical reduction of carbon dioxide to more energy-rich raw materials.

Dr. Tomáš Zakar is a postdoctoral fellow in the Bioelectrodynamics research team (Institute of Photonics and Electronics of the Czech Academy of Sciences). He received his M.Sc. and Ph.D. degrees as a plant biologist from the University of Szeged in 2013 and 2019. During his studies, he gained experience in the methodology of protein biochemistry, biophysics, and plant microbiology. His current research focuses on the effects of the micro- and nanosecond pulsed electric field on proteins and protein structures such as tubulin and microtubules.

Dr. Viliam Kolivoška is an independent researcher and deputy head of Electrochemistry at the Nanoscale department at J. Heyrovsky Institute of Physical Chemistry of the Czech Academy of Sciences. He obtained MSc. (2008) in physical chemistry at Charles University in Prague and Ph.D. (2011) in physical chemistry at University of Chemistry and Technology in Prague. From 2011 to 2013 he was a SCIEX postdoctoral fellow at University of Bern in Switzerland, exploring charge transfer and transport phenomena in single molecule electronic elements. His current research interests involve physical electrochemistry and electrocatalysis, focusing on the use of advanced manufacturing techniques in the development of electrochemical devices

Dr. Michal Cifra is a senior scientist and head of Bioelectrodynamics research team (Institute of Photonics and Electronics of the Czech Academy of Sciences). He obtained MSc. (2006) in Biomedical Engineering (University of Žilina, Slovakia) and Ph.D. (2009) in Radioelectronics (Czech Technical University in Prague, Czechia). Apart from ~1 year biophotonics research experience from Germany (RWTH, Aachen/ IIB, Neuss), he also gained experience with high-frequency bioelectronic interfaces (8 months, University of Chicago, USA). His research interests are in advanced high-frequency and microwave biochips, micro-/nanosensors, and nanoscale and molecular electrodynamic phenomena in biosystems.

7 Results

The results of the research presented in this thesis were published in scientific journals (see the list of author's publications on the page 87). The core of the dissertation consists of three main parts, namely Chapters 4, 5, and 6 and one paper in the Appendix, Section A. Full bibliographic citation, the contribution of the candidate, and acknowledgments are stated at the beginning of each section.

The fourth chapter (Chap. 4) reviews methods for monitoring oxidation mainly in biochemical systems, cells and tissue cultures and mentions their basic characteristics. The second part is focused on the particular chemiluminescent method – BAL and its correlations with various aspects. The pros and cons of this method are discussed. The review provides an overview of BAL employment to report on various aspects of oxidation processes starting from oxygen consumption to the generation of oxidation products such as carbonyls.

In further chapter 5, the correlation between BAL from yeast *Saccharomyces cerevisiae* and selected physical, chemical, or biological parameters are analyzed. For example, the BAL signal increased together with the number of ROS (resulting from the Fenton reaction) in a sample, while it increased just up to a certain limit and then started to decrease together with increasing yeast concentration. The addition of the antioxidant ascorbic acid to the sample suppressed the BAL signal for some time or completely depending on the antioxidant dose. Short-time oxidation of yeast cells by Fenton reagents did not cause any damage observable under a microscope, just increased the tendency of the cells to cluster. Additionally, higher H_2O_2 concentrations caused prolongation of the lag phase of yeast growth. During yeast culture growth in a bioreactor, the BAL intensity increased together with the number of cells, while the pH and glucose concentration decreased. The changes in oxygen partial pressure were nonlinear. After approximately 12 hours, when the glucose concentration was low and the yeast growth phase changed ('diauxic shift'), the BAL signal sharply decreased. These results contribute to real-time non-invasive methodologies for monitoring oxidative processes in biomedicine and biotechnology.

Section 6 engages BAL employment for monitoring oxidation in a BSA solution caused by PEF treatment. A special PEF chamber was designed and manufactured for this purpose. Comparison of a stainless steel anode (commonly used for PEF treatments) with a glassy carbon (anodically inert material) anode showed that the glassy carbon anode evinced significantly higher chemiluminescence signals than the steel one for our setup and measurement parameters. Variation of the applied voltage magnitude showed that the chemiluminescence signal increases together with increasing current, confirming that the origin of observed chemiluminescence is in electrogenerated ROS. The chemiluminescence signal increase in the BSA sample compared to the phosphate buffer (with the same conductivity) indicates involvement of BSA molecules in processes leading to biochemiluminescence. BAL based on BSA oxidation by electrogenerated ROS is probably due to excited triplet carbonyl groups and singlet oxygen originating from the oxidative damage of aliphatic regions in the protein molecule. This proposed reaction mechanism was supported by the results of spectroscopic analysis of protein carbonyls and measurement of changes in fluorescence of aromatic amino acid residues.

Possible approaches for enhancement of very low BAL signals are reviewed in the article in Appendix, Section A. Enhancement of the intensity by the application of electric or magnetic field and employment of nanoparticles (such as gold ones) into cells are discussed.

8 Conclusions

8.1 Contribution of the dissertation

This thesis provided an overview of available methods for monitoring oxidation in biosamples and their basic characteristics and capabilities (Chap. 4). It immersed deeply into one of these methods, namely the one employing BAL, and focused on the correlations between BAL characteristics and selected physical, chemical, and biological parameters (Chap. 4). References related to the BAL correlations with various aspects influencing the BAL process (such as ROS generation or various oxidative products) were separated into two groups according to the level of sample complexity and summarized in Chap. 4 (Table 2). Possibilities of the enhancement of the very low BAL signals were also discussed (Appendix, Section A).

Experimental results confirmed ROS participation in the reaction mechanism leading to BAL and the positive correlation between the number of ROS and BAL intensity (Chap. 5 and 6). Additionally, a proposal of a reaction scheme in a BSA sample where BAL was significantly enhanced by electrogenerated ROS was provided (Chap. 6, Fig. 5). The thesis also contributed to the extension of current knowledge of BAL correlations with various physical, chemical or biological parameters or aspects related to 1) spontaneous BAL of yeast *Saccharomyces cerevisiae* cell culture during its cultivation in a bioreactor (Chap. 5), 2) chemically enhanced BAL (by a hydroxyl radical originated from the Fenton reaction) from yeast cell culture (Chap. 5) and from the protein BSA (Chap. 6), and 3) physically enhanced BAL (by PEF) from the protein BSA (Chap. 6). The results of the thesis support the possibility of BAL employment as a non-invasive monitoring and diagnostic method in medicine and food industry.

In conclusion, the goals of the thesis summarized in Chapter 3 were fulfilled in Sections 4–6 and in the article in Appendix, part A.

8.2 Future directions

During my work, I have pioneered and optimized multiple experimental protocols, mainly connected with measurement of BAL from yeast cell culture and PEF-induced BAL from the protein. It provides scope for other

experiments with the great model organism, the simplest eukaryote, single cell - yeast *Saccharomyces cerevisiae* and also for studying the influence of PEF on various other proteins or other biosamples. For example, putting together, a natural next step could be measurement of BAL from yeast treated by PEF.

BIBLIOGRAPHY

[1] R. S. Balaban, S. Nemoto, and T. Finkel, "Mitochondria, oxidants, and aging," vol. 120, no. 4, pp. 483–495. [Online]. Available: https://linkinghub.elsevier.com/retrieve/pii/S0092867405001091

[2] A. A. Starkov, "The role of mitochondria in reactive oxygen species metabolism and signaling," vol. 1147, pp. 37–52. [Online]. Available: https://www.ncbi.nlm.nih.gov/pmc/articles/PMC2869479/

[3] F. Cristiana and A. Elena, *Reactive Oxygen Species (ROS) in Living Cells*. BoD – Books on Demand, google-Books-ID: hnCQDwAAQBAJ.

[4] C. Wilson and C. González-Billault, "Regulation of cytoskeletal dynamics by redox signaling and oxidative stress: implications for neuronal development and trafficking," vol. 9. [Online]. Available: https://www.ncbi.nlm.nih.gov/pmc/articles/PMC4588006/

[5] V. B. O'Donnell and A. Azzi, "High rates of extracellular superoxide generation by cultured human fibroblasts: involvement of a lipid-metabolizing enzyme." vol. 318, pp. 805–812. [Online]. Available: https://www.ncbi.nlm.nih.gov/pmc/articles/PMC1217690/

[6] E. Gross, C. S. Sevier, N. Heldman, E. Vitu, M. Bentzur, C. A. Kaiser, C. Thorpe, and D. Fass, "Generating disulfides enzymatically: Reaction products and electron acceptors of the endoplasmic reticulum thiol oxidase ero1p," vol. 103, no. 2, pp. 299–304. [Online]. Available: http://www.pnas.org/cgi/doi/10.1073/pnas.0506448103

[7] J. S. McNally, M. E. Davis, D. P. Giddens, A. Saha, J. Hwang, S. Dikalov, H. Jo, and D. G. Harrison, "Role of xanthine oxidoreductase and NAD(p)h oxidase in endothelial superoxide production in response to oscillatory shear stress," vol. 285, no. 6, pp. H2290–H2297. [Online]. Available: https://www.physiology.org/doi/10.1152/ajpheart.00515.2003

[8] A. San Martín and K. K. Griendling, "Redox control of vascular smooth muscle migration," vol. 12, no. 5, pp. 625–640. [Online]. Available: https://www.ncbi.nlm.nih.gov/pmc/articles/PMC2829046/

[9] A. A. Alfadda and R. M. Sallam, "Reactive oxygen species in health and disease," vol. 2012. [Online]. Available: https://www.ncbi.nlm.nih.gov/pmc/articles/PMC3424049/

[10] A. Catalano, S. Rodilossi, P. Caprari, V. Coppola, and A. Procopio, "5-lipoxygenase regulates senescence-like growth arrest by promoting ROS-dependent p53 activation," vol. 24, no. 1, pp. 170–179. [Online]. Available: https://www.ncbi.nlm.nih.gov/pmc/articles/PMC544914/

[11] F. J. Gonzalez, "Role of cytochromes p450 in chemical toxicity and oxidative stress: studies with CYP2e1," vol. 569, no. 1, pp. 101–110. [Online]. Available: https://linkinghub.elsevier.com/retrieve/pii/S0027510704003756

[12] H. Sies and D. P. Jones, "Reactive oxygen species (ROS) as pleiotropic physiological signalling agents." [Online]. Available: http://www.nature.com/articles/s41580-020-0230-3

[13] K. Brieger, S. Schiavone, J. Miller, and K. Krause, "Reactive oxygen species: from health to disease." [Online]. Available: http://doi.emh.ch/smw.2012.13659

[14] A. Valdivia, C. Duran, and A. Martin, "The role of nox-mediated oxidation in the regulation of cytoskeletal dynamics," vol. 21, no. 41, pp. 6009–6022. [Online]. Available: http://www.eurekaselect.com/openurl/content.php?genre=article&issn=1381-6128&volume=21&issue=41&spage=6009

[15] K. Das and A. Roychoudhury, "Reactive oxygen species (ROS) and response of antioxidants as ROS-scavengers during environmental stress in plants," vol. 2, pp. 53–65. [Online]. Available: http://journal.frontiersin.org/article/10.3389/fenvs.2014.00053/abstract

[16] C. L. Hawkins and M. J. Davies, "Detection, identification, and quantification of oxidative protein modifications," vol. 294, no. 51, pp. 19 683–19 708. [Online]. Available: https://www.ncbi.nlm.nih.gov/pmc/articles/PMC6926449/

[17] S. Zhang, R. Yang, W. Zhao, Q. Liang, and Z. Zhang, "The first ESR observation of radical species generated under pulsed electric fields processing," vol. 44, no. 4, pp. 1233–1235. [Online]. Available: https://linkinghub.elsevier.com/retrieve/pii/S0023643810003932

[18] Merck, "Modern methods in oxidative stress research." [Online]. Available: https://www.merckmillipore.com/CZ/cs/life-science-research/antibodies-assays/antibodies-overview/Research-Areas/neuroscience/oxidative-stress/NLib.qB.eW0AAAFPwH11gPuJ,nav

[19] M. Ohyagi, T. Nagata, K. Ihara, K. Yoshida-Tanaka, R. Nishi, H. Miyata, A. Abe, Y. Mabuchi, C. Akazawa, and T. Yokota, "DNA/RNA heteroduplex oligonucleotide technology for regulating lymphocytes in vivo," vol. 12, no. 1, p. 7344. [Online]. Available: https://www.nature.com/articles/s41467-021-26902-8

[20] J. Yun, P. Rocic, Y. F. Pung, S. Belmadani, A. C. R. Carrao, V. Ohanyan, and W. M. Chilian, "Redox-dependent mechanisms in coronary collateral growth: The "redox window" hypothesis," vol. 11, no. 8, pp. 1961–1974. [Online]. Available: https://www.ncbi.nlm.nih.gov/pmc/articles/PMC2848513/

[21] P. Jamnik and P. Raspor, "Methods for monitoring oxidative stress response in yeasts," vol. 19, no. 4, pp. 195–203. [Online]. Available: http://doi.wiley.com/10.1002/jbt.20091

[22] C. M. Spickett and A. R. Pitt, "Oxidative lipidomics coming of age: Advances in analysis of oxidized phospholipids in physiology and pathology," vol. 22, no. 18, pp. 1646–1666. [Online]. Available: https://www.ncbi.nlm.nih.gov/pmc/articles/PMC4486145/

[23] A. Reis and C. M. Spickett, "Chemistry of phospholipid oxidation," vol. 1818, no. 10, pp. 2374–2387. [Online]. Available: https://linkinghub.elsevier.com/retrieve/pii/S0005273612000387

[24] E. Cabiscol Català, J. Tamarit Sumalla, and J. Ros Salvador, "Oxidative stress in bacteria and protein damage by reactive oxygen species," publisher: Springer-Verlag Ibérica.

[25] H. Esterbauer, R. J. Schaur, and H. Zollner, "Chemistry and biochemistry of 4-hydroxynonenal, malonaldehyde and related aldehydes," vol. 11, no. 1, pp. 81–128. [Online]. Available: https://linkinghub.elsevier.com/retrieve/pii/0891584991901926

[26] C. L. Hawkins, P. E. Morgan, and M. J. Davies, "Quantification of protein modification by oxidants," vol. 46, no. 8, pp. 965–988. [Online]. Available: https://linkinghub.elsevier.com/retrieve/pii/S089158490900029X

[27] C. L. Hawkins and M. J. Davies, "Generation and propagation of radical reactions on proteins," vol. 1504, no. 2, pp. 196–219. [Online]. Available: http://linkinghub.elsevier.com/retrieve/pii/S0005272800002528

[28] H. Sies, "Damage to plasmid DNA by singlet oxygen and its protection," vol. 299, no. 3, pp. 183–191. [Online]. Available: https://linkinghub.elsevier.com/retrieve/pii/016512189390095U

[29] H. Sies and C. F. Menck, "Singlet oxygen induced DNA damage," vol. 275, no. 3, pp. 367–375.

[30] A. Hartwig, "Sensitive analysis of oxidative DNA damage in mammalian cells: use of the bacterial fpg protein in combination with alkaline unwinding," vol. 88, no. 1, pp. 85–90. [Online]. Available: https://linkinghub.elsevier.com/retrieve/pii/0378427496037228

[31] C. L. Hawkins and M. J. Davies, "Detection and characterisation of radicals in biological materials using EPR methodology," vol. 1840, no. 2, pp. 708–721. [Online]. Available: https://linkinghub.elsevier.com/retrieve/pii/S0304416513001281

[32] I. Dalle-Donne, R. Rossi, D. Giustarini, A. Milzani, and R. Colombo, "Protein carbonyl groups as biomarkers of oxidative stress," vol. 329, no. 1, pp. 23–38. [Online]. Available: http://linkinghub.elsevier.com/retrieve/pii/S0009898103000032

[33] P. Jamnik and P. Raspor, "Stress response of yeastcandida intermedia to cr(VI)," vol. 17, no. 6, pp. 316–323. [Online]. Available: http://doi.wiley.com/10.1002/jbt.10093

[34] P. Pospíšil, A. Prasad, and M. Rác, "Mechanism of the formation of electronically excited species by oxidative metabolic processes: Role of reactive oxygen species," vol. 9, no. 7, p. 258. [Online]. Available: https://www.mdpi.com/2218-273X/9/7/258

[35] D. Balasigamani, M. Usa, and H. Inaba, "Biophotons: ultraweak light emission from living systems," vol. 2, no. 2, pp. 188–193. [Online]. Available: http://www.sciencedirect.com/science/article/pii/S1359028697800642

[36] M. Cifra and P. Pospišil, "Ultra-weak photon emission from biological samples: Definition, mechanisms, properties, detection and applications," vol. 139, pp. 2–10. [Online]. Available: https://www.sciencedirect.com/science/article/pii/S1011134414000463

[37] E. Cadenas, A. Boveris, and B. Chance, "Low-level chemiluminescence of bovine heart submitochondrial particles," vol. 186, no. 3, pp. 659–667. [Online]. Available: http://www.biochemj.org/content/186/3/659.abstract

[38] A. Boveris, E. Cadenas, R. Reiter, M. Filipowski, Nasake, and B. Chance, "Organ chemiluminescence—noninvasive assay for oxidative radical reaction," vol. 77, pp. 347–351. [Online]. Available: http://www.jstor.org/stable/pdf/8201.pdf

[39] M. Havaux, C. Triantaphylides, and B. Genty, "Autoluminescence imaging: a non-invasive tool for mapping oxidative stress," vol. 11, no. 10, pp. 480–484.

[40] S. Cohen and F. Popp, "Biophoton emission of the human body," vol. 40, no. 2, pp. 187–189.

[41] J. Siegrist and H. Sies, "Disturbed redox homeostasis in oxidative distress: A molecular link from chronic psychosocial work stress to coronary heart disease?" vol. 121, no. 2, pp. 103–105. [Online]. Available: https://www.ahajournals.org/doi/10.1161/CIRCRESAHA.117.311182

[42] A. M. Shah, "Free radicals and redox signalling in cardiovascular disease," vol. 90, no. 5, pp. 486–487. [Online]. Available: http://heart.bmj.com/cgi/doi/10.1136/hrt.2003.029389

[43] S. S. Sabharwal and P. T. Schumacker, "Mitochondrial ROS in cancer: initiators, amplifiers or an achilles' heel?" vol. 14, no. 11, pp. 709–721. [Online]. Available: http://www.nature.com/doifinder/10.1038/nrc3803

[44] M. G. Lambrechts and I. S. Pretorius, "Yeast and its importance to wine aroma - a review," vol. 21, no. 1, pp. 97–129, number: 1. [Online]. Available: https://www.journals.ac.za/index.php/sajev/article/view/3560

[45] E. J. Pires, J. A. Teixeira, T. Brányik, and A. A. Vicente, "Yeast: the soul of beer's aroma—a review of flavour-active esters and higher alcohols produced by the brewing yeast," vol. 98, no. 5, pp. 1937–1949. [Online]. Available: https://doi.org/10.1007/s00253-013-5470-0

[46] I. Borodina and J. Nielsen, "Advances in metabolic engineering of yeast saccharomyces cerevisiae for production of chemicals," vol. 9, no. 5, pp. 609–620, _eprint: https://onlinelibrary.wiley.com/doi/pdf/10.1002/biot.201300445. [Online]. Available: https://onlinelibrary.wiley.com/doi/abs/10.1002/biot.201300445

[47] M. M. Bradford, "A rapid and sensitive method for the quantitation of microgram quantities of protein utilizing the principle of protein-dye binding," vol. 72, no. 1, pp. 248–254, publisher: Elsevier.

[48] Y. Xiao and S. N. Isaacs, "Enzyme-linked immunosorbent assay (ELISA) and blocking with bovine serum albumin (BSA)—not all BSAs are alike," vol. 384, no. 1, pp. 148–151. [Online]. Available: https://linkinghub.elsevier.com/retrieve/pii/S0022175912001706

[49] C. A. Kreader, "Relief of amplification inhibition in PCR with bovine serum albumin or t4 gene 32 protein," vol. 62, no. 3, pp. 1102–1106. [Online]. Available: https://journals.asm.org/doi/10.1128/aem.62.3.1102-1106.1996

[50] M.-S. Han and K. Niwa, "Effects of BSA and fetal bovine serum in culture medium on development of rat embryos," vol. 49, no. 3, pp. 235–242. [Online]. Available: http://www.jstage.jst.go.jp/article/jrd/49/3/49_3_235/_article

[51] R. Queiroz, G. Varca, S. Kadlubowski, P. Ulanski, and A. Lugão, "Radiation-synthesized protein-based drug carriers: Size-controlled BSA nanoparticles," vol. 85, pp. 82–91. [Online]. Available: https://linkinghub.elsevier.com/retrieve/pii/S0141813015302592

[52] R. Snyderman, J. K. Phillips, and S. E. Mergenhagen, "BIOLOGICAL ACTIVITY OF COMPLEMENT IN VIVO," vol. 134, no. 5, pp. 1131–1143. [Online]. Available: https://rupress.org/jem/article/134/5/1131/31730/BIOLOGICAL-ACTIVITY-OF-COMPLEMENT-IN-VIVO-ROLE-OF

[53] T. Topală, A. Bodoki, L. Oprean, and R. Oprean, "Bovine serum albumin interactions with metal complexes," vol. 87, no. 4, pp. 215–219. [Online]. Available: https://www.medpharmareports.com/index.php/mpr/article/view/357

[54] T. I. Quickenden and S. S. Q. Hee, "Weak luminescence from the yeast saccharomyces cerevisiae and the existence of mitogenetic radiation," vol. 60, no. 2, pp. 764–770.

[55] ——, "The spectral distribution of the luminescence emitted during growth of the yeast saccharomyces cerevisiae and its relationship to mitogenetic radiation," vol. 23, no. 3, pp. 201–204.

[56] T. Quickenden and R. Tilbury, "Growth dependent luminescence from cultures of normal and respiratory deficient saccharomyces cerevisiae," vol. 37, no. 3, pp. 337–344.

[57] T. I. Quickenden and R. N. Tilbury, "Luminescence spectra of exponential and stationary phase cultures of respiratory deficient saccharomyces cerevisiae," vol. 8, no. 2, pp. 169–174. [Online]. Available: http://www.sciencedirect.com/science/article/pii/101113449180055M

[58] R. Tilbury and T. Quickenden, "Luminescence from the yeast candida utilis and comparisons across three genera," vol. 7, no. 4, pp. 245–253.

[59] Miranda-Apodaca, Hananya, Velázquez-Campoy, Shabat, and Arellano, "Emissive enhancement of the singlet oxygen chemiluminescence probe after binding to bovine serum albumin," vol. 24, no. 13, p. 2422. [Online]. Available: https://www.mdpi.com/1420-3049/24/13/2422

[60] J. Yu, F. Wan, C. Zhang, M. Yan, X. Zhang, and S. Wang, "Molecularly imprinted polymeric microspheres for determination of bovine serum albumin based on flow injection chemiluminescence sensor," vol. 26, no. 2, pp. 632–637. [Online]. Available: https://linkinghub.elsevier.com/retrieve/pii/S0956566310003842

[61] Z. Wang, Z. Song, and D. Chen, "Study on the binding behavior of bovine serum albumin with cephalosporin analogues by chemiluminescence method," vol. 83, no. 2, pp. 312–319. [Online]. Available: https://linkinghub.elsevier.com/retrieve/pii/S003991401000740X

[62] G. Serša, M. Bosnjak, M. Čemažar, and R. Heller, "Preclinical studies on electrochemotherapy," in *Handbook of Electroporation*, D. Miklavčič, Ed. Springer International Publishing, pp. 1511–1525. [Online]. Available: http://link.springer.com/10.1007/978-3-319-32886-7_45

[63] V. Todorovic and M. Cemazar, "Combined treatment of electrochemotherapy with immunomodulators," in *Handbook of Electroporation*, pp. 1717–1731.

[64] J. Gehl and G. Serša, "Electrochemotherapy and its clinical applications," in *Handbook of Electroporation*, D. Miklavčič, Ed. Springer International Publishing, pp. 1771–1786. [Online]. Available: http://link.springer.com/10.1007/978-3-319-32886-7_91

[65] S. Bhonsle, R. E. Neal, and R. V. Davalos, "Preclinical studies on irreversible electroporation," in *Handbook of Electroporation*, pp. 1527–1542.

[66] A. A. Bulysheva and R. Heller, "Gene electrotransfer for ischemic tissue," in *Handbook of Electroporation*, D. Miklavčič, Ed. Springer International Publishing, pp. 1665–1677. [Online]. Available: http://link.springer.com/10.1007/978-3-319-32886-7_58

[67] S. A. Shirley, "Delivery of cytokines using gene electrotransfer," in *Handbook of Electroporation*, D. Miklavčič, Ed. Springer International Publishing, pp. 1755–1768. [Online]. Available: http://link.springer.com/10.1007/978-3-319-32886-7_189

[68] L. Liu, M. P. Morrow, and M. Bagarazzi, "Clinical use of DNA vaccines," in *Handbook of Electroporation*, D. Miklavčič, Ed. Springer International Publishing, pp. 1933–1952. [Online]. Available: http://link.springer.com/10.1007/978-3-319-32886-7_106

[69] C. Rosazza, S. Haberl Meglic, A. Zumbusch, M.-P. Rols, and D. Miklavcic, "Gene electrotransfer: A mechanistic perspective," vol. 16, no. 2, pp. 98–129. [Online]. Available: http://www.ingentaconnect.com/contentone/ben/cgt/2016/00000016/00000002/art00005

[70] W. Zhao and R. Yang, "Pulsed electric fields for inactivation of endogenous enzymes in foods," in *Handbook of Electroporation*, D. Miklavčič, Ed. Springer International Publishing, pp. 2239–2251. [Online]. Available: http://link.springer.com/10.1007/978-3-319-32886-7_130

[71] F. Schottroff, A. Krottenthaler, and H. Jäger, "Stress induction and response, inactivation, and recovery of vegetative microorganisms by pulsed electric fields," in *Handbook of Electroporation*, D. Miklavčič, Ed. Springer International Publishing, pp. 2539–2557. [Online]. Available: http://link.springer.com/10.1007/978-3-319-32886-7_183

[72] A. Patras, P. Choudhary, and A. Rawson, "Recovery of primary and secondary plant metabolites by pulsed electric field treatment," in *Handbook of Electroporation*, D. Miklavčič, Ed. Springer International Publishing, pp. 2517–2537. [Online]. Available: http://link.springer.com/10.1007/978-3-319-32886-7_182

[73] J. R. Sarkis, N. Boussetta, and E. Vorobiev, "Application of pulsed electric energies for oil and polyphenol extraction from sesame cake and sesame seeds," in *Handbook of Electroporation*, pp. 2699–2712.

[74] E. Vorobiev and N. Lebovka, "Application of pulsed electric fields for root and tuber crops biorefinery," in *Handbook of Electroporation*, pp. 2899–2922.

[75] D. E. Chafai, V. Sulimenko, D. Havelka, L. Kubínová, P. Dráber, and M. Cifra, "Reversible and irreversible modulation of tubulin self-assembly by intense nanosecond pulsed electric fields," vol. 31, no. 39, p. 1903636. [Online]. Available: https://doi.org/10.1002/adma.201903636

[76] S. Y. Ho, G. S. Mittal, and J. D. Cross, "Effects of high field electric pulses on the activity of selected enzymes," vol. 31, no. 1, pp. 69–84. [Online]. Available: https://www.sciencedirect.com/science/article/pii/S0260877496000520

[77] K. Zhong, X. Hu, G. Zhao, F. Chen, and X. Liao, "Inactivation and conformational change of horseradish peroxidase induced by pulsed electric field," vol. 92, no. 3, pp. 473–479. [Online]. Available: https://linkinghub.elsevier.com/retrieve/pii/S0308814604006247

[78] A. Guionet, T. Fujiwara, H. Sato, K. Takahashi, K. Takaki, M. Matsui, T. Tanino, and T. Ohshima, "Pulsed electric fields act on tryptophan to inactivate -amylase," vol. 112, p. 103597. [Online]. Available: https://www.sciencedirect.com/science/article/pii/S0304388621000462

[79] W. Jin, Z. Wang, D. Peng, W. Shen, Z. Zhu, S. Cheng, B. Li, and Q. Huang, "Effect of pulsed electric field on assembly structure of -amylase and pectin electrostatic complexes," vol. 101, p. 105547. [Online]. Available: https://www.sciencedirect.com/science/article/pii/S0268005X19321587

[80] M. L. Yarmush, A. Golberg, G. Serša, T. Kotnik, and D. Miklavčič, "Electroporation-based technologies for medicine: Principles, applications, and challenges," vol. 16, no. 1, pp. 295–320. [Online]. Available: http://www.annualreviews.org/doi/10.1146/annurev-bioeng-071813-104622

[81] P. Marracino, D. Havelka, J. Průša, M. Liberti, J. Tuszynski, A. T. Ayoub, F. Apollonio, and M. Cifra, "Tubulin response to intense nanosecond-scale electric field in molecular dynamics simulation," vol. 9, no. 1, p. 10477. [Online]. Available: https://doi.org/10.1038/s41598-019-46636-4

[82] J. Wang, S. K. Vanga, and V. Raghavan, "Structural responses of kiwifruit allergen act d 2 to thermal and electric field stresses based on molecular dynamics simulations and experiments," vol. 11, no. 2, pp. 1373–1384, publisher: The Royal Society of Chemistry. [Online]. Available: http://dx.doi.org/10.1039/C9FO02427A

[83] S. K. Vanga, A. Singh, and V. Raghavan, "Effect of thermal and electric field treatment on the conformation of ara h 6 peanut protein allergen," vol. 30, pp. 79–88. [Online]. Available: https://www.sciencedirect.com/science/article/pii/S1466856415000508

[84] J. Průša and M. Cifra, "Molecular dynamics simulation of the nanosecond pulsed electric field effect on kinesin nanomotor," vol. 9, no. 1, p. 19721. [Online]. Available: http://www.nature.com/articles/s41598-019-56052-3

[85] P. Marracino, F. Apollonio, M. Liberti, G. d'Inzeo, and A. Amadei, "Effect of high exogenous electric pulses on protein conformation: Myoglobin as a case study," vol. 117, no. 8, pp. 2273–2279. [Online]. Available: http://pubs.acs.org/doi/abs/10.1021/jp309857b

[86] P. Ojeda-May and M. E. Garcia, "Electric field-driven disruption of a native -sheet protein conformation and generation of a helix-structure," vol. 99, no. 2, pp. 595–599. [Online]. Available: http://linkinghub.elsevier.com/retrieve/pii/S0006349510005382

[87] N. J. English and D. A. Mooney, "Denaturation of hen egg white lysozyme in electromagnetic fields: A molecular dynamics study," vol. 126, no. 9, p. 091105. [Online]. Available: http://scitation.aip.org/content/aip/journal/jcp/126/9/10.1063/1.2515315

[88] Q. Zhang, D. Shao, P. Xu, and Z. Jiang, "Effects of an electric field on the conformational transition of the protein: Pulsed and oscillating electric fields with different frequencies," vol. 14, no. 1, p. 123, number: 1 Publisher: Multidisciplinary Digital Publishing Institute. [Online]. Available: https://www.mdpi.com/2073-4360/14/1/123

[89] A. Sinelnikova, T. Mandl, C. Östlin, O. Grånäs, M. N. Brodmerkel, E. G. Marklund, and C. Caleman, "Reproducibility in the unfolding process of protein induced by an external electric field," vol. 12, no. 6, pp. 2030–2038, publisher: The Royal Society of Chemistry. [Online]. Available: https://pubs.rsc.org/en/content/articlelanding/2021/sc/d0sc06008a

[90] F. Toschi, F. Lugli, F. Biscarini, and F. Zerbetto, "Effects of electric field stress on a -amyloid peptide," vol. 113, no. 1, pp. 369–376. [Online]. Available: http://pubs.acs.org/doi/abs/10.1021/jp807896g

[91] J. Průša, A. T. Ayoub, D. E. Chafai, D. Havelka, and M. Cifra, "Electro-opening of a microtubule lattice in silico," vol. 19, pp. 1488–1496. [Online]. Available: https://www.sciencedirect.com/science/article/pii/S2001037021000581

[92] N. Todorova, A. Bentvelzen, N. J. English, and I. Yarovsky, "Electromagnetic-field effects on structure and dynamics of amyloidogenic peptides," vol. 144, no. 8, p. 085101. [Online]. Available: http://scitation.aip.org/content/aip/journal/jcp/144/8/10.1063/1.4941108

[93] W. Zhao, R. Yang, R. Lu, Y. Tang, and W. Zhang, "Investigation of the mechanisms of pulsed electric fields on inactivation of enzyme: Lysozyme," vol. 55, no. 24, pp. 9850–9858. [Online]. Available: https://pubs.acs.org/doi/10.1021/jf072186s

[94] W. Zhao and R. Yang, "Experimental study on conformational changes of lysozyme in solution induced by pulsed electric field and thermal stresses," vol. 114, no. 1, pp. 503–510. [Online]. Available: https://pubs.acs.org/doi/10.1021/jp9081189

[95] ——, "Protective effect of sorbitol on enzymes exposed to microsecond pulsed electric field," vol. 112, no. 44, pp. 14 018–14 025. [Online]. Available: https://pubs.acs.org/doi/10.1021/jp8062367

[96] R. Wang, Q.-H. Wen, X.-A. Zeng, J.-W. Lin, J. Li, and F.-Y. Xu, "Binding affinity of curcumin to bovine serum albumin enhanced by pulsed electric field pretreatment," vol. 377, p. 131945. [Online]. Available: https://linkinghub.elsevier.com/retrieve/pii/S0308814621029514

[97] H. W. Yeom, Q. H. Zhang, and C. P. Dunne, "Inactivation of papain by pulsed electric fields in a continuous system," p. 7.

[98] W. Zhao and R. Yang, "Comparative study of inactivation and conformational change of lysozyme induced by pulsed electric fields and heat," vol. 228, no. 1, pp. 47–54. [Online]. Available: https://doi.org/10.1007/s00217-008-0905-z

[99] G. Urabe, T. Katagiri, and S. Katsuki, "Intense pulsed electric fields denature urease protein," p. bioe.2019.0021. [Online]. Available: https://www.liebertpub.com/doi/10.1089/bioe.2019.0021

[100] L. Wu, W. Zhao, R. Yang, and W. Yan, "Pulsed electric field (PEF)-induced aggregation between lysozyme, ovalbumin and ovotransferrin in multi-protein system," vol. 175, pp. 115–120. [Online]. Available: http://linkinghub.elsevier.com/retrieve/pii/S0308814614018743

[101] Y.-F. Liu, I. Oey, P. Bremer, A. Carne, and P. Silcock, "Effects of pH, temperature and pulsed electric fields on the turbidity and protein aggregation of ovomucin-depleted egg white," vol. 91, pp. 161–170. [Online]. Available: https://www.sciencedirect.com/science/article/pii/S0963996916305993

[102] P. Ruzgys, V. Novickij, J. Novickij, and S. Šatkauskas, "Influence of the electrode material on ROS generation and electroporation efficiency in low and high frequency nanosecond pulse range," vol. 127, pp. 87–93. [Online]. Available: https://linkinghub.elsevier.com/retrieve/pii/S1567539418305176

[103] B. Gabriel and J. Teissie, "Generation of reactive-oxygen species induced by electropermeabilization of chinese hamster ovary cells and their consequence on cell viability," vol. 223, no. 1, pp. 25–33. [Online]. Available: http://onlinelibrary.wiley.com/doi/10.1111/j.1432-1033.1994.tb18962.x/full

[104] M. Maccarrone, N. Rosato, and A. F. Agro, "Electroporation enhances cell membrane peroxidation and luminescence," vol. 206, no. 1, pp. 238–245.

[105] M. Maccarrone, C. Fantini, A. F. Agrò, and N. Rosato, "Kinetics of ultraweak light emission from human erythroleukemia k562 cells upon electroporation," vol. 1414, no. 1, pp. 43–50.

[106] O. N. Pakhomova, V. A. Khorokhorina, A. M. Bowman, R. Rodaitė-Riševičienė, G. Saulis, S. Xiao, and A. G. Pakhomov, "Oxidative effects of nanosecond pulsed electric field exposure in cells and cell-free media," vol. 527, no. 1, pp. 55–64. [Online]. Available: http://linkinghub.elsevier.com/retrieve/pii/S0003986112003037

[107] Y. Zhang, F. Dong, Z. Liu, J. Guo, J. Zhang, and J. Fang, "Nanosecond pulsed electric fields promoting the proliferation of porcine iliac endothelial cells: An in vitro study," vol. 13, no. 5, p. e0196688, publisher: Public Library of Science. [Online]. Available: https://journals.plos.org/plosone/article?id=10.1371/journal.pone.0196688

[108] W. Szlasa, A. Kiełbik, A. Szewczyk, N. Rembiałkowska, V. Novickij, M. Tarek, J. Saczko, and J. Kulbacka, "Oxidative effects during irreversible electroporation of melanoma cells—in vitro study," vol. 26, no. 1, p. 154, number: 1 Publisher: Multidisciplinary Digital Publishing Institute. [Online]. Available: https://www.mdpi.com/1420-3049/26/1/154

[109] W. Zhao, R. Yang, X. Shi, K. Pan, S. Zhang, W. Zhang, and X. Hua, "Oxidation of oleic acid under pulsed electric field processing," vol. 44, no. 5, pp. 1463–1467. [Online]. Available: https://linkinghub.elsevier.com/retrieve/pii/S0963996911001797

[110] W. Zhao and R. Yang, "Pulsed electric field induced aggregation of food proteins: Ovalbumin and bovine serum albumin," vol. 5, no. 5, pp. 1706–1714. [Online]. Available: https://doi.org/10.1007/s11947-010-0464-8

[111] K. Yogesh, "Pulsed electric field processing of egg products: a review," p. 12.

[112] L. Wu, W. Zhao, R. Yang, and X. Chen, "Effects of pulsed electric fields processing on stability of egg white proteins," vol. 139, pp. 13–18. [Online]. Available: https://linkinghub.elsevier.com/retrieve/pii/S026087741400168X

[113] M. Takeda, M. Kobayashi, M. Takayama, S. Suzuki, T. Ishida, K. Ohnuki, T. Moriya, and N. Ohuchi, "Biophoton detection as a novel technique for cancer imaging," vol. 95, no. 8, pp. 656–661. [Online]. Available: http://doi.wiley.com/10.1111/j.1349-7006.2004.tb03325.x

[114] J. Kim, J. Lim, H. Kim, S. Ahn, S.-B. Sim, and K.-S. Soh, "Scanning spontaneous photon emission from transplanted ovarian tumor of mice using a photomultiplier tube," vol. 25, no. 2, pp. 97–102. [Online]. Available: http://www.tandfonline.com/doi/full/10.1080/15368370600719000

[115] A. Keshavarzian, D. Zapeda, T. List, and S. Mobarhan, "High levels of reactive oxygen metabolites in colon cancer tissue: Analysis by chemiluminescence probe," vol. 17, no. 3, pp. 243–249. [Online]. Available: http://www.tandfonline.com/doi/abs/10.1080/01635589209514193

[116] I. Al-Ogaidi, H. Gou, Z. P. Aguilar, S. Guo, A. K. Melconian, A. K. A. Al-kazaz, F. Meng, and N. Wu, "Detection of the ovarian cancer biomarker CA-125 using chemiluminescence resonance energy transfer to graphene quantum dots," vol. 50, no. 11, pp. 1344–1346. [Online]. Available: http://xlink.rsc.org/?DOI=C3CC47701K

[117] M. Iranifam, "Analytical applications of chemiluminescence methods for cancer detection and therapy," vol. 59, pp. 156–183. [Online]. Available: https://linkinghub.elsevier.com/retrieve/pii/S0165993614000818

[118] C. Zong, J. Wu, C. Wang, H. Ju, and F. Yan, "Chemiluminescence imaging immunoassay of multiple tumor markers for cancer screening," vol. 84, no. 5, pp. 2410–2415. [Online]. Available: https://pubs.acs.org/doi/10.1021/ac203179g

[119] S. Ram and C. Siar, "Chemiluminescence as a diagnostic aid in the detection of oral cancer and potentially malignant epithelial lesions," vol. 34, no. 5, pp. 521–527. [Online]. Available: https://linkinghub.elsevier.com/retrieve/pii/S0901502704002899

[120] R. Shashidara, H. S. Sreeshyla, U. S. Sudheendra, and others, "Chemiluminescence: A diagnostic adjunct in oral precancer and cancer: A review," vol. 10, no. 3, p. 487, publisher: Medknow Publications.

[121] F. Licastro, M. C. Morini, L. J. Davis, P. Malpassi, D. Cucinotta, R. Parente, C. Melotti, and G. Savorani, "Increased chemiluminescence response of neutrophils from the peripheral blood of patients with senile dementia of the alzheimer's type," vol. 51, no. 1, pp. 21–26. [Online]. Available: https://linkinghub.elsevier.com/retrieve/pii/0165572894901244

[122] M. Arcaro, C. Fenoglio, M. Serpente, A. Arighi, G. G. Fumagalli, L. Sacchi, S. Floro, M. D'Anca, F. Sorrentino, C. Visconte, A. Perego, E. Scarpini, and D. Galimberti, "A novel automated chemiluminescence method for detecting cerebrospinal fluid amyloid-beta 1-42 and 1-40, total tau and phosphorylated-tau: Implications for improving diagnostic performance in alzheimer's disease," vol. 10, no. 10, p. 2667. [Online]. Available: https://www.mdpi.com/2227-9059/10/10/2667

[123] L. Agnello, T. Piccoli, M. Vidali, L. Cuffaro, B. Lo Sasso, G. Iacolino, V. R. Giglio, F. Lupo, P. Alongi, G. Bivona, and M. Ciaccio, "Diagnostic accuracy of cerebrospinal fluid biomarkers measured by chemiluminescent enzyme immunoassay for alzheimer disease diagnosis," vol. 80, no. 4, pp. 313–317. [Online]. Available: https://www.tandfonline.com/doi/full/10.1080/00365513.2020.1740939

[124] Repetto, Reides, Evelson, Kohan, De Lustig, and Llesuy, "Peripheral markers of oxidative stress in probable alzheimer patients: Oxidative stress in alzheimer's disease," vol. 29, no. 7, pp. 643–649. [Online]. Available: http://doi.wiley.com/10.1046/j.1365-2362.1999.00506.x

[125] C. Lu, G. Song, and J.-M. Lin, "Reactive oxygen species and their chemiluminescence-detection methods," vol. 25, no. 10, pp. 985–995. [Online]. Available: https://linkinghub.elsevier.com/retrieve/pii/S0165993606001683

[126] Y. A. Vladimirov and E. V. Proskurnina, "Free radicals and cell chemiluminescence," vol. 74, no. 13, pp. 1545–1566. [Online]. Available: http://link.springer.com/10.1134/S0006297909130082

[127] A. Agarwal, S. S. Allamaneni, and T. M. Said, "Chemiluminescence technique for measuring reactive oxygen species," vol. 9, no. 4, pp. 466–468. [Online]. Available: https://linkinghub.elsevier.com/retrieve/pii/S1472648310612849

[128] W. Vessey, A. Perez-Miranda, R. Macfarquhar, A. Agarwal, and S. Homa, "Reactive oxygen species in human semen: validation and qualification of a chemiluminescence assay," vol. 102, no. 6, pp. 1576–1583.e4. [Online]. Available: https://linkinghub.elsevier.com/retrieve/pii/S001502821402161X

[129] C.-H. Tsai, A. Stern, J.-F. Chiou, C.-L. Chern, and T.-Z. Liu, "Rapid and specific detection of hydroxyl radical using an ultraweak chemiluminescence analyzer and a low-level chemiluminescence emitter: Application to hydroxyl radical-scavenging ability of aqueous extracts of food constituents," vol. 49, no. 5, pp. 2137–2141. [Online]. Available: https://pubs.acs.org/doi/10.1021/jf001071k

[130] S. A. Nesbitt and M. A. Horton, "A nonradioactive biochemical characterization of membrane proteins using enhanced chemiluminescence," vol. 206, no. 2, pp. 267–272. [Online]. Available: https://linkinghub.elsevier.com/retrieve/pii/000326979290365E

[131] B. Li and Y. He, "Simultaneous determination of glucose, fructose and lactose in food samples using a continuous-flow chemiluminescence method with the aid of artificial neural networks," vol. 22, no. 4, pp. 317–325. [Online]. Available: https://onlinelibrary.wiley.com/doi/10.1002/bio.965

[132] L. Xu, J. Zhou, S. Eremin, A. C. P. Dias, and X. Zhang, "Development of ELISA and chemiluminescence enzyme immunoassay for quantification of histamine in drug products and food samples," vol. 412, no. 19, pp. 4739–4747. [Online]. Available: https://link.springer.com/10.1007/s00216-020-02730-5

[133] Z. Song and L. Wang, "Chemiluminescence investigation of detection of rutin in medicine and human urine using controlled-reagent-release technology," vol. 49, no. 12, pp. 5697–5701. [Online]. Available: https://pubs.acs.org/doi/10.1021/jf010354p

[134] L. Wu, X.-P. Ding, D.-N. Zhu, B.-Y. Yu, and Y.-Q. Yan, "Study on the radical scavengers in the traditional chinese medicine formula shengmai san by HPLC–DAD coupled with chemiluminescence (CL) and ESI–MS/MS," vol. 52, no. 4, pp. 438–445. [Online]. Available: https://linkinghub.elsevier.com/retrieve/pii/S0731708510000245

[135] J. Zhou, Z. Long, Y. Tian, X. Ding, L. Wu, and X. Hou, "A chemiluminescence metalloimmunoassay for sensitive detection of alpha-fetoprotein in human serum using fe-MIL-88b-NH $_2$ as a label," vol. 51, no. 7, pp. 517–526. [Online]. Available: http://www.tandfonline.com/doi/full/10.1080/05704928.2016.1141293

[136] T. Miyazawa, "Determination of phospholipid hydroperoxides in human blood plasma by a chemiluminescence-HPLC assay," vol. 7, no. 2, pp. 209–218. [Online]. Available: https://linkinghub.elsevier.com/retrieve/pii/0891584989900178

[137] A. K. Campbell, "Chemiluminescence. principles and applications in biology and medicine." [Online]. Available: https://www.osti.gov/etdeweb/biblio/6603431

[138] M. Liu, Z. Lin, and J.-M. Lin, "A review on applications of chemiluminescence detection in food analysis," vol. 670, no. 1, pp. 1–10. [Online]. Available: https://linkinghub.elsevier.com/retrieve/pii/S0003267010004952

[139] Y. Quan, M. Chen, Y. Zhan, and G. Zhang, "Development of an enhanced chemiluminescence ELISA for the rapid detection of acrylamide in food products," vol. 59, no. 13, pp. 6895–6899. [Online]. Available: https://pubs.acs.org/doi/10.1021/jf200954w

[140] K. Papadopoulos, T. Triantis, D. Dimotikali, and J. Nikokavouras, "Evaluation of food antioxidant activity by photostorage chemiluminescence," vol. 433, no. 2, pp. 263–268. [Online]. Available: https://linkinghub.elsevier.com/retrieve/pii/S0003267001007875

[141] R. Créton, J. A. Kreiling, and L. F. Jaffe, "Calcium imaging with chemiluminescence," vol. 46, no. 6, pp. 390–397. [Online]. Available: https://onlinelibrary.wiley.com/doi/10.1002/(SICI)1097-0029(19990915)46:6<390::AID-JEMT7>3.0.CO;2-S

[142] H. Higuchi, H. Nagahata, H. Teraoka, and H. Noda, "Relationship between the chemiluminescent response of bovine neutrophils and changes in intracellular free calcium concentration." vol. 61, no. 1, p. 57, publisher: Canadian Veterinary Medical Association.

[143] S. Paciotti, F. N. Sepe, P. Eusebi, L. Farotti, S. Cataldi, L. Gatticchi, and L. Parnetti, "Diagnostic performance of a fully automated chemiluminescent enzyme immunoassay for alzheimer's disease diagnosis," vol. 494, pp. 74–78. [Online]. Available: https://linkinghub.elsevier.com/retrieve/pii/S0009898119317176

[144] W. Baeyens, S. Schulman, A. Calokerinos, Y. Zhao, A. Garcıa Campaña, K. Nakashima, and D. De Keukeleire, "Chemiluminescence-based detection: principles and analytical applications in flowing streams and in immunoassays," vol. 17, no. 6, pp. 941–953. [Online]. Available: https://linkinghub.elsevier.com/retrieve/pii/S0731708598000624

[145] H. Ou-Yang, G. Stamatas, C. Saliou, and N. Kollias, "A chemiluminescence study of UVA-induced oxidative stress in human skin in vivo," vol. 122, no. 4, pp. 1020–1029. [Online]. Available: https://linkinghub.elsevier.com/retrieve/pii/S0022202X15307569

[146] H. Ou-Yang, "The application of ultra-weak photon emission in dermatology," vol. 139, pp. 63–70. [Online]. Available: http://linkinghub.elsevier.com/retrieve/pii/S1011134413002224

[147] C. M. Magalhães, J. C. G. EstevesdaSilva, and L. PintodaSilva, "Chemiluminescence and bioluminescence as an excitation source in the photodynamic therapy of cancer: A critical review," vol. 17, no. 15, pp. 2286–2294. [Online]. Available: https://onlinelibrary.wiley.com/doi/10.1002/cphc.201600270

[148] D. Mao, W. Wu, S. Ji, C. Chen, F. Hu, D. Kong, D. Ding, and B. Liu, “Chemiluminescence-guided cancer therapy using a chemiexcited photosensitizer,” vol. 3, no. 6, pp. 991–1007. [Online]. Available: https://linkinghub.elsevier.com/retrieve/pii/S2451929417304308

[149] L. Gámiz-Gracia, A. M. García-Campaña, J. F. Huertas-Pérez, and F. J. Lara, “Chemiluminescence detection in liquid chromatography: Applications to clinical, pharmaceutical, environmental and food analysis—a review,” vol. 640, no. 1, pp. 7–28. [Online]. Available: https://linkinghub.elsevier.com/retrieve/pii/S0003267009003985

[150] F. J. Lara, D. Airado-Rodríguez, D. Moreno-González, J. F. Huertas-Pérez, and A. M. García-Campaña, “Applications of capillary electrophoresis with chemiluminescence detection in clinical, environmental and food analysis. a review,” vol. 913, pp. 22–40. [Online]. Available: https://linkinghub.elsevier.com/retrieve/pii/S0003267016301349

LIST OF ABBREVIATIONS

BAL = biological autoluminescence

BSA = bovine serum albumine

EF = electric field

PEF = pulsed electric field

ROS = reactive oxygen species

List of author's publications

Papers in Peer-Reviewed Journals with Impact Factor

- Vahalová, Petra; Cifra, Michal. Biological autoluminescence as a perturbance-free method for monitoring oxidation in biosystems. Progress in Biophysics and Molecular Biology, 2023, 177: 80–108
  Candidate's contribution: 80 %
- Vahalová, Petra; Červinková, Kateřina; Cifra, Michal. Biological autoluminescence for assessing oxidative processes in yeast cell cultures. Scientific Reports, 2021, 11.1: 10852.
  Candidate's contribution: 80 %
- Vahalová, Petra; Havelka, Daniel; Vaněčková, Eva; Zakar, Tomáš; Kolivoška, Viliam Cifra, Michal. Biochemiluminescence Sensing of Protein Oxidation by Reactive Oxygen Species Generated by Pulsed Electric Field. Sensors and Actuators B: Chemical, 2023, 385: 133676.
  Candidate's contribution: 65 %

Chapter in the Book plus Papers and Abstracts in Conference Proceedings

- Sardarabadi, Hadi; Zohrab, Fatemeh; Vahalová, Petra; Cifra, Michal. Ultra-Weak Photon Emission from Biological Systems: Endogenous Biophotonics and Intrinsic Bioluminescence, Chapter Selected biophysical methods for enhancing biological autoluminescence. Springer, accepted.
- Bereta, Martin; Teplan, Michal; Vahalová, Petra; Cifra, Michal. Monitoring of Hydroxyl Radical Induced Oxidation of Yeast Cells Using Biological Autoluminescence, 2019 12^{th} International Conference on Measurement. IEEE, 2019, p. 248-251.
- Vahalová, Petra; Červinková, Kateřina; Poplová, Michaela; Cifra, Michal. Endogenous biological chemiluminescence as an indicator of oxidation. 2017 Electroporation-based Technologies and Treatments, p. 128.
- Cifra, Michal; Červinková, Kateřina; Havelka, Daniel; Krivosudský, Ondrej, Poplová, Michaela; Průša, Jiři; Vahalová, Petra. High-frequency chips and oxidation induced chemiluminescence. 2016 Electroporation-based Technologies and Treatments, p. 128.

APPENDIX

This chapter includes the accepted chapter *Selected biophysical methods for enhancing biological autoluminescence* for the currently prepared book "Ultra-Weak Photon Emission from Biological Systems: Endogenous Biophotonics and Intrinsic Bioluminescence" (Section A) and the supplementary data of Chapter 5 (Section B) and Chapter 6 (Section C).

A Selected biophysical methods for enhancing biological autoluminescence

This chapter is a version of:

Hadi Sardarabadi, Fatemeh Zohrab, Petra Vahalová, Michal Cifra,

Ultra-Weak Photon Emission from Biological Systems: Endogenous Biophotonics and Intrinsic Bioluminescence, Chapter Selected biophysical methods for enhancing biological autoluminescence,

Springer, accepted.

The manuscript carries the following acknowledgements:

MC and PV thank the Czech Science Foundation project no. 20-06873X for the support and they are also participating in the bilateral exchange project between the Czech and Slovak Academy of Sciences, no. SAV-18-11. The Science Editorium is acknowledged for the language check.

Selected biophysical methods for enhancing biological autoluminescence

Hadi Sardarabadi a, Fatemeh Zohrab b, Petra Vahalova c, Michal Cifra c

Corresponding author

Michal Cifra, Ph.D.

Institute of Photonics and Electronics of the Czech Academy of Sciences, Prague, Czechia

E-mail address: cifra@ufe.cz

a Zanjan Pharmaceutical Nanotechnology Research Center (ZPNRC), Zanjan University of Medical Sciences, 45139-56184 Zanjan, Iran.

b Department of Medical Biotechnology, Faculty of Medicine, Qom University of Medical Science, Qum, Iran.

c Institute of Photonics and Electronics of the Czech Academy of Sciences, Prague, Czechia

Abstract

All organisms, including humans, emit ultraweak luminescence (10 – 1000 photons·s^{-1}·cm^{-2} in the wavelength range of at least 350 – 1270 nm). These photons can be detected by very sensitive photomultiplier tubes or charge-coupled device imaging detectors. Biological autoluminescence (BAL) is an endogenously generated light and does not depend on external excitation by chemical means or light irradiation. It is widely accepted that BAL originates from electron-excited states, which are produced during oxidation reactions of biomolecules in living cells, i.e., it is related to the formation of reactive oxygen species (ROS). Because oxidative metabolism, as the main generating source of ROS, continues throughout the life of a living organism, it is possible to identify the health or disease status of a living system by analyzing the properties of these photons. Although BAL signals might contain valuable information about the physiological environment of a living cell, the detection of their ultraweak signal is a challenge for future *in vivo* diagnostic applications. Therefore, the development of appropriate strategies for enhancement of the BAL signal is necessary. Here we review novel biophysical approaches for enhancement of BAL.

Key words: Biological autoluminescence; Signal enhancement, Nanoparticles, Short intense electric pulses, Reactive oxygen species.

Abbreviations:

(BAL): Biological autoluminescence, (**ECL):** Electrochemiluminescence, (**LFE):** Low field effect, (**ROS):** Reactive oxygen species, (**NP**): Nanoparticle

1. Introduction

Biological autoluminescence (BAL) is known to be generated by electronically excited states of molecules in biosystems [1-12]. The typical intensity is <1000 photons·s^{-1}·cm^{-2}. These rays cover a range of the electromagnetic wave spectrum 350 – 1270 nm (depending on the type of emitter molecule), which includes a significant portion of the visible range, and hence is also called ultra-weak photon emission, biophotons, endogenous bioluminescence, autoluminescence, weak luminescence, low-level chemiluminescence, spontaneous chemiluminescence, spontaneous ultra-weak light emission, or ultra-weak bioluminescence [9]. BAL is endogenously generated and, unlike other luminescence phenomena, does not depend on exogenous chemical, physical, or electrical excitations. In fact, BAL is emitted from endogenously excited biomolecules. Extensive indirect investigation of BAL as light dates back to the 1920s [13, 14] when it was referred to as mitogenetic rays [15]. The existence of this phenomenon was controversial until the 1950s, when the first photomultiplier tubes were used to reliably confirm this phenomenon in a number of species [16, 17] and further supported using charge-coupled device camera systems in the 1990s [18]. To date, a widely accepted view regarding the origin of BAL is that the oxidative reactions of biomolecules initiate the generation of electron excited molecular species. There are also other hypotheses: one of them, which is not accepted by the wider scientific community because of the lack of experimental evidence, claims that endogenous biological light emanates from a coherent electromagnetic field and the main source of these emissions could be inside the DNA molecule and other intracellular cavity resonators [19]. Although profiling the genes (genomics), proteins (proteomics), and other cellular biomarkers (metabolomics) provide promising methods to detect different physiological states, these methods depend on applying invasive sampling methods. Therefore, the monitoring of intracellular and intercellular events at the appropriate time and location without the use of invasive methods is a major goal of future research in various disciplines. As all metabolically active cells (both eukaryotic and prokaryotic) generate electronically excited biomolecules during their metabolism as the main source of BAL, it can be considered as a new non-invasive diagnosis approach [20]. A significant increase in the BAL signal intensity of in vivo implanted tumors has been observed [21]. Researchers have shown that there is a strong relationship between the enhancement of the BAL signals intensity and an increase in tumor size [22]. In normal tissue, generated ROS are quickly eliminated by the enzymatic (as self-defense antioxidant mechanisms of living cells) or non-enzymatic pathways [23]. Compared with normal tissue, cancer tissue has a lower concentration of ROS eliminators, such as superoxide dismutase and catalase [24]. Such evidence shows the potential application of BAL as a noninvasive monitoring method for the early detection of cancer. Recently, cancer biomarkers have also been successfully detected by the analysis of BAL intensity. Among all human tissues, the skin is the most prone to oxidative damage. Considering the powerful relationship between the BAL intensity and oxidative processes, skin-related diseases could also be studied using BAL [25-29]. Several studies have shown that neuronal tissue activity can be studied by BAL [30-32]. In agriculture, the intensity and the spectrum of biologically generated photons can be used to evaluate plant responses to pathogens [33], drought stress [34], salinity stress [35], and herbicides [36]. The researchers also indicate it is possible to study physiological changes during

metamorphosis non-invasively by imaging of BAL [37]. Despite widespread efforts to optimally exploit the valuable properties of BAL, the weak intensity of these signals is considered as a major constraint both in *in vivo* and *in vitro* applications [38-42]. Hence, BAL signal enhancement studies are strongly required.

In this chapter, selected biophysical approaches for modulating the BAL signal intensity are introduced. First, the related mechanisms that are involved in the generation of electronically excited species are described. Then, we reviewed selected experimental studies that are related to the field of BAL signal enhancement.

2. Mechanisms of the BAL generation as a starting point for signal enhancement

Radiative relaxation of chemically generated electronically excited states of molecules (generated during the oxidative cell metabolism or stress) are recognized as the main sources of endogenous radiative processes we term here as BAL [43]. The general working hypothesis is displayed in Fig. 1. and is described in the following text.

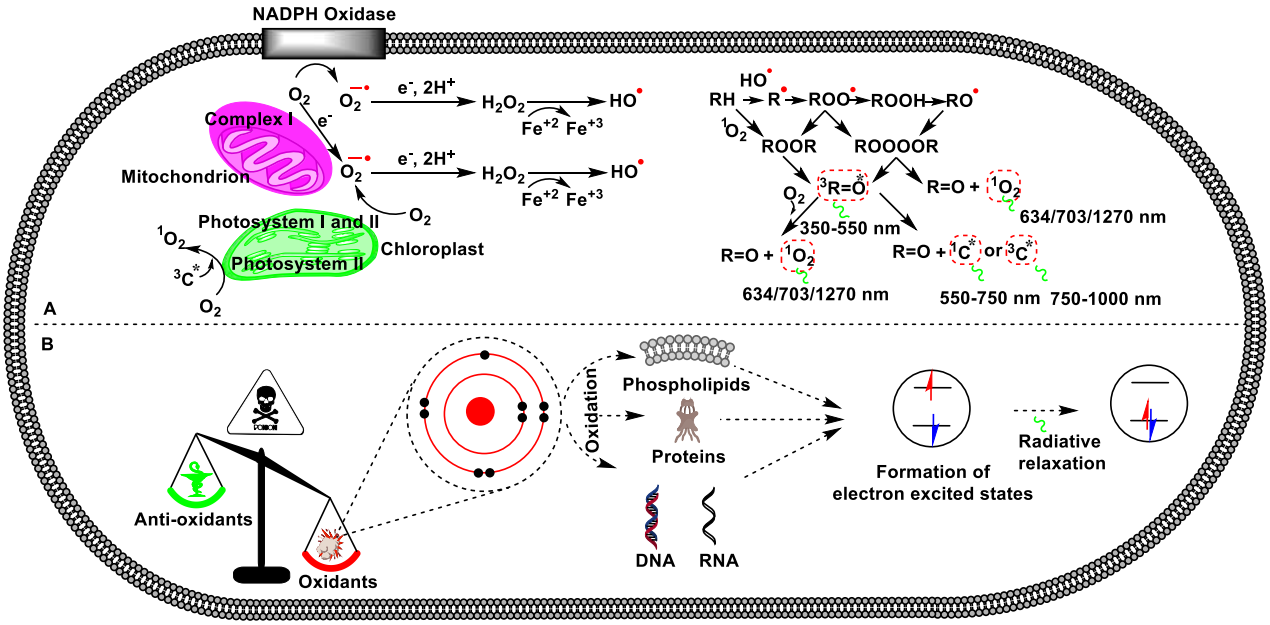

Fig. 1. Biological autoluminescence during dynamic metabolic processes. A) Formation of ROS and electronically excited states of molecules in metabolically active cells. B) The BAL emission from electron excited states of molecules caused by an imbalance between oxidants and antioxidants.

There are several pathways that lead to the formation of various ROS, reactive molecules standing at the beginning of the BAL generation. The one-electron reduction of molecular oxygen leads to the formation of a superoxide anion radical ($O_2^{\bullet-}$) and occurs in the mitochondria during cellular respiration, in the chloroplast during light exposure, and in the membrane-bound enzyme complex NADPH oxidase during the oxidative burst [44]. Although $O_2^{\bullet-}$ is preferentially formed at a neutral pH, it is converted into $HO_2^{\bullet}$ in an acidic microenvironment because pK_a ($HO_2^{\bullet}$) = 4.8 [45]. One-electron reduction of $O_2^{\bullet-}$ (occurring spontaneously or catalyzed by various types of superoxide dismutases in mitochondria, peroxisomes, and cytoplasm) [44] or two-electron oxidation of H_2O (in water splitting manganese complex in photosystem II in chloroplasts) [46] lead to the creation of hydrogen peroxide (H_2O_2). A hydroxyl radical ($HO^{\bullet}$) is formed through the one-electron reduction of H_2O_2 mediated by free metal ions such as Fe^{2+} [47]. Triplet-singlet energy transfer from excited triplet chromophores ($^3C^*$) to molecular oxygen leads to the formation of singlet oxygen ($^1O_2$). Radical ROS with unpaired electrons have high positive redox potential so they are highly reactive. An appropriate amount of ROS in the right place plays an important role in cellular signaling pathways, immune defense systems, apoptosis, or aging. On the other hand, undesirable reactions with biomolecules lead to the damage of cells.

ROS, especially $HO^{\bullet}$ and $HO_2^{\bullet}$, can react with organic matter RH and form organic radicals $R^{\bullet}$. In the presence of molecular oxygen, peroxyls $ROO^{\bullet}$ can be created. The hydrogen abstraction from another RH by $ROO^{\bullet}$ leads to ROOH and $R^{\bullet}$ formation. ROOH can be also created "directly" from RH during reaction with $^1O_2$ via an 'ene' reaction. If transition metals, such as Fe^{2+}, Mn^{2+}, Cu^{+}, or Zn^{+}, and reducing agents are in proximity to ROOH, reduction of ROOH leads to the creation of alkoxyl radicals $RO^{\bullet}$ [43].

The recombination of peroxyls $ROO^{\bullet}$ results in the formation of unstable high-energetic tetroxide ROOOOR, which is decomposed either to ground-state carbonyl, $^1O_2$, and organic hydroxide ROH, or to triplet excited carbonyl $^3R{=}O^*$, molecular oxygen, and ROH. Cyclization of $ROO^{\bullet}$ or cycloaddition of $^1O_2$ to polyunsaturated fatty acids or amino acids lead to the creation of another high-energetic intermediate, 1,2-dioxetane ROOR, which decomposes to $^3R{=}O^*$ and R=O [48].

Excited triplet carbonyls $^3R{=}O^*$ can relax to the ground state and emit light in the spectrum region 350 – 550 nm. In the presence of natural chromophores, such as tetrapyrroles (porphyrin, bilirubin), flavins (FMN, RAD), pyridine nucleotides (NADH, NADPH), melanin, urocanic acid, or pterins, excitation energy can be transferred from $^3R{=}O^*$ to the chromophore. As a consequence of the triplet–singlet or triplet–triplet energy transfer, singlet ($^1C^*$) or triplet excited ($^3C^*$) chromophores are formed. During their radiative transition to the ground state, they emit photons in the range 550 – 750 nm ($^1C^*$) or 750 – 1000 nm ($^3C^*$). For example, excited chlorophylls emit in the red part of the spectrum (670 – 740 nm) [49]. In aerobic conditions, the triplet–singlet energy transfer from $^3R{=}O^*$ and $^3C^*$ to molecular oxygen causes the formation of $^1O_2$. Its transition to the ground triplet state is accompanied by monomol photon emission at 1270 nm. A collision of two $^1O_2$ results in dimol photon emission at 634 and 703 nm. However, not all emitters are created with the same probability.

For example, the formation of $^3R{=}O^*$ is lower by 3 – 4 orders of magnitude than the generation of $^1O_2$ (3 – 14 %) during recombination of two $ROO^{\bullet}$ [43]. However, measurement of BAL is focused on the near UV and visible part of the spectrum because BAL intensity in the near infra-red region is comparable with photon emission caused by thermal excitation (Fig. 1-A). In general, BAL generation stems from oxidation reactions of the ROS with practically all types of biomolecules, such as lipids, proteins, or DNA (Fig. 1-B).

3. The BAL signal enhancement strategies

Here we review several biophysical approaches that could lead to an increase of the intensity of BAL by modulating the rate of processes across the whole chain of reactions leading to BAL: from the production of free radicals to radiative transitions of the electronically excited species.

3.1 Application of the magnetic fields

The most important possible biophysical mechanism involved in magnetic field modifying effects on biological responses to UV radiation and other oxidizing agents is the "radical-pair mechanism" [50]. Based on this mechanism, the low (below approximately 1 mT) and high field magnetic field can affect specific types of chemical reactions, which involve pair of radical molecules, by generally increasing or decreasing the concentration of free radicals in low and high fields, respectively. The low field effect (LFE) could explain the effects reported at 100 μT. Experimental studies have shown that the radical-pair mechanism is involved not only in cell-free biochemical systems but also has bioeffects in cells. For example, some studies have shown that the 50-Hz magnetic fields of approximately 100 μT have been able to alter the biological responses to ultraviolet (UV) radiation in yeast cells [51] and in mouse skin [52, 53]. Also, several other studies of biological samples treated with physical or chemical agents and exposed to a magnetic field indicate a similar radical-pair mechanism. Therefore, considering the ability of a small-magnitude LFE to generate a high radical level, LFE potentially has multiple effects on biological functions. In a normal cell, a crucial balance exists between the generation and elimination of radicals. If any external or internal agent disturbs this balance, the oxidative stress phenomenon will occur. Because the initial outcome of LFE exposure is generation of high radical levels, the oxidative stress is not unexpected and has meaningful effects on biological functions [54] and can also affect BAL intensity [55, 56].

3.2 Application of electric fields

3.2.1. Pulsed electric field

Pulsed electric field has been used for a long time to generate electroporation or electropermeabilization, with potential biomedical applications leveraging the delivery of various molecules such as exogenous genetic material and proteins into cells [57]. The permeability of the eukaryotic (human, animal, plant) cell membrane could be transiently increased by applying monopolar electric pulses or polarity alternating (bipolar) pulses (Fig. 2) [58]. It has also been shown that by reducing the duration of the applied electric pulses, some vital organelles such as mitochondria can be temporarily more permeable.

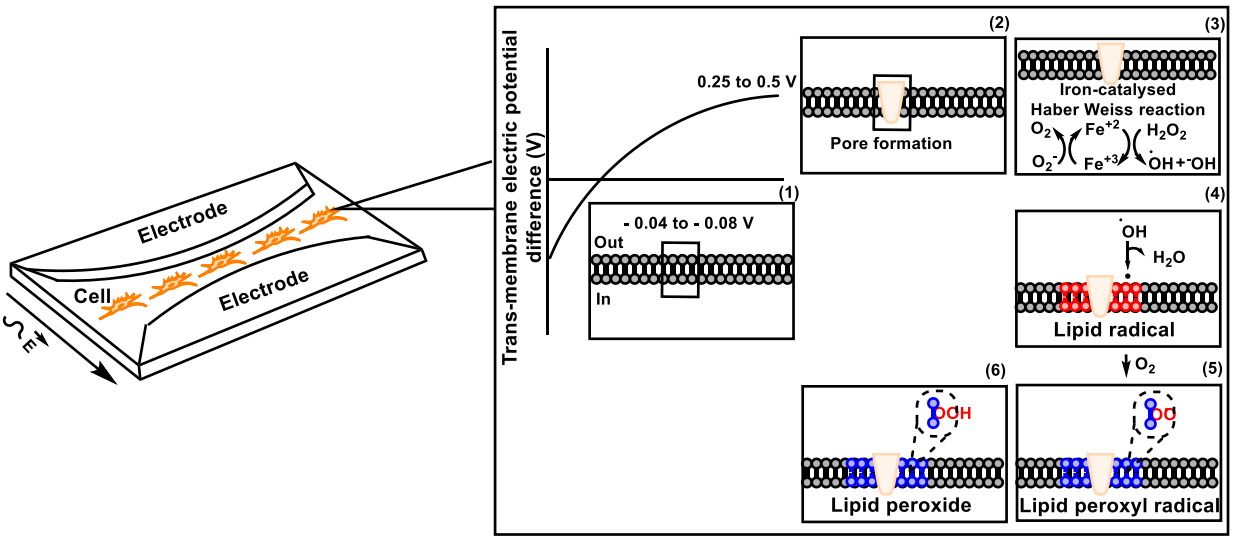

Fig 2. Molecular mechanism of lipid peroxidation and ROS generation in the presence of a pulsed electric field. Increasing the trans-membrane potential (1) caused the temporary formation of the pore (2). Generated Hydroxyl radical near the pore (3) can produce lipid radical (4), and such a radical eventually can generate the lipid peroxyl radical (5) and lipid peroxide (6) in the presence of molecular oxygen as BAL generating source.

In theory, electric field can directly or indirectly generate ROS. Direct generation is owing to reduction-oxidation (redox) reactions of the molecules at the electrode-electrolyte interface, when voltage is applied and exceeds a certain electrochemical threshold, which is almost always the case for intense electric pulses [59]. Indirect ROS generation by an electric field could also occur from electric-field-induced

cellular stress (permeabilization of membranes, leakage of ions) [60]. There are experimental works that support both the direct and indirect regime of ROS generation [61, 62]. Several works employing direct physical contact of electrodes with a biological sample have shown that pulsed electric fields cause oxidation in bio(molecular) systems. Interestingly, increased oxidation of biomolecules has also been found after delivery of intense electric pulses without contact through the antenna [63]. Furthermore, electric pulses have been demonstrated to induce cellular stress and biological production of ROS [62].

Table 1. The oxidation effect of short intense electric pulses

Cell type	Pulsing buffer	Cell/ml concentration	Signal time interval (ns)	Electric field strength (kV.cm^{-1})	Voltage (V)	Distance between electrodes or gap size (cm)	Signal enhancement mechanism	Ref
WTT CHO	(A): sucrose, potassium phosphate $MgCl_2$; (B): buffer A treated with Chelex-100 resin; (C): sucrose, potassium phosphate; (D): buffer C treated with Chelex-100 resin; (E): sucrose, potassium phosphate,$MgCl_2$, 69 mM KCI	$4 \cdot 10^8$	10^5	1.4	Not-specified	Not-specified	Chemiluminescence: Metal-ion- catalyzed Haber-Weiss reaction	[62]
K562	RPMI 1640 with 10% fetal bovine serum	$1.25 \cdot 10^6$	Not-specified	1.1	300	0.4	Chemiluminescence: Lipid peroxidation and generation of singlet oxygen and excited triplet carbonyl	[67]
PIEC	RPMI 1640 with 10% fetal bovine serum	$1.1 \cdot 10^6$	100	5, 10 and 20	60000	0.2	Chemiluminescence: ROS generation	[68]

The generated ROS are able to oxidize cellular biomolecules (lipids, proteins, or DNA) and very likely initiate reactions leading to the formation of electron excited states and eventually to BAL [26, 64-66]. The factors influencing the effects of pulsed electric field on cells and on BAL include the cell type and cell concentration, time duration, pulsing buffer conductivity and osmolarity, temperature, signal time interval, electric field strength, distance between electrodes or gap size, and electrode material. The oxidation effects of short intense electric pulses on BAL signal enhancement are summarized in Table 1.

Although it has not yet been possible to visualize all the mechanisms involved in the electroporation process in detail, evidence from various studies has shown that the localized generated ROS in the permeabilized part of the plasma membrane causes the direct or indirect production of further ROS.

3.2.2. Electrochemiluminescence

The direct generation of ROS and consequent BAL might be conceptually very similar to the phenomenon of electrochemiluminescence (synonymous with electrogenerated chemiluminescence) (ECL) [69, 70], which is a widely explored research topic (Fig. 3).

Definition box

In electrochemiluminescence (ECL), electrogenerated species undergo electron-transfer reactions (in the vicinity of a working electrode) to form excited species, and these species relax to the ground state with the release of energy in the form of light. Fundamental research on ECL since the mid-1960s with smart compounding of electrochemistry with chemiluminescence has revealed that ECL is a powerful potential diagnosis tool over optical methods [71]. First, because ECL does not require any external light as a triggering source, this not only simplifies ECL devices but also eliminates the background noise that originates from internal luminous impurities and scattered light. Second, ECL responses aren't affected by luminous position changes because the ECL emission occurs close to the surface of the electrode; hence ECL shows preferable control toward the position. Third, due to the relationship between the ECL luminophore and co-reactants, ECL has an excellent specificity. Because the luminophore excited states can be operated by using an alternative applied potential, ECL has satisfactory selectivity. Finally, ECL reproducibility is related to its controllability over time. Considering the high sensitivity, low background, and excellent controllability of ECL signals, ECL has attracted much attention in various fields of analysis including bioassay (DNA sensing, enzymatic detection), clinical diagnostics, drug screening, biodefense [72], environmental monitoring (such as food and water safety), and other application such as solid-state electrochemiluminescence sensor [73, 74]. Furthermore, the combination of ECL with other analytical techniques such as capillary electrophoresis, flow injection analysis, high-performance liquid chromatography, and micro total analysis has brought good results [75-80].

However, in contrast to typical electrochemiluminescent systems, in which donor and acceptor molecules are selected by design, endogenous ECL might involve a plethora of endogenously present donor and acceptor molecules and complex reaction dynamics taking place.

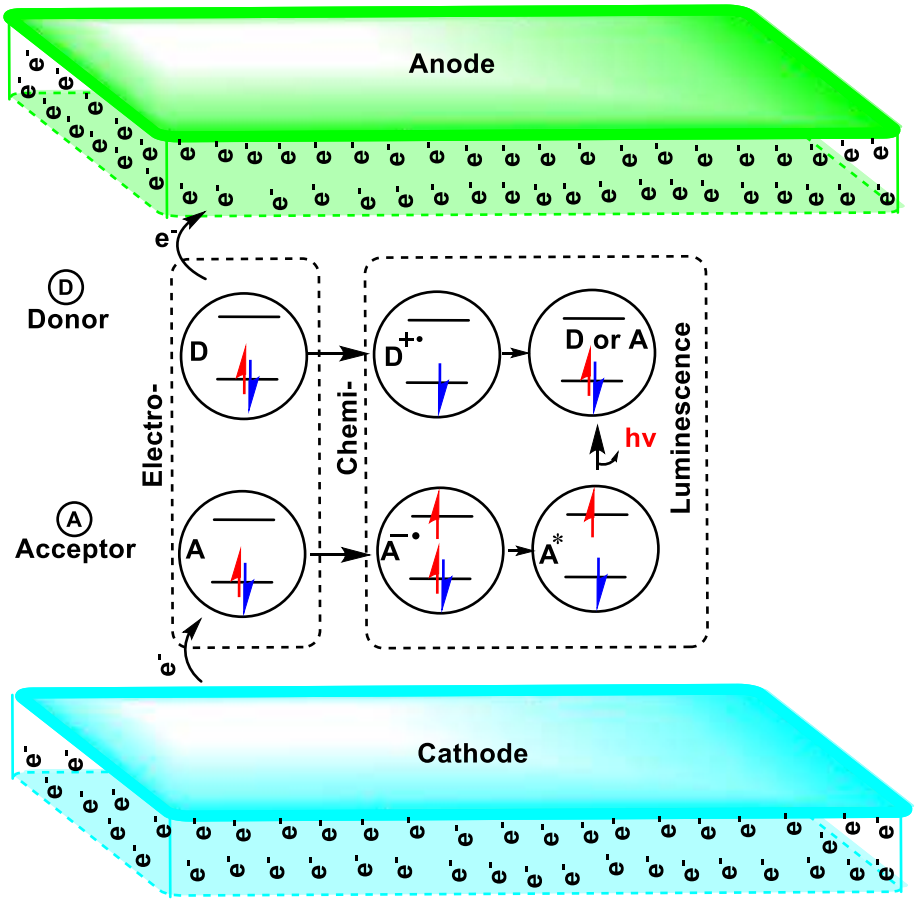

Fig 3. Schematic diagrams showing the general principles of electrochemiluminescence. Electron is transferred from the cathode to electron acceptor to form a radical. Electron donor transfers an electron to the anode and becomes a radical. The acceptor-based radical transfers a ground state electron to the donor radical and electron excited state of an acceptor is generated. The excited state can decay radiatively to generate luminescence.

3.3. Application of nanoparticles into the cell

The size similarity between nanoparticles and various intracellular components not only facilitates the delivery of particles into the cell [81], but can also cause subtle interactions with various intracellular molecules and organelles [82, 83]. Therefore, we consider nanoscale particles as a promising tool for manipulating processes leading to BAL, potentially leading to BAL signal enhancement.

Here we review two main classes of mechanisms for the prospective BAL signal enhancement by nanoscale particles, then a combination of electric field and nanoparticles, and finally the current evidence of BAL enhancement using nanoparticles in cells.

3.3.1. Nanoparticle-mediated increase of ROS production

Nanoscale particles contribute to the increase of BAL intensity via ROS production. Increased formation of reactive groups on the nanoparticle (NP) surface with decreasing particle size [84-86], active redox cycling on the surface of the NPs [87, 88] and the interaction of NPs with different intracellular components [89, 90] are probably three main possibilities of how metal NPs could affect the BAL through ROS production. Some studies have shown that gold nanoparticles (AuNPs) are able to promote oxidation of biomolecules within the cells [2, 91]. How AuNPs can enhance the BAL signal through the production of electron-excited species is summarized in Figure 4. Interaction of the free radicals ($CO_3^{\bullet-}$ and $O_2^{\bullet-}$) and AuNP results in the formation of emissive intermediate complex (Gold (I)), carbon dioxide dimers, and singlet oxygen molecular pairs (Fig. 4-A.). [92]. These intermediates species relax to their ground state via radiative relaxation.

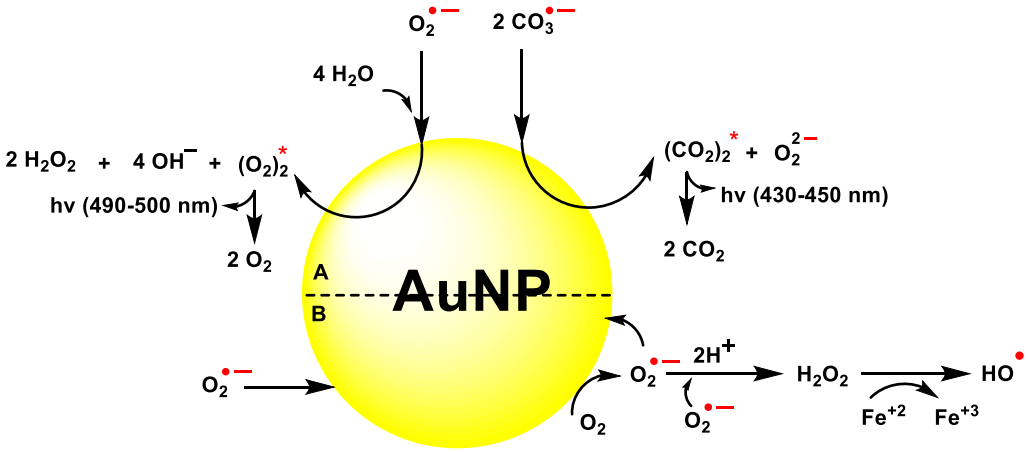

Fig 4. Formation of emissive intermediate gold(I) complex. AuNP interaction with $CO_3^{\bullet-}$ and $O_2^{\bullet-}$ caused formation of excited molecules on AuNP surface [92].

Also, during the mitochondrial metabolism, this organelle produces various free radicals (mainly superoxide anion radical) [93]. In the presence of AuNPs, it is

possible to form a complex between AuNPs and superoxide radicals. After formation of this complex, the superoxide radical acts as an electron donor and transfers its $2\pi^*$ electron to the gold conducting bond (Fig. 4-B.). Mitochondria is the main molecular oxygen consumption organelle within the cell. By the arrival of the molecular triplet oxygen to the AuNP surface, this molecule is able to receive the one electron from the conducting electron band and finally convert to another superoxide radical. This superoxide radical can go to two distinct routes: Combine with another superoxide radical and form hydrogen peroxide (by action of mitochondrial superoxide dismutase (SOD) enzyme) or return to the surface of the AuNP. Because the absorption spectra of the Au surface plasmon bond remain unchanged upon adsorption of the radicals, the electron density at the surface remains essentially unchanged. The mechanism is likely based on the exchange interactions between the unpaired electrons of radicals and conduction-band electrons of the metal. The superoxide radical can convert to singlet oxygen in two processes. First, it can act as a donor and transfer one of its $2\pi^*$ electron to the conducting bond. Second, this molecule can be converted to the singlet oxygen via spin conversion relaxation. (Note: singlet oxygen has the same electron spin on its $2\pi^*$) [93].

3.3.2. Nanoparticle-mediated manipulation of the radiative yield of electron excited species

From a chemical point of view, owing to the low efficiency of reactions that generate BAL, several strategies have been developed to enhance the BAL intensity. In this chapter, we do not consider fluorescent molecules (such as fluorescein [94] or DBAS (9,10-Dibromoanthracene-2-sulfonic Acid) [95]), which can accept electron excitation energy from otherwise weakly emitting endogenously generated electron excited states and emit the energy in the form of a photon with high efficiency. Rather, we focus on more “physical”, material science-based and nanoscale approaches for BAL enhancement.

One such physical approach is metal-enhanced chemiluminescence, which is another novel strategy in which plasmonic nanoparticles such as gold, silver, and platinum are used for the enhancement of chemiluminescence [96-98]. In metal-enhanced chemiluminescence, excitation of the metal surface plasmons by electronically excited molecules of chemiluminescent species can enhance the chemiluminescence intensity. Two mechanisms have been proposed for the enhancement effect of plasmonic nanoparticles: (1) increasing the local electromagnetic field [99] and (2) interaction of the plasmons with chemiluminescence species [97, 98].

This mechanism for the BAL signal enhancement in the presence of AuNPs is based on the plasmonic antenna effects of the AuNPs. The metal nanoparticles have been shown to modulate and to potentially enhance the radiative yield of electron-excited molecules [100]. Triplet excited carbonyls, one of the primary excited states produced chemically in the process preceding BAL emission, have very low radiative yield because of quenching by molecular oxygen [4]. Hence, enhancing radiative yield

of triplet excited state due to AuNPs antenna effects [101] could be another potential mechanism for the BAL signal enhancement in the presence of AuNPs.

Quantum dots (QDs) are zero-dimensional nanoparticles that have been used as potential alternatives to chemiluminescence emitters owing to their excellent electronic and optical properties [102]. There are three possible mechanisms for QDs as chemiluminescence enhancers: (1) modulators of the radiative relaxation rate of chemically generated excitons after direct electron- and hole-injection, (2) acting as the catalysts or energy acceptor, and (3) acting as emitter species after chemiluminescence resonance energy transfer (CRET).

3.3.3. Combination of electric field and nanoparticles

Since the first report of ECL on silicon QDs, ECL enhancement using other alloyed or core−shell structure QDs including CdSe, CdS, CdTe, ZnS, and Ag_2Se has also been reported [104-110]. Furthermore, polymer dots, carbon nanodots, graphite like carbon nitride, upconversion nanoparticles, and noble metal nanoclusters such as Au [110, 111], Ag [112-115], Cu [116-118], Pd [119], Pt [117, 120-123] are other ECL emitters. In this section we discuss metal nanoparticles as a new ECL component.

Because of the unique properties of metal nanoclusters, including high electrical conductivity, good water solubility, and stability, they are ECL luminophores, quenchers, and catalysts [125-127]. For example, the discrete electronic energy level (due to the comparable size to the Fermi wavelength of electrons) and direct electron transition of gold nanoclusters (GNCs) caused their use as new ECL nanomaterial. However, because of the low ECL efficiency of GNCs, increasing the ECL efficiency of GNCs by decreasing the nonradiative transition and complications from mass transport between the reactants has been investigated [103, 128]. Functionalization of gold nanocluster with luminol resulted in up to 100-fold enhancement in ECL intensity for alkaline phosphatase detection [129]. Hybrid gold nanocluster (AuNCs/graphene) showed a low detection limit (0.1 fM to 0.1 nM) of pentacholophenol [130]. A AuNPs-modified ECL electrode showed high sensitivity and good stability in immunoassays and DNA assays [131-133]. Although enhancement of the ECL signals of cell with a AuNPs-modified electrode is mainly attributed to its high surface area, the powerful electrons transfer properties of AuNPs caused sensitivity enhancements of 10- and 6-fold for detection of some biological material such as bovine serum albumin (BSA) and immunoglobulin G (IgG) [134]. Also, the catalytic effect of AuNPs on the redox of ECL-emitting species is considered as another reason for the enhancement of the ECL intensity in the presence of AuNPs. By using the gold nanorods, the intensities of ECL peaks were enhanced approximately 2 – 10-fold on a gold-nanorod-modified gold electrode [135]. AuNP also shows catalytic activity for the generation of ROS. Actually, AuNP surface can generate the ROS and these species are ultimately able to produce ECL by combination with ECL reagent (Fig. 5) [136].

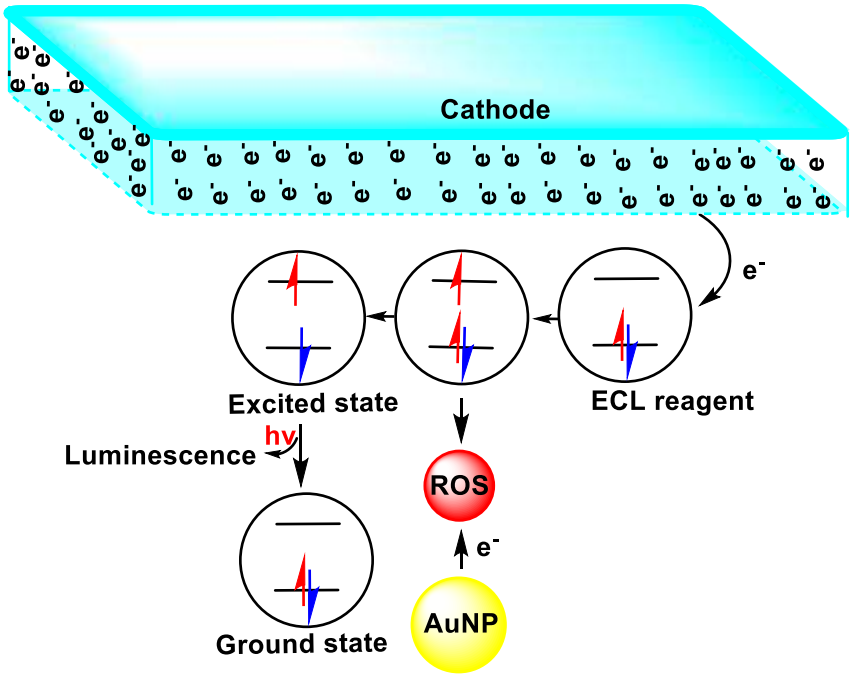

Fig. 5. AuNP surface can generate ROS and these species are ultimately able to produce ECL by combination with ECL reagent. ECL reagent accepts an electron from cathode. Subsequently, ROS gains the low-energy electron from the intermediate ECL reagent and convert it to the excited state. The final excited species radiatively relax and emit a photon.

3.3.4. Nanoparticle-mediated BAL enhancement - evidence from cells

In this section, we briefly outline recent reports in which nanoparticle-mediated BAL enhancement has been demonstrated.

BAL signal enhancement by metal nanoparticles under *in vitro* conditions has revealed a few valuable endpoints related to the importance of manipulating the ROS as the main source of BAL. An exponential increase in the BAL signal was observed when prostate cancer cells (10^5 cell·ml^{-1}) were treated with a 10 nM silver nanoparticle (AgNPs) solution (6 – 20 nm in diameter). The main reason for such an enhancement is related to the increase in the number of ROS, especially singlet oxygen in the presence of AgNPs [137]. Similarly, the treatment of 5 mm thick disks of sweet potato roots with 1 nM AgNPs (8-15 nm in diameter) resulted in BAL signal enhancement through two proposed mechanisms: ROS generation and energy resonance transfer [138].

Given that mitochondria are the most important source of BAL (approximately 90% of ROS are produced by mitochondria [139]), it is expected that the amount of generated BAL can be increased by affecting this vital organelle. F or example, in a

recent study, we showed that mitochondrial-targeted delivery by liposomal gold nanoparticles nanocarriers could significantly increase the intensity of BAL in a completely safe manner (Fig. 6) [140].

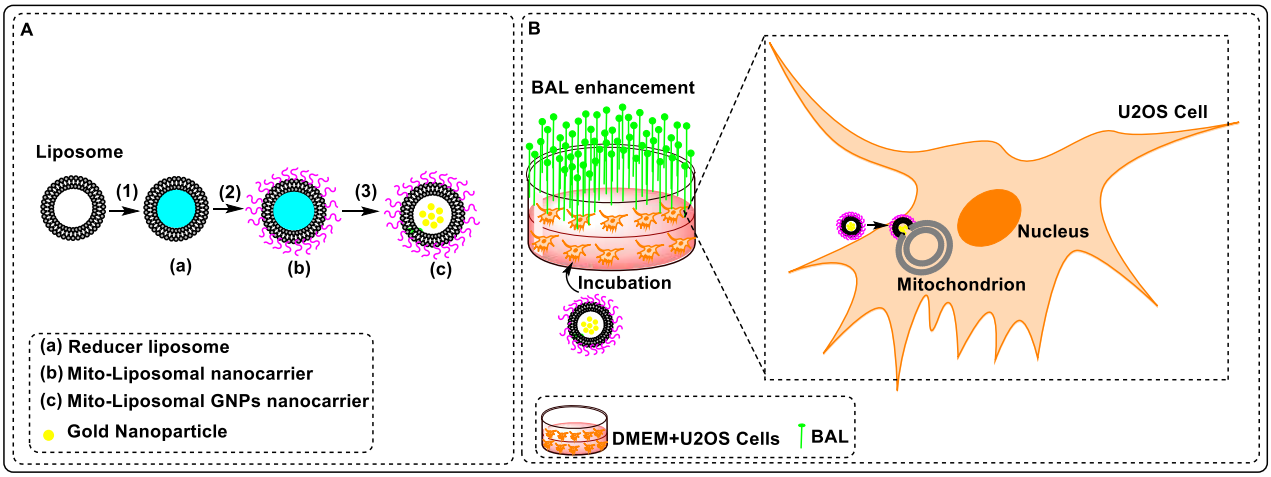

Figure 6. Mito-liposomal gold nanoparticles nanocarriers for the enhancement of the BAL signal. A) Functionalization of reducer liposome (1) with mitochondrial penetrating peptides (2) produced the Mito-liposomal GNPs nanocarrier (3). B) Incubated Mito-liposomal GNP nanocarriers can enhanced the UPE of U2OS cells by affecting the mitochondria

4. Conclusion

Biological autoluminescence detection is a potentially important non-invasive diagnostic method. However, owing to the ultraweak intensity of BAL signals, it is necessary to enhance it to be able to detect an unknown biological condition. Here, we reviewed novel approaches for the enhancement of the BAL signal by selected biophysical means by focusing on the application of electric and magnetic fields and metal nanoscale particles.

Acknowledgement

MC and PV thank the Czech Science Foundation project no. 20-06873X for the support and they are also participating in the bilateral exchange project between the Czech and Slovak Academy of Sciences, no. SAV-18-11. The Science Editorium is acknowledged for the language check.

References

1. Burgos, R.C.R., et al., *Ultra-weak photon emission as a dynamic tool for monitoring oxidative stress metabolism.* Scientific reports, 2017. **7**(1): p. 1229.
2. Wang, P., et al., *Interaction of gold nanoparticles with proteins and cells.* Science and technology of advanced materials, 2015. **16**(3): p. 034610.
3. Gabe, Y., O. Osanai, and Y. Takema, *The relationship between skin aging and steady state ultraweak photon emission as an indicator of skin oxidative stress in vivo.* Skin Research and Technology, 2014. **20**(3): p. 315-321.
4. Cilento, G. and W. Adam, *From free radicals to electronically excited species.* Free Radical Biology and Medicine, 1995. **19**(1): p. 103-114.
5. Van Wijk, R., *Introduction: biophoton emission, stress and disease.* Cellular and Molecular Life Sciences, 1992. **48**(11): p. 1029-1030.
6. Nakamura, K. and M. Hiramatsu, *Ultra-weak photon emission from human hand: influence of temperature and oxygen concentration on emission.* Journal of Photochemistry and photobiology B: Biology, 2005. **80**(2): p. 156-160.
7. Okano, Y., H. Masaki, and H. Sakurai, *Pentosidine in advanced glycation end-products (AGEs) during UVA irradiation generates active oxygen species and impairs human dermal fibroblasts.* Journal of dermatological science, 2001. **27**: p. 11-18.
8. Rastogi, A. and P. Pospísil, *Spontaneous ultraweak photon emission imaging of oxidative metabolic processes in human skin: effect of molecular oxygen and antioxidant defense system.* Journal of Biomedical Optics, 2011. **16**(9): p. 096005.
9. Cifra, M. and P. Pospíšil, *Ultra-weak photon emission from biological samples: definition, mechanisms, properties, detection and applications.* Journal of Photochemistry and Photobiology B: Biology, 2014. **139**: p. 2-10.
10. Cadenas, E. and H. Sies, *[26] Low-level chemiluminescence as an indicator of singlet molecular oxygen in biological systems*, in *Methods in enzymology*. 1984, Elsevier. p. 221-231.
11. Boveris, A., et al., *Organ chemiluminescence: noninvasive assay for oxidative radical reactions.* Proceedings of the National Academy of Sciences, 1980. **77**(1): p. 347-351.
12. Nakano, M., *Low-level chemiluminescence during lipid peroxidations and enzymatic reactions.* Journal of bioluminescence and chemiluminescence, 1989. **4**(1): p. 231-240.
13. Beloussov, L.V., J.M. Opitz, and S.F. Gilbert, *Life of Alexander G. Gurwitsch and his relevant contribution to the theory of morphogenetic fields.* International Journal of Developmental Biology, 2004. **41**(6): p. 771-777.
14. Gurwitsch, A., *A historical review of the problem of mitogenetic radiation.* Experientia, 1988. **44**(7): p. 545-550.
15. Volodyaev, I. and L.V. Beloussov, *Revisiting the mitogenetic effect of ultra-weak photon emission.* Frontiers in physiology, 2015. **6**: p. 241.

16. Coil, L., *Further measurement of the biolumine scence of the seedings.* Experientia, 1995. **11**: p. 479-481.

17. Colli, L. and U. Facchini, *Light emission by germinating plants.* Il Nuovo Cimento (1943-1954), 1954. **12**(1): p. 150-153.

18. Scholkmann, F., et al., *Spatio-temporal dynamics of spontaneous ultra-weak photon emission (autoluminescence) from human hands measured with an EMCCD camera: Dependence on time of day, date and individual subject.* Matters, 2018. **4**(3): p. e201803000001.

19. Popp, F.-A., *Quantum phenomena of biological systems as documented by biophotonics*, in *Quo Vadis Quantum Mechanics?* 2005, Springer. p. 371-396.

20. Bókkon, I., et al., *Endogenous spontaneous ultraweak photon emission in the formation of eye-specific retinogeniculate projections before birth.* Reviews in the Neurosciences, 2016. **27**(4): p. 411-419.

21. Takeda, M., et al., *Biophoton detection as a novel technique for cancer imaging.* Cancer Sci, 2004. **95**(8): p. 656-61.

22. Takeda, M., et al., *A novel method of assessing carcinoma cell proliferation by biophoton emission.* Cancer Lett, 1998. **127**(1-2): p. 155-60.

23. Agarwal, A., A. Hamada, and S.C. Esteves, *Insight into oxidative stress in varicocele-associated male infertility: part 1.* Nature Reviews Urology, 2012. **9**(12): p. 678-690.

24. Oberley, L.W. and D.R. Spitz, *[61] Assay of superoxide dismutase activity in tumor tissue.* Methods in enzymology, 1984. **105**: p. 457-464.

25. Khabiri, F., et al., *Non-invasive monitoring of oxidative skin stress by ultraweak photon emission (UPE)-measurement. I: mechanisms of UPE of biological materials.* Skin Research and Technology, 2008. **14**(1): p. 103-111.

26. Ou-Yang, H., et al., *A chemiluminescence study of UVA-induced oxidative stress in human skin in vivo.* Journal of investigative dermatology, 2004. **122**(4): p. 1020-1029.

27. Prasad, A. and P. Pospísil, *Ultraweak photon emission induced by visible light and ultraviolet A radiation via photoactivated skin chromophores: in vivo charge coupled device imaging.* Journal of biomedical optics, 2012. **17**(8): p. 085004.

28. Rastogi, A. and P. Pospíšil, *Ultra-weak photon emission as a non-invasive tool for monitoring of oxidative processes in the epidermal cells of human skin: comparative study on the dorsal and the palm side of the hand.* Skin research and technology, 2010. **16**(3): p. 365-370.

29. Sauermann, G., et al., *Ultraweak photon emission of human skin in vivo: influence of topically applied antioxidants on human skin*, in *Methods in enzymology*. 1999, Elsevier. p. 419-428.

30. Salari V, Valian H, Bassereh H, Bókkon I, Barkhordari A. *Ultraweak photon emission in the brain. Journal of integrative neuroscience*. 2015;14(03):419-29.

31. Bókkon I, Scholkmann F, Salari V, Császár N, Kapócs G. *Endogenous spontaneous ultraweak photon emission in the formation of eye-specific retinogeniculate projections before birth*. Reviews in the Neurosciences. 2016;27(4):411-9.

33. Esmaeilpour T, Fereydouni E, Dehghani F, Bókkon I, Panjehshahin M-R, Császár-Nagy N, et al. *An experimental investigation of ultraweak photon emission from adult murine neural stem cells*. Scientific reports. 2020;10(1):1-13.

33. Iyozumi, H., K. Kato, and T. Makino, *Spectral Shift of Ultraweak Photon Emission from Sweet Potato During a Defense Response*¶. Photochemistry and photobiology, 2002. **75**(3): p. 322-325.

34. Ohya, T., et al., *Biophoton emission due to drought injury in red beans: possibility of early detection of drought injury.* Japanese journal of applied physics, 2002. **41**(7R): p. 4766.

35. Ohya, T., et al., *Early detection of salt stress damage by biophotons in red bean seedling.* Japanese Journal of Applied Physics, 2000. **39**(6R): p. 3696.

36. Inagaki, H., et al., *Difference in ultraweak photon emissions between sulfonylurea-resistant and sulfonylurea-susceptible biotypes of Scirpus juncoides following the application of a sulfonylurea herbicide.* Weed biology and management, 2008. **8**(2): p. 78-84.

37. Usui, S., M. Tada, and M. Kobayashi, *Non-invasive visualization of physiological changes of insects during metamorphosis based on biophoton emission imaging.* Scientific reports, 2019. **9**(1): p. 1-7.

38. Cifra, M. and P. Pospisil, *Ultra-weak photon emission from biological samples: definition, mechanisms, properties, detection and applications.* J Photochem Photobiol B, 2014. **139**: p. 2-10.

39. Pospisil, P., A. Prasad, and M. Rac, *Role of reactive oxygen species in ultra-weak photon emission in biological systems.* J Photochem Photobiol B, 2014. **139**: p. 11-23.

40. *Non-equilibrium and coherent systems in biology, biophysics and biotechnology. 2nd International Alexander Gurwitsch Conference. Moscow, Russia, September 6-10, 1999. Abstracts.* Riv Biol, 2000. **93**(1): p. 103-61.

41. Popp, F.A., K. Li, and Q. Gu, *Recent advances in biophoton research and its applications*. 1992: World Scientific.

42. Beloussov, L.V., V.L. Voeikov, and V.S. Martynyuk, *Biophotonics and coherent systems in biology*. 2007: Springer Science & Business Media.

43. Pospíšil, P., A. Prasad, and M. Rác, *Mechanism of the formation of electronically excited species by oxidative metabolic processes: role of reactive oxygen species.* Biomolecules, 2019. **9**(7): p. 258.

44. Auchère, F. and F. Rusnak, *What is the ultimate fate of superoxide anion in vivo?* JBIC Journal of Biological Inorganic Chemistry, 2002. **7**(6): p. 664-667.

45. Bielski, B.H., et al., *Reactivity of HO2/O− 2 radicals in aqueous solution.* Journal of physical and chemical reference data, 1985. **14**(4): p. 1041-1100.

46. Kale, R., et al., *Amino acid oxidation of the D1 and D2 proteins by oxygen radicals during photoinhibition of Photosystem II.* Proceedings of the National Academy of Sciences, 2017. **114**(11): p. 2988-2993.

47. Prousek, J., *Fenton chemistry in biology and medicine.* Pure and applied chemistry, 2007. **79**(12): p. 2325-2338.

48. Pospíšil, P., A. Prasad, and M. Rác, *Role of reactive oxygen species in ultra-weak photon emission in biological systems.* Journal of Photochemistry and Photobiology B: Biology, 2014. **139**: p. 11-23.

49. Hideg, E. and H. Inaba, *Biophoton emission (ultraweak photoemission) from dark adapted spinach chloroplasts.* Photochemistry and photobiology, 1991. **53**(1): p. 137-142.

50. Barnes, F.S. and B. Greenebaum, *The effects of weak magnetic fields on radical pairs.* Bioelectromagnetics, 2015. **36**(1): p. 45-54.

51. Markkanen, A., et al., *Effects of 50 Hz magnetic field on cell cycle kinetics and the colony forming ability of budding yeast exposed to ultraviolet radiation.* Bioelectromagnetics: Journal of the Bioelectromagnetics Society, The Society for Physical Regulation in Biology and Medicine, The European Bioelectromagnetics Association, 2001. **22**(5): p. 345-350.

52. Kumlin, T., et al., *p53-independent apoptosis in UV-irradiated mouse skin: possible inhibition by 50 Hz magnetic fields.* Radiation and environmental biophysics, 2002. **41**(2): p. 155-158.

53. Kumlin, T., et al., *Effects of 50 Hz magnetic fields on UV-induced skin tumourigenesis in ODC-transgenic and non-transgenic mice.* International journal of radiation biology, 1998. **73**(1): p. 113-121.

54. Pizzino, G., et al., *Oxidative stress: harms and benefits for human health.* Oxidative medicine and cellular longevity, 2017. **2017**.

55. Bereta, M., et al., *Biological autoluminescence as a noninvasive monitoring tool for chemical and physical modulation of oxidation in yeast cell culture.* Scientific reports, 2021. **11**(1): p. 1-11.

56. Cheun, B., et al., *Biophoton emission of MDCK cell with hydrogen peroxide and 60 Hz AC magnetic field.* Journal of environmental biology, 2007. **28**(4): p. 735-740.

57. Rols, M.-P., *Electropermeabilization, a physical method for the delivery of therapeutic molecules into cells.* Biochimica et Biophysica Acta (BBA)-Biomembranes, 2006. **1758**(3): p. 423-428.

58. Sweeney, D.C., T.A. Douglas, and R.V. Davalos, *Characterization of cell membrane permeability in vitro part II: computational model of electroporation-mediated membrane transport.* Technology in cancer research & treatment, 2018. **17**: p. 1533033818792490.

59. Pataro, G., G. Donsì, and G. Ferrari, *Modeling of Electrochemical Reactions During Pulsed Electric Field Treatment*, in *Handbook of Electroporation*, D. Miklavcic, Editor. 2016, Springer International Publishing: Cham. p. 1-30.

60. Pakhomova, O.N., et al., *Oxidative effects of nanosecond pulsed electric field exposure in cells and cell-free media.* Archives of biochemistry and biophysics, 2012. **527**(1): p. 55-64.

61. Teissie, J., *Involvement of reactive oxygen species in membrane electropermeabilization.* Handbook of Electroporation, 2017: p. 1-15.

62. Gabriel, B. and J. Teissie, *Generation of reactive-oxygen species induced by electropermeabilization of Chinese hamster ovary cells and their consequence on cell viability.* European Journal of Biochemistry, 1994. **223**(1): p. 25-33.

63. Breton Marie, A.C., René Vezinet, LLuis M. Mir, *Chemical Study of the Effects of UltraWide Band and Narrow Band Signals on Membranes*, in *Proceedings of BIOEM2016*. 2016. p. 17–19.

64. Barnard, M.L., et al., *Protein and amino acid oxidation is associated with increased chemiluminescence.* Archives of biochemistry and biophysics, 1993. **300**(2): p. 651-656.

65. Ou-Yang, H., G. Stamatas, and N. Kollias, *Dermal contributions to UVA-induced oxidative stress in skin.* Photodermatology, photoimmunology & photomedicine, 2009. **25**(2): p. 65-70.

66. Sander, C.S., et al., *Photoaging is associated with protein oxidation in human skin in vivo.* Journal of Investigative Dermatology, 2002. **118**(4): p. 618-625.

67. Maccarrone, M., N. Rosato, and A.F. Agrò, *Electroporation enhances cell membrane peroxidation and luminescence.* Biochemical and biophysical research communications, 1995. **206**(1): p. 238-245.

68. Zhang, Y., et al., *Nanosecond pulsed electric fields promoting the proliferation of porcine iliac endothelial cells: An in vitro study.* PloS one, 2018. **13**(5): p. e0196688.

69. Bard, A.J., et al., *Electrochemical methods: fundamentals and applications*. Vol. 2. 1980: wiley New York.

70. Bard, A.J., *Electrogenerated chemiluminescence*. 2004: CRC Press.

71. Bouffier, L. and N. Sojic, *Introduction and Overview of Electrogenerated Chemiluminescence.* 2019.

72. Bruno, J.G. and J.C. Cornette, *An Electrochemiluminescence Assay Based on the Interactionof Diaminotoluene Isomers with Gold (I) and Copper (II) Ions.* Microchemical journal, 1997. **56**(3): p. 305-314.

73. Kong, S.H., et al., *Light-Emitting Devices Based on Electrochemiluminescence: Comparison to Traditional Light-Emitting Electrochemical Cells.* ACS Photonics, 2017. **5**(2): p. 267-277.

74. Spehar-Délèze, A.-M., S. Almadaghi, and C.K. O'Sullivan, *Development of solid-state electrochemiluminescence (ECL) sensor based on Ru (bpy) 32+-encapsulated silica nanoparticles for the detection of biogenic polyamines.* Chemosensors, 2015. **3**(2): p. 178-189.

75. Rizwan, M., et al., *A highly sensitive and label-free electrochemiluminescence immunosensor for beta 2-microglobulin.* Analytical Methods, 2017. **9**(17): p. 2570-2577.

76. Inoue, Y., et al., *Sensitive detection of glycated albumin in human serum albumin using electrochemiluminescence.* Analytical chemistry, 2017. **89**(11): p. 5909-5915.

77. Roy, S., et al., *A novel, sensitive and label-free loop-mediated isothermal amplification detection method for nucleic acids using luminophore dyes.* Biosensors and Bioelectronics, 2016. **86**: p. 346-352.

78. Yao, J., et al., *Quantum dots: from fluorescence to chemiluminescence, bioluminescence, electrochemiluminescence, and electrochemistry.* Nanoscale, 2017. **9**(36): p. 13364-13383.

79. Cui, H., et al., *Analytical electrochemiluminescence*. 2016, Springer.

80. Bist, I., K. Bano, and J.F. Rusling, *Screening Genotoxicity Chemistry with Microfluidic Electrochemiluminescent Arrays.* Sensors, 2017. **17**(5): p. 1008.

81. Blanco, E., H. Shen, and M. Ferrari, *Principles of nanoparticle design for overcoming biological barriers to drug delivery.* Nat Biotech, 2015. **33**(9): p. 941-951.

82. Cai, K., et al., *Bio-nano interface: The impact of biological environment on nanomaterials and their delivery properties.* Journal of Controlled Release, 2017.

83. Nel, A.E., et al., *Understanding biophysicochemical interactions at the nano-bio interface.* Nat Mater, 2009. **8**(7): p. 543-557.

84. Fu, P.P., et al., *Mechanisms of nanotoxicity: generation of reactive oxygen species.* Journal of food and drug analysis, 2014. **22**(1): p. 64-75.

85. Xia, T., et al., *Comparison of the mechanism of toxicity of zinc oxide and cerium oxide nanoparticles based on dissolution and oxidative stress properties.* ACS nano, 2008. **2**(10): p. 2121-2134.

86. Nel, A., et al., *Toxic potential of materials at the nanolevel.* science, 2006. **311**(5761): p. 622-627.

87. Li, N., T. Xia, and A.E. Nel, *The role of oxidative stress in ambient particulate matter-induced lung diseases and its implications in the toxicity of engineered nanoparticles.* Free Radical Biology and Medicine, 2008. **44**(9): p. 1689-1699.

88. Huang, Y.-W., C.-h. Wu, and R.S. Aronstam, *Toxicity of transition metal oxide nanoparticles: recent insights from in vitro studies.* Materials, 2010. **3**(10): p. 4842-4859.

89. Risom, L., P. Møller, and S. Loft, *Oxidative stress-induced DNA damage by particulate air pollution.* Mutation Research/Fundamental and Molecular Mechanisms of Mutagenesis, 2005. **592**(1): p. 119-137.

90. Knaapen, A.M., et al., *Inhaled particles and lung cancer. Part A: Mechanisms.* International Journal of Cancer, 2004. **109**(6): p. 799-809.

91. Khan, H.A., et al., *Effect of gold nanoparticles on glutathione and malondialdehyde levels in liver, lung and heart of rats.* Saudi journal of biological sciences, 2012. **19**(4): p. 461-464.

92. Cui, H., Z.-F. Zhang, and M.-J. Shi, *Chemiluminescent reactions induced by gold nanoparticles.* The Journal of Physical Chemistry B, 2005. **109**(8): p. 3099-3103.

93. Razzaq, H., et al., *Interaction of gold nanoparticles with free radicals and their role in enhancing the scavenging activity of ascorbic acid.* Journal of Photochemistry and Photobiology B: Biology, 2016. **161**: p. 266-272.

94. White, E.H., et al., *Chemilunimescence of luminol: The chemcial reaction.* Journal of the American Chemical Society, 1964. **86**(5): p. 940-941.

95. Velosa, A.C., et al., *1, 3-diene probes for detection of triplet carbonyls in biological systems.* Chemical research in toxicology, 2007. **20**(8): p. 1162-1169.

96. Aslan, K. and C.D. Geddes, *Metal-enhanced chemiluminescence: advanced chemiluminescence concepts for the 21st century.* Chemical Society Reviews, 2009. **38**(9): p. 2556-2564.

97. Chowdhury, M.H., et al., *Metal-enhanced chemiluminescence.* Journal of fluorescence, 2006. **16**(3): p. 295-299.

98. Chowdhury, M.H., et al., *Metal-enhanced chemiluminescence: Radiating plasmons generated from chemically induced electronic excited states.* Applied physics letters, 2006. **88**(17): p. 173104.

99. Abel, B., et al., *Enhancement of the chemiluminescence response of enzymatic reactions by plasmonic surfaces for biosensing applications.* Nano biomedicine and engineering, 2015. **7**(3): p. 92.

100. Park, J.-E., J. Kim, and J.-M. Nam, *Emerging plasmonic nanostructures for controlling and enhancing photoluminescence.* Chemical science, 2017. **8**(7): p. 4696-4704.

101. Herrmann, J.F., et al., *Antenna-Enhanced Triplet-State Emission of Individual Mononuclear Ruthenium (II)-Bis-terpyridine Complexes Reveals Their Heterogeneous Photophysical Properties in the Solid State.* ACS Photonics, 2016. **3**(10): p. 1897-1906.

102. Chen, H., et al., *Quantum dots-enhanced chemiluminescence: mechanism and application.* Coordination Chemistry Reviews, 2014. **263**: p. 86-100.

103. Wang, T., et al., *Near-infrared electrogenerated chemiluminescence from aqueous soluble lipoic acid Au nanoclusters.* Journal of the American Chemical Society, 2016. **138**(20): p. 6380-6383.

104. Huan, J., et al., *Amplified solid-state electrochemiluminescence detection of cholesterol in near-infrared range based on CdTe quantum dots decorated multiwalled carbon nanotubes@ reduced graphene oxide nanoribbons.* Biosensors and Bioelectronics, 2015. **73**: p. 221-227.

105. Zhang, X., et al., *Molecular-counting-free and electrochemiluminescent single-molecule immunoassay with dual-stabilizers-capped CdSe nanocrystals as labels.* Analytical chemistry, 2016. **88**(10): p. 5482-5488.

106. Jie, G. and G. Jie, *Sensitive electrochemiluminescence detection of cancer cells based on a CdSe/ZnS quantum dot nanocluster by multibranched hybridization*

chain reaction on gold nanoparticles. RSC Advances, 2016. **6**(29): p. 24780-24785.

107. Lv, X., et al., *Electrochemiluminescent immune-modified electrodes based on Ag2Se@ CdSe nanoneedles loaded with polypyrrole intercalated graphene for detection of CA72-4.* ACS applied materials & interfaces, 2014. **7**(1): p. 867-872.

108. Stewart, A.J., et al., *A cholesterol biosensor based on the NIR electrogenerated-chemiluminescence (ECL) of water-soluble CdSeTe/ZnS quantum dots.* Electrochimica Acta, 2015. **157**: p. 8-14.

109. Jie, G., et al., *Autocatalytic amplified detection of DNA based on a CdSe quantum dot/folic acid electrochemiluminescence energy transfer system.* Analyst, 2015. **140**(1): p. 79-82.

110. Zhang, J., Z. Gryczynski, and J.R. Lakowicz, *First observation of surface plasmon-coupled electrochemiluminescence.* Chemical physics letters, 2004. **393**(4-6): p. 483-487.

111. Richter, M.M. and A.J. Bard, *Electrogenerated chemiluminescence. 58. Ligand-sensitized electrogenerated chemiluminescence in europium labels.* Analytical chemistry, 1996. **68**(15): p. 2641-2650.

112. Lei, Y.-M., et al., *Silver Ions as Novel Coreaction Accelerator for Remarkably Enhanced Electrochemiluminescence in a PTCA–S2O82–System and Its Application in an Ultrasensitive Assay for Mercury Ions.* Analytical chemistry, 2018. **90**(11): p. 6851-6858.

113. Chowdhury, M.H., et al., *First observation of surface plasmon-coupled chemiluminescence (SPCC).* Chemical physics letters, 2007. **435**(1-3): p. 114-118.

114. Bruno, J.G., et al., *Preliminary electrochemiluminescence studies of metal ion–bacterial diazoluminomelanin (DALM) interactions.* Journal of bioluminescence and chemiluminescence, 1998. **13**(3): p. 117-123.

115. Jingru, A. and L. Jinming, *Determination of Trace Silver (I) in Basic Aqueous Solution by Electrochemiluminescence of a New Reagent 6-(2-Hydroxy-4-Diethylaminophenylazo)-2, 3-Dihydro-1, 4-Phthalazine-1, 4-Dione.* CHEMICAL RESEARCH IN CHINESE UNIVERSITES, 1991. **7**(1): p. 32-36.

116. Bolleta, F., et al., *Polypyridine transition metal complexes as light emission sensitizers in the electrochemical reduction of the persulfate ion.* Inorganica Chimica Acta, 1982. **62**: p. 207-213.

117. Vogler, A. and H. Kunkely, *Electrochemiluminescence of organometallics and other transition metal complexes.* 1987.

118. McCall, J., et al., *Electrochemiluminescence of Copper (I) Bis (2, 9-dimethyl-1, 10-phenanthroline).* Analytical chemistry, 2001. **73**(19): p. 4617-4620.

119. Tokel-Takvoryan, N.E. and A.J. Bard, *Electrogenerated chemiluminescence. XVI. ECL of palladium and platinum α, β, γ, δ-tetraphenylporphyrin complexes.* Chemical Physics Letters, 1974. **25**(2): p. 235-238.

120. Vogler, A. and H. Kunkely, *Electrochemiluminescence of tetrakis (diphosphonato) diplatinate (II).* Angewandte Chemie International Edition in English, 1984. **23**(4): p. 316-317.

121. Gross, E.M., N.R. Armstrong, and R.M. Wightman, *Electrogenerated chemiluminescence from phosphorescent molecules used in organic light-emitting diodes.* Journal of the Electrochemical Society, 2002. **149**(5): p. E137-E142.

122. Kim, J., et al., *Electrogenerated chemiluminescence on the electrogenerated chemiluminescence (ECL) of tetrakis (pyrophosphito) diplatinate (II), Pt2 (P2O5H2) 44−.* Chemical physics letters, 1985. **121**(6): p. 543-546.

123. Bonafede, S., et al., *Electrogenerated chemiluminescence of an ortho-metalated platinum (II) complex.* The Journal of Physical Chemistry, 1986. **90**(16): p. 3836-3841.

124. Kane-Maguire, N., et al., *Photoluminescence and electrogenerated chemiluminescence of palladium (0) and platinum (0) complexes of dibenzylideneacetone and tribenzylideneacetylacetone.* Inorganic Chemistry, 1988. **27**(17): p. 2905-2907.

125. Wang, H., et al., *Electrogenerated chemiluminescence detection for deoxyribonucleic acid hybridization based on gold nanoparticles carrying multiple probes.* Analytica chimica acta, 2006. **575**(2): p. 205-211.

126. Sun, X., et al., *Method for effective immobilization of Ru (bpy) 32+ on an electrode surface for solid-state electrochemiluminescene detection.* Analytical chemistry, 2005. **77**(24): p. 8166-8169.

127. Wang, X., et al., *A controllable solid-state Ru (bpy) 32+ electrochemiluminescence film based on conformation change of ferrocene-labeled DNA molecular beacon.* Langmuir, 2008. **24**(5): p. 2200-2205.

128. Han, S., et al., *Chemiluminescence and electrochemiluminescence applications of metal nanoclusters.* Science China Chemistry, 2016. **59**(7): p. 794-801.

129. Nie, F., et al., *Novel preparation and electrochemiluminescence application of luminol functional-Au nanoclusters for ALP determination.* Sensors and Actuators B: Chemical, 2015. **218**: p. 152-159.

130. Luo, S., et al., *Ultrasensitive detection of pentachlorophenol based on enhanced electrochemiluminescence of Au nanoclusters/graphene hybrids.* Sensors and Actuators B: Chemical, 2014. **194**: p. 325-331.

131. Zhang, L., et al., *A novel alcohol dehydrogenase biosensor based on solid-state electrogenerated chemiluminescence by assembling dehydrogenase to Ru (bpy) 32+–Au nanoparticles aggregates.* Biosensors and Bioelectronics, 2007. **22**(6): p. 1097-1100.

132. Yin, X.-B., et al., *4-(Dimethylamino) butyric acid labeling for electrochemiluminescence detection of biological substances by increasing sensitivity with gold nanoparticle amplification.* Analytical chemistry, 2005. **77**(11): p. 3525-3530.

133. Li, Y., et al., *Detection of DNA immobilized on bare gold electrodes and gold nanoparticle-modified electrodes via electrogenerated chemiluminescence*

using a ruthenium complex as a tag. Microchimica Acta, 2009. **164**(1-2): p. 69.

134. Zhao, C., et al., *Electrochemiluminescence of gold nanoparticles and gold nanoparticle-labelled antibodies as co-reactants.* RSC advances, 2018. **8**(63): p. 36219-36222.

135. Dong, Y.-P., H. Cui, and C.-M. Wang, *Electrogenerated chemiluminescence of luminol on a gold-nanorod-modified gold electrode.* The Journal of Physical Chemistry B, 2006. **110**(37): p. 18408-18414.

136. Higashi, Y., et al. *Electrochemiluminscence Based Biosensors with AuNP Showing Catalytic ROS Generation*. in *Multidisciplinary Digital Publishing Institute Proceedings*. 2017.

137. Hossu, M., et al., *Enhancement of biophoton emission of prostate cancer cells by Ag nanoparticles.* Cancer nanotechnology, 2013. **4**(1): p. 21-26.

138. Hossu, M., L. Ma, and W. Chen, *Nonlinear enhancement of spontaneous biophoton emission of sweet potato by silver nanoparticles.* Journal of Photochemistry and Photobiology B: Biology, 2010. **99**(1): p. 44-48.

139. Zhang W, Hu X, Shen Q, Xing D. *Mitochondria-specific drug release and reactive oxygen species burst induced by polyprodrug nanoreactors can enhance chemotherapy*. Nature communications. 2019;10(1):1-14.

140. Sardarabadi, H., et al., Enhancement of the biological autoluminescence by mito-liposomal gold nanoparticle nanocarriers. Journal of Photochemistry and Photobiology B: Biology, 2020. **204**: p. 111812.

B | Supplementary data of Section 5

This section include the supplementary data of chapter 5 - *Biological autoluminescence for assessing oxidative processes in yeast cell cultures*.

Supplementary data for ”Biological autoluminescence for assessing oxidative processes in yeast cell cultures”

Petra Vahalová[1], **Kateřina Červinková**[1], **and Michal Cifra**[1,*]

[1]Institute of Photonics and Electronics of the Czech Academy of Sciences, Prague, Czechia
[*]cifra@ufe.cz

ABSTRACT

In this supplementary information, we provide additional data to BAL measurements: the autoluminescence signal from media without any cells, data showing the effect of a glucose injection on the BAL intensity, and simultaneous detection of cell and glucose concentration .

Water background of (chemi)autoluminescence induced by the Fenton reaction

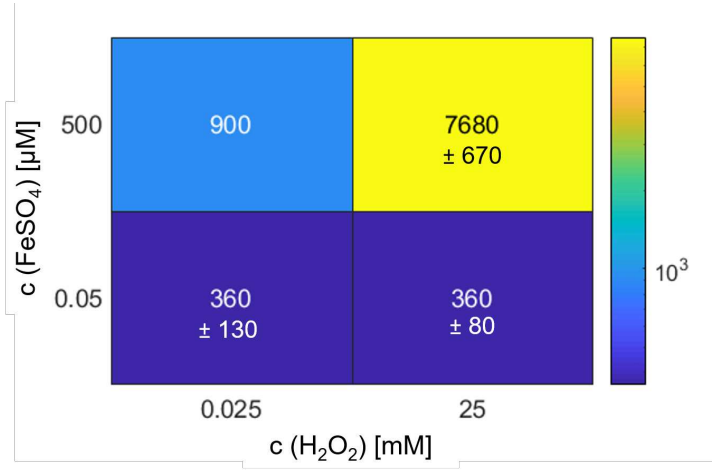

Figure S1. BAL from medium alone (Q water without any yeast cells) induced by the Fenton reagents at edge concentrations. The colour indicates the sum of the BAL intensities during the first 60 s after injection of H_2O_2 with a subtracted background (the previous 10 s before the injection of H_2O_2). The given numbers are usually the average from 3 measurements and the standard deviation.

BAL of YPD measured in bioreactor

Luminescence recovery after addition of glucose

In Fig. S3 the effect of addition of glucose into the yeast sample after sharp decrease of the BAL signal (approximately at seventeenth hour of the measurement) is shown. The measurement protocol was little bit different than for other experiments. Yeast cells were cultivated in an orbital shaking incubator just for 16 hours (standart YPD, 30 °C, 180 rpm). Yeast concentration was established using Bürker chamber. Required amount of cultivated yeast was transferred to 200 mL of cold YPD medium at initial concentration $5{\cdot}10^6$ cells·mL^{-1} placed in Erlemeyer flask covered with cotton stopper. The sample was bubbled with filtered room air. The experimental setup for BAL measurements was similar to the setup for measurements of induced

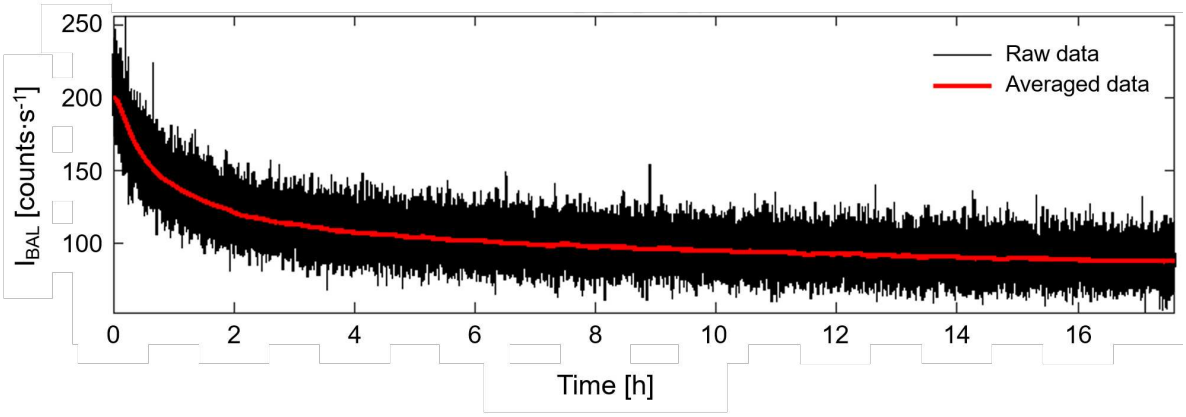

Figure S2. BAL signal from YPD medium (without yeast cells) measured in bioreactor for almost 18 hours. Initial higher BAL intensity was caused by the illumination of the sample during its preparation in the normal laboratory light conditions.

BAL from samples in a Petri dish, just instead of a Petri dish an Erlenmeyer flask was placed in a special black box (30 °C) with a photomultiplier module H7360-01. After the sharp decrease of the BAL intensity (approximately after 17 hours of measurement), 11 mL of 40% glucose was injected into the sample. The measurement was several times interrupted in order to establish the yeast concentration.

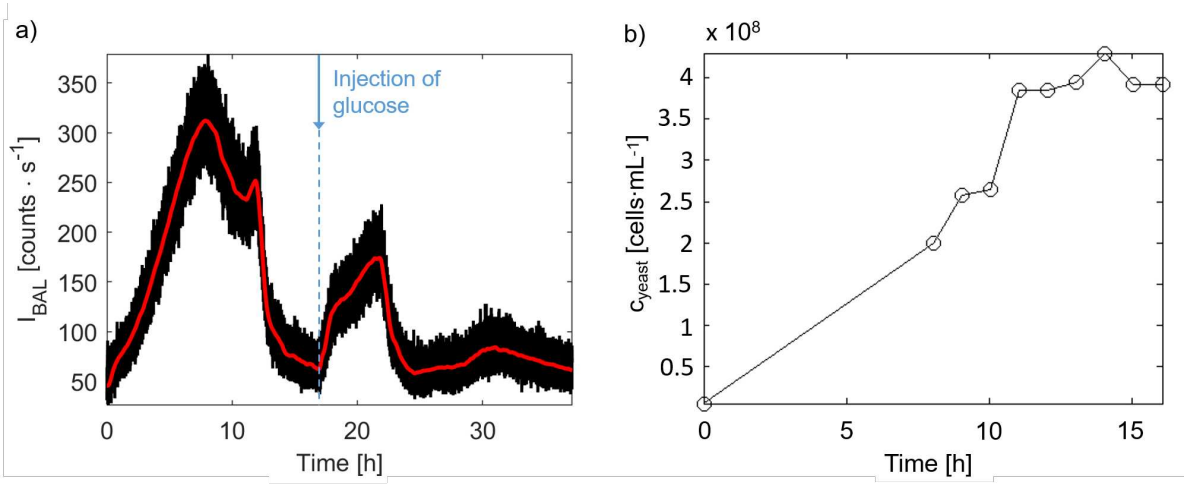

Figure S3. Development of BAL intensity during yeast growth in Erlenmeyer flask and repeated increase of the BAL signal after injection of glucose.

Development of glucose concentration in a growing yeast culture

Fig. S4 shows the development of glucose concentration during the yeast culture growth in bioreactor that is depicted by yeast cell concentration. Yeast concentration was evaluated by a cell counter (Beckman Coulter, Z2 series) in the range 3 - 9 μm. Glucose concentration was established by a commercial glucose kit (Glu 1000, Erba Lachema). Optical density was measured at 500 nm and subsequently recalculated to a real glucose concentration in mM (using calibration solutions at known glucose concentration). Both measurements are subject to a large deviation. However, trends are clear: with increasing amount of cells in the sample, glucose decreases. In other words, low concentration of glucose is correlated with the change of yeast growth phase and the change of yeast metabolism.

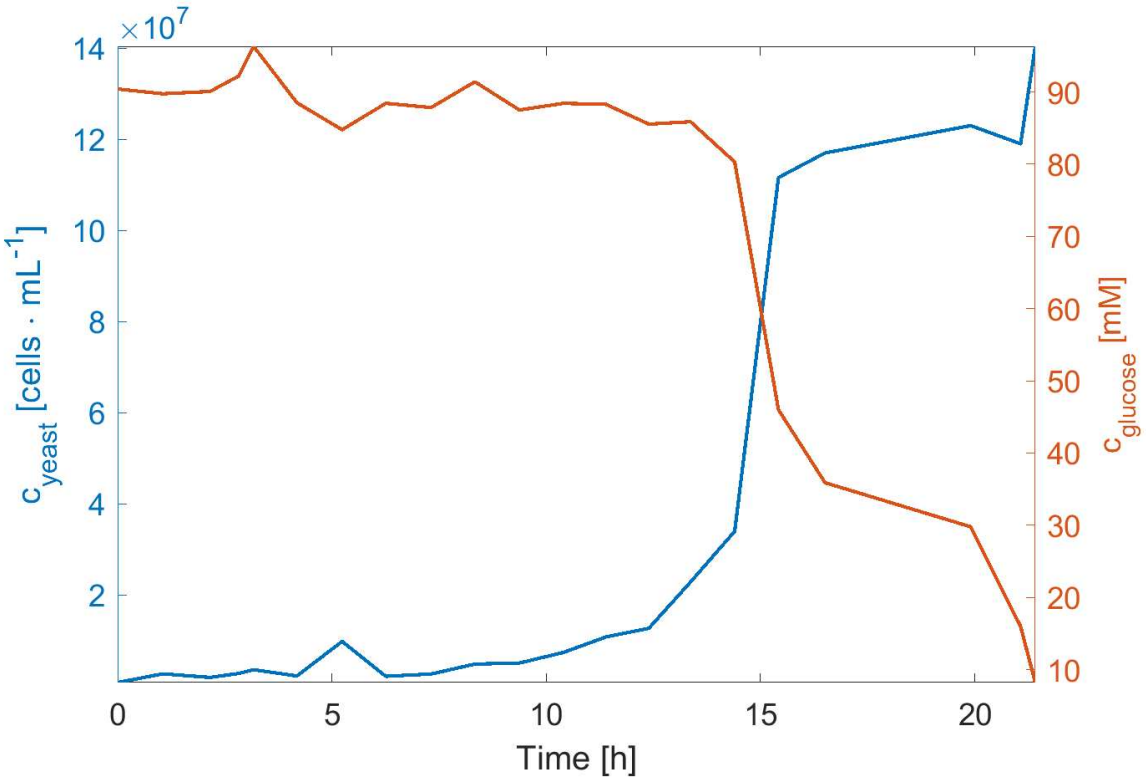

Figure S4. Simultaneous measurement of concentrations of glucose and yeast cells during their growth in a bioreactor. While the small measurement errors are visible, the trend is clear.

Raw data description

The source data can be found under https://doi.org/10.5281/zenodo.4382342 and are sorted according to the figure number and parts. For plotting the mean and the standard deviation of several (3 - 7) independent measurements in the Fig. 3a, 3d, and 4a, the predefined Matlab function 'shadedErrorBar' was used. Figures 4(ab), S2, and S3 contain smoothed data obtained by function 'rsmooth'[1]. To create Fig. 3c and S1 the Matlab command 'heatmap' was used.

References

1. Garcia, D. Robust smoothing of gridded data in one and higher dimensions with missing values. *Computational Statistics & Data Analysis* **54**, 1167–1178 (2010). URL https://linkinghub.elsevier.com/retrieve/pii/S0167947309003491.

C | Supplementary data of Section 6

This section include the supplementary data of chapter 6 - *Biochemiluminescence Sensing of Protein Oxidation by Reactive Oxygen Species Generated by Pulsed Electric Field*.

Supplementary information 1 for: Biochemiluminescence sensing of protein oxidation by reactive oxygen species generated by pulsed electric field

Petra Vahalová[a], Daniel Havelka[a], Eva Vaněčková[b], Tomáš Zakar[a], Viliam Kolivoška[b*], Michal Cifra[a*]

[a]*Institute of Photonics and Electronics of the Czech Academy of Sciences, Prague, 18200, Czechia*
[b]*J. Heyrovský Institute of Physical Chemistry of the Czech Academy of Sciences, Prague, 18200, Czechia*
[c]*corresponding authors: cifra@ufe.cz, viliam.kolivoska@jh-inst.cas.cz*

Abstract

Supplementary information

Keywords: luminescence, pulsed electric field, proteins, albumin, sensing, monitoring

S1-1. Materials and Methods

The sample preparation, assembly of the measurement setup and experiments were performed at ambient pressure and temperature ranging from 20 to 25 °C.

S1-1.1. Chemicals, preparation of samples

Bovine serum albumin (BSA; Sigma, A3803) was selected as a model biomolecule. Solid BSA was dissolved in Milli-Q water (Millipore, resistivity 18.2 MΩ·cm) at a concentration 20 mg·mL^{-1} (0.30 mM, ~ pH 7.1). As a control sample, phosphate buffer (PB, 0.36 mM NaH_2PO_4 and 0.83 mM Na_2HPO_4 , ~ pH 7.5, obtained from solid phosphate salts ($NaH_2PO_4 \cdot 2\,H_2O$ (P-Lab, D 03102), $Na_2HPO_4 \cdot 12\,H_2O$ (P-Lab, H 08102)) containing no BSA was employed. The concentration of PB constituents was selected so that the resulting solution had the same conductivity (approximately 190 µS·cm^{-1}) and similar pH (7.5) as the BSA sample (7.1). The employed conductometer (SevenCompact S230, probe InLab 751-4mm, Mettler Toledo) was calibrated with a standard solution 84 µS·cm^{-1} (T = 25 °C). Iron(III) nitrate nonahydrate ($Fe(NO_3)_3.9H_2O$, p.a.) and potassium thiocyanate (KSCN, p.a.) were purchased from Lach-Ner, Czech Republic. Hydrogen peroxide (H_2O_2, non-stabilized 30 % solution, p.a.) and sulfuric acid (H_2SO_4, 96 %, p.a.) were obtained from Penta. Hydrochloric acid (HCl, 30 %, suprapure) and nitric acid (HNO_3, 65 %, suprapure) were purchased from Merck.

S1-1.2. PEF chamber

PEF treatment of the samples was executed in a special chamber designed and manufactured in the Institute of Photonics and Electronics of the Czech Academy of Sciences, Prague, Czechia (Fig. 1). The chamber consists of a dielectric (transparent polymethylmethacrylate, PLEXIGLAS GS, Zenit) housing equipped with an anode (bottom electrode) and a cathode (top electrode) positioned in a parallel-plate arrangement. Two types of anodes were employed - glassy carbon (Sigradur G, Hochtemperatur-Werkstoffe GmbH, Germany) and stainless steel (type 1.4571, AKROS), both with a diameter 26 mm, defining the cross-sectional area of the liquid sample in the PEF chamber (5.31 10^{-4} cm^{-2}) . In the case of the glassy carbon electrode, a 3 mm thick carbon disk was fixed to a thin stainless steel support by adhesive conductive copper foil (1182, 3M), with the final resistance of ~ 10 Ω. The cathode was manufactured from stainless steel (type 1.4304, thickness 130 µm, PragoBoard). The central part of the cathode was perforated by hexagonally arranged holes with a diameter of 1.0 mm and spacing of 1.5 mm between the centers of the holes, creating 50 % voids. The cathode-anode gap was 2.00 and 1.88 mm for the steel and glassy carbon anode, respectively. The corresponding voltage to gap ratio (electric field strength magnitude) was 0.75 MV/m (7.5 kV/cm) for the 2.00 mm gap and 0.80 MV/m (8.0 kV/cm) for the 1.88 mm gap for the highest used voltage 1500 V. For the lowest used voltage (300 V), the values were 0.15 MV/m (1.5 kV/cm) for the 2.00 mm gap and 0.16 MV/m (1.6 kV/cm) for the 1.88 mm gap.

S1-1.3. PEF treatment and measurement setup

Before the PEF experiment, both the cathode and anode were cleaned with an aqueous 8.79 M solution of H_2O_2 for at least 10 min. The anode was cleaned as integrated in the PEF chamber by introducing the cleaning agent to its surface. The cathode was cleaned by immersion in the solution in a separate beaker. Cleaning was followed by copious rinsing with Milli-Q water and drying with dust-free wiping paper. Afterwards, a freshly prepared sample (either PB or BSA solution, see above) was introduced into the PEF chamber in volumes of 1.08 mL (in the case of the glassy carbon anode) or 1.24 mL (in the case of the steel anode). The assembly was finalized by mounting the steel cathode, the contacting ring and closing the PEF chamber, see Fig. 1. In all experiments, the same glassy carbon or steel anode and the same steel cathode were used.

A PEF was generated by a pulse generator (ELECTROcell B15, Leroy-Biotech) that simultaneously recorded the applied voltage and resulting current. The PEF consisted of 30 pulses with 100 µs width fired at a frequency of 1 Hz and voltage amplitude as a variable (ranging from 300 to 1500 V in increments of 300 V). Characteristics of the first pulse of each PEF sequence were additionally recorded by high voltage (P5100, Durlclth) and current (ICP5150, Instrance) probes connected to the oscilloscope (GDS-2202E, GW Instek). To verify proper chamber assembly, an LCR meter (BK891, BK PRECISION) was used to measure the impedance magnitude and phase shift between the anode and the cathode of the chamber before and after the PEF treatment.

Measurements of PEF-induced (bio)chemiluminescence were performed using a photon counting regime in a light-tight box equipped with a photomultiplier tube (PMT) module H7360-01 (Hamamatsu Photonics K.K.), which was selected as appropriate for the intended experiments due to its spectral range (300 to 650 nm). The luminescence sensing setup further comprised a C8855 counting unit (Hamamatsu Photonics K.K.), which also served as an interface to PC. The setup enabled tuning the distance between the chamber and the PMT module. The distance between the PMT module and the cathode was always set to 8.2 mm. To obtain the background response, sensing of photons was commenced 120 s before the beginning of the PEF treatment and the signal was additionally recorded for another 450 s after the PEF treatment. A schematic diagram of the experimental setup is shown in Fig. 2.

S1-1.4. Protein carbonyl assay

To determine the amount of carbonyl moieties in BSA samples, a commercial kit (Protein carbonyl content assay kit, Sigma-Aldrich, MAK094) and the corresponding measurement protocol (see lower) were used. The assay was based on the spectrophotometric determination of products of the reaction between carbonyls in the analyzed samples and 2,4-dinitrophenylhydrazine (Brady's test). As a negative control, the analysis was performed for pristine (untreated) BSA sample. Subsequently, BSA samples treated by PEF with either a glassy carbon or a steel anode employed were inspected. Additionally, the analysis was performed for BSA samples subjected to extended PEF treatment, in which the number of pulses was increased from 30 to 240. Extended PEF treatment was separated into 8 pulsing series with 30 pulses in each series, with 90 s pauses between the series to avoid excessive heating. As a positive control, a BSA sample treated with Fenton reagent was investigated. The latter involved iron(II) sulfate ($FeSO_4$, obtained from P-LAB, final concentration 1 µM) and hydrogen peroxide (H_2O_2, final concentration 146.5 mM). The mixture of BSA and the Fenton reagent was prepared by introducing $FeSO_4$ to the BSA solution and then adding H_2O_2, with final concentration of BSA being 0.30 mM. Such obtained reaction mixture was left at room temperature for 70 – 80 min. After execution of all the sample handling steps prescribed by the measurement protocol (see lower for the full protocol), the absorbance of the reaction mixture was measured at 375 nm employing a transparent 96-well plate (269620, Thermo Scientific) with 100 µL of a sample in each well was used. The measurement was performed with a multiwell plate reader (Tecan Spark). Each sample (untreated, treated by PEF or by the Fenton reagent) was inspected at least four times, with each individual measurement being an average from at least four wells. The carbonyl content (presented in units of µmole/L denoting the concentration in the protein solution further in this work) was determined based on Lambert-Beer's law, with background (solvent) subtraction being performed. Calculations underlying the determination of carbonyl content in BSA samples inspected in this work are presented in the detailed protocol lower.

S1-1.5. Iron assay

To determine the total amount of iron in purchased BSA, the sample (100 mg) was dissolved in 1.0 mL of water and mixed with 4.0 mL of aqueous 65 % solution of HNO_3. The resulting mixture was heated to 75 °C for 6 hours

and then left overnight at room temperature. The treatment by strongly oxidizing and acidic agent guarantees that the entire amount of iron present in the sample is converted to the Fe^{3+} ion. The sample was then heated to 75 °C to reduce its volume to approximately 1 mL. The remaining content was quantitatively transferred to a 5 mL volumetric flask, with the rest of the volume being filled with 3 % aqueous solution of HCl. Subsequently, 1.0 mL of the sample was introduced to Suprasil quartz cuvette (10 mm light path, purchased from Hellma Analytics) and its absorption spectrum in the range of 200 to 1100 nm (used further as a blank) was obtained using an Agilent 8453 UV-Vis-NIR diode array detector spectrometer. Afterwards, 20 mg of solid KSCN as an agent to determine Fe^{3+} ion was introduced to the sample in the cuvette, the mixture was homogenized and the absorption spectrum was measured again. Subsequently, five 10 μL aliquots of 1.00 mM $Fe(NO_3)_3$ used as the internal standard (corresponding to a concentration range of 10 to 50 μM) were sequentially introduced to the sample in the cuvette, with absorption spectra being recorded upon each addition. The content of Fe^{3+} ion in the solution was determined based on absorbance values evaluated at 480 nm.

S1-1.6. Tryptophan and tyrosine fluorescence

In addition to analyzing the carbonyl content, the BSA samples, treated as described above, were probed for the amount of aromatic amino acid residues employing fluorescence spectroscopy. The excitation wavelength was set to 280 nm, which falls within the absorption bands of tryptophan and tyrosine, implying that the cumulative content of these two amino acids was determined in the analysis. Emission spectra of samples were obtained in the wavelength range of 318 and 398 nm with a 5 nm step. The signal analyzed and presented further was evaluated at the emission maximum of 338 nm. The fluorescence analysis utilized multiwell plate reader Spark (Tecan) and black 96-well plates (Thermo Scientific, 237105). Each kind of BSA sample was measured at least 4 times. As a negative control, the analysis was carried out with the PB sample replacing the BSA sample, subjected to the same treatment. Each kind of PB sample was measured at least 3 times. Within individual measurements, the fluorescence signal presented further was obtained as an average from 3 – 6 wells, filled with 100 µL of the same sample.

S1-1.7. Chemiluminescence detection using multiwell plate reader

To detect (bio)chemiluminescence from either pure water, PB or BSA solutions (see above for their respective chemical composition) across a large range of concentrations of Fenton reagents (Fe^{2+} and H_2O_2), we utilized multiwell plate reader Spark (Tecan) and black 96-well plates (236105, Thermo Scientific). The plate reader luminescence detector is sensitive in the wavelength range from 370 to 700 nm. The plate wells were filled using a multichannel pipette (PB, water, iron solutions) or an electronic repeater pipette Eppendorf Multipette E3X (BSA solutions) to prevent bubble formation. The plate reader was set to inject the solution of H_2O_2 and luminescence measurement started right after the H_2O_2 injection (< 1 s). The luminescence signal was collected for 1 minute (using kinetic mode setting in the plate reader). After the measurement, the signals were integrated to obtain the total counts per 1 minute. Injected volumes were always the same across the experiments (hence the concentration in the final mixture was varied by the concentration of the stock solutions) and the final volume was always 200 µL per well. The experiments were performed at 28 °C. In the 96-well plate, we varied concentrations of H_2O_2 and $FeSO_4$ across different columns (1–12) and made N=8 repetitions along the single column (i.e. A–H). The final concentrations were 0, 0.01, 0.1, 1, 10 and 100 mM for H_2O_2 and 0, 0.01, 0.1, 1, 10 and 100 µM for $FeSO_4$.

S1-2. Difference in mechanisms of PEF action on membranes vs. proteins

It is well known that PEF enables electropermeabilization and electroporation of membranes with EF strengths starting from the order of kV/cm (depending on the pulse duration); therefore, membranes are the first and canonical targets of PEF [1]. The physical reason is that biological membranes are practically electrical insulators that cause a voltage drop (large difference in electrical potential across them) [2] effectively enhancing the EF strength in their interior by orders of magnitude compared to an external EF. This enhancement effect is absent in water-soluble biomolecules, which reside outside the membrane. Therefore, substantially less data is available on the effect of PEF on soluble proteins than on membranes, because much higher EF strengths are typically needed to affect the proteins physically. Nevertheless, the progress in technology has resulted in more powerful electric pulse generators in a lab bench format, enabling EF strengths [3, 4] that are now capable of direct action on the electromechanics of

proteins. The EF thresholds required to induce an effect are largely unexplored and uncertain because of the much wider diversity of protein structures compared to membranes. However, methods for controlling protein structure and function, which PEF might enable, are extremely important for several vast areas of science and industry: proteins are by mass the most abundant biomolecules in most biological cells, crucial food constituents, and potential bio-nanotechnological workhorses. Therefore, the new technology-enabled opportunities and potential research and industrial impact of potential PEF effects on proteins strongly motivate research in this area.

Protein carbonyl content assay kit (Sigma-Aldrich)

Before measurement

- Place 10 mL of acetone in -25 °C freezer.
- Place appropriate amount of 6 M guanidine solution into a test tube and leave it to come to room temperature (200 µL for each sample + 4x 100 µL as a reference).
- For each sample put 100 µL of DNPH solution into a 1.5 mL eppendorf and leave it to come to room temperature.

Protocol

1. To each 1.5 mL eppendorf with 100 µL of DNPH solution, add 100 µL of a sample (4x each sample), vortex, incubate for 10 min at room temperature.
2. Approximately 2 min before the end of incubation time, take out 87 % TCA from fridge and put it into the ice.
3. Add 30 µL of 87% TCA to each sample, vortex, incubate on ice for 5 min.
4. Centrifuge samples at 13000 g for 2 min.
5. Remove supernatant carefully, do not disturb the pellet.
6. Add 500 µL of ice-cold acetone to each pellet.
7. Place samples in a sonication bath for 1 min.
8. Incubate samples in a freezer for 5 min.
9. Centrifuge samples at 13000g for 2 min.
10. Carefully remove acetone from pellet.
11. Add 500 µL of ice-cold acetone to each pellet.
12. Place samples in a sonication bath for 1 min.
13. Incubate samples in freezer for 5 min.
14. Centrifuge samples at 13000 g for 2 min.
15. Carefully remove acetone from pellet.
16. Add 200 µL of 6 M guanidine solution (room temperature) to pellets, sonicate briefly (samples should be homogenous).
17. Transfer 100 µL of each sample to the 96-well plate.
18. Measure absorbance at 375 nm.

Protein carbonyl quantification

- Subtract background (absorbance of 6 M guanidine solution) from absorbance of a sample.
- Calculate amount of carbonyl in sample well according Lambert-Beer's law:

$$\mathrm{C}\left(\frac{\mathrm{nmol}}{\mathrm{well}}\right) = \frac{\mathrm{A375_{sub}} * \mathrm{V}}{\mathrm{L} \cdot \varepsilon}$$

  where $\mathrm{A375_{sub}}$ is measured absorbance at 375 nm after background subtraction, L = 0.2893 cm is path-length in a well for 96-well plate, ε = 22 $\mathrm{mM^{-1} \cdot cm^{-1}}$ is molar extinction coefficient of the product of the reaction between DNPH and carbonyl moieties and V = 100 µL refers to total volume in well.

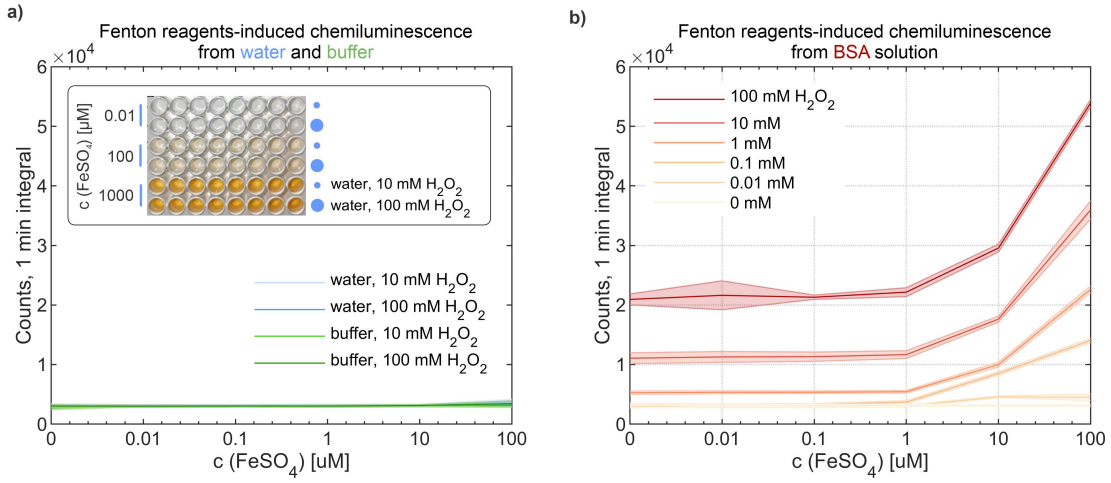

Figure S1-1: (Bio)chemiluminescence from a) water, phosphate buffer, and b) BSA solution (in water) induced by various concentrations of H_2O_2 and $Fe^{2+}SO_4$. The data mean is depicted as a thick line and the standard deviation from N=8 measurements (wells) is depicted as a shaded error bar. The inset in a) is a photo of an example plate after the experiment.

- To recalculate carbonyl content into micromoles per liter, it is necessary to multiply the obtained number C (nmol/well) by 10.

S1-3. (Bio)chemiluminescence due to BSA oxidation by Fenton reagent

When cleaning glassware employed to prepare stock solutions of BSA by Piranha solution (96 % H_2SO_4 and 30 % H_2O_2 freshly mixed in 3/1 v/v ratio) we noticed formation of gas bubbles (attributed to oxygen and ROS) with a rate higher than typical for this cleaning procedure. This observation motivated us to perform an additional experiment focusing on the oxidation of BSA dissolved in water by Piranha solution. In particular, 4 mL of Piranha solution were mixed either with 1 mL of water (a control experiment) or 1 mL of aqueous BSA solution (its concentration in the resulting mixture was set to 20 mg/mL, i.e., identical to that in PEF experiments). We stress here that this experiment involves mixing of a very potent oxidizing agent with organic matter and has to be performed at a very well-ventilated environment and employing protective equipment (face-shield, gloves, lab coat). In the absence of BSA, the resulting mixture became warm, but remained quiescent, with hardly detectable bubble formation. In the presence of BSA, additionally to warming, gas bubbles were vigorously formed, accumulated at the surface of the liquid phase (see Fig. S1-5) and an intense ozone odor was sensed. This striking difference suggests that BSA (or its oxidation products or impurities contained in the sample) facilitates the formation of oxygen and ROS from H_2O_2 in a strongly acidic environment.

These results stimulated us to monitor the formation of ROS from H_2O_2 and their subsequent reactions with BSA by (bio)chemiluminescence measurements. To make a bridge to the above-presented experiments with electrochemically generated ROS by PEF, we replaced the strongly acidic Piranha solution by neutral environments (pure water, PB and BSA samples). We examined these systems with H_2O_2 introduced as the ROS precursor at concentrations ranging from 0.01 to 100 mM in a decadic logarithm spacing. At the same time, we explored the influence of Fe^{2+} employed as the catalyst in the Fenton reagent on the kinetics of the ROS formation and action, by introducing $FeSO_4$ at concentrations ranging from 0.01 to 100 μM. Biologically relevant values for H_2O_2 concentration are in the range of nM-mM [5, 6, 7], which is well within the concentration range we explored. The biologically relevant concentration values of iron are in the range of 0.1–10 mM, where the iron is often present in a bound form [8, 9, 10]. The maximum $FeSO_4$ concentration was set to 0.1 mM in our experiments due to solibility limits, as a higher value

(1 mM) caused a substantial formation of precipitates (see inset of Fig. S1-1), presumably composed of poorly soluble hydrated iron(III) oxide formed by oxidative hydrolysis of Fe^{2+} ions in neutral solutions saturated with ambient oxygen. These precipitates would distort measured luminescence signal by light scattering and absorption phenomena. Besides concentration-resolved measurements, control experiments were performed in the absence of H_2O_2 and/or $FeSO_4$.

Fig. S1-2 shows averaged luminescence transients obtained immediately upon the introduction of H_2O_2 solution to the BSA sample containing $FeSO_4$, with the highest H_2O_2 (10 and 100 mM) and $FeSO_4$ (10 and 100 μM) concentrations used in this work. For both H_2O_2 and $FeSO_4$, a ten-fold concentration increase lead to significantly elevated luminescence signals, implying that these agents are involved in the reaction sequence leading to photoemissive processes. In water or PB and the same concentrations of H_2O_2 and $FeSO_4$, the obtained luminescence signals (Fig. S1-3,S1-4) were practically equal to the dark count of the measurement apparatus (60 counts/s). This confirms that the vast majority of the signal observed for the BSA sample is due to biochemiluminescence resulting from reactions involving protein molecules. Integrals evaluated for luminescence transients obtained for the entire inspected range of H_2O_2 and $FeSO_4$ concentrations are cumulatively depicted in Fig. S1-1 (panel A for water and PB, panel B for BSA). For BSA and the absence of $FeSO_4$, the signal is elevated for H_2O_2 concentrations equal to and greater than 1 mM, i.e. for values exceeding the concentration of dissolved BSA (0.3 mM). The same picture is preserved for $FeSO_4$ concentrations up to 1 μM. This suggests that under these conditions, H_2O_2 species are either spontaneously decomposed (i.e. without the need for Fe^{2+}/Fe^{3+} as the catalyst) or that a certain amount of catalyst species is contained in the BSA sample. To ascertain which scenario is more plausible, we analyzed a sample of BSA used in this work for the total iron content. The assay was realized by thermal mineralization of 20 mg/mL BSA solution in concentrated HNO_3 and subsequent spectrophotometric determination of such formed Fe^{3+} exploiting its reaction with SCN^- anion as the specifically binding colorizing agent (see Experimental part for details). The analysis led us to the conclusion that the BSA sample contained 6 ± 3 ppm of total iron, which, for 20 mg/mL solution of BSA, translated to 2 ± 1 μM. This result corresponds well to the upper end of the $FeSO_4$ concentration range (1 μM) for which a constant biochemiluminescence signal was observed. We conclude that the signal obtained in solutions with $FeSO_4$ concentrations of 1 μM and lower is due to the intrinsic catalytic activity of iron species contained in the BSA sample, while for higher $FeSO_4$ concentrations, elevated reaction rates are due to externally introduced catalyst. Note that the oxidation of the BSA by the Fenton reagent composed of 1 μM $FeSO_4$ and 146.5 mM H_2O_2 lead to a noticeable increase of the carbonyl content in the sample (see Fig. 6), implying that profound oxidation of molecules takes place under these conditions.

An absence of a chemiluminescence signal in water and PB (samples without BSA) as underlying media for Fenton reactions indicates that the overall reaction rate is low for concentration ranges and pH selected in this work. While the reaction between the Fe^{2+} and H_2O_2 (Eq. 1) has a rate constant of ca. 100 M^{-1} s^{-1} [11], converting the majority of the catalyst to the Fe^{3+} form, the regeneration of the Fe^{2+} form (Eq. 2) is much slower (ca. 0.001 M^{-1} s^{-1}) [11], being the rate-limiting step in the catalytic cycle. Note that anodically generated ROS were found to produce a significant chemiluminescence response in the absence of BSA. High rates of reactions underpinning photoemissive processes may be rationalized by the reactive nature of electrogenerated ROS ($OH^\bullet$ and $HO_2^\bullet$) [12, 13, 14] combined with their spatial confinement to the electrode/electrolyte interface. In the Fenton reagent, the chemiluminescence intensity is limited by rates of reactions among relatively stable species (Fe^{2+}, Fe^{3+} and H_2O_2) diluted in the entire solution. This comparison points to the advantages of electrochemical approaches based on carbon anodes enabling localized production of ROS of desired amounts via polarizing electrodes by voltage steps and pulses performed in customized reactor geometries.

S1-4. Measurement of electrolyte heating due to PEF

The temperature increase in the electrolyte due to Joule heating was estimated theoretically for the highest applied voltage (1500 V) and observed current (8 A) considering the geometry of the employed PEF chamber (see Experimental part) and specific heat capacity of water (4184 J kg^{-1} K^{-1}), with heat transport through electrodes being neglected. The temperature increase calculated for one and thirty 100 μs pulses amounts to 0.3 and 8.4 °C, respectively. Sensing performed during the PEF experiment by a thermal imaging camera revealed a temperature increase of ca. 2 K implying that losses due to heat transport are significant. Importantly, such a low change in temperature is assumed to have no influence on the chemical structure, reactivity, and chemiluminescence of BSA molecules.

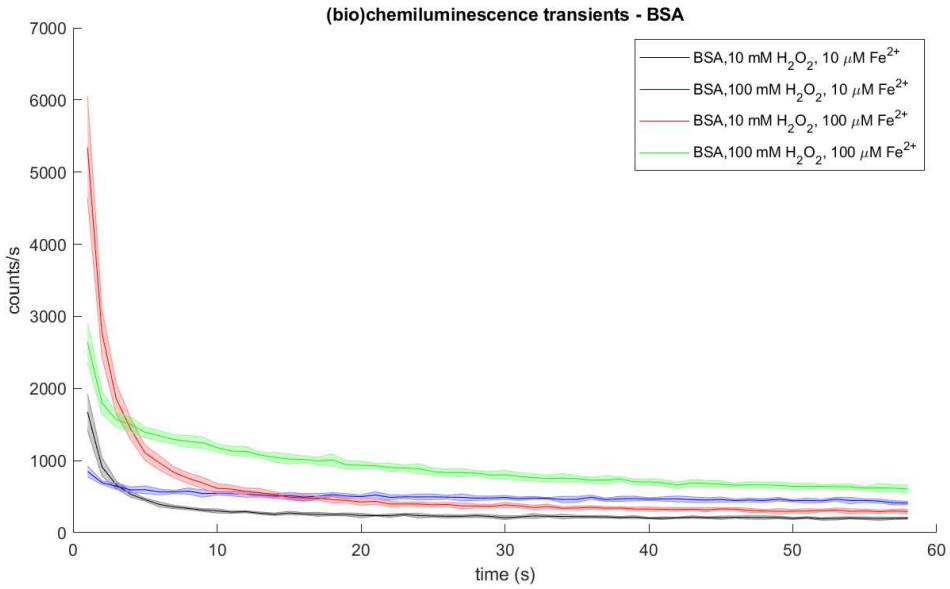

Figure S1-2: Chemiluminescence transients induced by Fenton reagents (H_2O_2 and Fe^{2+}) in 20 mg/mL BSA solutions as measured with luminescence module of Tecan SPARK multiwell plate reader.

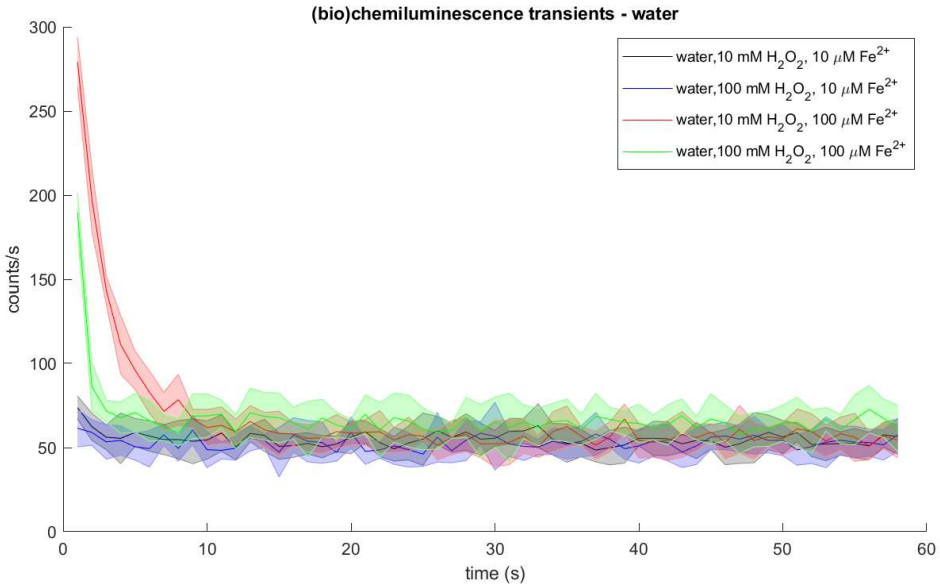

Figure S1-3: Chemiluminescence transients induced by Fenton reagents (H_2O_2 and Fe^{2+}) in water as measured with luminescence module of Tecan SPARK multiwell plate reader.

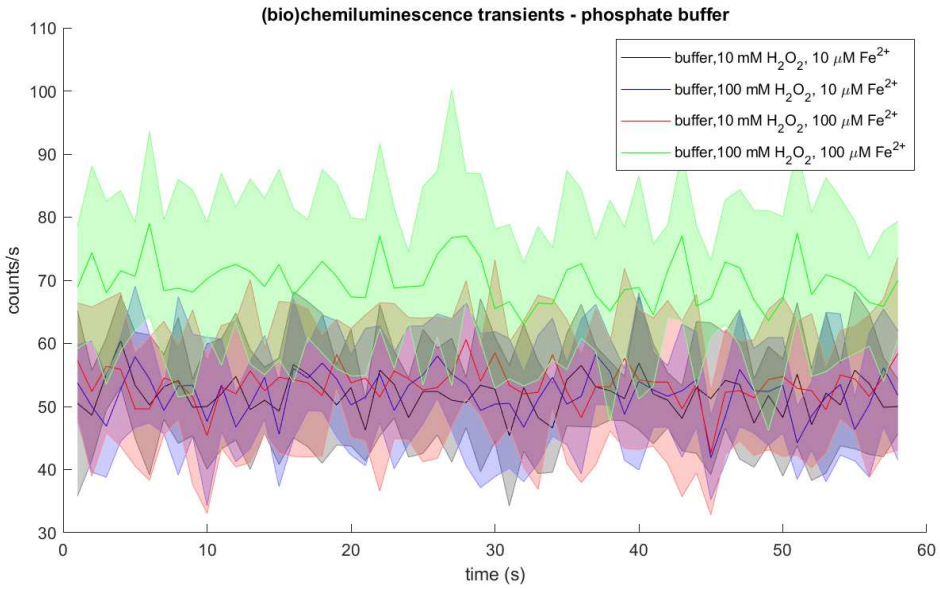

Figure S1-4: Chemiluminescence transients induced by Fenton reagents (H_2O_2 and Fe^{2+}) in phosphate buffer (0.36 mM NaH_2PO_4 and 0.83 mM Na_2HPO_4) as measured with luminescence module of Tecan SPARK multiwell plate reader.

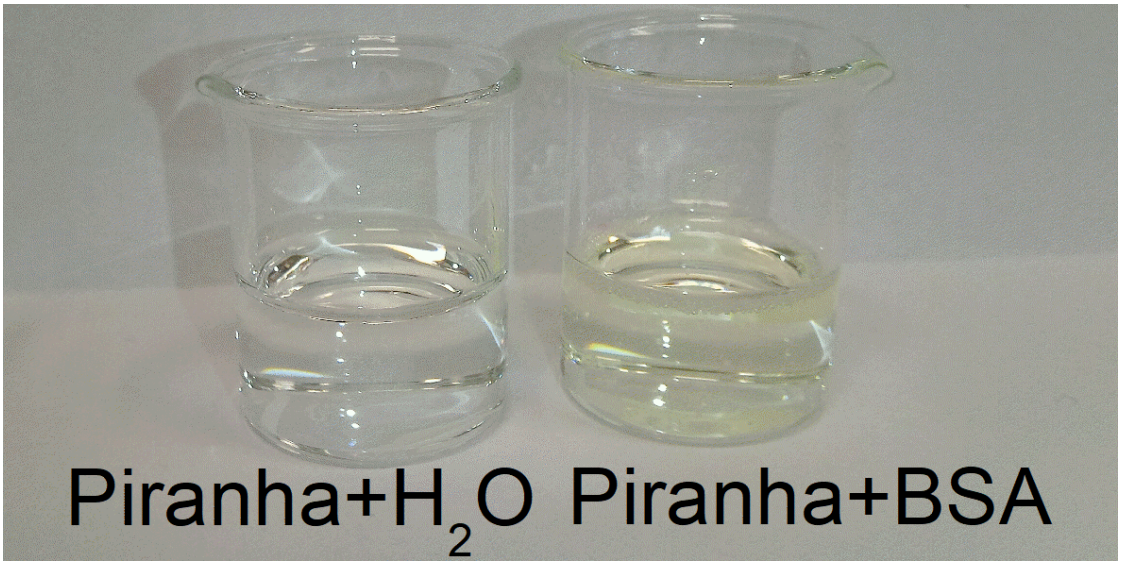

Figure S1-5: Optical photograph of freshly prepared Piranha solution (3 mL of 96 % H_2SO_4 and 1 mL of 30 % H_2O_2) mixed with 1 mL of water (left) and 1 mL of aqueous BSA solution (final concentration of 20 mg/mL, right).

Abbreviations

DNPH = 2,4-dinitrophenylhydrazine

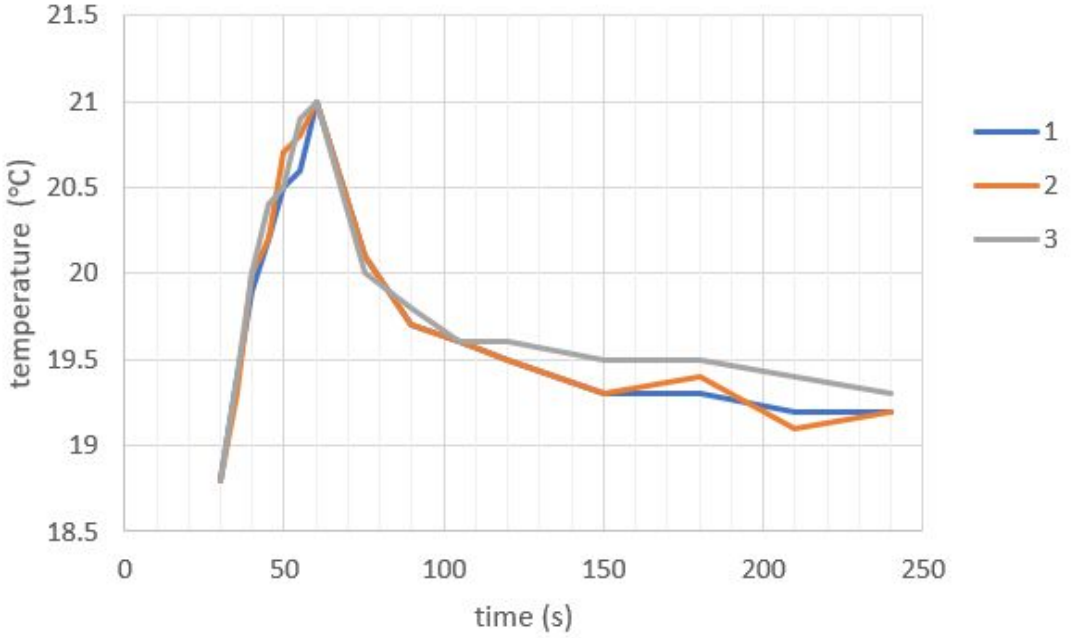

Figure S1-6: Evolution of temperature of the 20 mg/mL (0.3 mM) BSA sample (ca. 200 µS) during one train of 30 pulses, 100 µs, 1 Hz, 1500 V. Legend refers to three replications of the experiments

TCA = trichloroacetic acid

References

[1] M. L. Yarmush, A. Golberg, G. Serša, T. Kotnik, D. Miklavčič, Electroporation-Based Technologies for Medicine: Principles, Applications, and Challenges, Annual Review of Biomedical Engineering 16 (1) (2014) 295–320. doi:10.1146/annurev-bioeng-071813-104622.
URL http://www.annualreviews.org/doi/10.1146/annurev-bioeng-071813-104622

[2] T. Kotnik, G. Pucihar, Induced transmembrane voltage-theory, modeling, and experiments, in: Advanced electroporation techniques in biology and medicine, 2010, pp. 51–70.
URL https://www.researchgate.net/profile/Tadej_Kotnik/publication/236681426_Induced_transmembrane_voltage__theory_modeling_and_experiments/links/02e7e518faa41a30c0000000.pdf

[3] G. Urabe, T. Sato, G. Nakamura, Y. Kobashigawa, H. Morioka, S. Katsuki, 1.2 MV/cm pulsed electric fields promote transthyretin aggregate degradation, Scientific Reports 10 (1) (2020) 12003. doi:10.1038/s41598-020-68681-0.
URL http://www.nature.com/articles/s41598-020-68681-0

[4] O. Lucia, T. Garcia-Sanchez, H. Sarnago, L. M. Mir, J. Burdio, Industrial Electronics for Biomedical Applications: Electroporation as a New Tool for Cancer Treatment, IEEE Industrial Electronics Magazinedoi:10.1109/MIE.2019.2942377.

[5] E. Cadenas, K. J. Davies, Mitochondrial free radical generation, oxidative stress, and aging, Free Radical Biology and Medicine 29 (3-4) (2000) 222–230.

[6] P. Niethammer, C. Grabher, A. T. Look, T. J. Mitchison, A tissue-scale gradient of hydrogen peroxide mediates rapid wound detection in zebrafish, Nature 459 (7249) (2009) 996–999. doi:10.1038/nature08119.
URL http://www.nature.com/articles/nature08119

[7] A. E. K. Loo, R. Ho, B. Halliwell, Mechanism of hydrogen peroxide-induced keratinocyte migration in a scratch-wound model, Free Radical Biology and Medicine 51 (4) (2011) 884–892. doi:10.1016/j.freeradbiomed.2011.06.001.
URL http://linkinghub.elsevier.com/retrieve/pii/S0891584911003595

[8] C. A. Martínez-Garay, R. de Llanos, A. M. Romero, M. T. Martínez-Pastor, S. Puig, Responses of Saccharomyces cerevisiae Strains from Different Origins to Elevated Iron Concentrations, Applied and Environmental Microbiology 82 (6) (2016) 1906–1916. doi:10.1128/AEM.03464-15.
URL http://aem.asm.org/lookup/doi/10.1128/AEM.03464-15

[9] N. F. Olivieri, Progression of iron overload in sickle cell disease, Seminars in Hematology 38 (2001) 57–62. doi:10.1016/S0037-1963(01)90060-5.
URL https://www.sciencedirect.com/science/article/pii/S0037196301900605

[10] J. C. Wood, Estimating Tissue Iron Burden: Current Status and Future Prospects, British journal of haematology 170 (1) (2015) 15–28. doi:10.1111/bjh.13374.
URL https://www.ncbi.nlm.nih.gov/pmc/articles/PMC4484399/

[11] J. De Laat, H. Gallard, Catalytic Decomposition of Hydrogen Peroxide by Fe(III) in Homogeneous Aqueous Solution: Mechanism and Kinetic Modeling, Environmental Science & Technology 33 (16) (1999) 2726–2732. doi:10.1021/es981171v.
URL https://pubs.acs.org/doi/10.1021/es981171v

[12] K. Sehested, O. L. Rasmussen, H. Fricke, Rate constants of OH with HO2,O2-, and H2O2+ from hydrogen peroxide formation in pulse-irradiated oxygenated water, The Journal of Physical Chemistry 72 (2) (1968) 626–631. doi:10.1021/j100848a040.
URL https://pubs.acs.org/doi/10.1021/j100848a040

[13] D. T. Sawyer, J. S. Valentine, How super is superoxide?, Accounts of Chemical Research 14 (12) (1981) 393–400. doi:10.1021/ar00072a005.
URL https://pubs.acs.org/doi/abs/10.1021/ar00072a005

[14] B. H. J. Bielski, D. E. Cabelli, R. L. Arudi, A. B. Ross, Reactivity of HO_2 /O^-_2 Radicals in Aqueous Solution, Journal of Physical and Chemical Reference Data 14 (4) (1985) 1041–1100. doi:10.1063/1.555739.
URL http://aip.scitation.org/doi/10.1063/1.555739